CENTER FOR INFRASTRUCTURE ENGINEERING STUDIES

UTC
ETT131

Geotechnical and Bridge Design Workshop: New Madrid Seismic Zone Experience

By

Dr. Genda Chen

University Transportation Center Program at

The Universitv of Missouri-Rolla

Disclaimer

Technical Report Documentation Page

1. Report No.	2. Government Accession No.	3. Recipient's Catalog No.
UTC ETT131		

4. Title and Subtitle	5. Report Date
Geotechnical and Bridge Design Workshop: New Madrid Seismic Zone Experience	Dec 2004
	6. Performing Organization Code
7. Author/s	8. Performing Organization Report No.
Dr. Genda Chen	00001352
9. Performing Organization Name and Address	10. Work Unit No. (TRAIS)
Center for Infrastructure Engineering Studies/UTC program University of Missouri - Rolla 223 Engineering Research Lab Rolla, MO 65409	11. Contract or Grant No. DTRS98-G-0021
12. Sponsoring Organization Name and Address	13. Type of Report and Period Covered
U.S. Department of Transportation Research and Special Programs Administration 400 7th Street, SW Washington, DC 20590-0001	Final
	14. Sponsoring Agency Code

15. Supplementary Notes

16. Abstract

A technology transfer workshop will be held in Cape Girardeau on October 28-29, 2004 to disseminate the research results from the UMR earthquake hazards mitigation research program. The workshop will cover the bridge design related topics in geophysics, seismology, geotechnical to structural engineering. Attempt will be made to work step-by-step through a complete design cycle for bridge systems, highlighting the contributions from the UMR efforts in each step.

17. Key Words	18. Distribution Statement
Bridge Structure, Earthquake Mitigation	No restrictions. This document is available to the public through the National Technical Information Service, Springfield, Virginia 22161.

19. Security Classification (of this report)	20. Security Classification (of this page)	21. No. Of Pages	22. Price
unclassified	unclassified		

Form DOT F 1700.7 (8-72)

GEOTECHNICAL AND BRIDGE SEISMIC DESIGN WORKSHOP

New Madrid Seismic Zone Experience

Drury Inn Lodge
Cape Girardeau, Missouri

October 28-29, 2004

Organizer: University of Missouri-Rolla (UMR)

Sponsors: Federal Highway Administration
Missouri Department of Transportation
University Transportation Center at UMR

PREFACE

The University of Missouri-Rolla (UMR) was awarded the project entitled "Earthquake Hazard Mitigation Research Program for Highway Systems" in 2002 by the U.S. Department of Transportation through the Federal Highway Administration. The period of performance was originally from January 30, 2002 through January 29, 2004, but was recently extended to February 28, 2005. Co-funded by the Missouri and Alaska Departments of Transportation, Missouri Department of Natural Resources, UMR, and the University Transportation Center at UMR, the project involves a multidisciplinary team of seismologists, geologists, geotechnical and structural engineers. Focused on the earthquake threat from the New Madrid Seismic Zone, the research project addresses several issues of national importance, including earthquake loss estimation, effect of near-field ground motions on bridge designs, post-earthquake assessment, and seismic retrofit techniques for Mid-American highway bridge systems.

At present, the research team is summarizing the findings and methodology developed from the research project. The final report is expected to become available in Spring 2005. As an integral part of the overall project, this Geotechnical and Bridge Seismic Design Workshop provides a forum for information dissemination. The main objective of the workshop is to present a methodology for the geotechnical and structural seismic design of bridge systems in the New Madrid Seismic Zone based on the recent research findings. The new methodology addresses the uniqueness of earthquake motions (near field and directivity), as well as the effects of deep soil stratigraphy on the seismic response in the New Madrid Seismic Zone. Participants in the workshop will apply this methodology to re-design an existing highway bridge in the vicinity of the New Madrid Seismic Zone.

This workshop is sponsored by the Federal Highway Administration (FHWA), the Missouri Department of Transportation (MoDOT), and the University Transportation Center at UMR; their support is greatly appreciated. The findings and opinions expressed in a series of presentations during the workshop reflect only those of the authors and do not necessarily represent those of the sponsors.

The investigators of the research project all contributed to the organization of this workshop by providing their inputs related to technical contents. The logistics of the workshop were coordinated by Ms. Victoria Bañales from the Continuing Education at UMR. The workshop was administrated by the Workshop Steering Committee, which consisted of Dr. Neil Anderson (Co-Chair), Dr. Genda Chen (Co-Chair), Peter Clogston (FHWA), Thomas Fennessey (MoDOT), and Timothy Chojnacki (MoDOT).

Genda Chen, Ph.D., P.E.
Associate Professor of Civil Engineering at UMR
Technical Director of the UMR Earthquake Hazard Mitigation Research Program

Neil Anderson, Ph.D.
Professor of Geology and Geophysics at UMR
Principal Investigator of the UMR Earthquake Hazard Mitigation Research Program

WORKSHOP PROGRAM

Thursday, October 28, 2004, State/Delta Room

7:45 – 8:30 am	Registration
8:30 – 8:45 am	Introduction (Drs. Neil Anderson/Genda Chen)
8:45 – 9:30 am	Earthquake loss estimation of St. Louis transportation highway system (Dr. Ronaldo Luna)
9:30 – 10:00 am	Post-earthquake condition assessment of RC structures: Part 1 cable sensor and Part 2 microwave technology (Dr. Genda Chen)
10:00 – 10:15 am	Coffee break
10:15 – 10:45 am	Recommended LRFD guidelines for the seismic design of highway bridges (Dr. Phillip Yen)
10:45 – 11:30 am	Seismic design procedure of highway bridges – an overview (Mr. Thomas Fennessey/Anousone Arounpradith)
11:30 – 12:00 pm	General geologic setting and seismicity of the FHWA project site in the New Madrid Seismic Zone (Mr. David Hoffman)
12:00 – 1:00 pm	Lunch
1:00 – 2:00 pm	Synthetic near-field rock motions in the New Madrid Seismic Zone (Dr. Genda Chen)
2:00 – 3:00 pm	Geotechnical site characterization (Drs. Neil Anderson/Richard Stephenson)
3:00 – 3:15 pm	Coffee break
3:15 – 4:00 pm	Site response analysis including liquefaction (Dr. Ronaldo Luna)
4:00 – 4:30 pm	Seismic performance of embankments (Dr. Richard Stephenson)
5:00 – 6:00 pm	Happy hour (Hayward Baker)
6:00 – 7:30 pm	Dinner Dinner Speech: brief overview of seismic threat posted by the New Madrid Seismic Zone (Dr. David Rogers)

Friday, October 29, 2004, State/Delta Room

8:00 – 8:45 am	Soil-pile-structure interaction – geotechnical aspects (Dr. Ronaldo Luna)
8:45 – 9:30 am	Bridge response to near-field ground motions (Dr. Genda Chen)
9:30 – 10:30 am	Seismic evaluation and retrofit of beam-column joints of Mid-America bridges: Part 1 carbon fiber reinforced polymer retrofit and Part 2 steel sheet and plate retrofit (Drs. Genda Chen/Pedro Silva)
10:30 – 10:45 am	Coffee break
10:45 – 11:15 am	Seismic design issues of long-span bridges (Mr. Steve Hague)
11:15 – 11:30 am	Closure (Dr. Genda Chen)
11:45 am –	Site visit – Bill Emerson Memorial Bridge (Mr. Steve Hague)

TABLE OF CONTENTS

PRESENTATION 1

INTRODUCTION

INTRODUCTION

Genda Chen, Ph.D., P.E.
Associate Professor of Civil Engineering
University of Missouri-Rolla (UMR)
gchen@umr.edu

Geotechnical and Bridge Seismic Design Workshop
New Madrid Seismic Zone Experience

October 28-29, 2004, Cape Girardeau, Missouri

UMR Earthquake Hazard Mitigation Research Program for Highway Systems

February 2002 – February 2005

Principal Investigator: Dr. Neil Anderson
Technical Director: Dr. Genda Chen, P.E.
Project Manager (FHWA): Dr. Phillip W. Yen, P.E.
Project Coordinator (MoDOT): Thomas Fennessey, P.E.

Collaboration

Project Funding

- **Total funding: $1,432,758**
  - $800,000 - Federal Highway Administration (Cooperative Agreement DTFH61-02-X-00009)
  - $197,271 - Missouri Department of Transportation (in-kind plus cash)
  - $110,000 - Alaska Department of Transportation
  - $4,000 - Missouri Department of Natural Resources (in kind)
  - $70,035 – University Transportation Center
  - $251,452 - University of Missouri-Rolla (in-kind)

List of Participants

- **UMR Faculty:**
  - Dr. Neil Anderson (Principal Investigator)
  - Dr. Genda Chen (Technical Director)
  - Dr. David Enke
  - Dr. Ronaldo Luna
  - Dr. Shamsher Prakash
  - Dr. David Rogers
  - Dr. Pedro Silva
  - Dr. Gary Spring
  - Dr. Richard Stephenson
  - Dr. Reza Zoughi
- **MODOT:**
  - Tom Fennessey
  - Paul Porter/Bryan Hartnagel
  - Carlis Callahan
- **MODNR:**
  - David Hoffmann
- **FHWA Regional Office**
  - Peter Clogston
- **St. Louis University:**
  - Dr. Robert Herrmann
- **University of Nevada at Reno**
  - Dr. Yuehua Zeng
- **Russian Scientist:**
  - Dr. Alexi A. Malovichko
- **Postdoctoral Research Associate:**
  - Dr. Mostafa Engebawy
  - Dr. Siasi Kociu
- **UMR Graduate Students:**
  - Don Deardorff/ Bill Lawrence /Chakkaphan Tirasirichai/Sripathy Kitta
  - Xiaofei Ying/Wenjian Wang
  - Wei Zheng/Wanxing Liu
  - Nick Ereckson/ Xi Huang

Overall Objectives

- To improve earthquake resistance and mitigate earthquake damage to highway transportation networks, including loss of bridges and highways, by developing new seismic design and assessment methodologies, by improving seismic retrofitting measures, and by exchanging and transferring new technologies.

Element Interaction

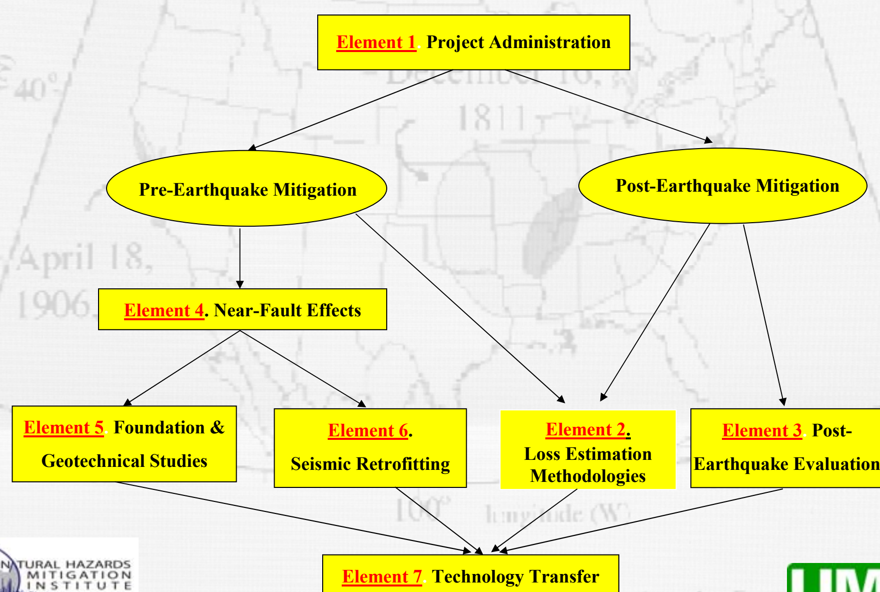

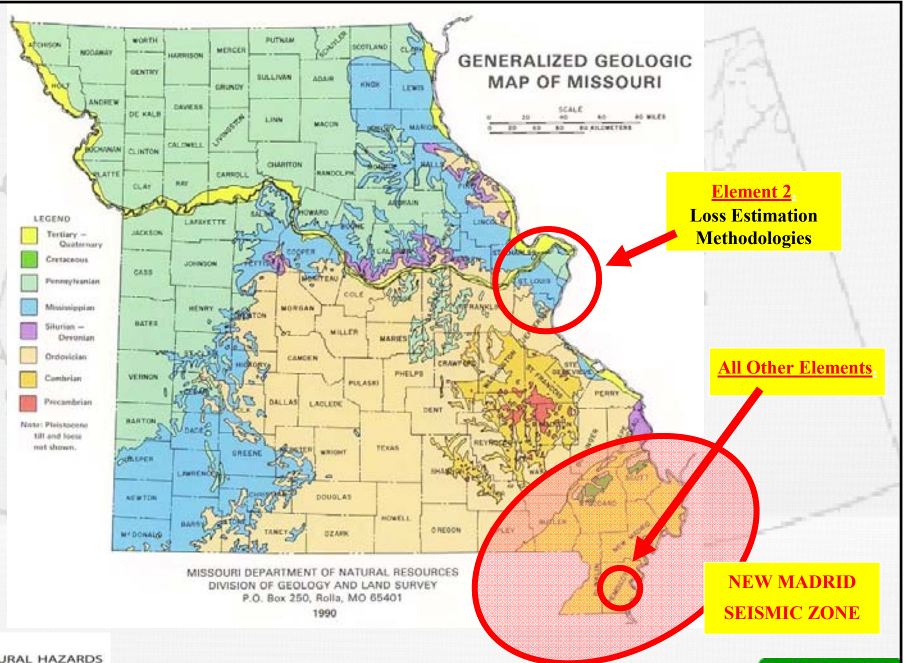

PRESENTATION 2

EARTHQUAKE LOSS ESTIMATION OF St. LOUIS TRANSPORTATION HIGHWAY SYSTEM

EARTHQUAKE LOSS ESTIMATION OF St. LOUIS TRANSPORTATION HIGHWAY SYSTEM

Ronaldo Luna, Ph.D., P.E.
Associate Professor of Civil Engineering
University of Missouri-Rolla (UMR)

Geotechnical and Bridge Seismic Design Workshop
New Madrid Seismic Zone Experience

October 28-29, 2004, Cape Girardeau, Missouri

NATURAL HAZARDS MITIGATION INSTITUTE

UMR
UNIVERSITY OF MISSOURI-ROLLA

EARTHQUAKE LOSS ESTIMATION OF St. LOUIS TRANSPORTATION HIGHWAY SYSTEM

Investigators (alphabetical order):

Genda Chen
Don Deardorff
Dave Enke
Dave Hoffman
Sripathy Jitta
Siasi Kociu
Bill Lawrence
Ronaldo Luna (Lead)
Gary Spring
Chakkaphan Tirasirichai
Ed Wang

NATURAL HAZARDS MITIGATION INSTITUTE

UMR
UNIVERSITY OF MISSOURI-ROLLA

Presentation Outline

- Goals & Objectives
- Project Timeline
- EQ Loss Estimation Methodology
- Scenarios & Results
- Summary
- Questions/Comments

FHWA Goal

- Develop or adopt an earthquake loss estimation procedure for earthquake damage to the highway system
  - Includes direct and indirect losses
- Demonstrate the methodology in the NMSZ area

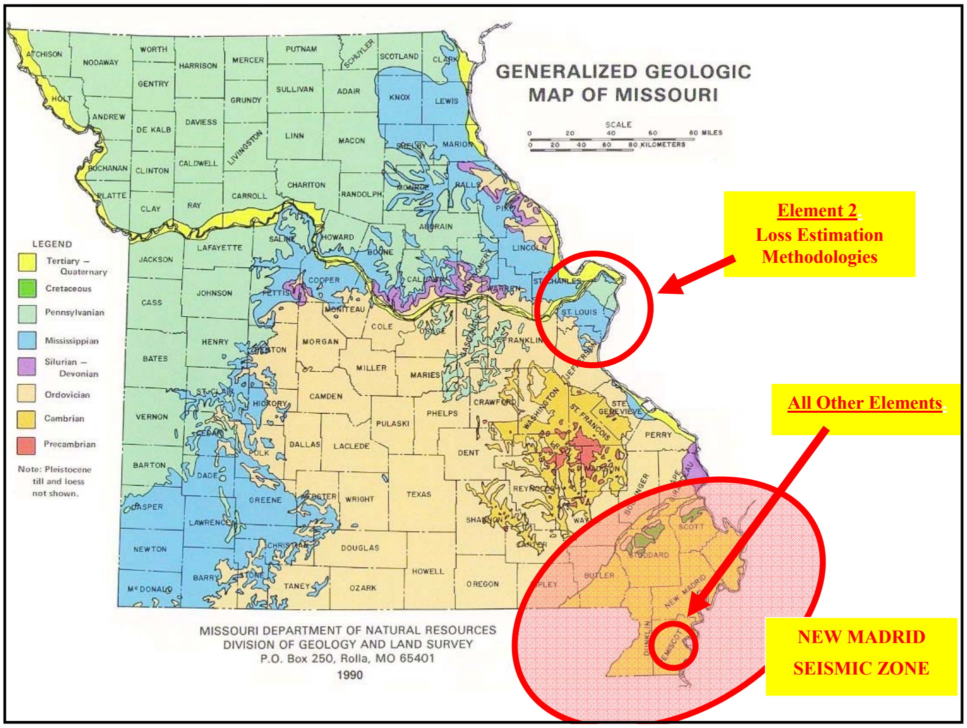
GENERALIZED GEOLOGIC MAP OF MISSOURI
Element 2
Loss Estimation Methodologies
All Other Elements
NEW MADRID SEISMIC ZONE
LEGEND
Tertiary – Quaternary
Cretaceous
Pennsylvanian
Mississippian
Silurian – Devonian
Ordovician
Cambrian
Precambrian
Note: Pleistocene till and loess not shown.
MISSOURI DEPARTMENT OF NATURAL RESOURCES
DIVISION OF GEOLOGY AND LAND SURVEY
P.O. Box 250, Rolla, MO 65401
1990

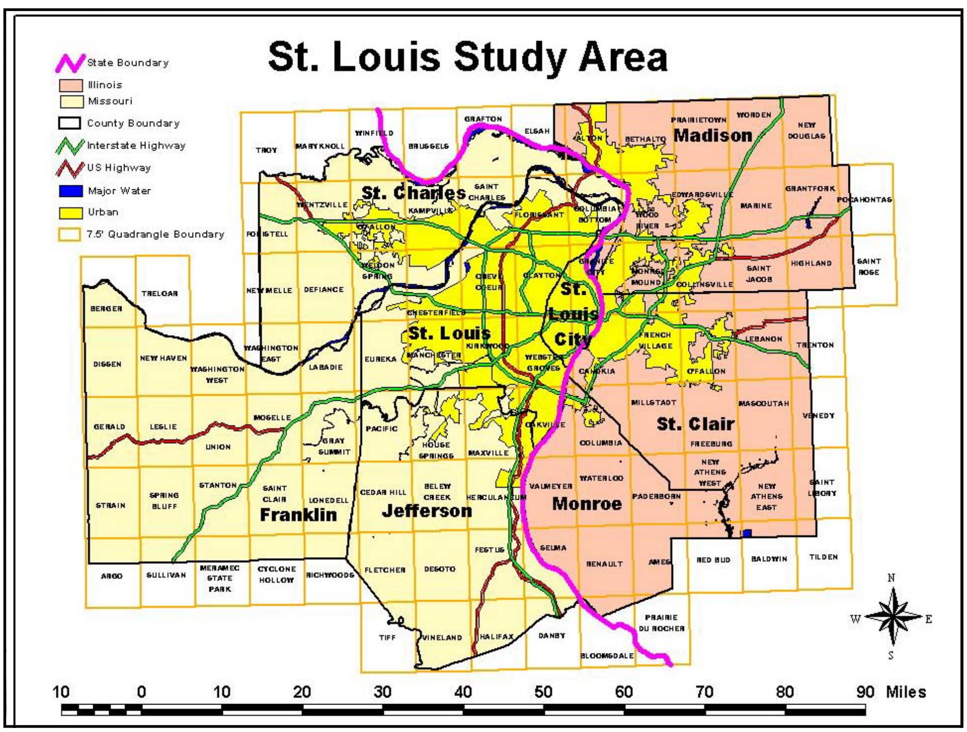
St. Louis Study Area
State Boundary
Illinois
Missouri
County Boundary
Interstate Highway
US Highway
Major Water
Urban
7.5' Quadrangle Boundary
Madison
St. Charles
St. Louis
St. Louis City
St. Clair
Franklin
Jefferson
Monroe
10 0 10 20 30 40 50 60 70 80 90 Miles

Previous Work

- No previous EQ Loss Estimation for any major metropolitan area in Missouri.
- MAE Center has looked at regional larger interstate network.
- Memphis Study: REDARS (Werner, et al., 2000)
- California: Los Angeles & San Francisco

EQ Loss Estimation Methodology

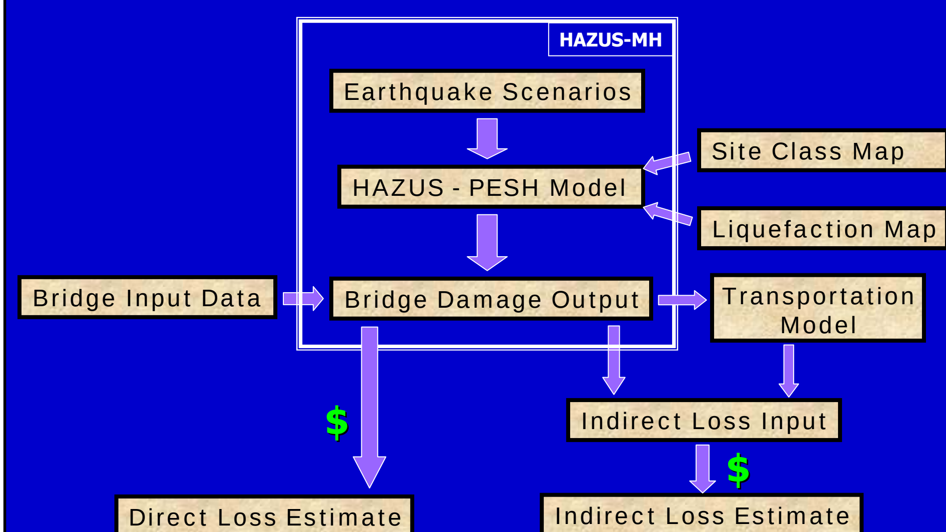

HAZUS – MH

Hazards US – Multi-Hazards

HAZUS-MH

- Software developed by FEMA under a contract with the National Institute of Building Sciences (NIBS) and their contractors.
- GIS driven software that manipulates maps and databases to estimate losses.
- 1997 → 1999 → 2004 (MH)
- Floods, Hurricanes & Earthquakes.

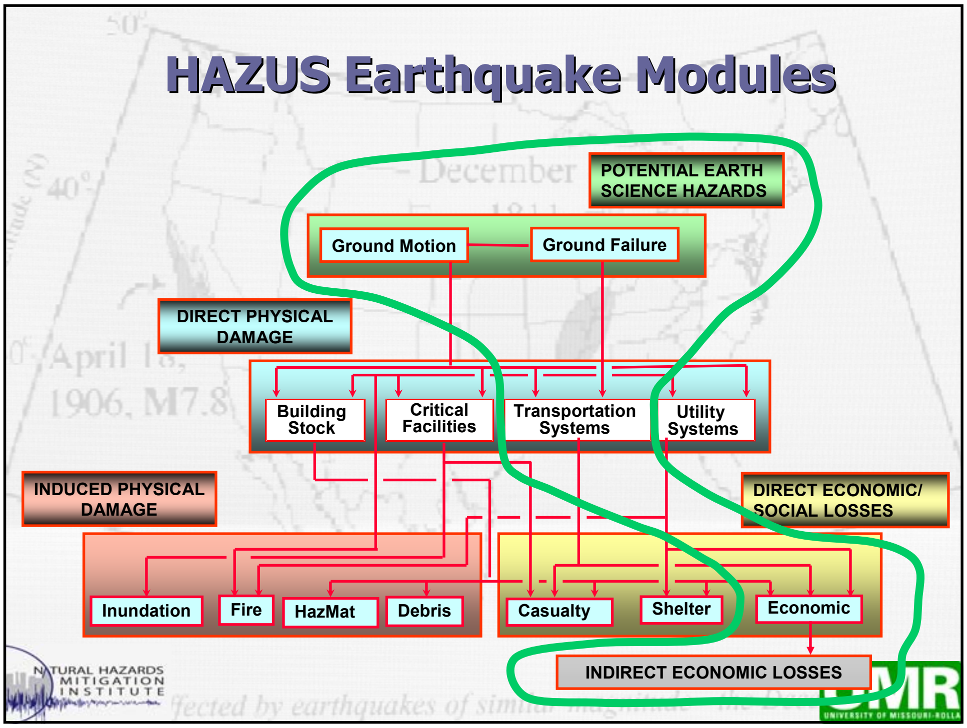
HAZUS Earthquake Modules
POTENTIAL EARTH SCIENCE HAZARDS
Ground Motion
Ground Failure
DIRECT PHYSICAL DAMAGE
Building Stock
Critical Facilities
Transportation Systems
Utility Systems
INDUCED PHYSICAL DAMAGE
DIRECT ECONOMIC/ SOCIAL LOSSES
Inundation
Fire
HazMat
Debris
Casualty
Shelter
Economic
INDIRECT ECONOMIC LOSSES
NATURAL HAZARDS MITIGATION INSTITUTE
UMR
UNIVERSITY OF MISSOURI-ROLLA

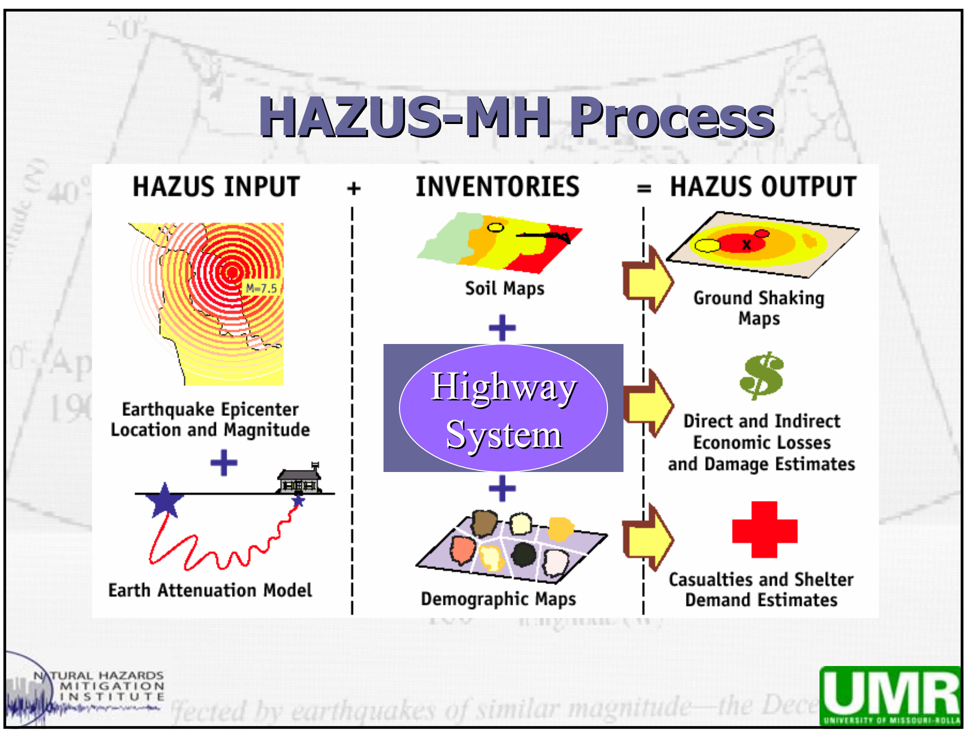
HAZUS-MH Process
HAZUS INPUT
+
INVENTORIES
=
HAZUS OUTPUT
M=7.5
Earthquake Epicenter Location and Magnitude
+
Earth Attenuation Model
Soil Maps
+
Highway System
+
Demographic Maps
Ground Shaking Maps
Direct and Indirect Economic Losses and Damage Estimates
Casualties and Shelter Demand Estimates
NATURAL HAZARDS MITIGATION INSTITUTE
UMR
UNIVERSITY OF MISSOURI-ROLLA

Three Levels of Usage

1. Default Databases: limited use due to site and bridge databases are based on national databases - not much detail data.
2. Modified Databases: to include local site effects and infrastructure, customized databases are used (requires significant user input).
3. Third party model integration to study special conditions.

NATURAL HAZARDS MITIGATION INSTITUTE

UMR UNIVERSITY OF MISSOURI-ROLLA

HAZUS-MH in this study

- Deterministic earthquake scenarios.
- PESH model developed distribution of PGA based on 2002 USGS attenuation relationships – database extended to include distances >200mi.
- Losses estimated based on 2002 $ value
- Site class & liquefaction maps developed
- Latest NBI adjusted for local bridges.

NATURAL HAZARDS MITIGATION INSTITUTE

UMR UNIVERSITY OF MISSOURI-ROLLA

HAZUS-MH within Study

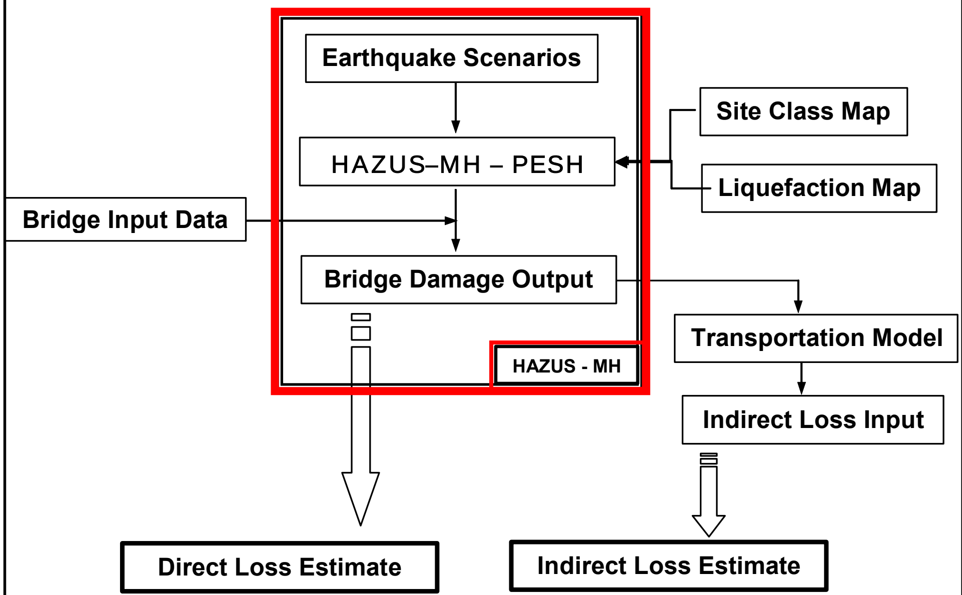

Transportation Model

UTMS

Transportation Model

- Urban Transportation Modeling System (UTMS) software used for planning.
- East-West Gateway Council (St. Louis) Transportation model – calibrated 2002
- MinUTP: trip generation, distribution and network assignment, given the user prepared link data, zone data, and friction factor data sets .

Four-step UTMS method

1. People decide to make a trip (generation)
2. Decide where to go (distribution)
3. Decide what mode to take (modal split)
4. Decide what route to use (assignment)

UTMS remains the standard modeling tool for the vast majority of metropolitan areas around the world, a wide variety of commercially available software packages is available to support UTMS-based modeling.

Earthquake Scenarios

for St. Louis, MO

Earthquake Scenarios

- Initially focused on the far field condition due to recently revised and released USGS National Seismic Hazard Maps (March 6, 2002)
- Most of the 2002 changes were for short period bridges near the 0.2 sec, not much change for longer period near 1 sec.
- Deterministic, historic, prehistoric and probabilistic methods used.
- Focused on geologic evidence worst case scenario.

Earthquake Scenarios - Missouri & Illinois

Name of EQ Source Zone	Source Zone Fault or Structure	Dist. From STL (miles)	M	Evidence for EQ source	Most recent EQ. (yrs BP)	Refs. ★
Arnold, Missouri	Unknown	18	5.2	Paleo-iquefaction features	< 2750	A, B, C
Germantown, Illinois	**Unknown**	**38**	**7.0**	**Paleo-liquefaction features**	**< 6,500**	**A, C**
Centralia, Illinois	Unknown -	56	7.5	Paleo-liquefaction features	< 6,500	A, C, D
Vincinnes, Indiana	Wabash Valley fault zone	146	7.5	Paleo-liquefaction features	6,100	C, E, F
New Madrid, Missouri	**New Madrid seismic zone**	**148**	**7.7**	**Historic earthquakes and paleo-liquefaction features**	**107**	**C, G**
St. Louis, Missouri	**USGS background seismicity**	**0**	**7.0**	**None - assumed possible anywhere in the Central U.S. inboard "craton" zone**	**Unknown**	**G**

NATURAL HAZARDS MITIGATION INSTITUTE

UMR UNIVERSITY OF MISSOURI-ROLLA

ST. LOUIS AREA MISSOURI AND ILLINOIS EARTHQUAKE SCENARIO SOURCE AREAS

References

Summary of EQ Input Parameters

Name Earthquake Scenario	Lat. (d,d)	Long. (d,d)	M_m	Epicenter Depth (km)	Attenuation Relationship
1. St. Louis, MO	38.63	-90.2	7.0	10	Project 2000 East
2. Germantown, IL	38.56	-89.5	7.0	10	Project 2000 East
3. New Madrid, MO	36.55	-89.54	7.7	10	Frankel (1996)

NATURAL HAZARDS MITIGATION INSTITUTE

UMR UNIVERSITY OF MISSOURI-ROLLA

PGA – Germantown EQ with bridge inventory

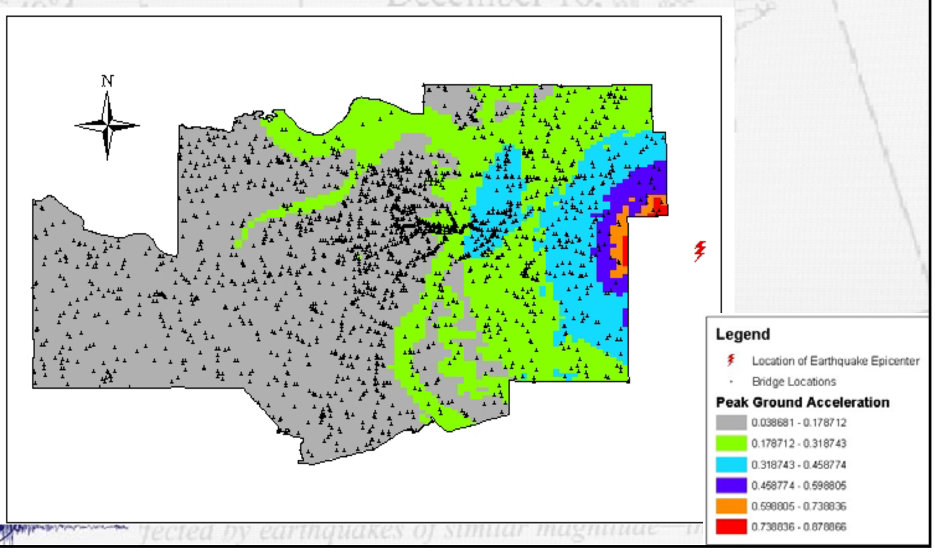

Site Class – GMA

- Ground Motion Amplification (GMA)
  - simplified site response factors based on amplification factors - NEHRP 1997.
- GIS maps were based on data from MoDNR and IGS for this purpose.
- USGS NEHRP is in the process to develop new maps for St. Louis including site specific data (available from geotechnical community and research projects).

NATURAL HAZARDS MITIGATION INSTITUTE

UMR UNIVERSITY OF MISSOURI-ROLLA

Liquefaction distribution

- A separate liquefaction potential map for Missouri and Illinois was prepared for use in a GIS HAZUS environment.
- A lateral spreading potential map was prepared as an area around the river channels, but areas are too small to be seen at a map scale suitable for page size.

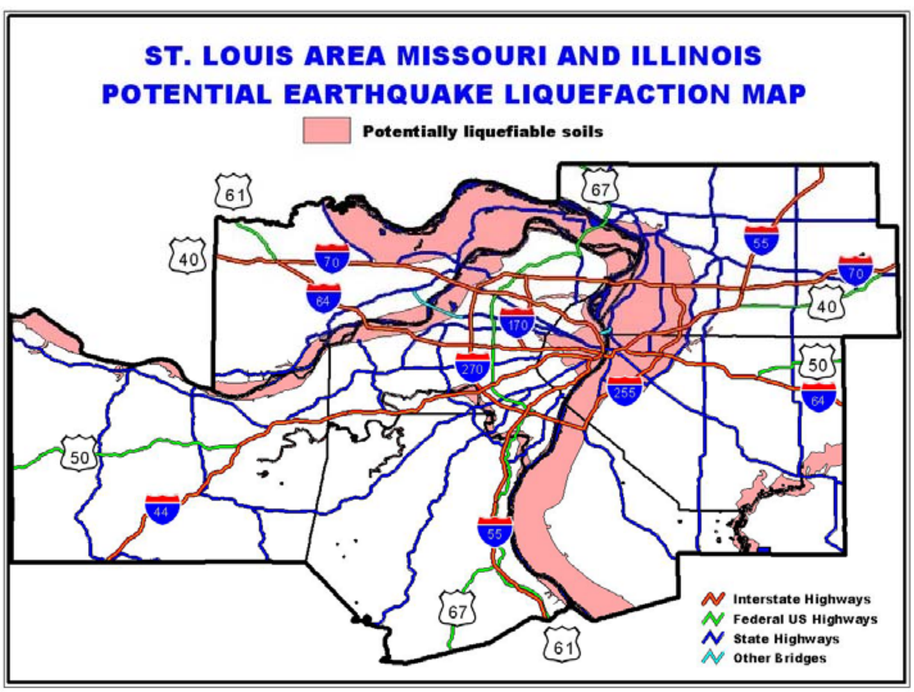

Bridge Inventories

- Major highways in the area include Interstates 70, 170, 270, 44, 55, 64 and Highway 67.
- National Bridge Inventory (NBI) produced by the Federal Highway Administration, Office of Bridge Technology.
- State DOT sources

Major MO/MS Rivers Bridges

Structure (NBI Item 8)	County (NBI Item 3)	Feature Intersected (NBI Item 6a)	Facility Carried (NBI Item 7)	Year Built (NBI Item 27)	1999 ADT (NBI Item 29,30)	Structure Length (NBI Item 49, m)
A40171 2	St. Charles	MISSOURI RIVER	US 40 (E)	1991	39969	796.7
A5585 4	St. Charles	MISSOURI RVR	MO 364	1999	72400	986.9
A4557 2	St. Charles	MISSOURI RVR	MO 370 (N)	1992	9532	1053.1
A4557 3	St. Charles	MISSOURI RVR	MO 370 (S)	1993	9532	1053.1
J10004 3	St. Charles	MISSOURI RVR	US 40 (W)	1935	39463	796.7
A3047 4	St. Charles	MISSOURI RVR	US 67	1979	32567	848.3
A4278 4	St. Charles	MISSISSIPPI RVR	US 67	1994	28565	1408.2
A3292R 2	St. Louis	MISSOURI RIVER	IS 70 (E)	1978	143463	1155.8
L05617 3	St. Louis	MISSOURI RVR	IS 70 (W)	1958	87752	1244.5
A1850 3	St. Louis	MISSISSIPPI RVR	IS 255 (W)	1985	28859	1220.1
A4936 2	St. Louis	MISSISSIPPI RVR	IS 255	1990	26393	1220.1
A 890 4	St. Louis City	MISSISSIPPI RVR	IS 270	1964	52299	824.8
A4856 1	St. Louis City	MISSISSIPPI RVR	MO 770	1900	41076	1222.2
A1500R3 4	St. Louis City	MISSISSIPPI RVR	IS 70	1963	149848	659.9
K09691 1	Franklin	MISSOURI RVR	MO 47	1934	8811	780.9

(Source: 2001 NBI by FHWA)

Multiple Bridge databases

Bridge Inventory	Media	Date Updated	Inventory Items
MoDOT GIS	GIS	2001	45
MoDOT District 6 (1)	Database	1999	6
MoDOT District 6 (2)	Database	2002	6
Illinois ISIS/SIMS	GIS/Database	2003	170
FEMA's HAZUS-MH	GIS/Database	2001	25
FHWA's NBI	GIS/Database	2002	116

NATURAL HAZARDS MITIGATION INSTITUTE

UMR UNIVERSITY OF MISSOURI-ROLLA

Multiple Bridge databases

Bridge Inventory	Media	Date Updated	Inventory Items
MoDOT GIS	GIS	2001	45
MoDOT District 6 (1)	Database	1999	6
MoDOT District 6 (2)	Database	2002	6
Illinois ISIS/SIMS	GIS/Database	2003	170
FEMA's HAZUS-MH	**GIS/Database**	**2001**	**25**
FHWA's NBI	GIS/Database	2002	116

NATURAL HAZARDS MITIGATION INSTITUTE

UMR UNIVERSITY OF MISSOURI-ROLLA

HAZUS-MH and NBI

- HAZUS-MH Release 28-D incorporates:
  - 2,645 bridges
  - 771 road segments
- into its database for the region of study selected for this project.
- 28 Bridge classes.
- 2001 NBI data set.

Items in HAZUS-MH bridge inventory

(Adapted from FEMA Metadata for HAZUS-MH Release 28-D.)

Item Name	Description
Highway Bridge Id	HAZUS-MH Internal ID
Bridge Class	Analysis Class
Tract	Census Tract
Name	Bridge Name
Owner	Bridge Owner
Bridge Type	Structure Type
Width	Bridge Width (m)
Number of Spans	Number of Spans
Length	Total Bridge Length (m)
Max Span Length	Maximum Span Length (m)
Skew Angle	Skew Angle (degrees)
Seat Length	Seat Length (m)
Seat Width	Seat Width (m)

Item Name	Description
Year Built	Year Bridge Was Built
Year Remodeled	Year Bridge Remodeled
Pier Type	Pier Type
Foundation Type	Foundation Type
Scour Index	Scour Index
Traffic	Daily Traffic (cars/day)
Traffic Index	Traffic Index
Condition	General Condition Rating
Cost	Replacement Cost (thous. $)
Latitude	Latitude of Bridge
Longitude	Longitude of Bridge
Comment	Misc. Comments

Direct Losses

Direct Losses

The cost to repair a bridge back to 100% capacity after incurring damage due to an earthquake event.

"Direct economic losses are computed based on:

(1) probabilities of being in a certain damage state,

(2) the replacement value of the component, and

(3) damage ratios for each damage state.

Economic losses are evaluated by multiplying the compounded damage ratio by the replacement value, where the compounded damage ratio is computed as the probabilistic combination of damage ratios." [HAZUS-MH (2002) Technical Manual, Pg. 15-31]

Number of Bridges Damaged St. Louis Earthquake, M=7.0

Probability of Occurrence	Initial Damage State				
	Complete	Exceed Extensive	Exceed Moderate	Exceed Slight	None
=1.0	0	0	0	0	81
≥0.75	29	163	216	367	1448
≥0.50	188	469	564	732	1913
≥0.25	521	836	997	1197	2278
>0	2216	2423	2480	2564	2645
≥0	2645	2645	2645	2645	2645

NATURAL HAZARDS MITIGATION INSTITUTE

UMR UNIVERSITY OF MISSOURI-ROLLA

Number of Bridges Damaged Germantown Earthquake, M=7.0

Probability of Occurrence	Initial Damage State				
	Complete	Exceed Extensive	Exceed Moderate	Exceed Slight	None
=1.0	0	0	0	0	81
≥0.75	0	0	2	232	2427
≥0.50	0	9	50	103	2542
≥0.25	9	112	155	218	2613
>0	1483	1999	2146	2239	2645
≥0	2645	2645	2645	2645	2645

NATURAL HAZARDS MITIGATION INSTITUTE

UMR UNIVERSITY OF MISSOURI-ROLLA

Number of Bridges Damaged
New Madrid Earthquake, M=7.7

Probability of Occurrence	Initial Damage State				
	Complete	Exceed Extensive	Exceed Moderate	Exceed Slight	None
=1.0	0	0	0	0	13
≥0.75	0	0	0	0	2494
≥0.50	0	0	5	58	2587
≥0.25	0	29	67	151	2645
>0	1738	2306	2471	2632	2645
≥0	2645	2645	2645	2645	2645

NATURAL HAZARDS MITIGATION INSTITUTE

UMR UNIVERSITY OF MISSOURI-ROLLA

Replacement Value for Bridges

System	Replacement Value ($ thousands)	Label	Component Classification
Highway	20,000	HWB1 / HWB2	Major Bridges
	5,000	HWB8, 9, 10, 11, 15, 16, 20, 21, 22, 23, 26, 27	Continuous Bridges
	1,000	HWB3, 4, 5, 6, 7, 12, 13, 14, 17, 18, 19, 24, 25, 28	Other Bridges

NATURAL HAZARDS MITIGATION INSTITUTE

UMR UNIVERSITY OF MISSOURI-ROLLA

Direct Economic Loss Estimate for Bridges at select EQ Scenarios

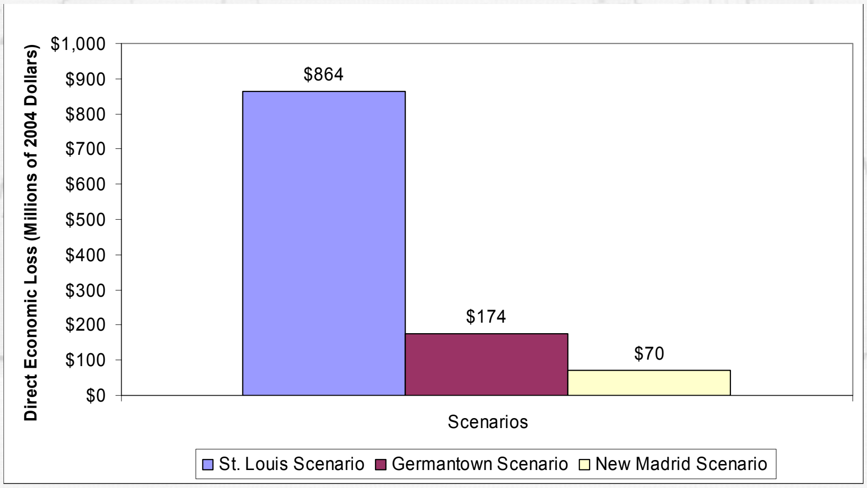

NATURAL HAZARDS MITIGATION INSTITUTE

UMR UNIVERSITY OF MISSOURI-ROLLA

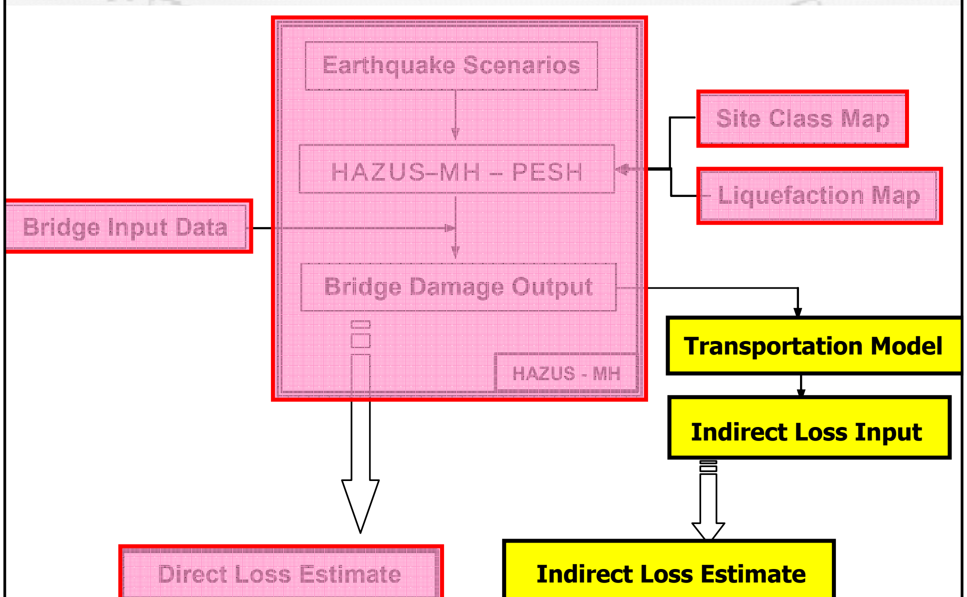

MITIGATION INSTITUTE

UMR UNIVERSITY OF MISSOURI-ROLLA

Transportation Modeling

St. Louis, MO

Transportation Modeling

- EWG provided transportation data, transportation data models, and results (forecasts) for the years of 2000, 2004, and 2010.
- The 2004 calibrated network was modified to represent each earthquake damage scenario.

Loading the Network

- St. Louis regional travel demand model covers the entire eight-county metropolitan area.
- The metropolitan area is divided in a series of traffic analysis zones (TAZ) with different demographic characteristics.
- The TAZs generate the corresponding travel trips from zone to zone
- These trips load the highway network - in addition to the trips coming into the study area.

NATURAL HAZARDS MITIGATION INSTITUTE

UMR UNIVERSITY OF MISSOURI-ROLLA

Transportation Analysis Zones

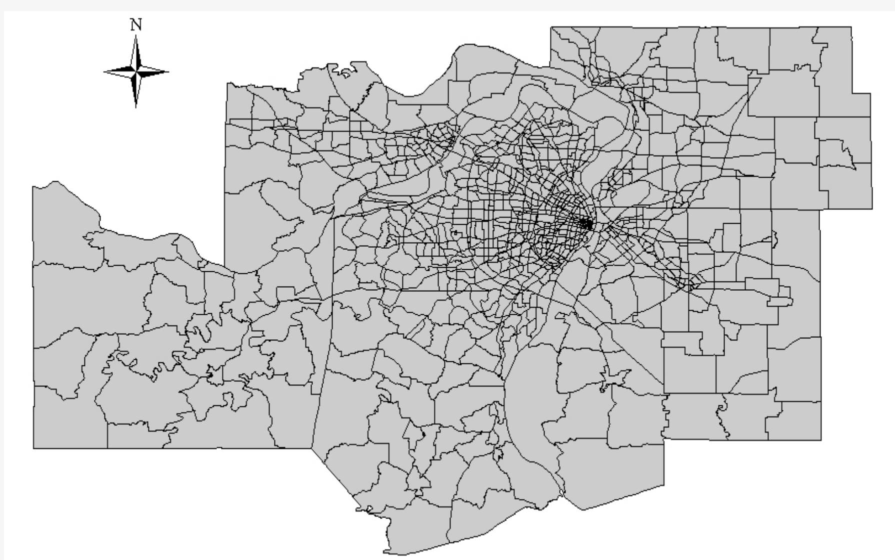

The St. Louis Road Network

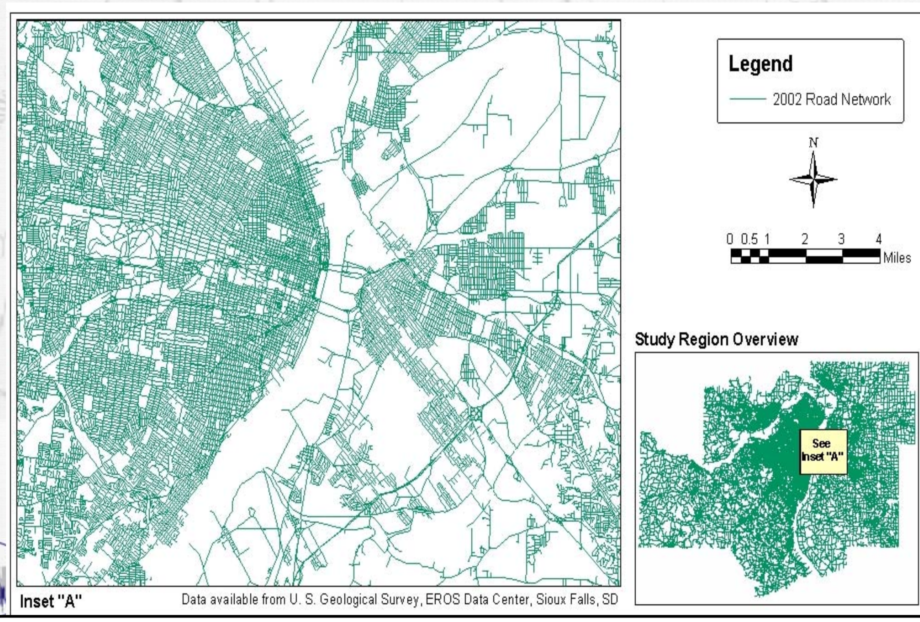

Network Model (link-nodes)

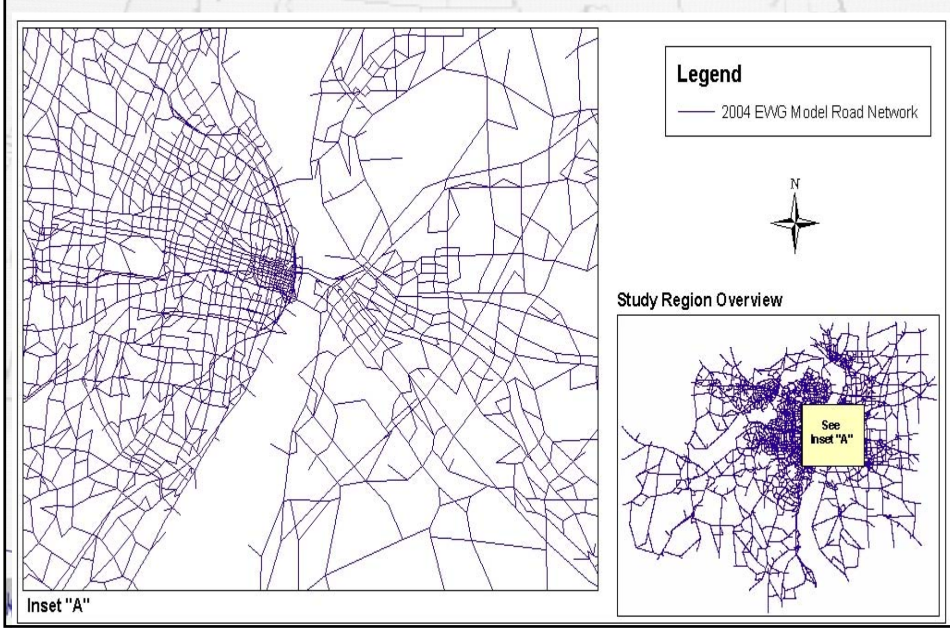

Transitions from HAZUS

1. HAZUS-MH output data interpretation,
2. Data preparation,
3. Model implementation and runs,
4. Output interpretation.

Model Link Removal

Scenario (2004)	@ Time (days)	No. Bridges from HAZUS 99/MH Output	No. Bridges Selected for EWG Runs	No. Links on EWG Model Altered
New Madrid	1	60	32	33
New Madrid	30	60	32	33
New Madrid	90	60	32	33
New Madrid	250	60	32	33
Germantown	1	50	17	19
Germantown	30	50	17	19
Germantown	90	50	17	19
Germantown	250	50	17	19
Germantown	400	50	17	19
St. Louis	1	29	23	19
St. Louis	30	29	23	19
St. Louis	90	29	23	19
St. Louis	250	29	23	19
St. Louis	350	29	23	19
St. Louis	400	29	23	19

Probability of Complete Damage ≥ 75% for a St. Louis M 7.0

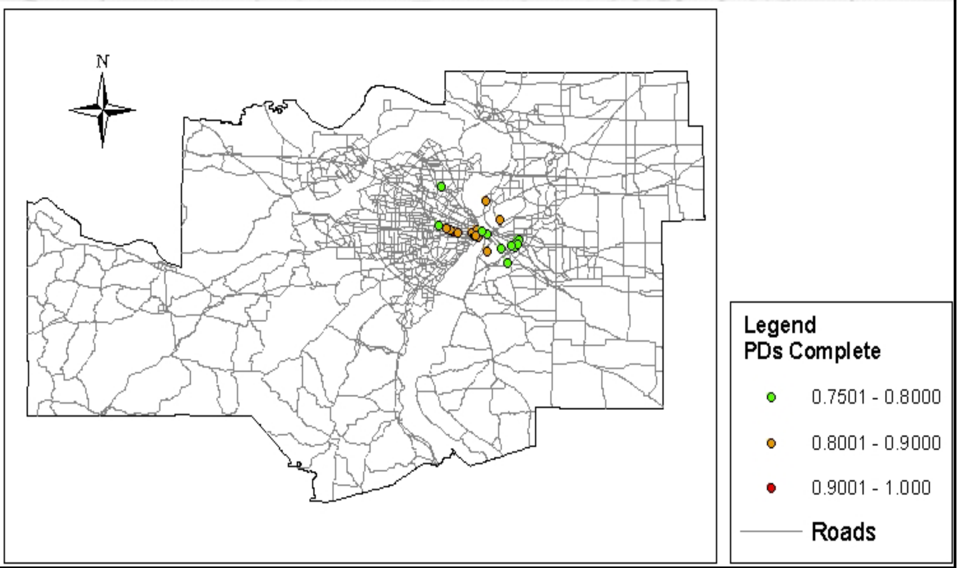

Probability of Moderate Damage ≥ 50% for a Germantown M 7.0

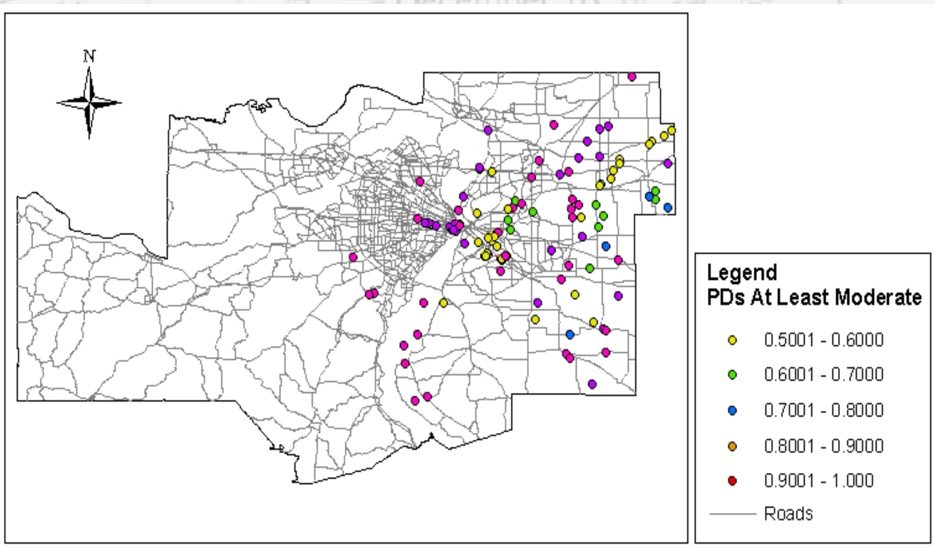

Probability of Moderate Damage ≥ 30% for a New Madrid M 7.7

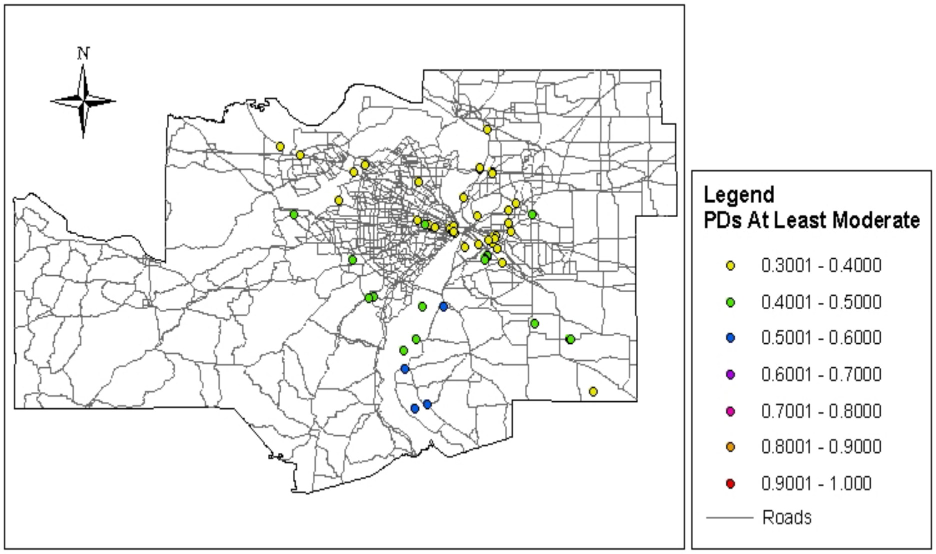

How HAZUS defines functionality

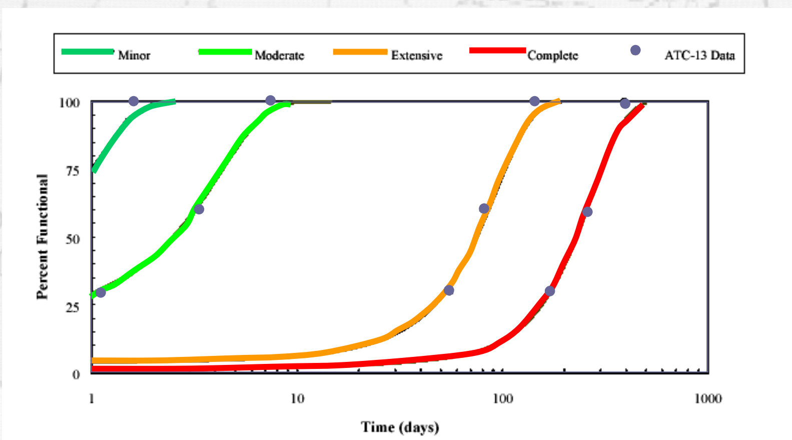

After ATC 13 (1985)

NATURAL HAZARDS MITIGATION INSTITUTE

UMR
UNIVERSITY OF MISSOURI-ROLLA

Model Runs at EW-Gateway

Idealistic Approach and with all the time in the world… we could do the following runs:

Earthquake Data			Functionality Approach - Reduced Capacities, Never Closed			
Scenario	Source	M	Functionality Curve (Multi-Point e.g. after 1,3,7,30,90,250 days)	Functionality Curve (4-Point e.g. after 1, 30, 90, 250 days)	Functionality Curve (2-Point e.g. after 1, 30 days)	Functionality Curve (1-Pt, 1 days)
1	St. Louis, MO	7.0	[redacted]	4	[redacted]	[redacted]
[redacted]	[redacted]	[redacted]	[redacted]	[redacted]	[redacted]	[redacted]
3	Germantown, IL	7.0	[redacted]	4	[redacted]	[redacted]
[redacted]	[redacted]	[redacted]	[redacted]	[redacted]	[redacted]	[redacted]
6	New Madrid, MO	7.7	[redacted]	4	[redacted]	[redacted]
	TOTAL NUMBER OF RUNS:		[redacted]	24	[redacted]	[redacted]
	TOTAL NUMBER OF EWGateway Meetings:		[redacted]	12	[redacted]	[redacted]

NATURAL HAZARDS MITIGATION INSTITUTE

UMR UNIVERSITY OF MISSOURI-ROLLA

Model Runs at EW-Gateway

- St. Louis Earthquake (M=7.0 & Dist=0 miles):
  - Removed bridges with P>0.75 (Day 0)
  - Modified bridge capacity according to HAZUS output using restoration curves (Day 30, 90 and 250).
- Germantown Earthquake (M=7.0 & Dist=38 miles)
  - Modified bridge capacity according to HAZUS output using restoration curves (Day 30, 90 and 250).
- New Madrid Earthquake (M=7.7 & Dist=148 miles)
  - Level of earthquake is too far away to cause damage in St. Louis. Attenuation functions in HAZUS control the results. The number of bridges affected is small.

NATURAL HAZARDS MITIGATION INSTITUTE

UMR UNIVERSITY OF MISSOURI-ROLLA

Indirect Losses

Analysis for Indirect Loss

- For each of the three scenarios, the MINUTP runs were created for days 1, 30, 90, and 250.
- The St. Louis and Germantown scenarios also included runs for day 350 and 400. These were not completed for the New Madrid run due to insignificant findings from the other 2 events at these times following the earthquake event.

Analysis for Indirect Loss

- The St. Louis run was created with day "1" links being completely removed from the EWG network, simulating the bridges being closed immediately following the earthquake event which is appropriate for bridges in the "complete" damage state.
- The runs for the Germantown and New Madrid earthquake events were made with day "1" links being reduced, but not removed, in order to simulate a reduced capacity while the bridge was still able to be used. This was more appropriate for the lesser damage states initially selected for the bridge selection in these events

Travel Time & Distance

- Another preparation for indirect loss estimates is the travel time delays and increased distance traveled by the public.
- This is computed in a matrix of all the trips generated by the network.
- The change in time and distance traveled is shown in the following charts.

Peak & Off-Peak Change in Travel Time

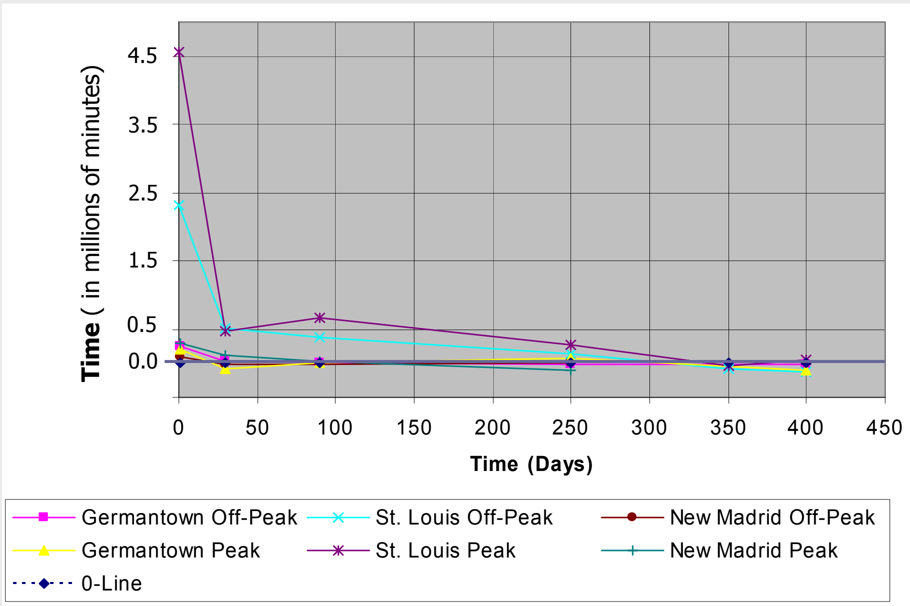

Peak & Off-Peak Change in Travel Distance

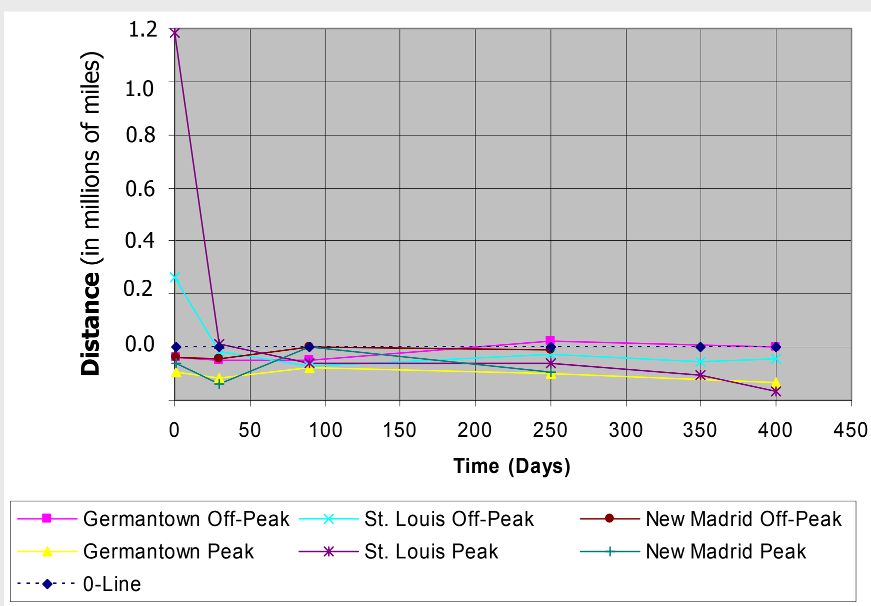

Indirect Losses - definition

Indirect economic loss will normally cover the economic loss to items not included in the normal restoration costs. Damage of the transportation network will incur an increase of transportation costs, lower productivity, among others. It is practically impossible to capture every indirect loss resulting from an earthquake by a single economic model.

Indirect Losses - definition

The indirect economic loss of this project is labeled as "Partial Indirect Economic Loss: The Impact on Highways for the Traveling Public". The definition of this partial indirect loss is defined as the expected financial loss that occurs from increases in transportation costs in the highway network.

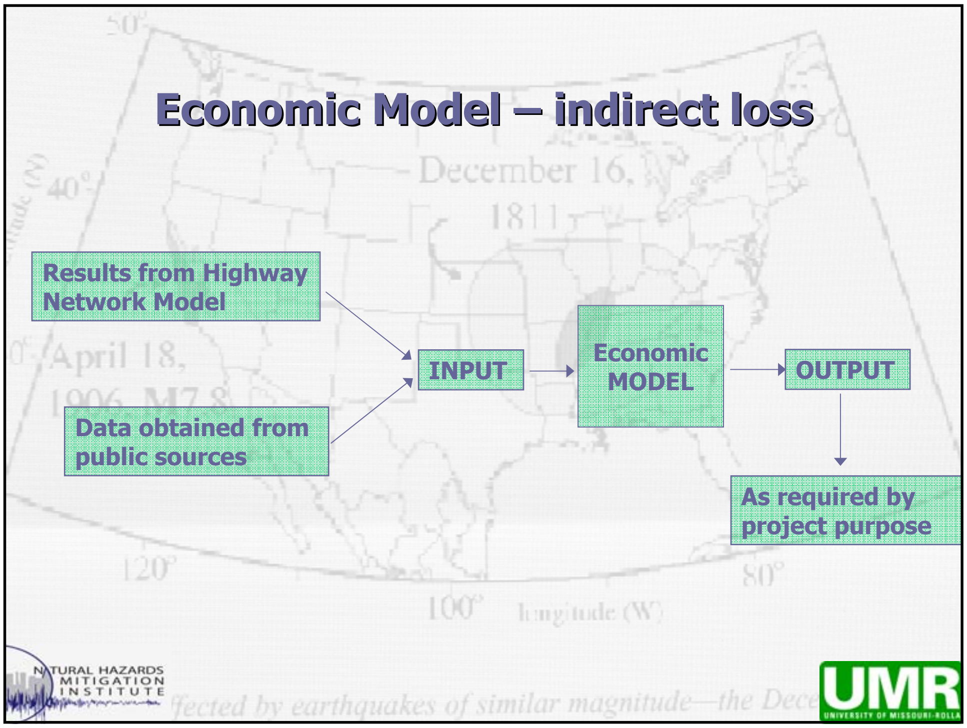
Economic Model – indirect loss
Results from Highway Network Model
Data obtained from public sources
INPUT
Economic MODEL
OUTPUT
As required by project purpose
NATURAL HAZARDS MITIGATION INSTITUTE
UMR
UNIVERSITY OF MISSOURI-ROLLA

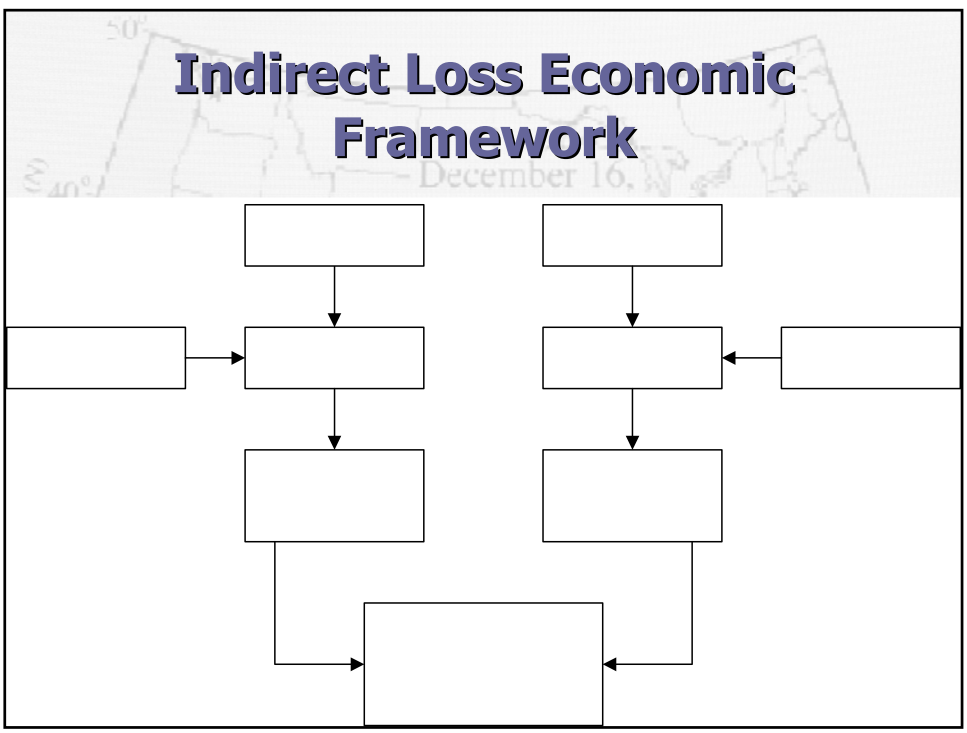
Indirect Loss Economic Framework

Formulation

$$\text{Total Partial Loss} = \sum_{i=1}^{n}\sum_{j=1}^{n} \text{Loss from increase travel time of route ij} +$$

$$\sum_{i=1}^{n}\sum_{j=1}^{n} \text{Loss from increase travel distance of route ij}$$

where: i = Route origin zone number

j = Route destination zone number

n = Total number of zones in the study area

NATURAL HAZARDS MITIGATION INSTITUTE

UMR UNIVERSITY OF MISSOURI-ROLLA

Commuting Trips

- Demographics will affect the value of the trips and are weighted accordingly.

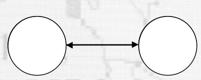	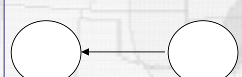	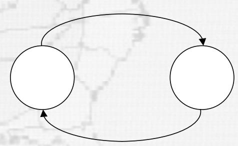
Trip of person in zone A from zone A to zone B	Trip of person in zone B from zone B to zone A	Trip of person in zone A from zone A to zone B and then his/her return trip from zone B to A

NATURAL HAZARDS MITIGATION INSTITUTE

UMR UNIVERSITY OF MISSOURI-ROLLA

Commercial Trips

- Those made by commercial freight.
- Divided into two categories:
  1. Trucks
  2. Tractor + Trailer

	Tractor & Trailer	Truck	Weighted
Value of Time Delayed (per hour)	$29.86	$26.97	$29.06
Value of Increased Distance (per km)	$0.76	$0.52	$0.70

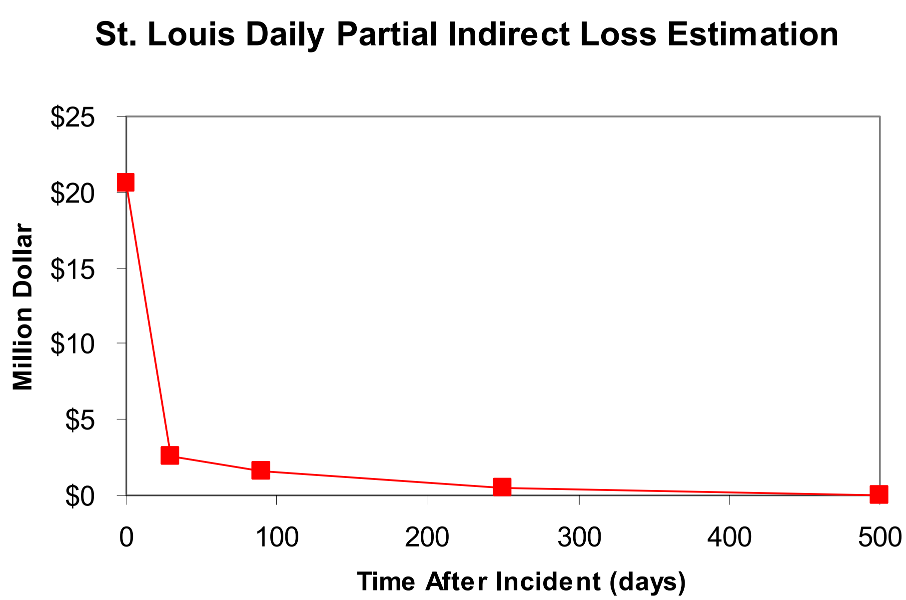

Partial Indirect Loss for Different Restoration Rate

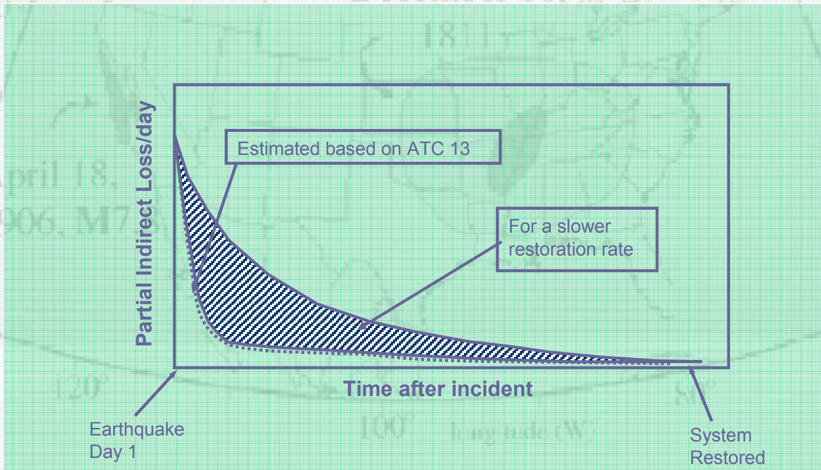

Summary & Conclusions

- The original objective to demonstrate that a loss estimate can be made for the St. Louis area was accomplished.
- Both direct and indirect losses have been calculated for select earthquake scenarios, including one in the NMSZ.

Summary & Conclusions (continued)

- HAZUS combined with transportation models can be used for earthquake loss estimation.
- Process is complex and tedious – a more streamlined software systems would ease this process, e.g., REDARS.
- Earthquake scenarios besides the NMSZ were considered for the St. Louis area.

Summary & Conclusions (continued)

- The geologic and soil conditions in St. Louis metro area contribute to the variability in ground motion.
- Large areas of liquefaction susceptibility increase the consequences for bridge damage.
- Most of the anticipated damage is on river crossings, old structures and on the Illinois side.

Summary & Conclusions (continued)

- Direct losses range from $70 to $800 million, depending on EQ scenario.
- Travel time delays and distance can be used to estimate a partial indirect loss.
- Partial indirect losses vary depending on the ability to restore the highway system– starting at $20 million/day at Day 1 and decreasing depending on the ability to restore transportation capacity.

NATURAL HAZARDS MITIGATION INSTITUTE

UMR UNIVERSITY OF MISSOURI-ROLLA

Summary & Conclusions (continued)

- Partial indirect losses over the entire period of highway network restoration could be $700 million, or higher depending on the ability to restore the transportation highway network.

NATURAL HAZARDS MITIGATION INSTITUTE

UMR UNIVERSITY OF MISSOURI-ROLLA

---------Appendix-------

- Following slides used in animations

> 75% Damage Map

- insert

Earthquake Scenarios Missouri & Illinois

Name of EQ Source Zone	Source Zone Fault or Structure	Dist. From STL (miles)	M	Evidence for EQ source	Most recent EQ. (yrs BP)	Refs. ★
Arnold, Missouri	Unknown	18	5.2	Paleo-iquefaction features	< 2750	A, B, C
Germantown, Illinois	Unknown	38	7.0	Paleo-liquefaction features	< 6,500	A, C
Centralia, Illinois	Unknown -	56	7.5	Paleo-liquefaction features	< 6,500	A, C, D
Vincinnes, Indiana	Wabash Valley fault zone	146	7.5	Paleo-liquefaction features	6,100	C, E, F
New Madrid, Missouri	New Madrid seismic zone	148	7.7	Historic earthquakes and paleo-liquefaction features	107	C, G
St. Louis, Missouri	USGS background seismicity	0	7.0	None - assumed possible anywhere in the Central U.S. inboard "craton" zone	Unknown	G

NATURAL HAZARDS MITIGATION INSTITUTE

References:

A. Tuttle, M., Chester, J., Lafferty, R., Dyer-Williams, K., and Cande, R., 1999, Paleoseismology Study Northwest of the New Madrid Seismic Zone U.S. Nuclear Regulatory Commission, NUREG/CR-5730

B. Tuttle, M. P., 2001 Personal communication

C. Crone, A. J., and Wheeler, R. L., 2002 Data for Quaternary faults, liquefaction features, and possible tectonic features in the Central and Eastern United States, east of the Rocky Mountain front U.S. Geological Survey, Open-File Report 00-260. http://pubs.usgs.gov/of/2000/ofr-00-0260/

D. Bauer, R., 2002, Personal communication by the Illinois State Geological Survey

E. Munson, P. J., and Munson, C. A., 1996, Paleoliquefaction Evidence for Recurrent Strong Earthquakes Since 20,000 Years BP in the Wabash Valley Area of Indiana, Report to USGS National Earthquake Hazards Reduction Program, Grant No. 14-08-0001-G2117

F. Martin, J. R., 199X, Seismic Parameters for the Central United States Based on Paleoliquefaction Evidence in the Wabash Valley.

G. Frankel, A. D., Petersen, M. D., Mueller, C. S., Haller, K. M., Wheeler, R. L., Leyendecker, E. V., Wesson, R. L., Harmsen, S. C., Cramer, C. H., Perkins, D. M., and Rukstales, K. S., 2002, Documentation for the 2002 Update of the National Seismic Hazard Maps, U.S. Geological Survey, Open-File Report 02-420 http://geohazards.cr.usgs.gov/eq/of02-420/OFR02-420.pdf

NATURAL HAZARDS MITIGATION INSTITUTE

References:

A. Tuttle, M., Chester, J., Lafferty, R., Dyer-Williams, K., and Cande, R., 1999, Paleoseismology Study Northwest of the New Madrid Seismic Zone U.S. Nuclear Regulatory Commission, NUREG/CR-5730

B. Tuttle, M. P., 2001 Personal communication

C. Crone, A. J., and Wheeler, R. L., 2002 Data for Quaternary faults, liquefaction features, and possible tectonic features in the Central and Eastern United States, east of the Rocky Mountain front U.S. Geological Survey, Open-File Report 00-260. http://pubs.usgs.gov/of/2000/ofr-00-0260/

D. Bauer, R., 2002, Personal communication by the Illinois State Geological Survey

E. Munson, P. J., and Munson, C. A., 1996, Paleoliquefaction Evidence for Recurrent Strong Earthquakes Since 20,000 Years BP in the Wabash Valley Area of Indiana, Report to USGS National Earthquake Hazards Reduction Program, Grant No. 14-08-0001-G2117

F. Martin, J. R., 199X, Seismic Parameters for the Central United States Based on Paleoliquefaction Evidence in the Wabash Valley.

G. Frankel, A. D., Petersen, M. D., Mueller, C. S., Haller, K. M., Wheeler, R. L., Leyendecker, E. V., Wesson, R. L., Harmsen, S. C., Cramer, C. H., Perkins, D. M., and Rukstales, K. S., 2002, Documentation for the 2002 Update of the National Seismic Hazard Maps, U.S. Geological Survey, Open-File Report 02-420 http://geohazards.cr.usgs.gov/eq/of02-420/OFR02-420.pdf

NATURAL HAZARDS MITIGATION INSTITUTE

HAZUS - PESH Model

- PESH=Potential Earth Science Hazards
- Ground shaking maps produced
  - Basis for ground shaking (Probabilistic Seismic Hazard Maps (USGS))
  - Standard shape of response spectra
  - Attenuation of ground shaking (CEUS Default-50% Frankel 1996 + 50% Toro 1997)
  - Amplification of ground shaking - local site conditions (site classes and soil amplification factors proposed for the *1997 NEHRP Provisions*)

NATURAL HAZARDS MITIGATION INSTITUTE

UMR UNIVERSITY OF MISSOURI-ROLLA

Site Class – GMA

- Ground Motion Amplification
  - simplified site response factors based on amplification factors based on NEHRP 1997.
- We have adopted MODNR Surficial deposits MAP for this purpose.
- USGS NEHRP is in the process to develop new maps for St. Louis

NATURAL HAZARDS MITIGATION INSTITUTE

UMR UNIVERSITY OF MISSOURI-ROLLA

HAZUS - Liquefaction Map

- Inputs
  - A geologic MAP based on the age, depositional environment, and the material characteristics of the geologic units were used to create a liquefaction susceptibility map (Liquefiable - Soil Site Class F)
  - Groundwater depth map is supplied with a default depth of 5 feet.
  - Earthquake Moment Magnitude (**M**)
- Output
  - Aerial map depicting estimated permanent ground deformations

NATURAL HAZARDS MITIGATION INSTITUTE

UMR UNIVERSITY OF MISSOURI-ROLLA

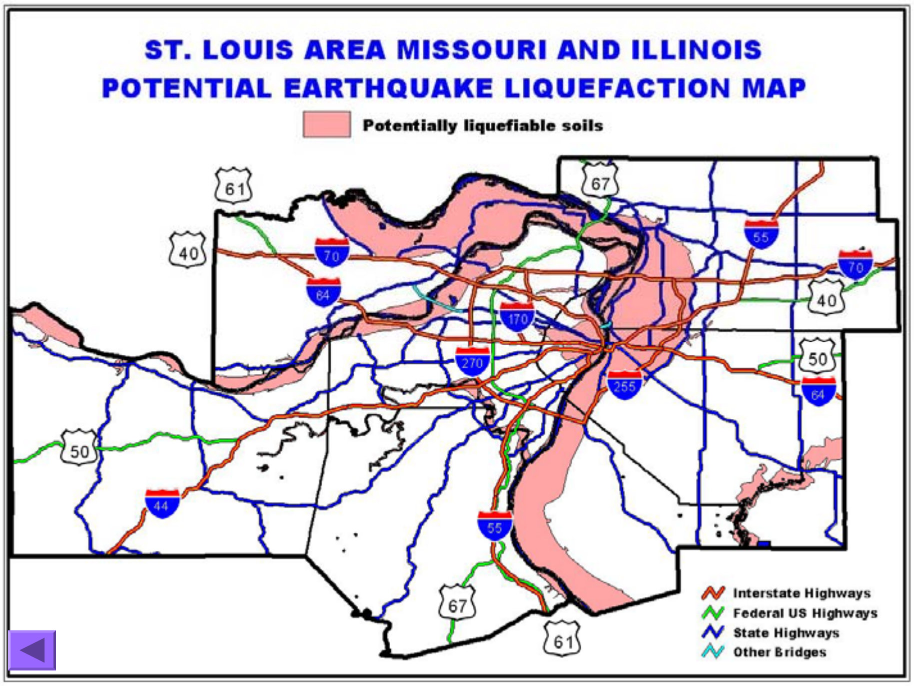

HAZUS – Bridge Input Data

- Bridges divided into 28 categories based on 1996 NBI database
- Inputs
  - Bridge Classification (based on the following structural characteristics: Seismic Design, Number of spans, Structure type, Pier type, Abutment type and bearing type, Span continuity)
  - Geographical location of bridge (longitude and latitude)
  - Spectral accelerations at 0.3 sec and 1.0 sec, and PGD at bridge (for fragility curves)
  - Peak Ground Acceleration (for PGD-related computations)

HAZUS – Damage Output

- % Damage
  - Initial damage state only
  - Output is in terms of probability of slight, moderate, extensive, or complete damage to occur for the input earthquake scenario
- % Functionality
  - Damage state over time
  - Output is in terms of % functionality at time periods of 1, 3, 7, 30, and 90 days

HAZUS – Direct Losses

- Limited to the cost of repairing damage to the lifeline system
- Output in 1994 dollars
- Default values are provided for replacement values of lifeline components as a guide

% Functionality…

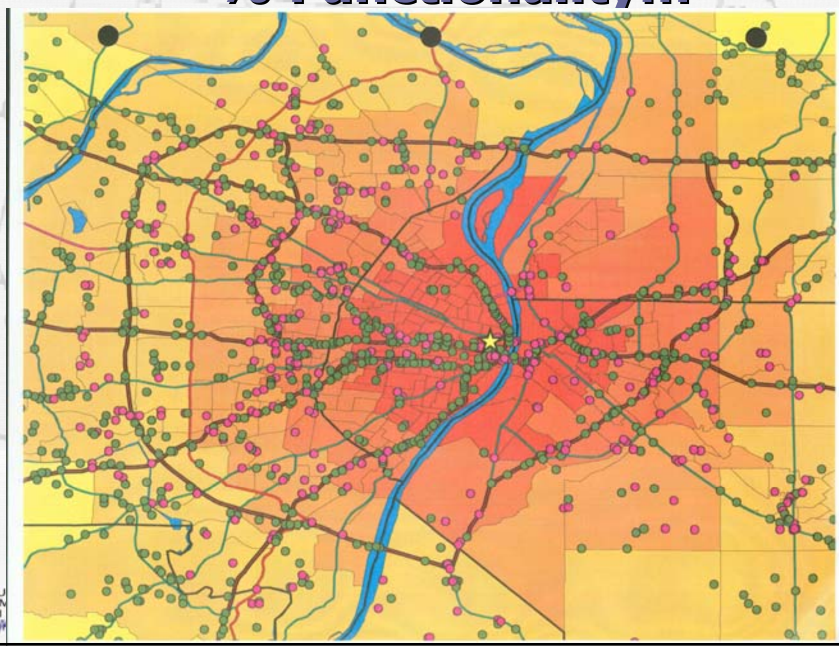

Indirect Losses - Input

- Calibrated urban transportation planning model (Minutp software from EWG)
  - 2004 baseline selected
  - Census Bureau demographic data from 2000 projected to 2004
  - Current transportation highway system
- Bridges to be removed from the network
  - Selected those from HAZUS runs with P (complete damage) > .75

Indirect Losses - Output

- Cost due to longer travel time
  - Delay =Final travel time – Baseline travel time
  - What is the value of time?
- Cost due to longer travel distance
  - Final travel dist. – Baseline travel dist.
  - Increase in dist. traveled =
    Final dist. – Baseline dist.
  - Cost of longer distance of travel
- Indirect transportation cost =
  Delay cost + Cost of longer travel distance

PRESENTATION 3

POST-EARTHQUAKE CONDITION ASSESSMENT OF RC STRUCTURES

POST-EARTHQUAKE CONDITION ASSESSMENT OF RC STRUCTURES PART 1: CRACK SENSOR

Genda Chen, Ph.D., P.E.
Associate Professor of Civil Engineering
University of Missouri-Rolla (UMR)
gchen@umr.edu

Geotechnical and Bridge Seismic Design Workshop
New Madrid Seismic Zone Experience

October 28-29, 2004, Cape Girardeau, Missouri

Participants

Genda Chen, Ph.D., P.E.: Associate Professor of Civil Engineering (Team Leader)

Ryan McDaniel: M.S. Graduate Student

David Pommerenke, Ph.D.: Associate Professor of Electrical Engineering

James L. Drewniak, Ph.D.: Professor of Electrical Engineering

Shishuang Sun: Ph.D. Graduate Student

Objectives

To introduce a general framework for structural condition assessment of RC members with measured surface crack pattern

To introduce distributed cable sensors and measurement principle

To validate the performance of cable sensors for crack detection for both location and severity

To illustrate the potential applications of sensors

A Framework for Condition Assessment of RC Member

A three-level strategy is proposed in this study to assess the damage of a RC structural system, using electromagnetic wave-guiding tools:

1. to apply the recently-developed, distributed cable sensors to locate and detect the near-surface cracks in any major member of the structure.
2. to apply microwave technology to refine the crack distribution at critical locations, such as near the beam-column joints or where the first-level detection has indicated the occurrence of excessive cracking.
3. to infer the structural condition of the member from the measured crack patterns by applying the mechanical principle [Nazmul and Matsumoto 2003].

Anatomy of a Crack Sensor

- Twisted silver plated copper wire serves as inner conducting core
- Teflon dielectric layer covers inner core
- Steel spiral layer serves as outer conductor
- Thin layer of solder coats the steel spiral layer

Measurement Principle: Electrical Time Domain Reflectometry

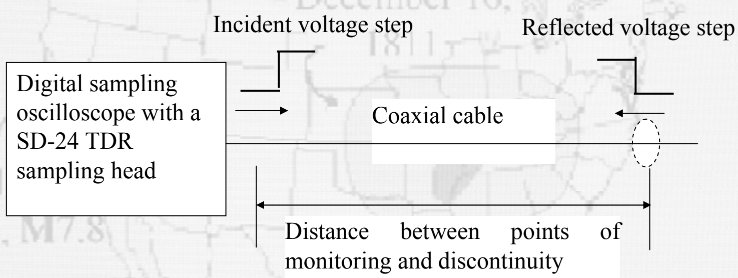

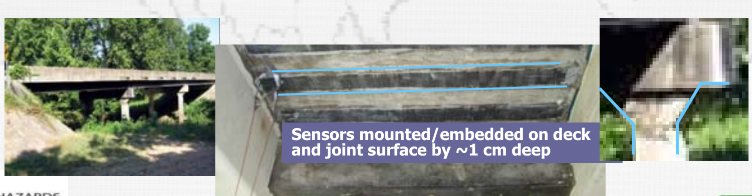

Performance Validation with Static, Cyclic, and Dynamic Tests

- Static testing on beam specimens
- Dynamic testing on column specimens
- Cyclic testing on 80%-scale beam-column specimens
- Load tests of the RC deck of Dallas County Bridge, MO

Installation of Distributed Sensors

- Sensors are near surface mounted on a member and installed in a 1.25cm x 1.25cm groove.
- Sensors are grouted into place with grout materials that are more brittle than concrete.

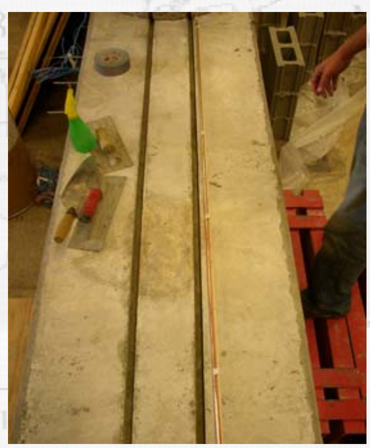

Data Acquisition

- Signals are acquired using the Electronic Time-Domain Reflectometery (ETDR)
- A Time Domain Reflectometer (TDR) digital oscilloscope is used in data acquisition
- Sampling rate is 200 kHz, corresponding time needed to retrieve full signal is on the order of 2.6 milliseconds

Equipment

Typical Reflected Waveform

Static Tests on Beam Specimens

- Sensor installed on 91-centimeter beams tested in flexure under static loads

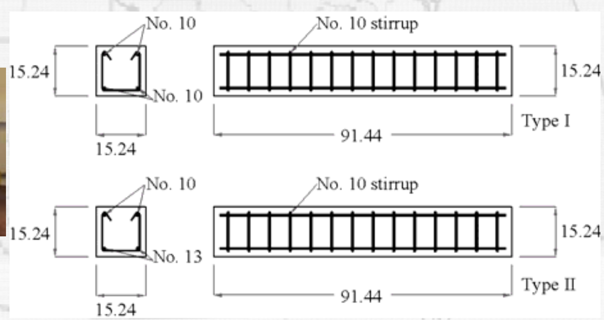

Design Details of RC Beams

Static Tests on Beam Specimens

- Crack pattern and reflected waveform

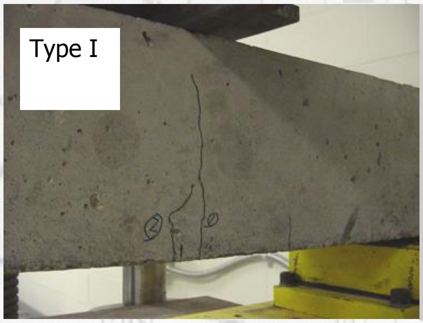

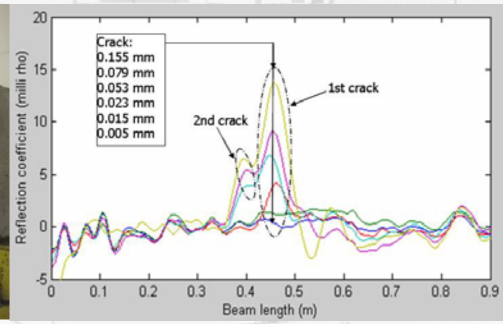

Static Tests on Beam Specimens

- Crack pattern and reflected waveform

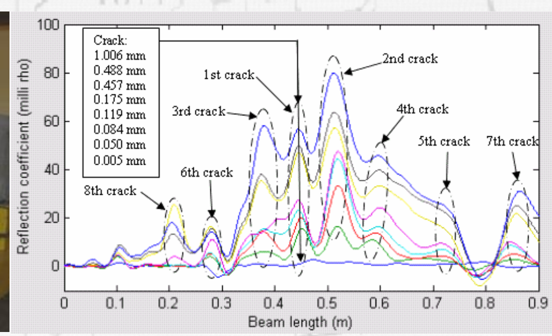

Dynamic Test Specimen

- 1.9m tall 20cm x 20cm square concrete column
- Rectangular footing for attachment to shake table
- 76cm x 76cm x 76cm mass of concrete on top of column to give the column a fundamental frequency of around 8 Hz
- 27.6 MPa concrete used in construction of column
- 1.25cm x 1.25 groove in face of column for sensor installation

Dynamic Test Specimen

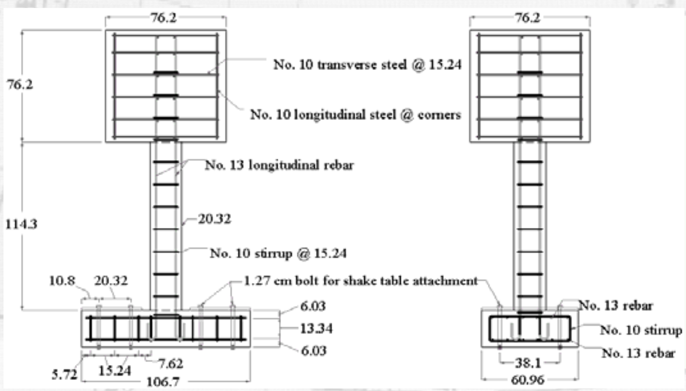

Dynamic Test Specimen Retrofit Schedule

Column	Retrofit	Stroke (mm)	Rubber-Sensor	Teflon-Sensor	Crack
C1	No	1.78	N/A	T1	Surface
C2	No	1.78	N/A	T2	Surface
C3	Yes	1.78	N/A	T3	Hidden
C4	Yes	1.78	N/A	T4	Hidden
C5	Yes	0.76	N/A	T5	Hidden
C6	No	0.76	R1	N/A	Surface

Purpose for Dynamic Tests

- Investigate the behavior of the sensor in a dynamic application (harmonic excitation)
- Investigate the ability of the sensor to detect cracks beneath retrofit (FRP)
- Investigate any fatigue effects
- Study the “memory” feature of the sensor

Results of Dynamic Tests

- Shows location and size of crack in column
- Detects crack in advance of visual detection
- Detects crack beneath FRP reinforcement

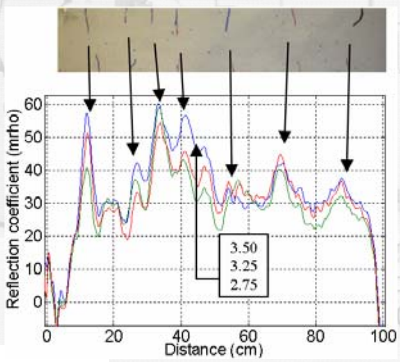

(a) Column C1

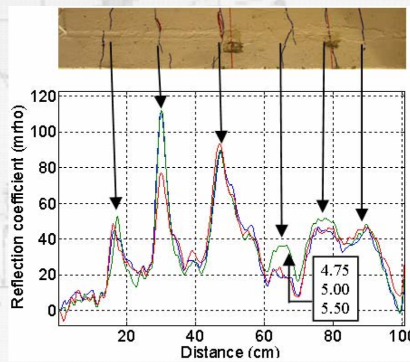

(b) Column C2

Results of Dynamic Tests

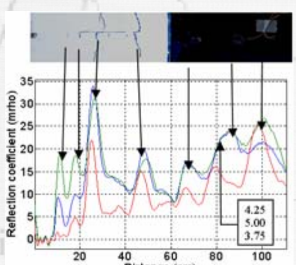

(c) Column C3

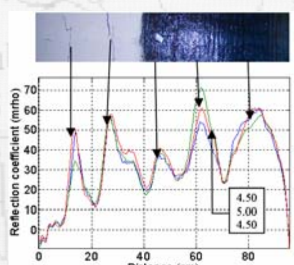

(d) Column C4

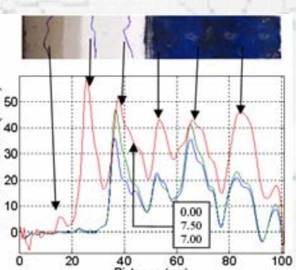

(e) Column C5

Results of Dynamic Tests

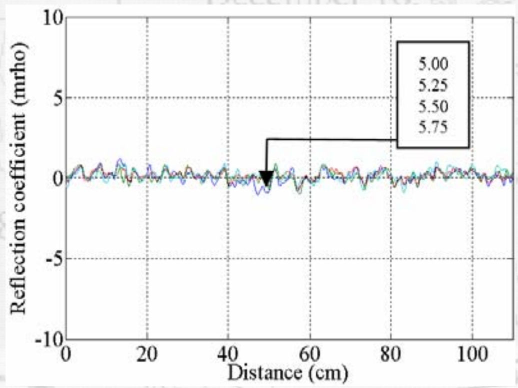

Column C6 with rubber-type sensor

Results of Dynamic Tests

- Shows the location of cracks beneath FRP

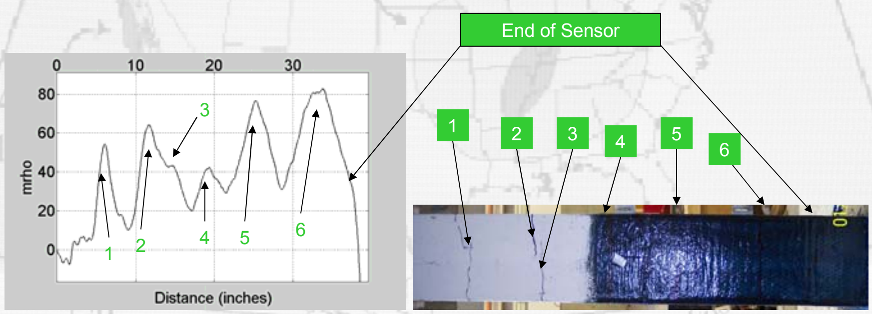

Fatigue of Sensor

- Sensor continues to operate after several test cycles (upwards of 20,000)
- Only one sensor ceased to operate, reason was because of connector, not actual sensor
- Sensor shows location of cracks after testing ceases (column reinforcement failure)

Discovery of Memory Feature

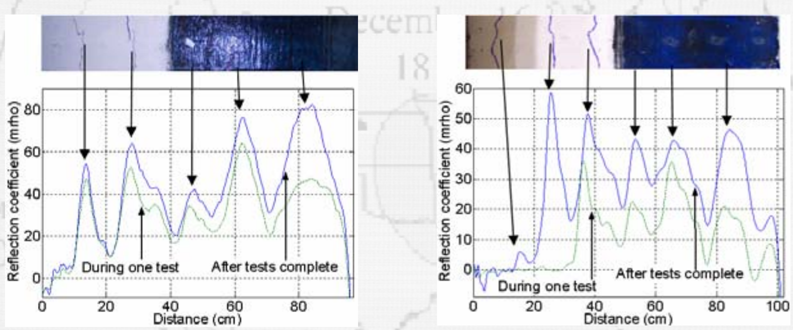

(a) Column C4 (b) Column C5

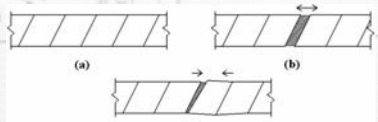

80% Bridge Column-Beam Specimen

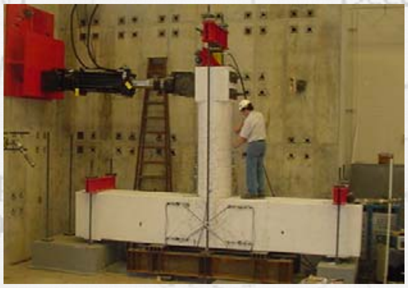

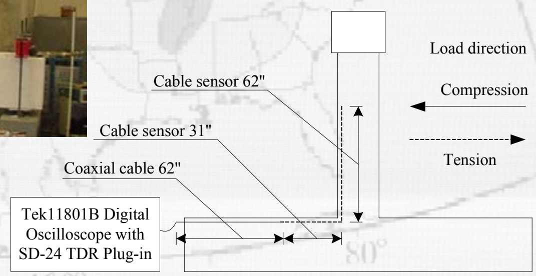

Specimen # 1 (Rubber Sensor)

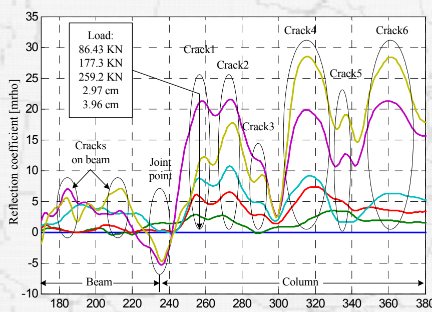

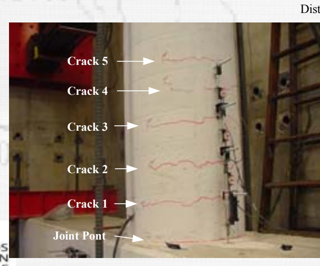

(a) Crack pattern at 177.3 kN

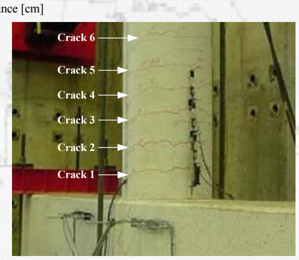

(b) Crack pattern at 1.98 cm

Specimen # 3

- Both rubber and Teflon sensor installed into specimen
- Specimen tested in December of 2003 without any retrofit
- Testing resumed August 2004 with retrofit scheme

Specimen # 3 Results (Teflon)

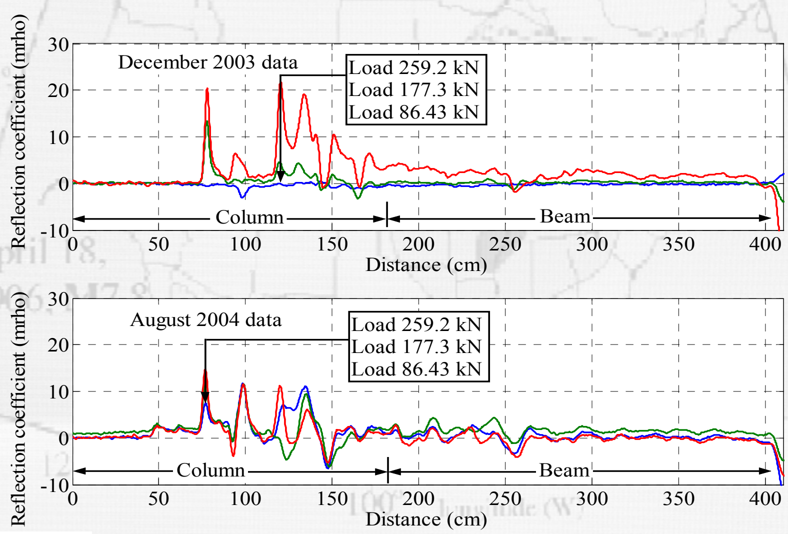

Specimen # 3 Results (Rubber)

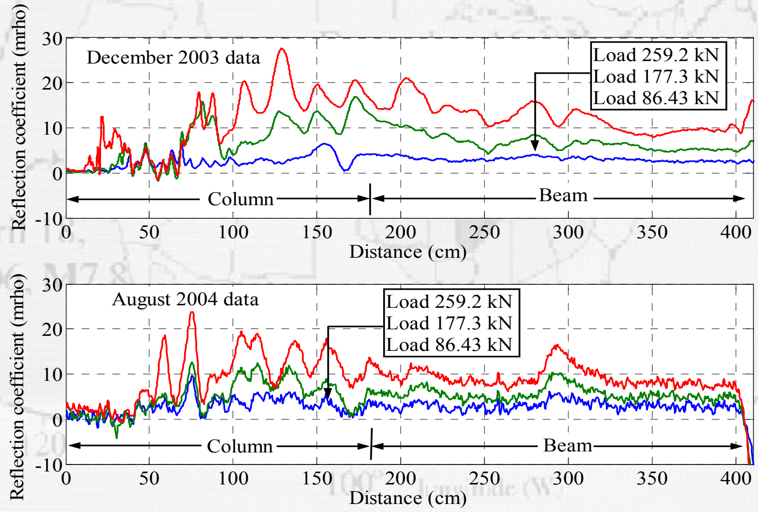

Specimen # 3 Results

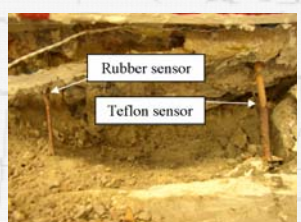

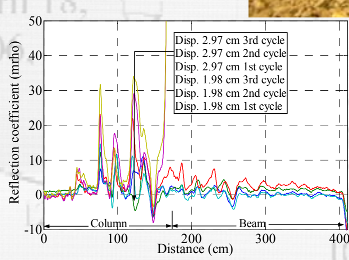

Teflon Sensor

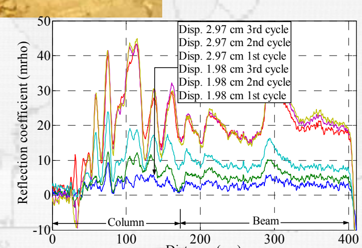

Rubber Sensor

Specimen # 3 Results

- After six months of inactivity sensors still show comparable results at same loading levels
- Both detect location and relative size of cracks
- 90^{o} bend at construction joint is a detriment to sensor performance

Monitoring of Bridge Deck under Load Testing

Dallas County Bridge, MO

Difference Signals Taken at Zero Loading (Sensor 1)

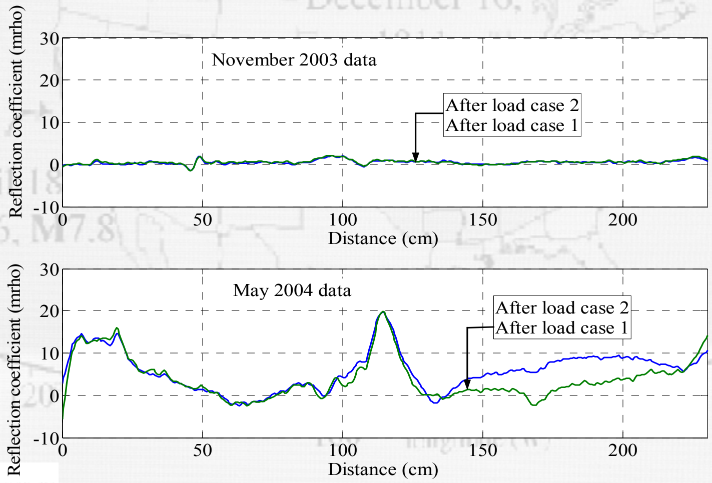

Difference Signals Taken at Zero Loading (Sensor 2)

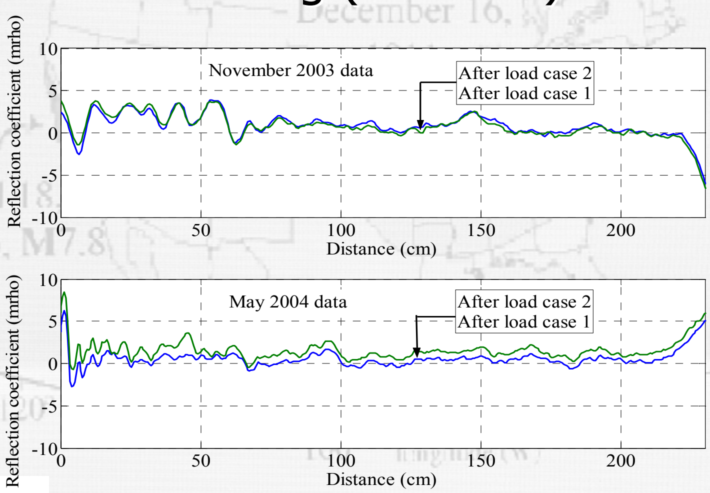

Results of Bridge Tests

- Sensors show no degradation after several months of exposing to the elements

Conclusions

- Sensors are demonstrated to be able to detect location and relative size of cracks
- Rubber type sensors are not recommended for dynamic application
- Sensors are rugged, surviving over 20,000 cycles of loading
- Teflon sensors have ability to record the most severe crack
- Sensors can detect cracks beneath retrofit schemes
- It is not recommended to install sensors across construction joints where large displacements are prone to occur
- No degradation is observed in sensors over a period of months in both lab conditions and in field conditions

POST-EARTHQUAKE CONDITION ASSESSMENT OF RC STRUCTURES PART 2: NEAR-FIELD MICROWAVE

Reza Zoughi, Ph.D. and Genda Chen*, Ph.D., P.E.
*Associate Professor of Civil Engineering
University of Missouri-Rolla (UMR)
gchen@umr.edu

Geotechnical and Bridge Seismic Design Workshop
New Madrid Seismic Zone Experience

October 28-29, 2004, Cape Girardeau, Missouri

Participants

Reza Zoughi, Ph.D.: Schlumberger Professor of Electrical Engineering (Team Leader)

Jagadish Nadakuduti: M.S. Graduate Student

Genda Chen, Ph.D., P.E.: Associate Professor of Civil Engineering

Objectives

The ultimate goal of this study is to extract crack information, width and depth, from a crack characteristic signal. This extraction process, however, is an inverse engineering problem, which is difficult to solve in practical applications. As a first step towards this endeavor, a forward model will be developed, allowing the simulation of the crack characteristic signal of a cracked concrete surface given the operating frequency, crack width, crack depth, dielectric property of the concrete, waveguide dimensions, and standoff distance. Specific objectives are

- To study how a crack characteristic signal changes with operational parameters (frequency, standoff distance, etc.) and crack sizes (width and depth) from calibration tests with a network analyzer.
- To develop a forward model with the commercial Ansoft HFSS platform.
- To develop an empirical way of constructing the crack characteristic signal

Terminology

Laboratory-Designed Microwave Reflectometer

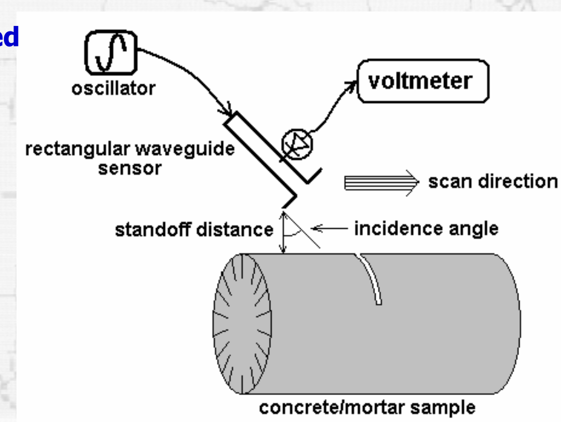

Crack characteristic signal: detector voltage plotted as a function of scanning distance, obtained when a crack is scanned over a waveguide aperture.

Microwave Images: Experimental Setup (Previous study)

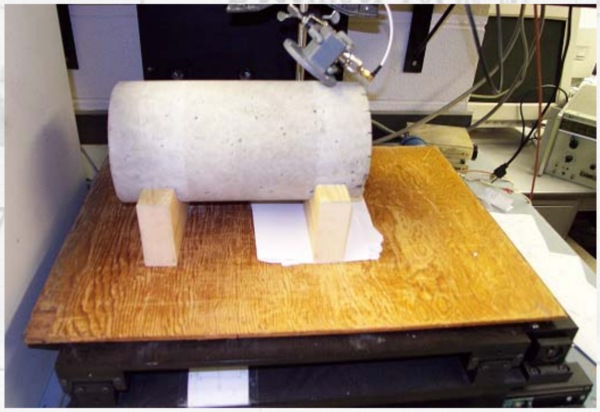

Operating frequency – 10.5 GHz (X-band: 8.2 – 12.4 GHz)
– 7.5 GHz (J-band: 5.85 – 8.2 GHz)

Microwave Images at X-band (pre-cracked cylinder)

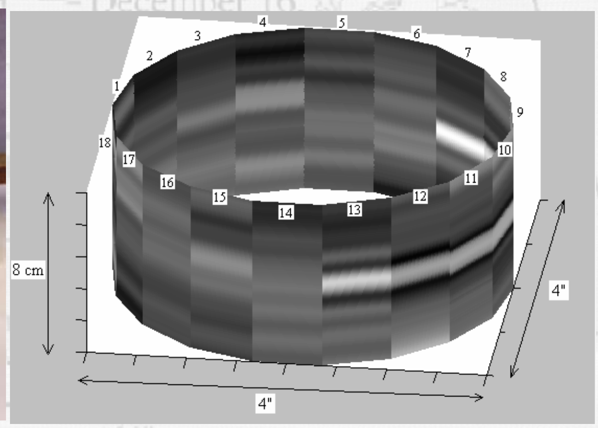

Microwave Images at X-Band (Cyclic stress induced cracks)

Schematic of testing procedure.

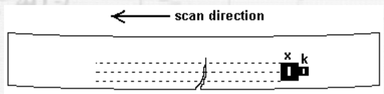

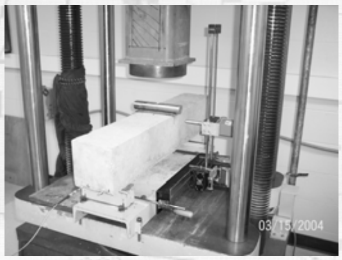

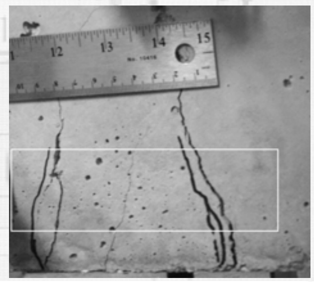

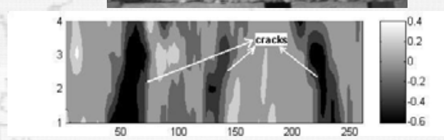

4 lines with 125 mm of scan length (2 data points/mm shown) with static variation removed.

Summary of Previous Study with Microwave Images at X-Band

Influences of
- Operating frequency
- Standoff distance
- Incidence angle
- Water content/moisture presence
- Polarization of waveguide sensor

on crack characteristic signals were investigated with microwave images.

Disadvantage:
Unable to identify the depth of a crack and approximate for crack width estimation.

Next step:
Measure both the magnitude and phase of a crack characteristic signal with a Vector Network Analyzer (VNA)

NATURAL HAZARDS MITIGATION INSTITUTE
UMR UNIVERSITY OF MISSOURI-ROLLA

Experimental Setup Employing VNA

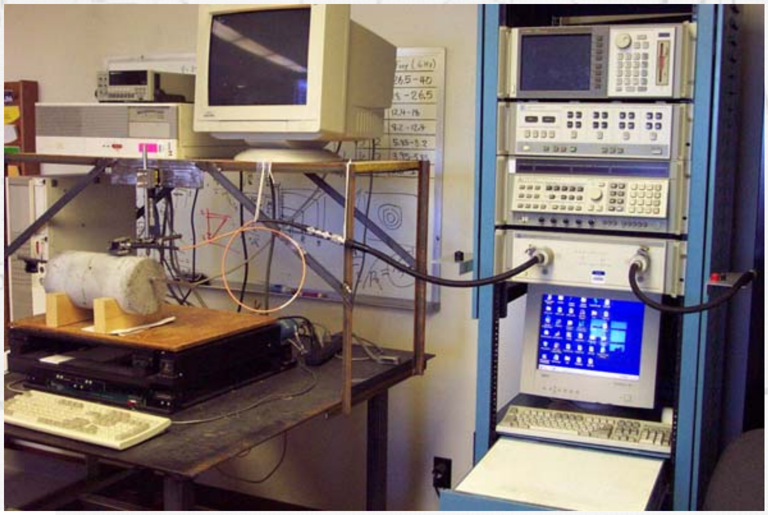

Magnitude and Phase of a Crack Characteristic Signal (CCS)

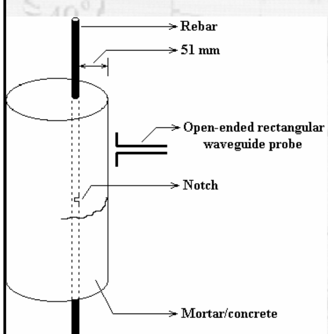

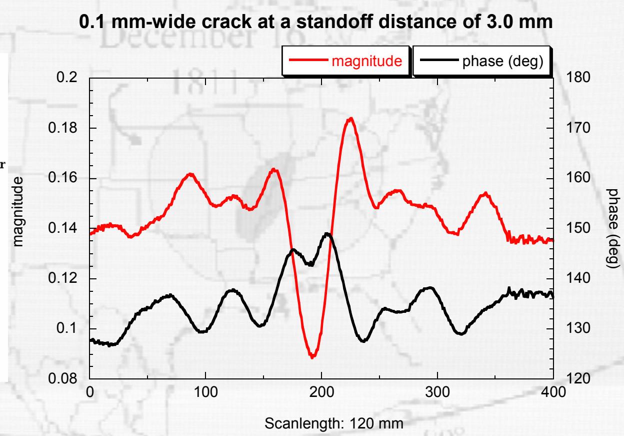

(Reflection co-efficient of X-band open-ended waveguide for a surface-breaking crack generated in mortar sample by externally loading the rebar)

Modeling of Probe Response to a Crack

- Why Electromagnetic Modeling?
  - Optimization of Measurement Parameters
  - Characterization of Crack Dimensions
- Forward Model: To simulate CCS given the
  - standoff distance,
  - operating frequency,
  - crack dimensions and
  - waveguide dimensions.
- Conduct measurements to record the magnitude and phase of CCS as a function of these parameters.

Specimens for Calibrated Measurements

Arrangement 1:
Cracks of Varying Width

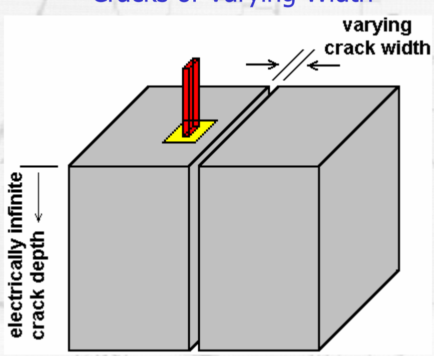

Two mortar cubes used to simulate cracks with varying crack width.

Arrangement 2:
Cracks of Varying Depth

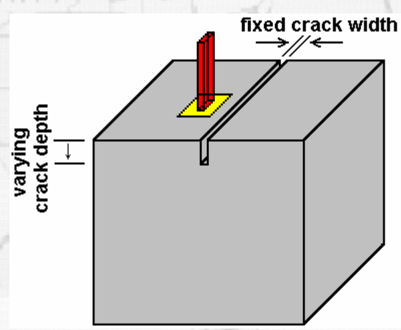

Cement-past cube with a notch cut using hacksaw to generate a crack of varying depth.

Influence of Standoff Distance

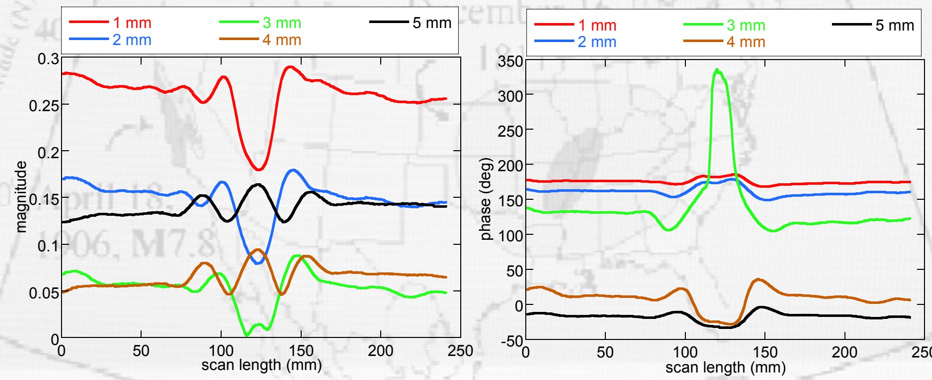

Magnitude and phase of reflection coefficient for a 2 mm-wide crack on day 13 at different standoff distances (Arrangement 1).

Influence of Crack Width

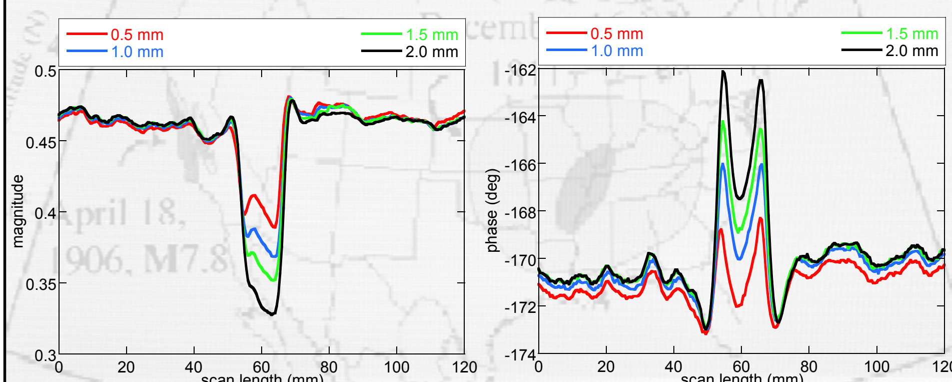

Magnitude and phase of reflection coefficient for different crack widths at a standoff distance of 0.05 mm (Arrangement 1).

Influence of Crack Depth

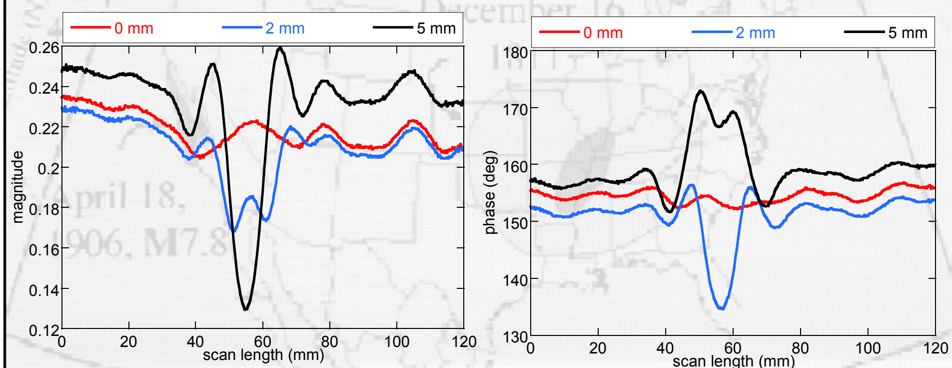

Magnitude and phase of reflection coefficient of a 1.14-mm wide crack for different crack widths at a standoff distance of 2.0 mm (Arrangement 2 @10 GHz).

Numerical Simulations Using an 3D Electromagnetic Field Solver: Ansoft HFSS

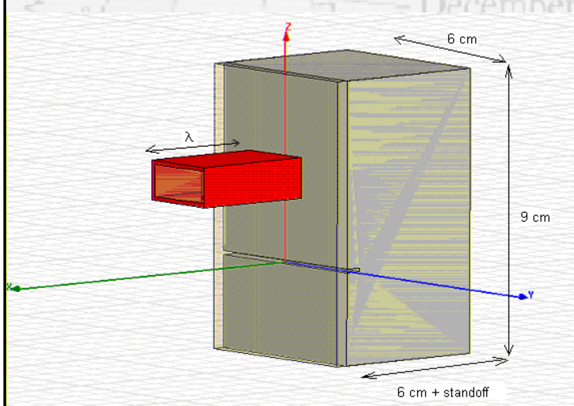

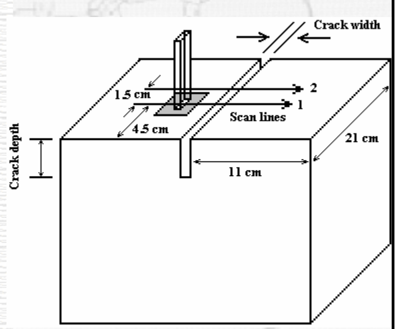

Schematic of HFSS model developed for simulating crack characteristic signals (CCS).

Results of Numerical Simulations of CCS using Ansoft HFSS

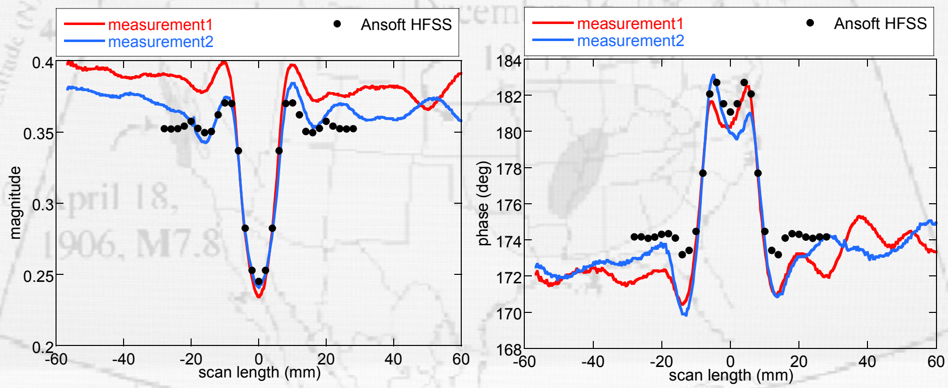

Magnitude and phase of measured and simulated crack characteristic signals for a crack of 1.14 mm wide, 5.0 mm deep, at a standoff distance of 1.0 mm and for a dielectric property of (5.96 – j1.02) at 10.0 GHz using *Arrangement 2.*

Complex Representation of CCS

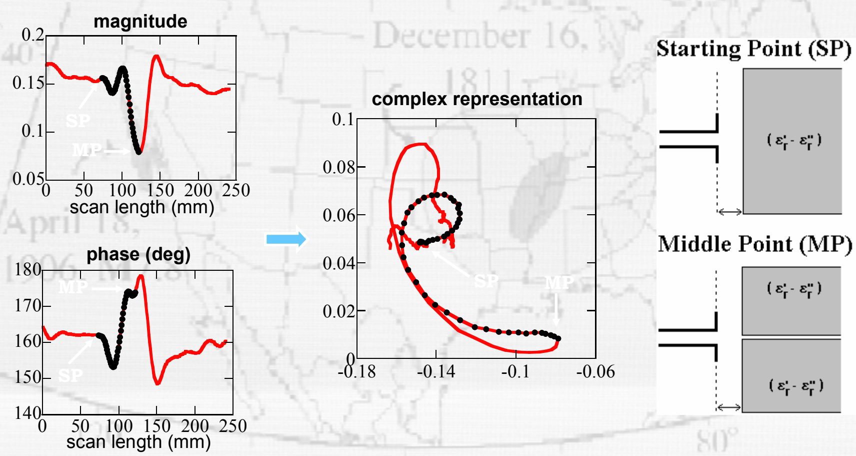

Complex plane representation of reflection coefficient of 2 mm-wide crack at a standoff distance of 2.0 mm on day 13.

Complex Plane Representations: CCS as Function of Standoff Distance

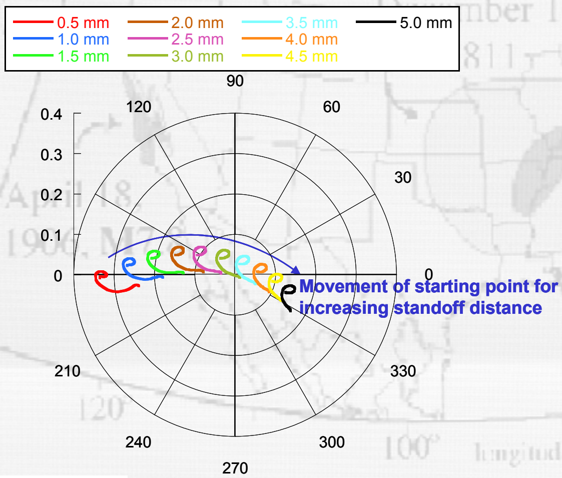

2 mm-wide crack for different standoff distances (Arrangement 1 @ 10 GHz)

Modeling of CCS in Complex Domain

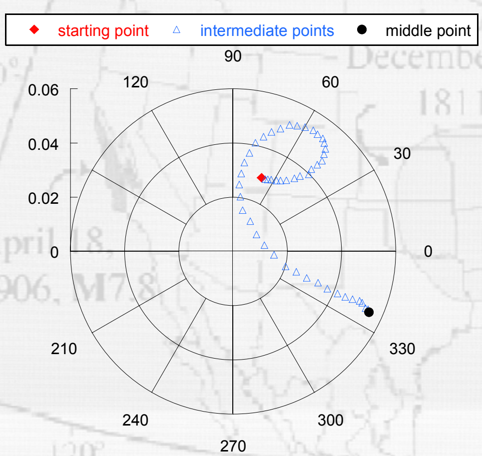

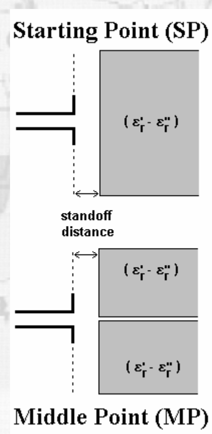

Measured crack characteristic signal of a 2.0 mm-wide crack at a standoff of 3.5 mm on day 13 comprising of starting point, intermediate points and middle point

Computing Starting Point

- This can be accomplished by using a custom-built electromagnetic model ("nlayer") available from previous studies for determining the reflection coefficient at the aperture of an open-ended rectangular waveguide radiating into a stratified media given the dielectric properties and thickness of each layer.

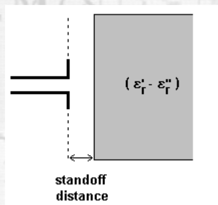

Schematic showing the inputs given to "nlayer" code for computing the starting point

Computing Starting Point: Using N-layer code

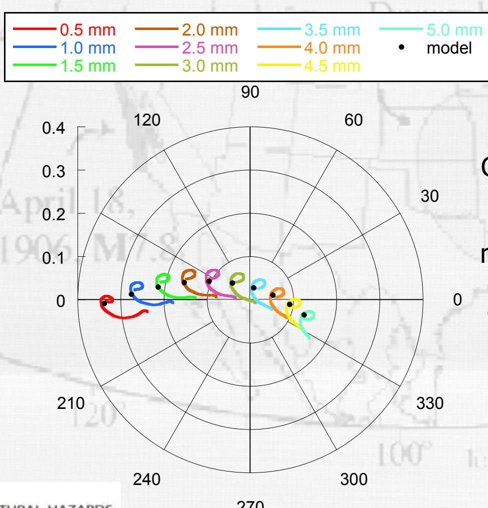

Comparison of starting points computed from "nlayer" and those obtained from the measured crack characteristic signals at different standoff distances for a 2.0 mm-wide crack in mortar (4.11-j0.56) at 10.0 GHz.

Difficulty in Computing Middle Point

- It is difficult to develop an electromagnetic model to accurately determine the middle point. The difficulty arises mainly because of:
  - the complex near-field interaction of probe field properties with discontinuities (presence of a crack in this case) in a dielectric material,
  - flange effect of the waveguide,
  - edge effect of the crack, etc.,

  to compute the middle point with reasonable accuracy.

Alternative to Compute Middle Point

- Use an 3D electromagnetic field solver (previously developed Ansoft HFSS model)
- This model takes approximately one hour to compute this single point.
- Simulating an entire crack characteristic signal is time consuming and hence only the middle point is computed using Ansoft HFSS for the overall empirical model.

Computing Intermediate Points

- The shape of the crack characteristic signal between the starting point and the middle point is dependant on standoff distance and crack dimensions.
- The shape of measured crack characteristic signals as a function of only one parameter (e.g. standoff distance) can be used to generate templates for a given value of that parameter.

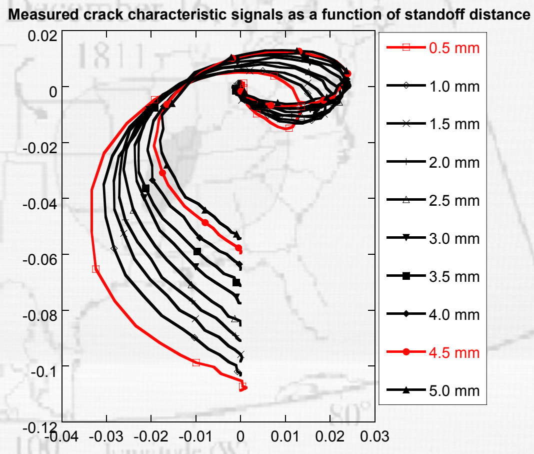

Computing Intermediate Points by Generating Templates

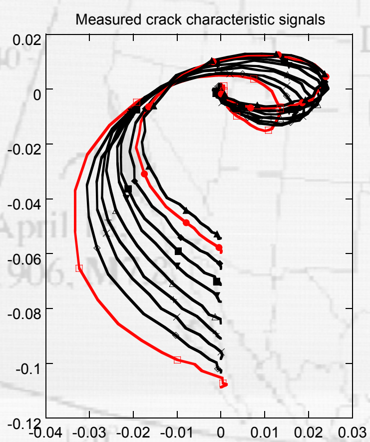

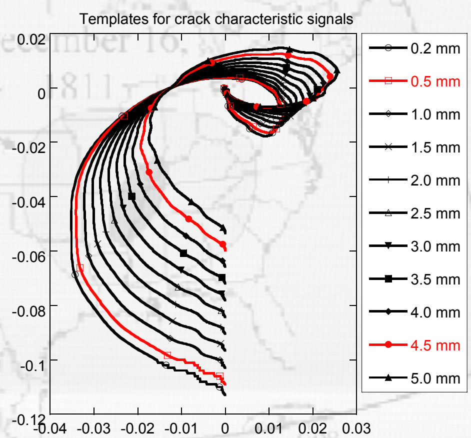

Templates at other standoff distances are obtained by interpolating or extrapolating the measurement signals at standoff distance of 0.5 mm and 4.5 mm

Modeling Crack Characteristic Signals

- Once the template signal is found for a given standoff distance, a scaled version of this signal is rotated and translated such that it fits in between the starting and the end points.
- Thus, the simulated crack characteristic signal in the complex domain is unwrapped to obtain magnitude and phase of CCS for a given standoff distance, crack dimensions and dielectric properties of the mortar cube.

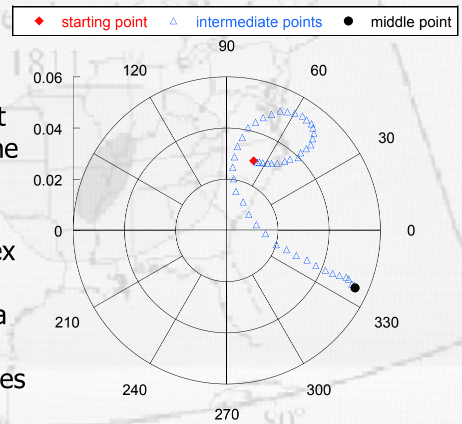

NATURAL HAZARDS MITIGATION INSTITUTE

UMR UNIVERSITY OF MISSOURI-ROLLA

Modeling CCS: Results

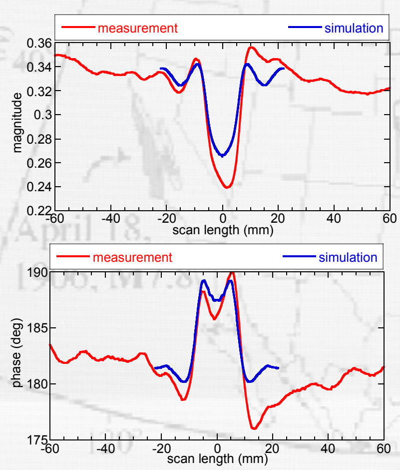

crack width of 2.0 mm
at standoff distance of 0.5 mm

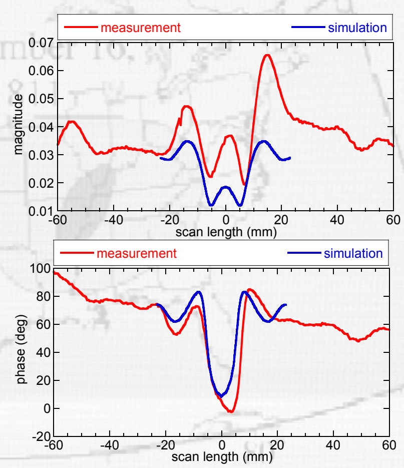

crack width of 1.0 mm
at standoff distance of 3.5 mm

NATURAL HAZARDS MITIGATION INSTITUTE

UMR UNIVERSITY OF MISSOURI-ROLLA

Conclusions

- Surface-breaking cracks can be successfully detected with open-ended rectangular waveguides.
- Influence of various measurement parameters on crack detection was discussed.
- The results of empirical modeling show that the simulated crack characteristic signals match well with the measured signals.
- The results presented here are only for infinitely deep cracks. For this empirical model to work for finite depth cracks, a database of template signals as a function of crack dimensions, operating frequency and waveguide dimensions must be created.

Future Considerations

- Generate a database of template signals (general shape of a crack characteristic signal) as a function of various parameters such as standoff distance, crack dimensions, waveguide aperture dimensions and the operating frequency.
- The model needs to be robust irrespective of the waveguide probe used and the operating frequency (test using K-band & J-band probes).
- An inverse model needs to be developed which can be used to extract information regarding crack dimensions (width and depth) from the magnitude and phase of crack characteristic signal assuming the dielectric properties of the material is known *a priori*.
- Extend this study to model interior cracks as well.

PRESENTATION 4

RECOMMENDED LRFD GUIDELINES FOR THE SEISMIC DESIGN OF HIGHWAY BRIDGES

Recommended LRFD Guidelines for the Seismic Design of Highway Bridges

W. Phillip Yen, PhD, PE

Office of Infrastructure, R&D FHWA

&

Lee Marsh

BERGER/ABAM Engineers

Cape Girardeau, MO
Oct. 28-29, 2004

Recommended LRFD Guidelines for the Seismic Design of Highway Bridges

For: *AASHTO LRFD Bridge Design Specifications*

(Load and Resistance Factor Design)

Sponsors:

- National Cooperative Highway Research Program (NCHRP) NCHRP 12-49
- Federal Highway Administration (FHWA)

Prepared by:

- ATC/MCEER Joint Venture
- MCEER Highway Project

NCHRP 12-49 Project Team

Ian Friedland, FHWA
Chris Rojahn, ATC
Ron Mayes, SGH

Don Anderson, CH2M Hill
Michel Bruneau, U Buffalo
Greg Fenves, UC Berkeley
John Kulicki, Modjeski & Masters
John Mander, U Buffalo
Geoff Martin, USC
Lee Marsh, BERGER/ABAM
Andy Nowak, U Michigan
Rick Nutt, consultant
Maury Power, Geomatrix
Andrei Reinhorn, U Buffalo

Others Involved

NCHRP Panel Chair
Harry Capers, NJDOT

NCHRP Panel and AASHTO T-3
Richard Land, Caltrans

NCHRP Panel and FHWA Liaison,
Phillip Yen, FHWA

ATC Project Engineering Panel Chair,
Ian Buckle, Univ Nevada Reno

Where The Process Stands

- Provisions for LRFD spec developed
- Stand-alone guidelines developed
- Trial designs / limited use as resource
- Barriers to AASHTO adoption:
  - Number of bridges in higher zones too large
  - Return period (2500 years) too long
  - Guidelines too complex
- Next step?

Key Concepts

- National hazard maps, site factors, spectra
- Performance objectives and design earthquakes
- Emphasis on capacity design principles
  - Selected yielding / damage sites
  - Essentially elastic response elsewhere
- Seismic Design and Analysis Procedures (SDAP)
- Improved foundation, abutment and liquefaction design procedures

Design Earthquakes

- Rare Event
  - 3 % probability of exceedance (PE) in 75 years (2500-year return period)
  - Deterministically capped near active faults
- Frequent Event
  - 50 % PE in 75 years (100–year return period)
  - Similar to flood and associated performance objectives
- Consistent with retrofit definitions
  - Probability of exceedance and not return period

Performance Objectives

	Performance Objective	
Probability of Exceedence	Life Safety	Operational
Rare EQ SL 3%/75yr *D*	Significant disruption *Significant*	Immediate *Minimal*
Freq EQ SL 50%/75yr *D*	Immediate *Minimal*	Immediate *None*

SL = Service Level *D = Damage*

Philosophy Behind the Guidelines

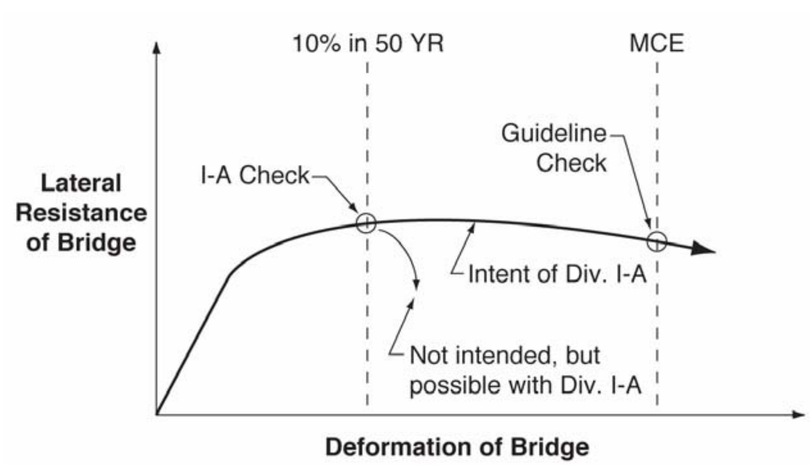

Logic Behind the Guidelines

- Seismic hazard is function of mapped acceleration and soil
  - 0.2-second spectral acceleration (S_S)
  - 1-second spectral acceleration (S_1)
  - Site coefficients (F_a and F_v)
- Increasing rigor in the provisions with hazard
  - Seismic Analysis and Design Procedures (SDAP)
  - Seismic Detailing Requirements (SDR)

Response Spectrum Construction

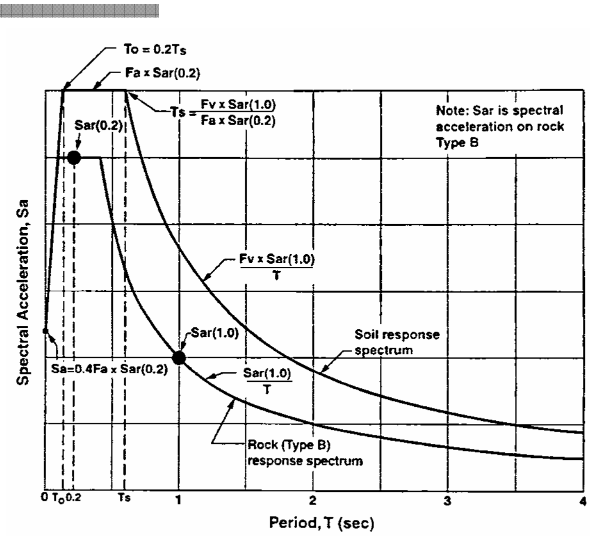

Seismic Hazard Levels

Seismic Hazard Level	Value of F_vS_1 (1-second)	Value of F_aS_s (0.2 –second)
I	$F_vS_1 \leq 0.15$	$F_aS_s \leq 0.15$
II	$0.15 < F_vS_1 \leq 0.25$	$0.15 < F_aS_s \leq 0.35$
III	$0.25 < F_vS_1 \leq 0.40$	$0.35 < F_aS_s \leq 0.60$
IV	$0.40 < F_vS_1$	$0.60 < F_aS_s$

Design Options

Seismic Design and Analysis Procedures (SDAP) and Seismic Design Requirements (SDR)

Seismic Hazard Level	Life Safety		Operational	
	SDAP	SDR	SDAP	SDR
I	A1	1	A2	2
II	A2	2	C/D/E	3
III	B/C/D/E	3	C/D/E	5
IV	C/D/E	4	C/D/E	6

"No Seismic Analysis"
SDAP B

- 'Regular' bridges in lower seismic hazard areas
- Bridge does not require seismic demand analysis
- Capacity design procedures used for detailing columns and connections
- No seismic design requirements for abutments

Capacity Spectrum
SDAP C

- Conceptually similar to Caltrans' displacement design method
- May be used for 'very regular' structures
- Period of vibration does not need to be calculated
- Designer sees explicit trade-offs between design forces and displacements

Elastic Response Spectrum SDAP D

- Same as current code, uses either the uniform load or multi-mode method of demand analysis.
- 'R-Factor' design force approach, similar to current code.
- Requires capacity design approach for superstructure, column shear, connections, abutments and foundations.

"Pushover" Analysis – SDAP E

- Perform multi-mode analysis, use 50% higher R-Factor for initial design, then check plastic rotations and displacements with pushover.
- Quantifies expected deformation demands in columns and foundations
- Highest R-Factors for column design
- Required for limited ductility systems so that actual demands on the elements are known.

Capacity Design Principles

- Include formal identification of earthquake resisting system
- Limit yielding/damage to preferred elements (e.g. columns – above ground)
- Reduce capacity if yielding not confined to preferred elements (e.g. drilled shafts - below ground)
- Increase capacity if pushover assessment used

Earthquake Resisting Systems (ERS) and Elements (ERE)

Three categories:

(1) Permissible (Preferred)
(2) Permissible with owner's permission
(3) Not recommended

ERE Example

Permissible Earthquake Resisting Elements that Require Owner's Approval

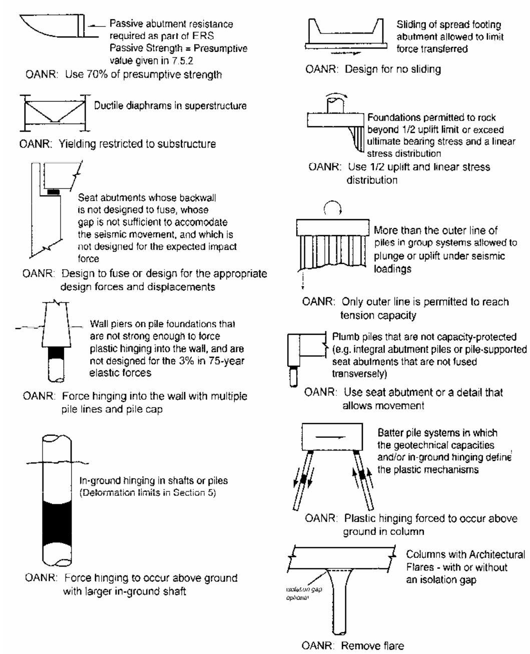

Foundations and Abutments

- Guidance for development of soil springs
- Guidance for assessment of performance
- Recognition of the beneficial contribution of abutment resistance
- Soil deformation effects considered in terms of structural and operational implications
- Design and detailing for liquefaction effects

Liquefaction Assessment

- State-of-the-art procedures for estimating liquefaction potential
- Quantification of liquefaction effects
  - lateral flow or spreading of approach fills
  - settlements of liquefied soils
- Use of ground improvement and pile resistance to limit soil movement
- Acceptance of plastic hinging in piles

Ground Movement vs. Structure Resistance Mechanisms

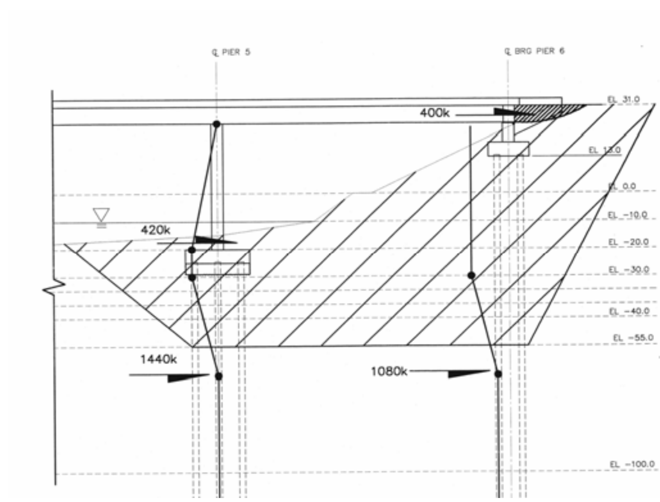

Parameter Study, Trial Designs and Design Examples

- 2400 simplified substructure designs
- 19 trial designs by state DOTs
- 2 design examples
- Broad, nationwide data sets included
- Costs similar to or only moderately higher (+/- 10%) than those by current provisions

Original Zone of Higher Seismic Design Requirements – Eastern US

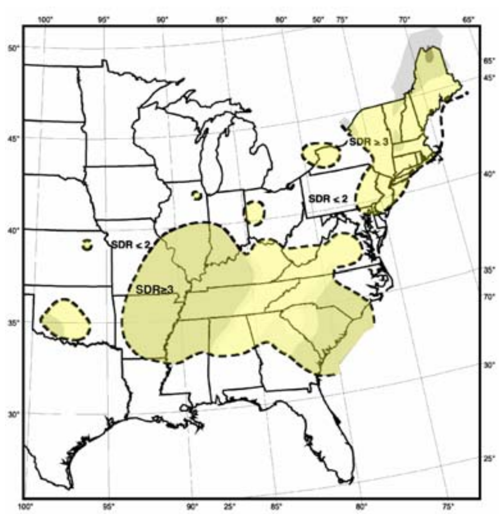

A Possible Revision to Seismic Design Boundaries – Eastern US

1500-year event

Hazard w/o soil factor

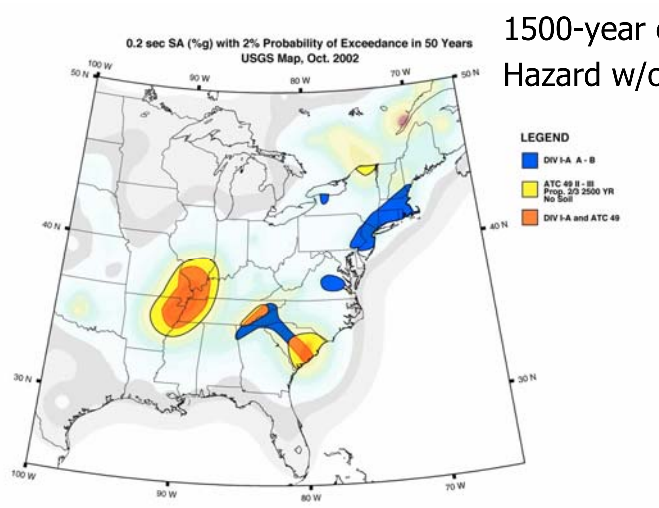

Conclusions

- Guidelines include many of the current "best practices" (a number of which were developed for special bridges)
- Design provisions are nationally consistent
- Designs produced have reasonable costs
- Guidelines provide reasonable platform for seismic design specifications

PRESENTATION 5

SEISMIC DESIGN PROCEDURE OF HIGHWAY BRIDGES – AN OVERVIEW

SEISMIC DESIGN PROCEDURE OF HIGHWAY BRIDGES -

A GEOTECHNICAL OVERVIEW

Thomas W. Fennessey, P.E.
Senior Materials Engineer
Geotechnical Section
Missouri Department of Transportation

Geotechnical and Bridge Seismic Design Workshop

New Madrid Seismic Zone Experience

October 28-29, 2004, Cape Girardeau, Missouri

1994 Northridge, CA EQ vs. 1895 Charleston, MO EQ

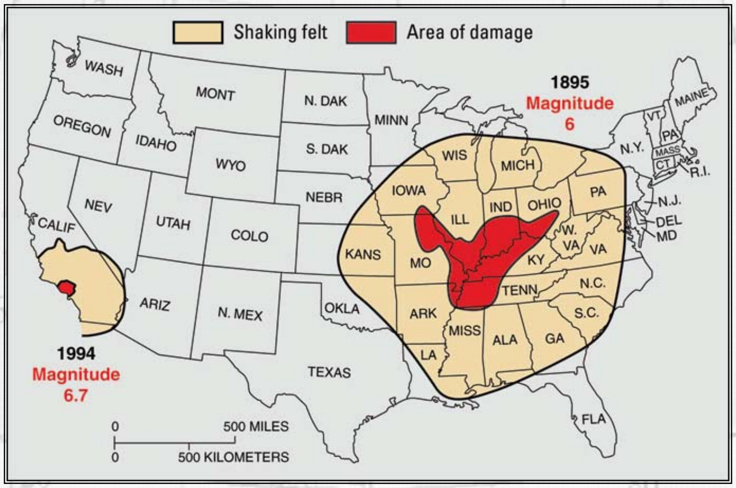

Source: http://geopubs.wr.usgs.gov/fact-sheet/fs017-03/

NATURAL HAZARDS MITIGATION INSTITUTE

MoDOT

UMR
UNIVERSITY OF MISSOURI-ROLLA

Peak Horizontal Acceleration in Rock, % g

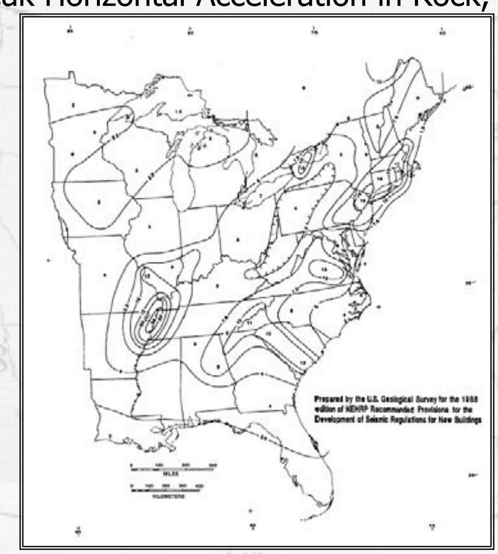

Source: AASHTO LRFD Bridge Design Specifications - Customary U.S Units – Third Edition- 2004

NATURAL HAZARDS MITIGATION INSTITUTE

MoDOT

UMR
UNIVERSITY OF MISSOURI-ROLLA

MoDOT Seismic Map

A = Peak Horizontal Acceleration in Rock, % g

Source: http://www.modot.mo.gov/business/manuals/documents/Section6.1.pdf

MoDOT Bridge Division Soil Design Parameters Request Form

Bridge Unit Request for Soil Properties

Job #: ______________
County: ______________
Bridge #: ______________
Route: ______________

N = N60 = SPT Blowcounts per 12" or per 300 mm to 60% machine efficiency for granular soil in Category A or for cohesive soil in Category A, B, C, or D.
N = (N1)60 = SPT Blowcounts per 12" or per 300 mm, corrected to 1 TSF overburden and to 60% machine efficiency for granular soil in Category B, C, or D.
ϕ = phi angle, internal angle of friction, degrees.
S_u = For clay, the undrained shear strength. For rock, the shear capacity, ksf or kPa.
γ = Weight per unit volume, pcf or kN/m³ (Saturated unit weight below water table, Natural unit weight above water table).
E = Elastic Modulus of soil, ksf or kPa, where: E = 2*(1+v)*G and v = Poisson's ratio = 0.35 (sand), 0.45 (clay), or 0.20 (rock).
Em = Rock mass modulus for intact rock, ksf or kPa (AASHTO Div. I, Section 4.4.8.2).
RQD = Rock Quality Designation, %.

Bent No's.	Structural Type (Seismic Category)	N #-#-#	ϕ (degrees)	S_u (ksf or kPa)	γ (pcf or kN/m³)	E or Em (ksf or kPa)	RQD (%)	Allowable friction (ksf or kPa)	Allowable Bearing (ksf or kPa)	* F.S. Liquefaction	Water table Elev. (ft or m)	** AASHTO soil profile type
	Bridge (Category A)	X									X	
	Bridge (Category B, C, or D)	X	X	X	X	X				X	X	X
	Drilled Shafts (Category A)	X	X	X	X	X	X	X	X		X	
	Drilled Shafts (Category B, C, or D)	X	X	X	X	X	X	X	X	X	X	X
	Retaining Wall (Category A)	X	X		X						X	
	Retaining Wall (Category B, C, or D)	X	X		X						X	

*** Provide safety factors for liquefaction for the recommended seismic magnitude at the bridge site. The magnitude shall be based on the probabilities of exceedance of 10% in 50 years (approximately corresponding to a return period of 500 years).**
**** Provide soil profile type (type I, II, III, or IV based on AASHTO Div. I-A, Sec. 3.5) at each boring location.**
Note: If an item above is checked, then "X" indicates the soil properties required at each boring location.

Other required soil properties:
(or special instructions)
1: ______________
2: ______________
3: ______________
4: ______________

Source: http://www.modot.mo.gov/business/manuals/documents/Section6.1.pdf

Failing 1500 Drill Rig

Typical Boring Data

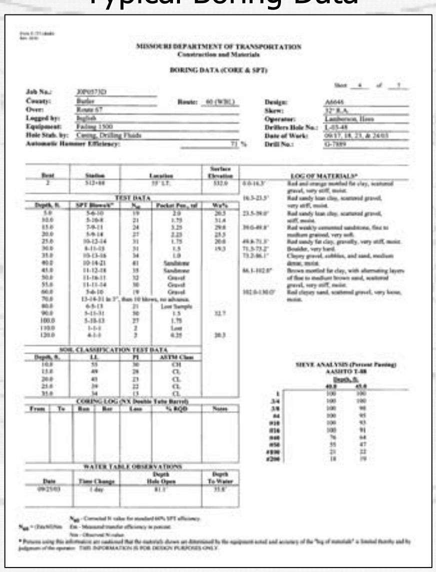

MISSOURI DEPARTMENT OF TRANSPORTATION
Construction and Materials

BORING DATA (CORE & SPT)

Sheet 4 of 7

Job No.: J0P0573D	Route: 60 (WBL)	Design:	A6646
County: Butler		Skew:	32° R.A.
Over: Route 67		Operator:	Lamberson, Hess
Logged by: English		Drillers Hole No.:	L-03-48
Equipment: Failing 1500		Date of Work:	09/17, 18, 23, & 24/03
Hole Stab. by: Casing, Drilling Fluids		Drill No.:	G-7889
Automatic Hammer Efficiency: 71 %			

Bent	Station	Location	Surface Elevation
2	512+88	35' LT.	332.0

TEST DATA

Depth, ft.	SPT Blows/6"	N_{60}	Pocket Pen., tsf	W%
5.0	5-6-10	19	2.0	20.5
10.0	5-10-8	21	1.75	31.4
15.0	7-9-11	24	3.25	29.6
20.0	5-9-14	27	2.25	23.3
25.0	10-12-14	31	1.75	20.6
30.0	8-11-13	31	1.5	19.3
35.0	10-13-16	34	1.0	
40.0	10-14-21	41	Sandstone	
45.0	11-12-18	35	Sandstone	
50.0	11-16-11	32	Gravel	
55.0	11-11-14	30	Gravel	
60.0	5-6-10	19	Gravel	
70.0	13-14-21 in 3", then 10 blows, no advance.			
80.0	6-5-13	21	Lost Sample	
90.0	5-11-31	50	1.5	32.7
100.0	5-10-13	27	1.75	
110.0	1-1-1	2	Lost	
120.0	4-1-1	2	0.25	20.3

LOG OF MATERIALS*

0.0-16.3'	Red and orange mottled fat clay, scattered gravel, very stiff, moist.
16.3-23.5'	Red sandy lean clay, scattered gravel, very stiff, moist.
23.5-39.0'	Red sandy lean clay, scattered gravel, stiff, moist.
39.0-49.8'	Red weakly cemented sandstone, fine to medium grained, very soft.
49.8-71.3'	Red sandy fat clay, gravelly, very stiff, moist.
71.3-73.2'	Boulder, very hard.
73.2-86.1'	Clayey gravel, cobbles, and sand, medium dense, moist.
86.1-102.0'	Brown mottled fat clay, with alternating layers of fine to medium brown sand, scattered gravel, very stiff, moist.
102.0-130.0'	Red clayey sand, scattered gravel, very loose, moist.

SOIL CLASSIFICATION TEST DATA

Depth, ft.	LL	PI	ASTM Class
10.0	55	30	CH
15.0	49	28	CL
20.0	45	23	CL
25.0	39	22	CL
35.0	34	13	CL

CORING LOG (NX Double Tube Barrel)

From	To	Run	Rec	Loss	% RQD	Notes

SIEVE ANALYSIS (Percent Passing)
AASHTO T-88

	Depth, ft. 40.0	45.0
1	100	100
3/4	100	100
3/8	100	98
#4	100	95
#10	100	93
#16	100	91
#40	76	64
#50	55	47
#100	21	22
#200	18	19

WATER TABLE OBSERVATIONS

Date	Time Change	Depth Hole Open	Depth To Water
09/25/03	1 day	81.1'	35.8'

N_{60} = (Em/60)Nm
N_{60} - Corrected N value for standard 60% SPT efficiency.
Em - Measured transfer efficiency in percent.
Nm - Observed N value.

* Persons using this information are cautioned that the materials shown are determined by the equipment noted and accuracy of the "log of materials" is limited thereby and by judgment of the operator. THIS INFORMATION IS FOR DESIGN PURPOSES ONLY.

Typical Earthquake Boring Log

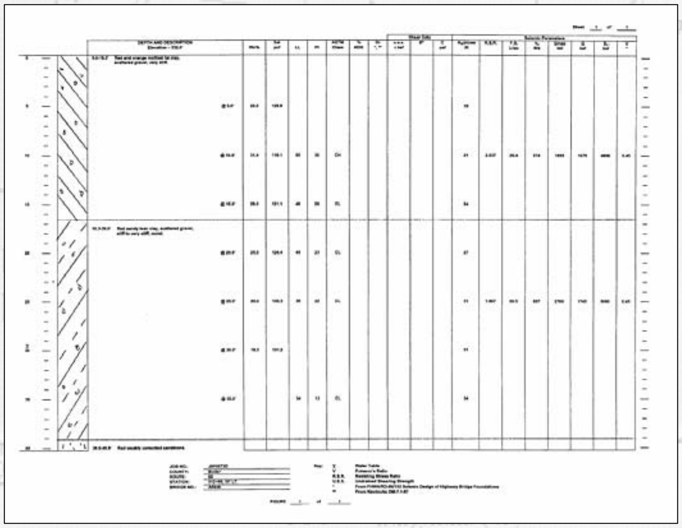

Typical Earthquake Boring Log Data

- Moisture Content
- Saturated Unit Weight
- Liquid Limit
- Plasticity Index
- ASTM Classification
- Percent < #200 Sieve
- Relative Density
- Undrained Shear Strength
- Friction Angle
- Cohesion
- Blow Count (N_{60})
- Resisting Stress Ratio
- Liquefaction F.S.
- Shear Wave Velocity
- Maximum Shear Modulus
- Shear Modulus
- Young's Modulus
- Poisson's Ratio

Hogentolgler Track Mounted Cone Penetrometer System

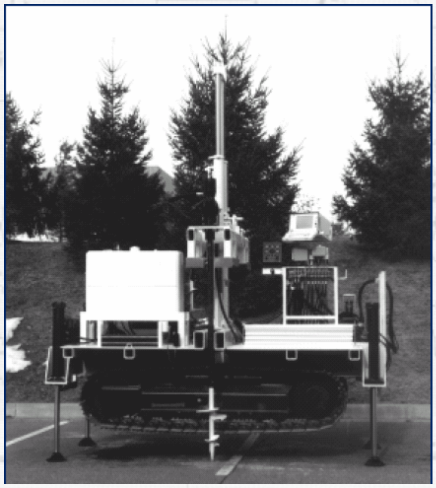

Typical Cone Penetrometer Data

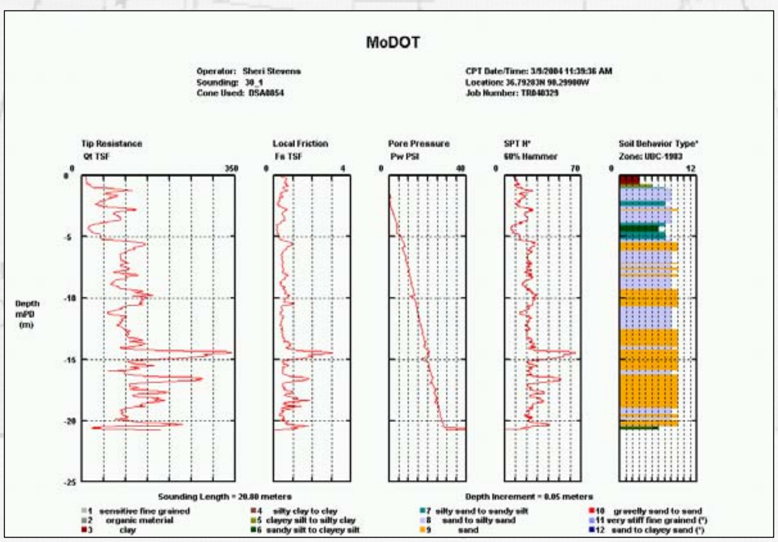

Typical Seismic Cone Penetrometer Data

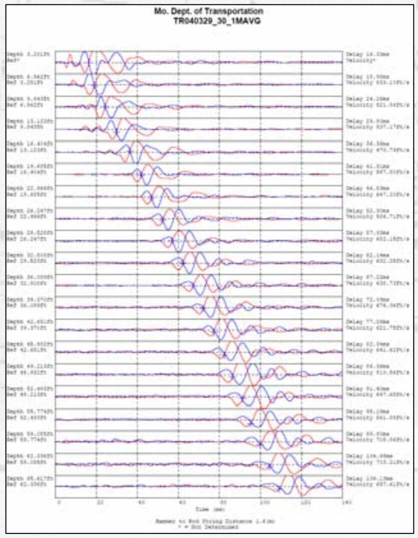

Spectral Analysis of Surface Waves

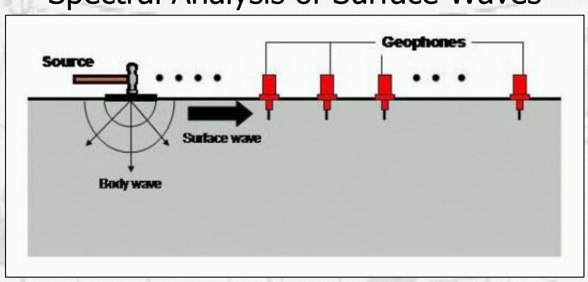

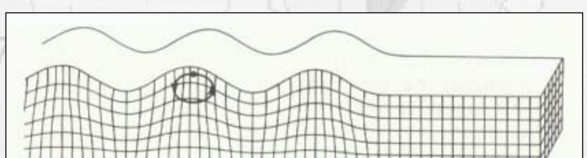

Rayleigh Wave Particle Motion

Plan View – St. Francis River Site

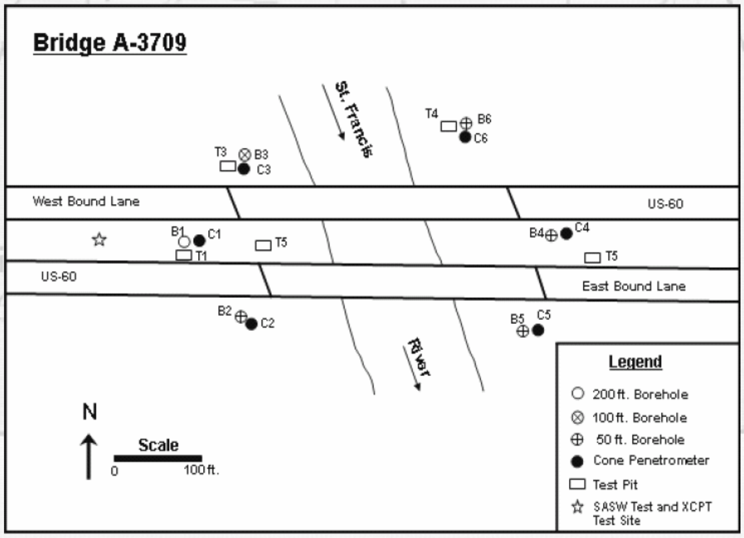

Shear Wave Velocity Profile - St. Francis River Site

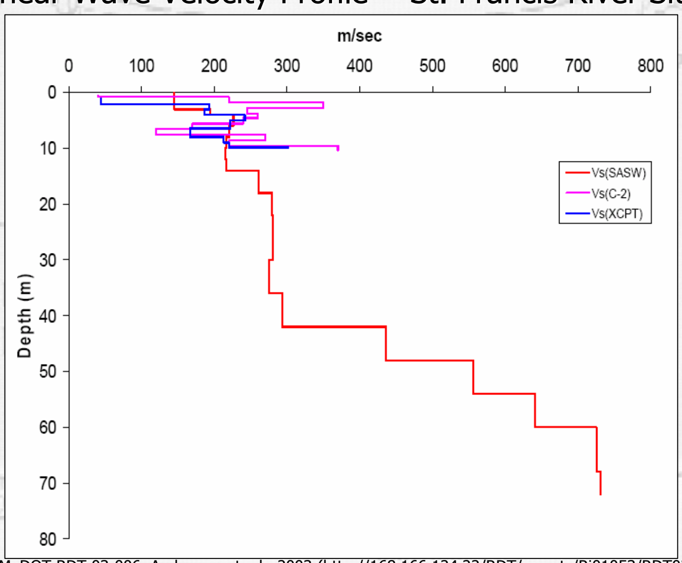

Source: MoDOT RDT 03-006, Anderson, et. al., 2003 (http://168.166.124.22/RDT/reports/Ri01053/RDT03006.pdf)

Earthquake Effects

Loma Prieta, CA
1989

SEISMIC DESIGN AND RETROFITTING FOR MISSOURI HIGHWAY BRIDGES

Presenting by

Anousone Arounpradith, MSCE, P.E.
Structural Project Manager, Bridge Division
Missouri Dept. of Transportation

Geotechnical and Bridge Seismic Design Workshop
New Madrid Seismic Zone Experience
October 28-29, 2004, Cape Girardeau, Missouri

Outlined Topics

- Bridge Overview
- Seismic Design for new bridges
- Seismic Retrofitting for existing bridges
- Summary

Bridge Overview

- First seismic design in 1989
- Structures in Missouri
  - Over 10,000 bridges in the state inventory
  - Currently 2,300 (23%) bridges in Seismic Cat. B, C & D
- Typical Bridges in Missouri
  - Plate Girder, PS I-Beams, Solid Slab, etc.
  - Multiple column bents, pile bents (steel and concrete)
  - Spread and Pile Footings

PS I-Beams Superstructure

Plate Girder Superstructure


MoDOT
Multiple Concrete Column Bents


MoDOT
Multiple (Steel) Pile Cap Bents
A6241T I-44 at Six Flags Rd.
bent 4 looking West
3/5/03 MVC-004F

Integral (monolithic) Abutment

Non-integral (free-standing) Abutment

Steel Pile Footings w/anchors

Spread Footings on Rock

Outlined Topics

- Bridge Overview
- Seismic Design for new bridges

Seismic Design

- Design References
  - 16th AASHTO Div. I-A (1996) and interims
  - Lam and Martin (1986)
  - Priestley and Seible (1996)
  - Wilson, J.C. (1988)
  - Etc.

- Seismic Map for Missouri
  - Rock Acc. Coeff. = 0.10 to 0.36
  - <1/3 of Missouri in Seismic Cat. B, C & D

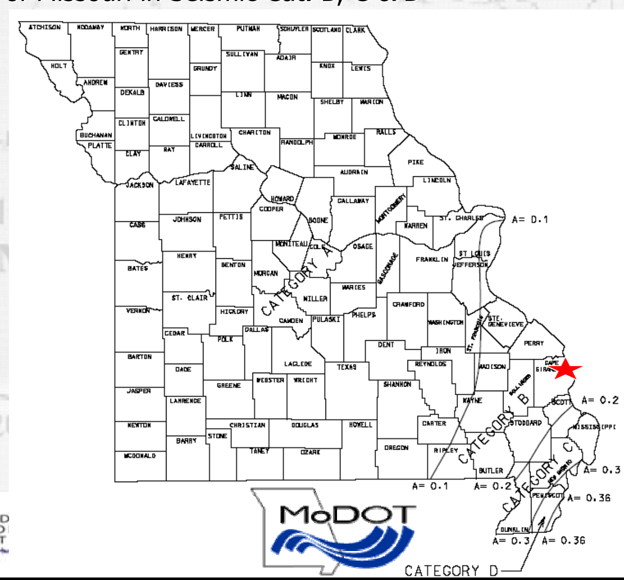

NATURAL HAZARD MITIGATION INSTITUTE

MoDOT

UMR
UNIVERSITY OF MISSOURI-ROLLA

Bridge Layout

- Multiple spans bridge with large skew
- Monolithic abutments with interior wing walls
- Multiple column bents
- Pile footings

Seismic Design

- Analysis/Design
  - Multi-mode response spectrum method
  - Liquefaction
  - Soil-Foundation Interaction
    - Footing springs
    - Abutment springs
    - Pile springs

Seismic Design

- Spread Footing Springs (Lam & Martin)
  - Equivalent circular footing
  - Six linear springs
    - 3 Translations &
    - 3 Rotations

$$[K] = (\beta)(\alpha)[Ko]$$

Ko – diagonal stiffness

β – embedment factor

α – shape correction factor

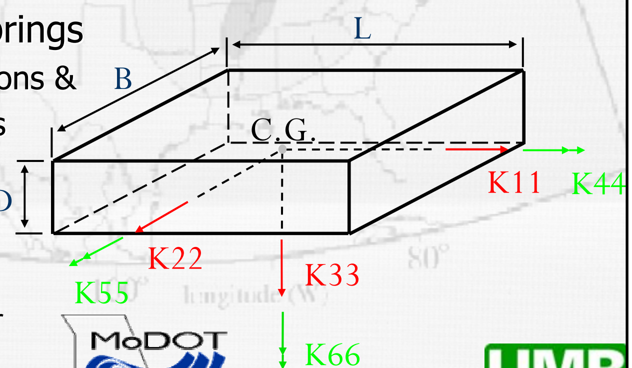

Seismic Design

- Abutment Springs
  - Wilson's models (1988)
  - 3 linear springs
    - Translation and
    - Two Rotations

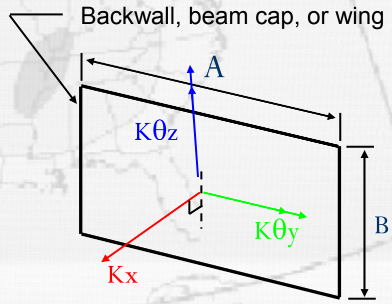

Pile Axial Spring

- SPILE Program (Urzua, 1993)
  - Piles subject to axial loads
  - Non-linear curve for soil-pile interaction
  - Equivalent Linear Spring (Secant Stiffness Approach, Q/2)

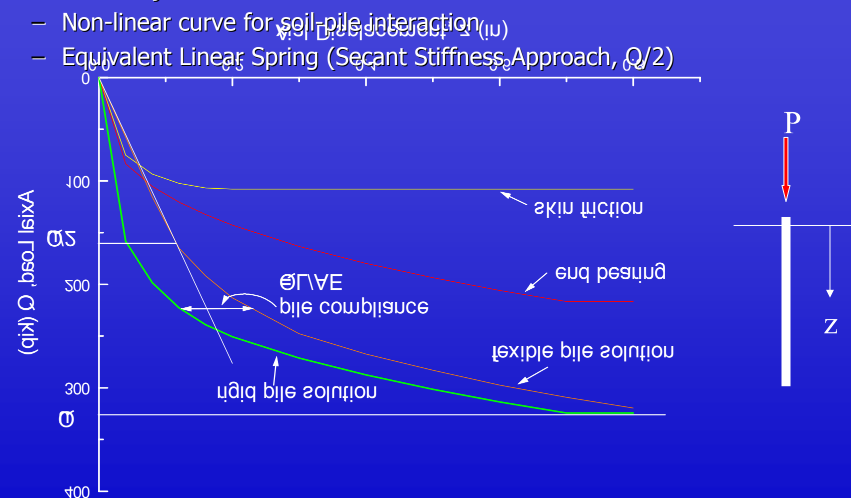

Pile Lateral & Rotational Springs

- COM624P Program (Wang & Reese, 1993)
  - Piles subject to lateral loads
  - Non-linear curve for soil-pile interaction
  - Equivalent Linear Spring (Secant Stiffness Approach, P(Mu)/2)

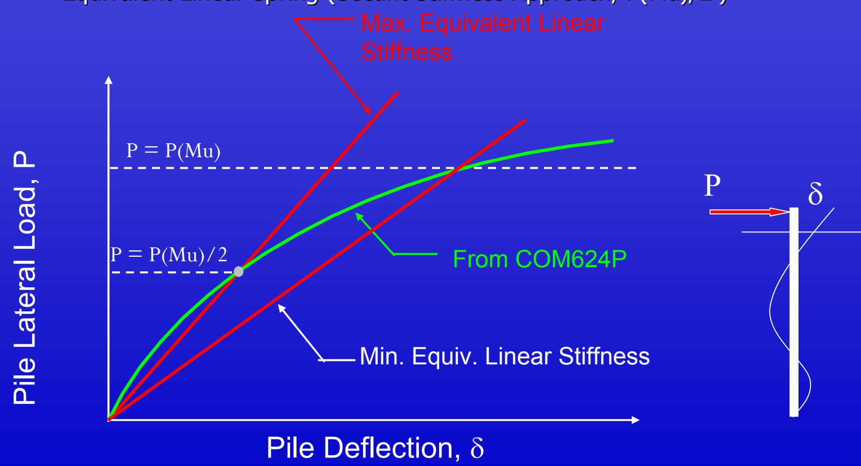

Foundation Spring Model

- Drilled shafts
- Footing on piles or rock

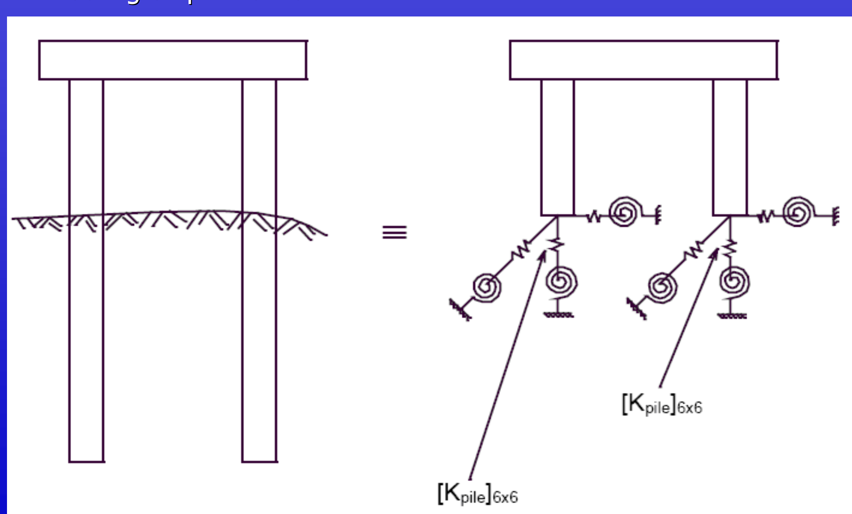

Abutment Springs

- Many equiv. linear springs
- Master joint at C.G. of superstructure

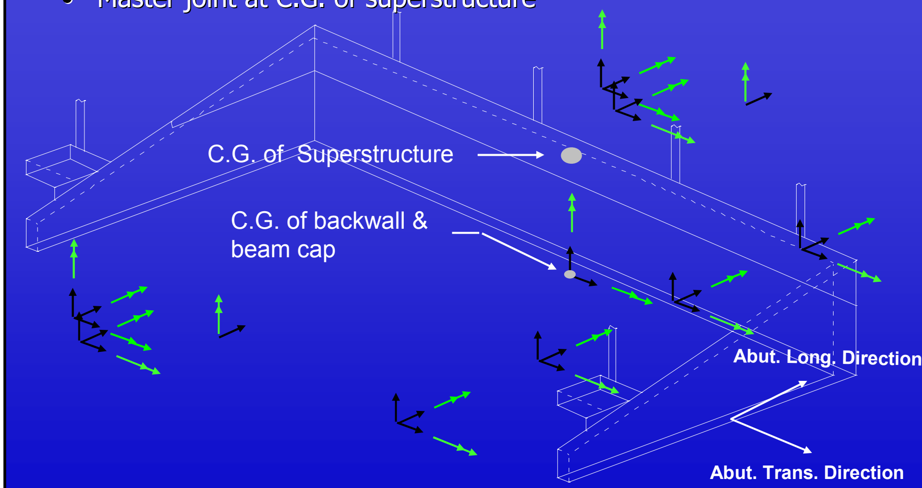

Seismic Design

- Analysis/Design (cont'.)
  - Rigid Body Transformation Technique
    - Combine springs (stiffness) at a master joint
    - Reduce # of degree-of-freedoms
    - Take account of coupling effects
    - Demand seismic forces for abut.'s components

Structure Modeling

- Multi-mode Response Spectrum Analysis
- [6x6] stiffness at abutment’s master joint
- [6x6] stiffness at foundation’s master joint
- “Full-Zero” abutment springs – 2 separated seismic analyses

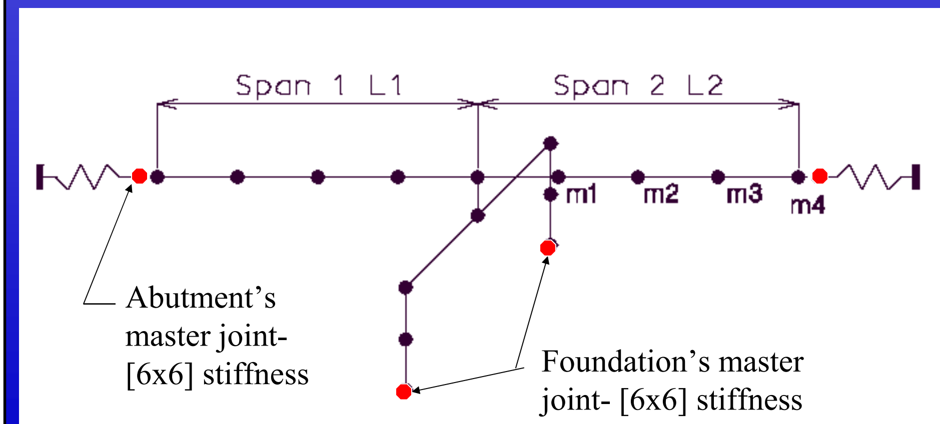

Seismic Design

- Analysis/Design (cont’.)
  - Iterative Abutment Procedure
    - Check soil passive pressure <7.7 ksf

NATURAL HAZARDS MITIGATION INSTITUTE

MoDOT

UMR UNIVERSITY OF MISSOURI-ROLLA

Passive Soil Pressure vs. Abutment Displ.

- Max. passive soil pressure 7.7 ksf at abutments
- Reduce abutment springs when abutment's pressure > 7.7 ksf

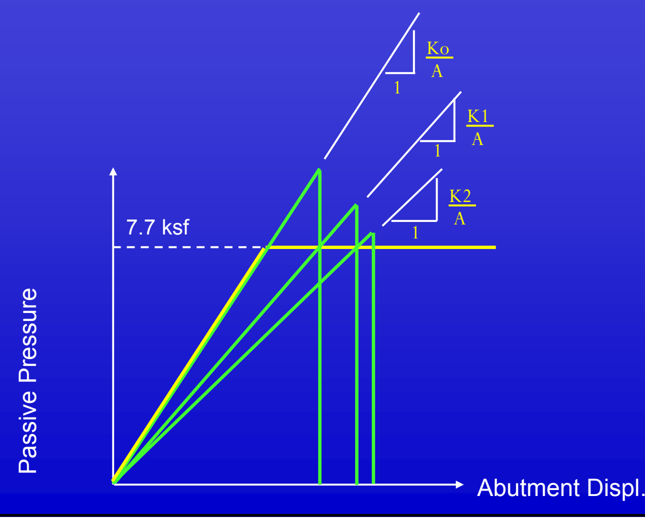

Seismic Design

- Analysis/Design (cont'.)
  - Iterative Abutment Procedure
    - Check soil passive pressure <7.7 ksf
    - Check pile stresses < allowable stresses
    - Check abutment's displacement at the master joint
  - Min. support length at expansion gaps
  - Consider both elastic and plastic designs
  - Design all main connections
    - Column to footing or beam cap (T-Joint Design)
    - Anchor bolts, shear blocks, crossframes
    - Etc.

Column-Beam Cap (T-Joint) Connection

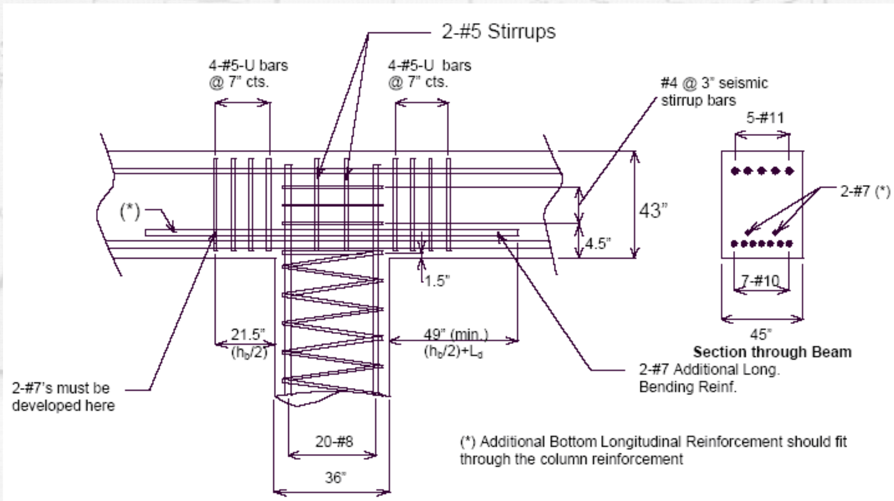

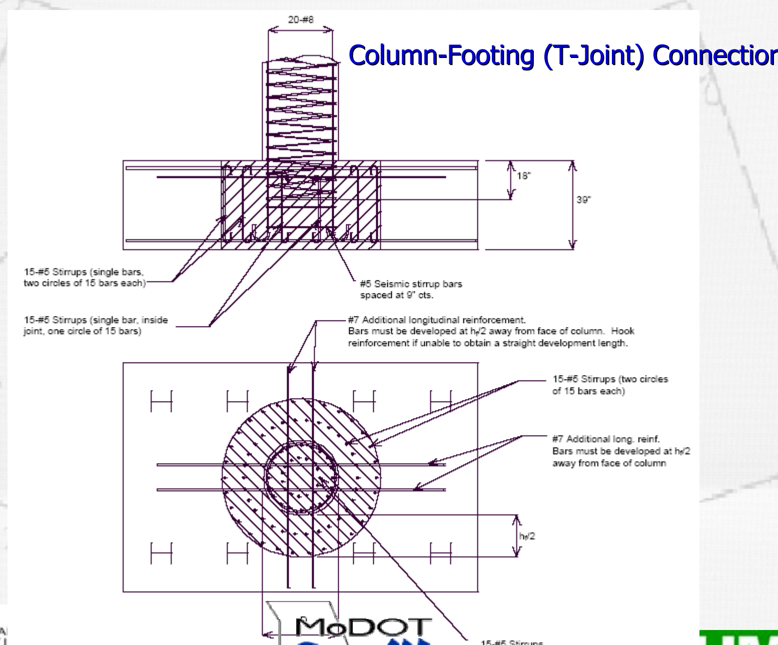

Outlined Topics

- Bridge Overview
- Seismic Design for new bridges
- Seismic Retrofit for existing bridges

SEISMIC RETROFIT

- Major bridge rehabilitations
  - Deck replacement
  - Bridge widening
  - Case-by-case basis
- Retrofitting vs. New bridge
  - Evaluate Pros and Cons
  - Cost-effective comparison
  - Availability of funding

SEISMIC RETROFIT

- Retrofit design
  - FHWA-RD-94-052 (May 1995)
  - Multi-mode Response Spectrum analysis
  - Capacity/Demand Ratio
- Types of Retrofitting
  - Restrainers
  - Bearing replacements
  - Deepen beam caps
  - Steel column jacketing
  - Widen footings

SEISMIC RETROFIT

- Restrainer System

SEISMIC RETROFIT

- Steel Column Jacketing

SEISMIC RETROFIT

- Retrofitting footings

Outlined Topics

- Bridge Overview
- Seismic Design for new bridges
- Seismic Retrofit for existing bridges
- Summary

SUMMARY

- Multi-mode Response Spectral Analysis
- Soil-Foundation Interaction
- Rigid Body Transformation
- T-Joint Connection Design
- Rigorous Analysis and Design
- Time-consuming Design

Questions ?

More Information,

Website: www.modot.state.mo.us

Look for "Business/bridge design/section 6.1 & 6.2"

Email: Anousone.Arounpradith@modot.mo.us.gov

Thank you!

PRESENTATION 6

GENERAL GEOLOGIC SETTING AND SEISMICITY OF THE FHWA PROJECT SITE IN THE NEW MADRID SEISMIC ZONE

General Geologic Setting and Seismicity of the FHWA Project Site in the New Madrid Seismic Zone

David Hoffman
University of Missouri – Rolla
Natural Hazards Mitigation Institute
Civil, Architectural & Environmental Engineering Department

dhoffman@umr.edu

NATURAL HAZARDS MITIGATION INSTITUTE

UMR

General Geologic Setting and Seismicity of the FHWA Project Site in the New Madrid Seismic Zone

- Central and Eastern United States Earthquake Hazard
- Regional geology, topography and seismicity
- Mississippi Embayment and Reelfoot Rift (Mississippi Valley Graben)
- Stratigraphy
- Geologic structure, faults and seismicity
- Sandblows
- Attenuation
- Local site alluvial soils
- Important Considerations

NATURAL HAZARDS MITIGATION INSTITUTE

UMR

General Geologic Setting and Seismicity of the FHWA Project Site in the New Madrid Seismic Zone

- **Central and Eastern United States Earthquake Hazard**
- Regional geology, topography and seismicity
- Mississippi Embayment and Reelfoot Rift (Mississippi Valley Graben)
- Stratigraphy
- Geologic structure, faults and seismicity
- Sandblows
- Attenuation
- Local site alluvial soils
- Important Considerations

NATURAL HAZARDS MITIGATION INSTITUTE

UMR

Central and Eastern United States Earthquake Hazard

Hazard Map

•Based on geology and seismology

•Probabilistic map

Geologic Factors Affecting Ground Motion

•Earthquake magnitude

•Source mechanism

•Distance

•Condition of rock along transmission path

•Local site conditions

•Duration of shaking

NATURAL HAZARDS MITIGATION INSTITUTE

UMR

The Central and Eastern United States Earthquake Hazard

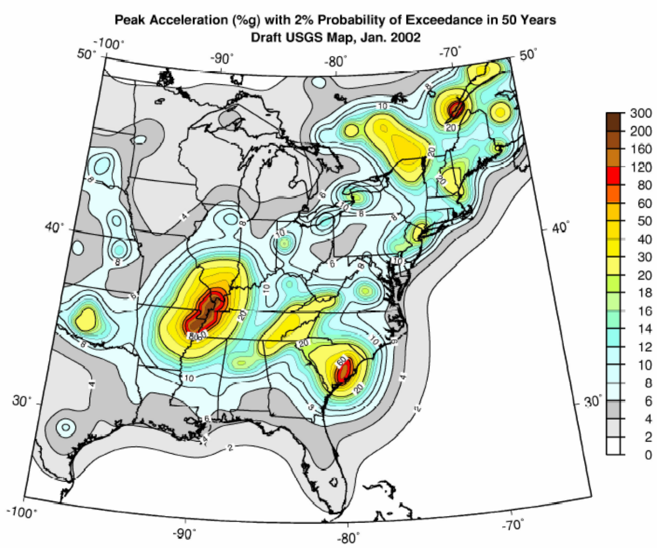

For Site Class B (amplification = 1.0)

Several areas of the Central and Eastern United States have know earthquake hazards. This is shown on engineering design maps.

FACTORS AFFECTING GROUND MOTION

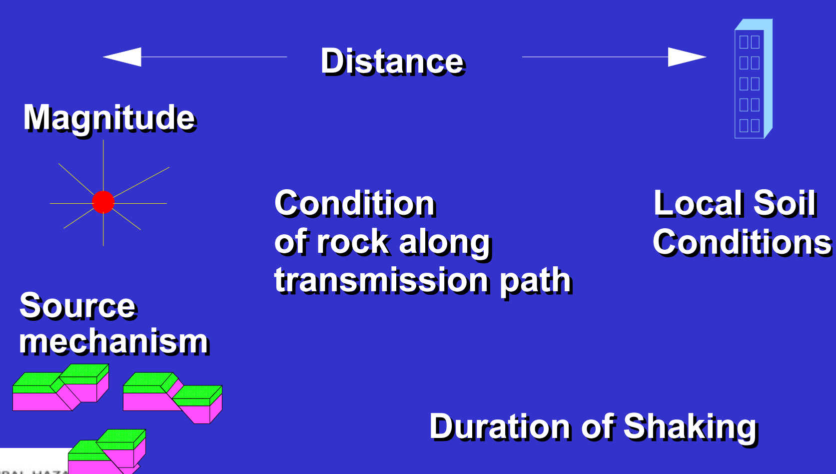

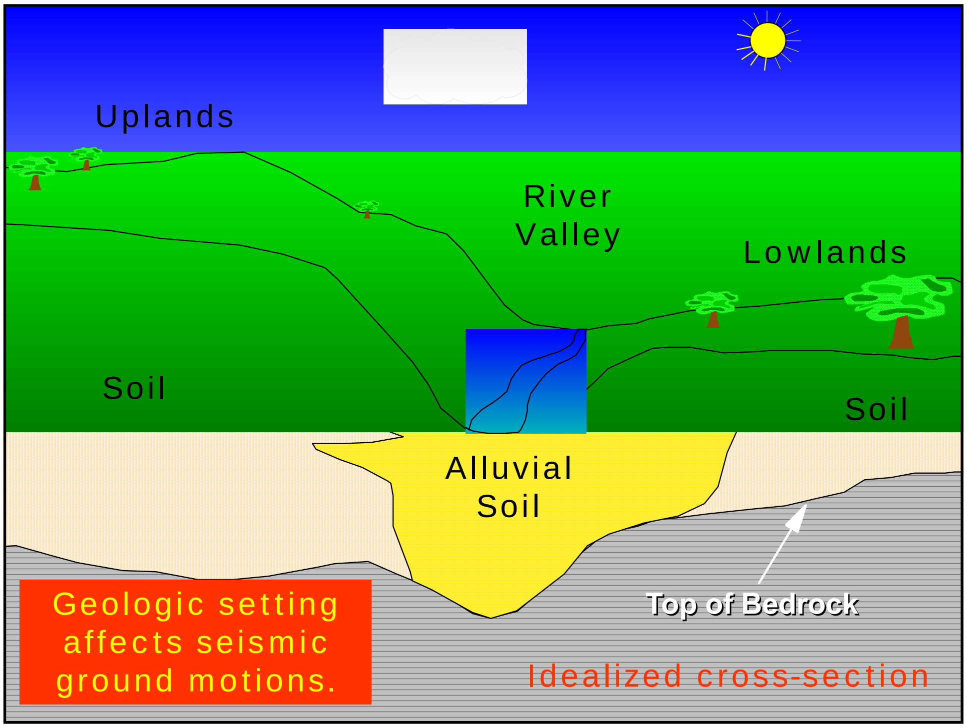
Uplands
River Valley
Lowlands
Soil
Soil
Alluvial Soil
Top of Bedrock
Geologic setting affects seismic ground motions.
Idealized cross-section

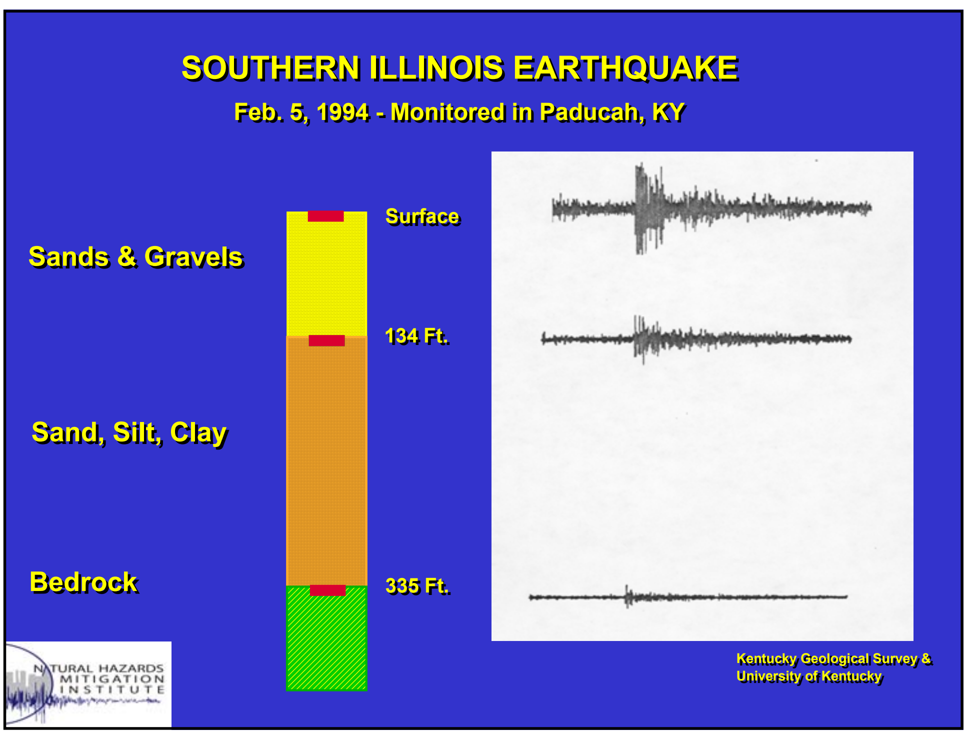
SOUTHERN ILLINOIS EARTHQUAKE
Feb. 5, 1994 - Monitored in Paducah, KY
Sands & Gravels
Sand, Silt, Clay
Bedrock
Surface
134 Ft.
335 Ft.
Kentucky Geological Survey & University of Kentucky
NATURAL HAZARDS MITIGATION INSTITUTE

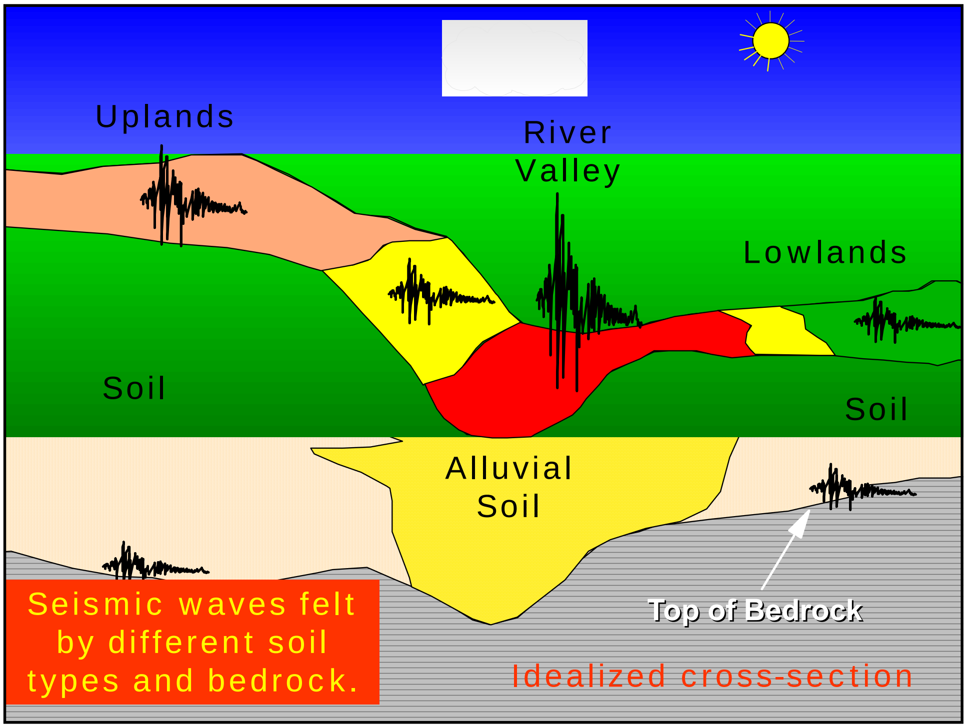

Soil Type and Properties Affect Site Amplification

Increasing Amplification

Soil Profile Type	Average Shear Wave Velocity (Ft/Sec)	Possible Amount of Amplification times bedrock Ground Motions
A	>5,000	0.8
B	2,500 - 5,000	1.0
C	1,200 - 2,500	1.3 - 1.7
D	600 - 1,200	1.5 - 2.4
E	<600	2.4 - 3.5
F	Not Applicable	Site Specific Investigation should be performed - can be <1 to as high as 10X

NATURAL HAZARDS MITIGATION INSTITUTE

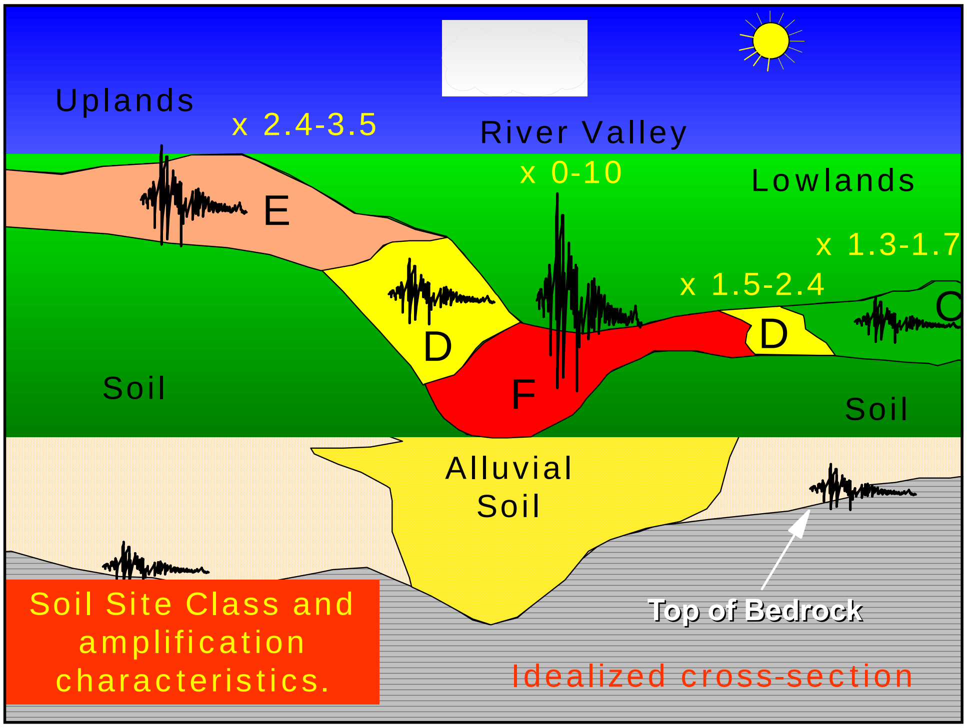
Uplands
x 2.4-3.5
River Valley
x 0-10
Lowlands
E
x 1.3-1.7
x 1.5-2.4
D
D
C
F
Soil
Soil
Alluvial
Soil
Top of Bedrock
Soil Site Class and amplification characteristics.
Idealized cross-section

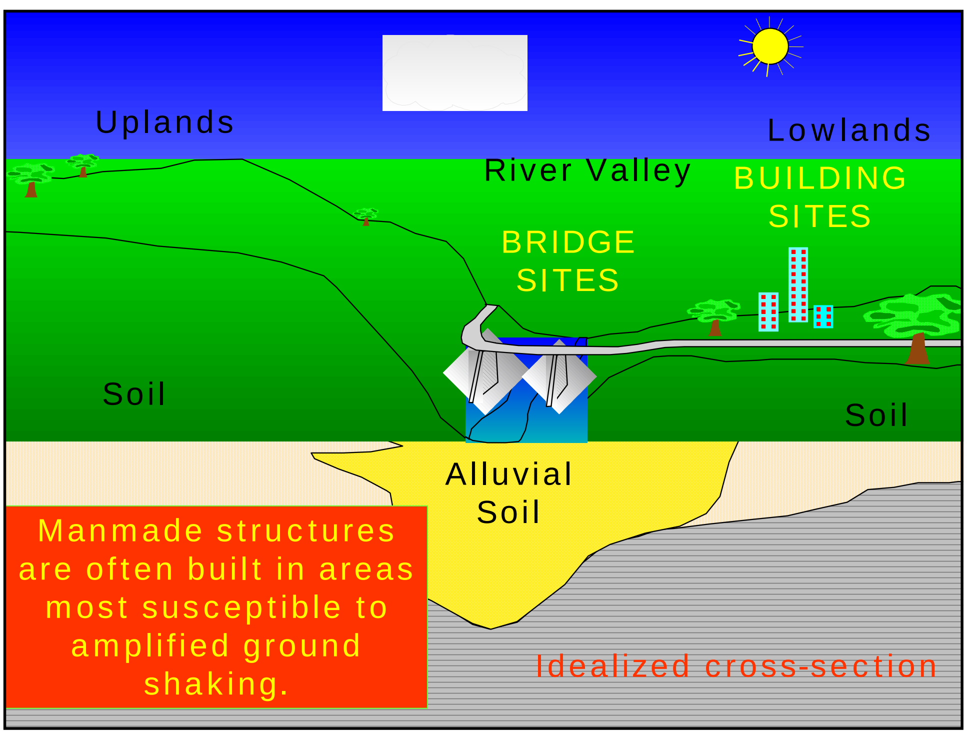
Uplands
Lowlands
River Valley
BUILDING SITES
BRIDGE SITES
Soil
Soil
Alluvial
Soil
Manmade structures are often built in areas most susceptible to amplified ground shaking.
Idealized cross-section

General Geologic Setting and Seismicity of the FHWA Project Site in the New Madrid Seismic Zone

- Central and Eastern United States Earthquake Hazard
- **Regional geology, topography and seismicity**
- Mississippi Embayment and Reelfoot Rift (Mississippi Valley Graben)
- Stratigraphy
- Geologic structure, faults and seismicity
- Sandblows
- Attenuation
- Local site alluvial soils
- Important Considerations

NATURAL HAZARDS MITIGATION INSTITUTE

UMR

Regional geology, topography and seismicity

Geology

- Stable contential interior
  - Older rocks
  - Glacial sediments
- Gulf Coastal Plain
- Mississippi Embayment
  - New Madrid Seismic Zone

Topography

- Very flat

Seismicity

- Northern Mississippi Embayment

NATURAL HAZARDS MITIGATION INSTITUTE

UMR

General Geology of the New Madrid Seismic Zone and Mississippi Embayment Area

The geology and related seismicity create the earthquake hazard.

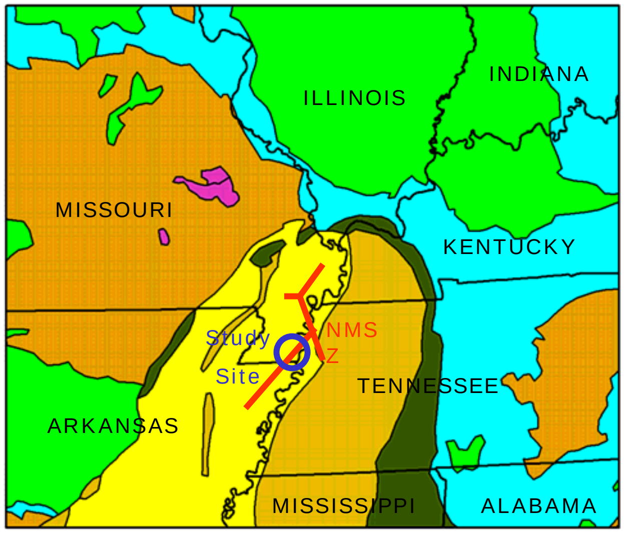

Mississippi Embayment

Soft Sediments
- Quaternary alluvium
- Tertiary
- Cretaceous

Older Bedrock
- Mississippian
- Pennsylvanian
- Ordovician
- Precambrian

Ground Elevation and Topographic Relief In the Central United States Area

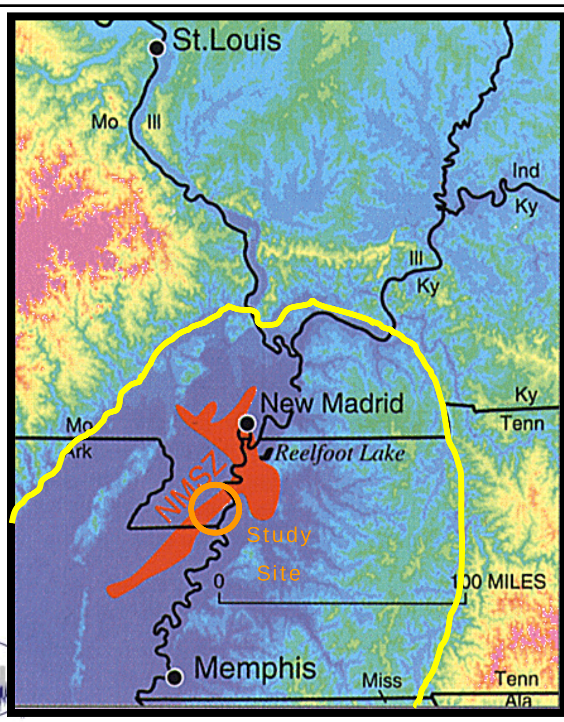

The New Madrid Seismic Zone (red) is in the flat lowlands (purple) of the Mississippi Embayment (yellow line). The Mississippi Embayment is a depressed area due to a weakness in the North American tectonic plate crust.

Central United States Seismicity & General Geology

Seismicity is associated with the Mississippi Embayment crustal weakness.

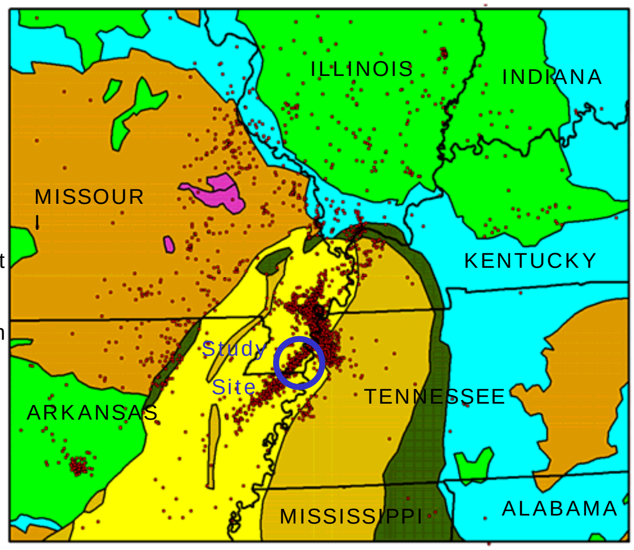

Mississippi Embayment

Soft Sediments

- Quaternary alluvium
- Tertiary
- Cretaceous

Older Bedrock

- Mississippian
- Pennsylvanian
- Ordovician
- Precambrian

● Earthquake Epicenters Since 1994

General Geologic Setting and Seismicity of the FHWA Project Site in the New Madrid Seismic Zone

- Central and Eastern United States Earthquake Hazard
- Regional geology, topography and seismicity
- **Mississippi Embayment and Reelfoot Rift (Mississippi Valley Graben)**
- Stratigraphy
- Geologic structure, faults and seismicity
- Sandblows
- Attenuation
- Local site alluvial soils
- Important Considerations

Mississippi Embayment and Reelfoot Rift (Mississippi Valley Graben)

Mississippi Embayment

- Basin with thick soft young sediments
- Hard bedrock very deep
- Flat lowlands and flat to genteelly rolling uplands

Reelfoot Rift (Mississippi Valley Graben

- Old weakness in Earth crust
- Identified by geoghysical methods
  - Magnetic signature
  - Gravity signature
- Location of seismicity

NATURAL HAZARDS MITIGATION INSTITUTE

UMR

Mississippi Embayment & Central United States Seismicity

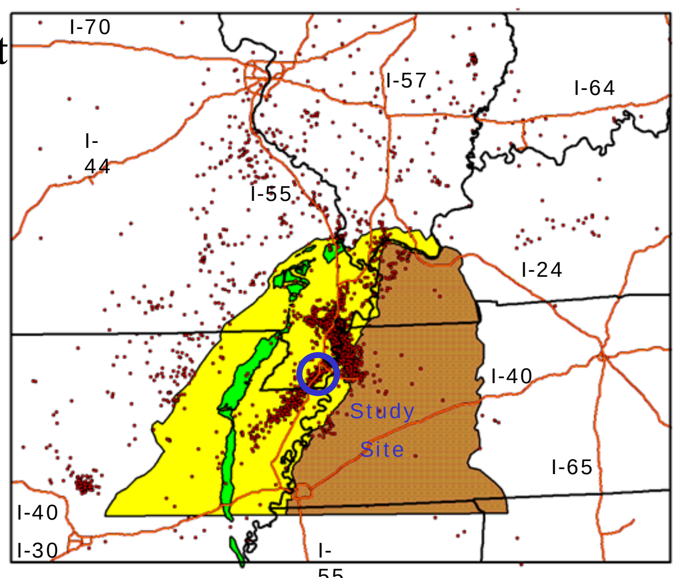

Lowlands: Alluvium

Uplands: Crowleys Ridge

Uplands: Kentucky & Tennessee

Earthquake Epicenters Since 1994

Interstate Highways

NATURAL HAZARDS MITIGATION INSTITUTE

UMR

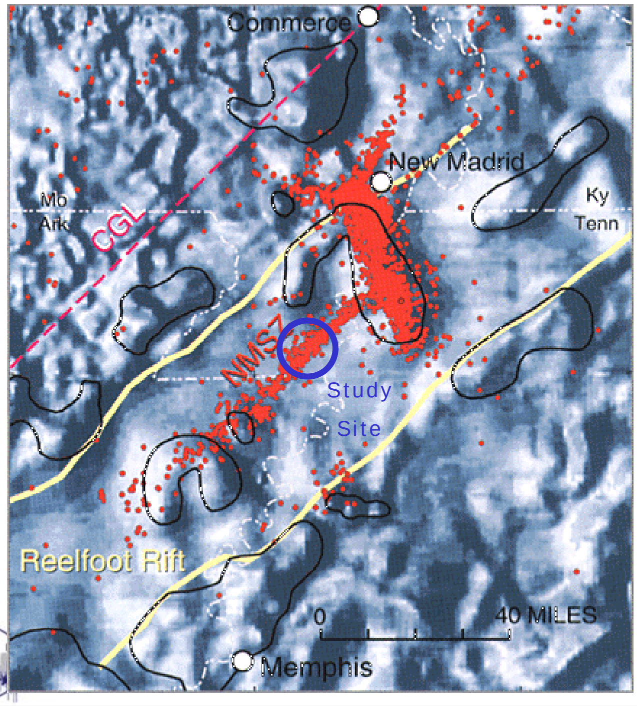

Magnetic Intensity Map Showing Reelfoot Rift and Associated New Madrid Seismic Zone Seismicity

3-D View of Reelfoot Rift

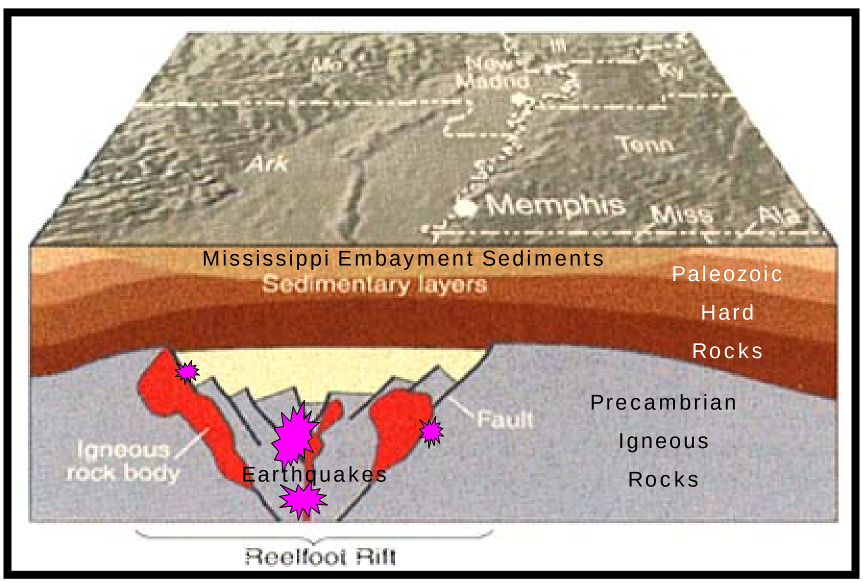

NATURAL HAZARDS MITIGATION INSTITUTE

UMR

General Geologic Setting and Seismicity of the FHWA Project Site in the New Madrid Seismic Zone

- Central and Eastern United States Earthquake Hazard
- Regional geology, topography and seismicity
- Mississippi Embayment and Reelfoot Rift (Mississippi Valley Graben)
- **Stratigraphy**
- Geologic structure, faults and seismicity
- Sandblows
- Attenuation
- Local site alluvial soils
- Important Considerations

Stratigraphy

Stratigraphic Column

- Alluvium
- Tertiary and Cretaceous unconsolidated sediments
- Bedrock

Structural Contour Maps

- Limited deep data
- Contours for various strata
- Profile
- Newer data sources

Generalized Stratigraphy of the Northern Mississippi Embayment

- Clay (unconsolidated)
- Silt (unconsolidated)
- Sand (unconsolidated)
- Gravel (unconsolidated)
- Sedimentary Rocks
- Precambrian Rocks

SOURCES
Hosman and Weiss, 1991
Crone, 1981
Grohskopf, 1955

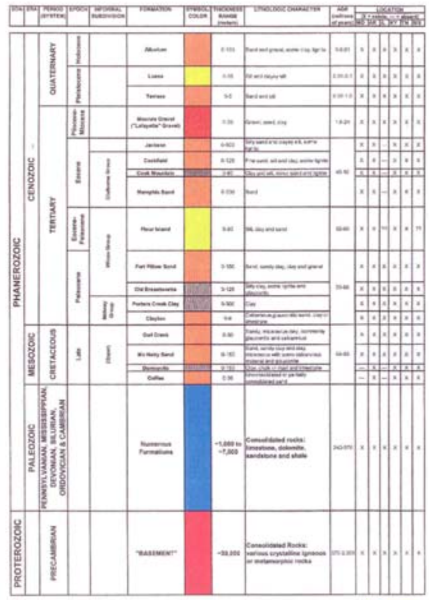

UMR

COLUMNAR SECTION

Southeastern Missouri Mississippi Embayment Area

ERA	SYSTEM		FORMATION	MAXIMUM THICKNESS (in feet)	LITHOLOGIC CHARACTER
CENOZOIC	QUATERNARY		Alluvium	275	Sand and gravel, some clay, lignite.
			Loess	80	Silt, yellow-brown.
	TERTIARY		"Lafayette"	60	Gravel, sand, clay.
		WILCOX GROUP	Holly Springs ? Ackerman ?	1300	Sand, several well-developed clay zones, thick basal sand.
		MIDWAY GROUP	Porters Creek	650	Clay, blue-gray, conchoidal fracture, siderite and silt in upper portion. Glauconitic and calcareous in lower portion.
			Clayton	15	Limestone and calcareous clay, fossiliferous, glauconitic.
MESOZOIC	CRETACEOUS		Owl Creek	70	Clay, brown, sandy, glauconitic. Very fossiliferous.
			Mc Nairy (Ripley)	250	Sand, sandy clay, glauconitic, fossiliferous.
			Ozan ? Marlbrook-Saratoga ?	250	Sand, calcareous sand and clay.
			Bailey	50	Limestone, very cherty.

NATURAL HAZARDS MITIGATION INSTITUTE

Paleozoic and Older Rocks

UMR

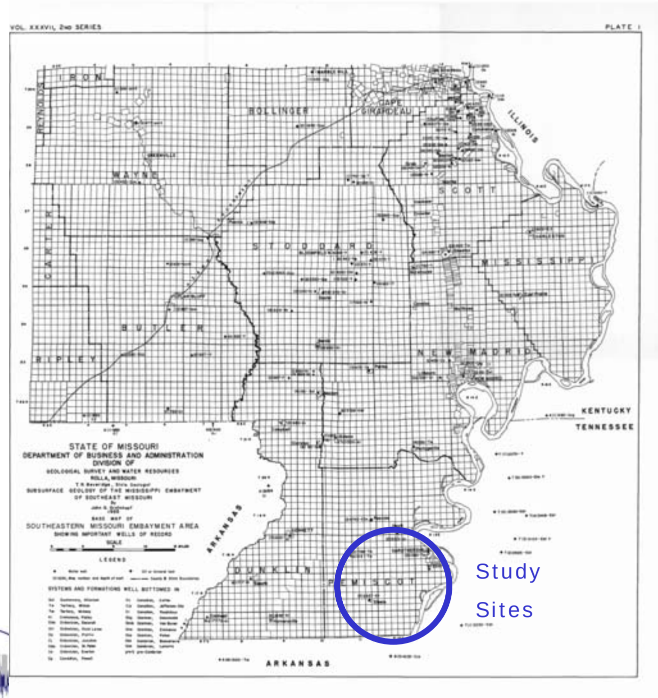

Southeast Missouri Mississippi Embayment Area Showing Important Deep Wells (Grohskopf, 1955)

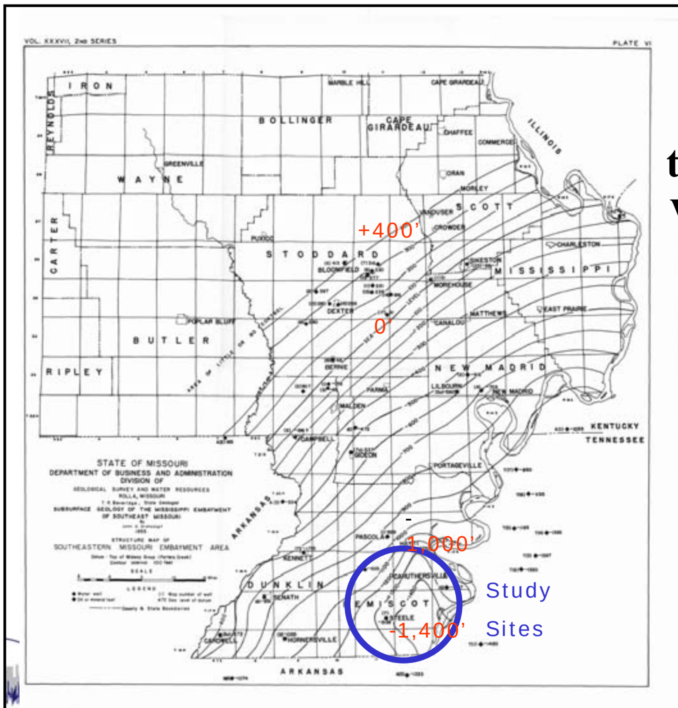

Structural Contours on the Base of the Wilcox Group or Top of the Midway Group (Grohskoph, 1955)

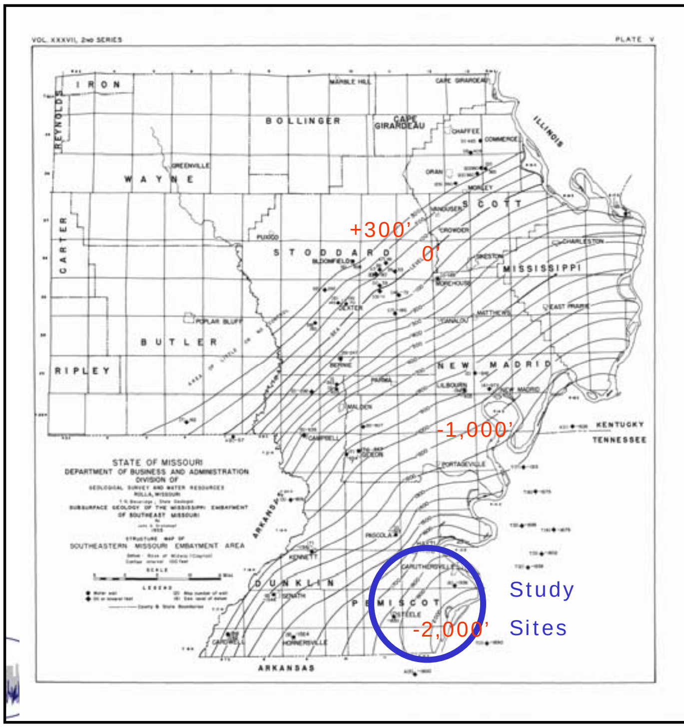

Structural Contours on he Base of the Midway Group or Top of the Cretaceous (Grohskopf, 1955)

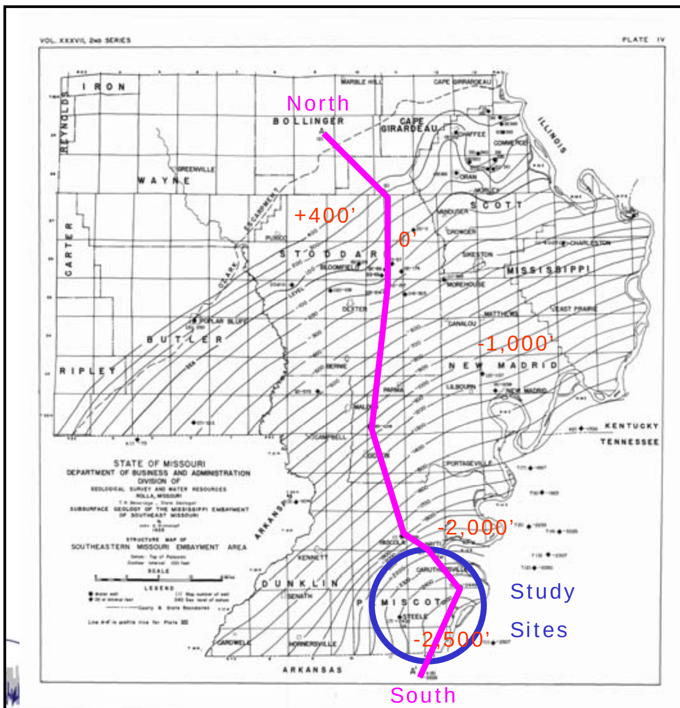

Structural Contours on the Base of the Cretaceous or Top of the Paleozoic (Grohskopf, 1955)

Profile Line

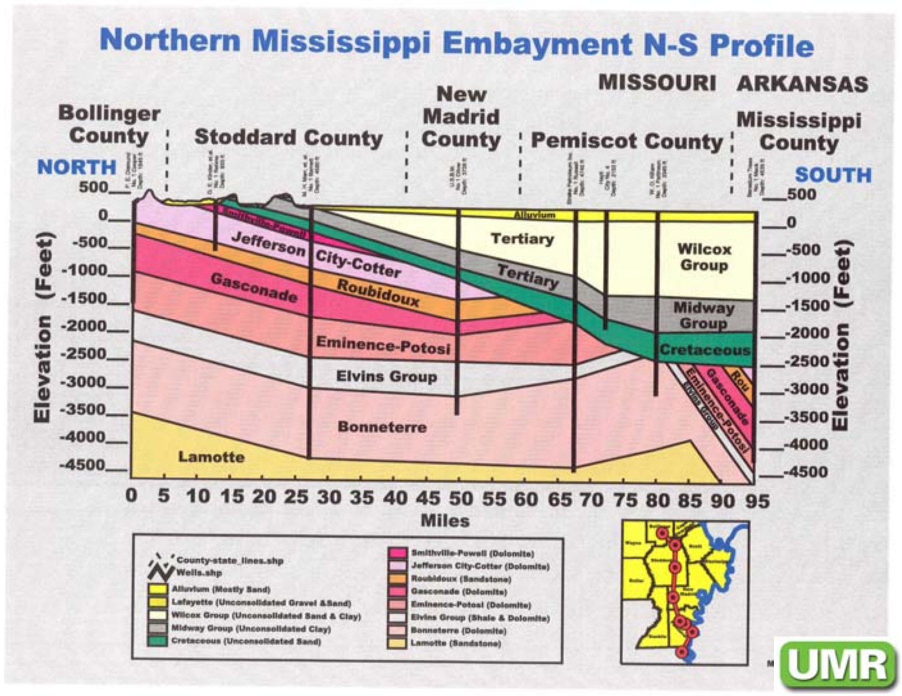

More Detailed Stratigraphic Data for Select Areas

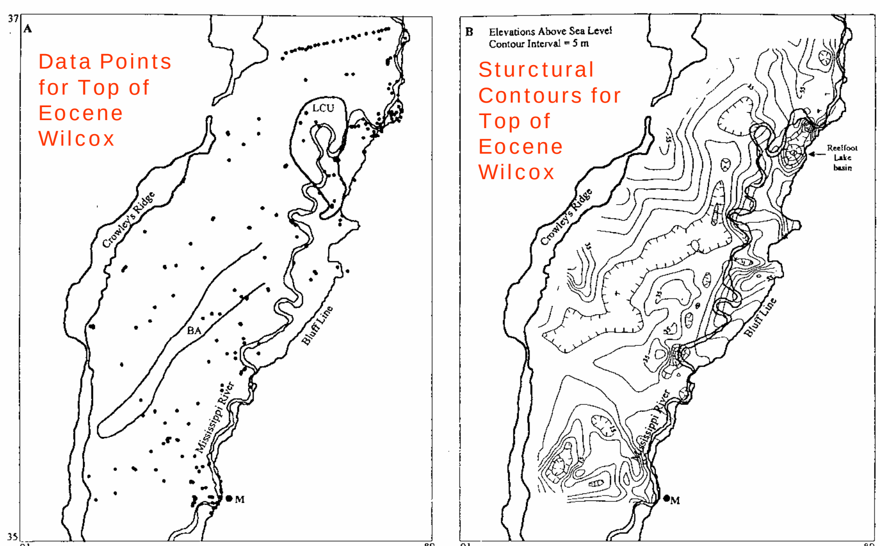

(Van Arsdale & TenBrink, 2000)

General Geologic Setting and Seismicity of the FHWA Project Site in the New Madrid Seismic Zone

- Central and Eastern United States Earthquake Hazard
- Regional geology, topography and seismicity
- Mississippi Embayment and Reelfoot Rift (Mississippi Valley Graben)
- Stratigraphy
- **Geologic structure, faults and seismicity**
- Sandblows
- Attenuation
- Local site alluvial soils
- Important Considerations

Geologic structure, faults and seismicity

Burried Rift

•East northeast-west southwest compression

Seismicity Pattern

•Four faults

  •Three near vertical strike-slip faults

  •One low angle reverse thrust fault

Bridge Sites

•Both near NMSZ southwest segment strike-slip fault

•One near NMSZ central segment reverse thrust fault

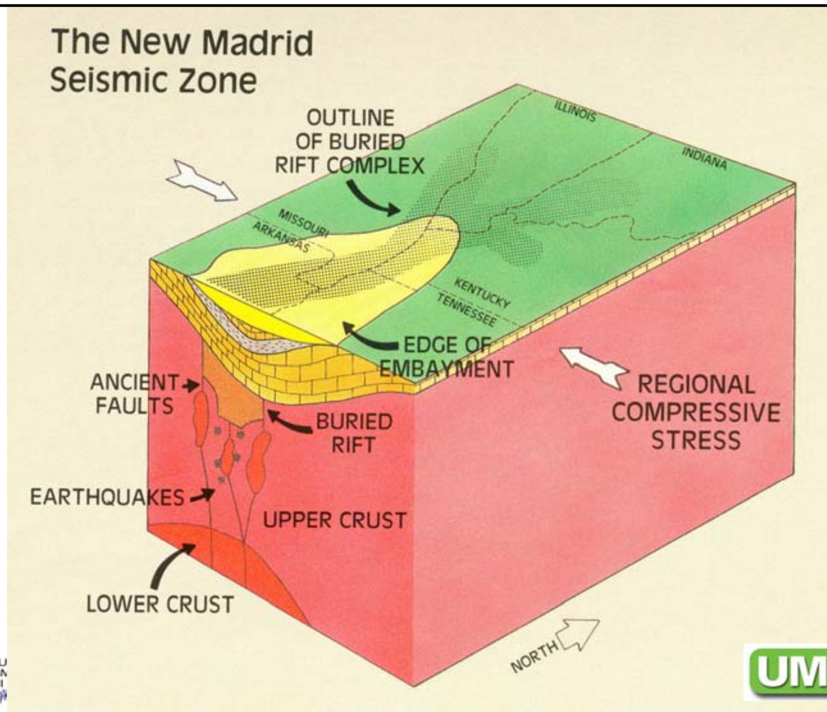

New Madrid Seismic Zone Seismicity Epicenters 1974-2004

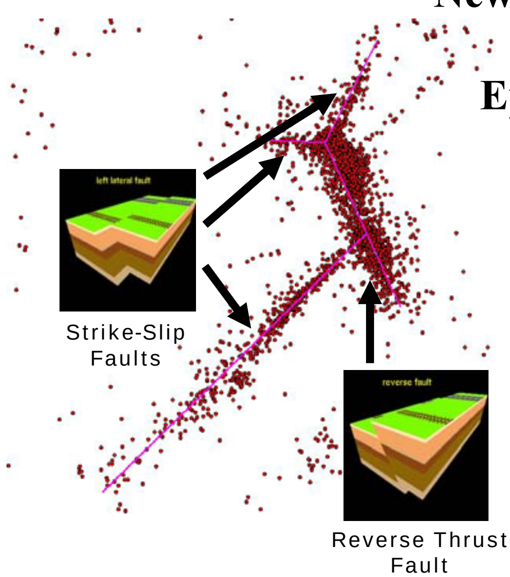

Several faults are outlined by the frequent seismic activity in the NMSZ. Most are vertical strike-slip faults with narrow zones of epicenters but one is a reverse thrust fault with epicenters spread over a wide zone.

Simplified Pattern and Direction of Movement for the 4 Major Faults in the New Madrid Seismic Zone

- Central Segment
  Reverse Thrust
- Southwest Segment
  Right Lateral Strike-Slip
- Northeast Segment
  Right Lateral Strike-Slip
- West Segment
  Left Lateral Strike-Slip

UMR

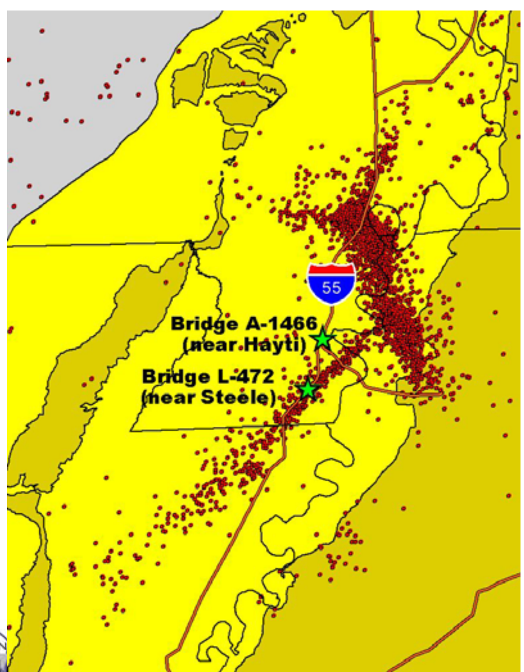

New Madrid Seismic Zone Seismicity and its Relationship to the Study Area

I-55 passes through the NMSZ. It is subject to the varied types of fault movements and ground motions. Studied bridges are on top of or very near to the southwest strike-slip segment of the NMSZ.

UMR

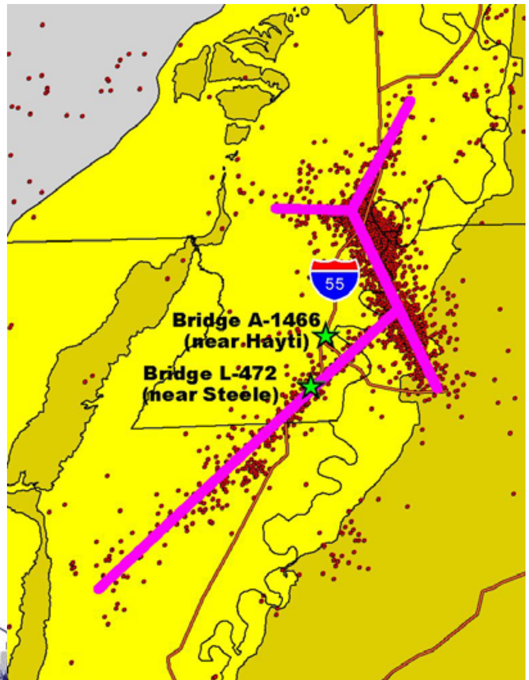

Seismicity and Simplified Pattern of Major Faults in the New Madrid Seismic Zone

Major faults in the NMSZ and their relationship to I-55 and the bridges studied. Alluvial lowlands in yellow and Mississippi Embayment uplands in tan.

General Geologic Setting and Seismicity of the FHWA Project Site in the New Madrid Seismic Zone

- Central and Eastern United States Earthquake Hazard
- Regional geology, topography and seismicity
- Mississippi Embayment and Reelfoot Rift (Mississippi Valley Graben)
- Stratigraphy
- Geologic structure, faults and seismicity
- **Sandblows**
- Attenuation
- Local site alluvial soils
- Important Considerations

Sandblows

Evidence of Past Intense Sandblows

- Casual observation
- Airphoto mapping
- Trench logging

Seismicity Associated with Sandblows

- Close correlation
- Hugh area affected
- Some variation related to local soils and site conditions

NATURAL HAZARDS MITIGATION INSTITUTE

UMR

Sandblows of the New Madrid Seismic Zone, Mississippi Embayment Lowlands

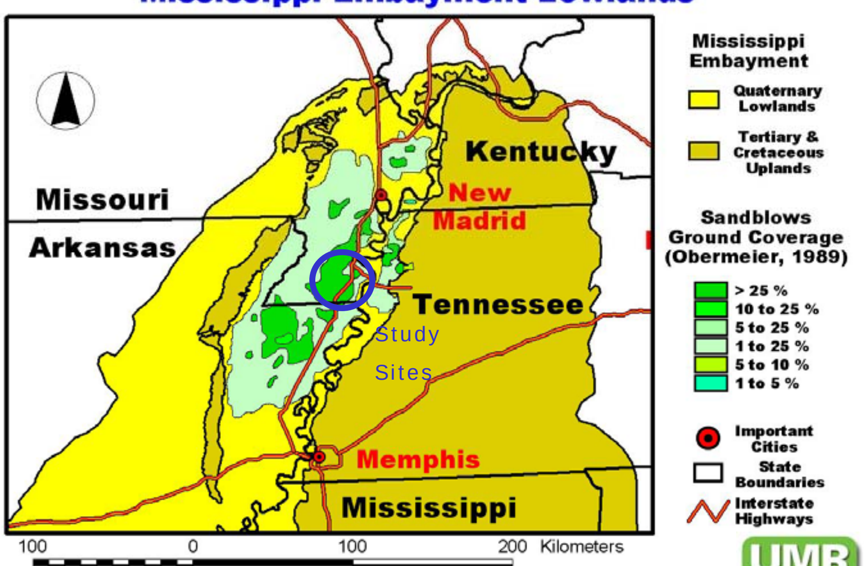

UMR

Sandblows & Seismicity of the New Madrid Seismic Zone, Mississippi Embayment Lowlands

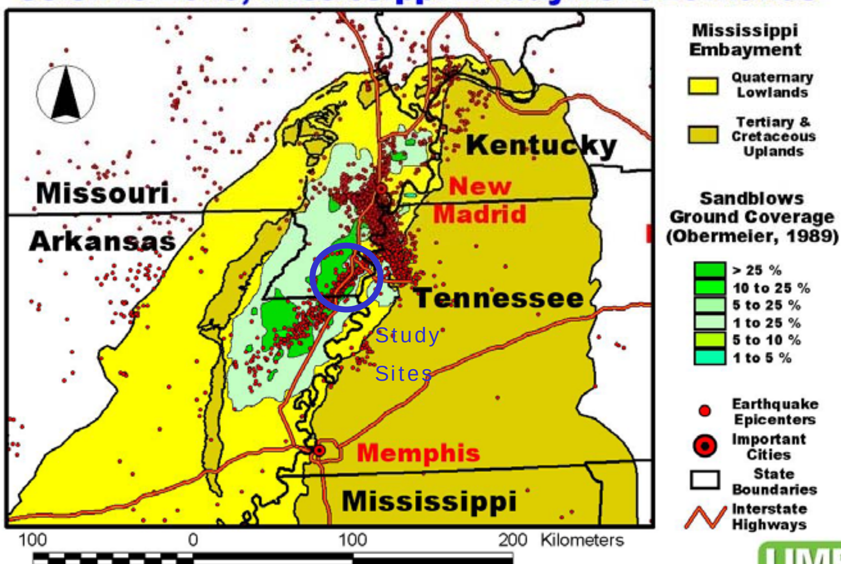

UMR

General Geologic Setting and Seismicity of the FHWA Project Site in the New Madrid Seismic Zone

- Central and Eastern United States Earthquake Hazard
- Regional geology, topography and seismicity
- Mississippi Embayment and Reelfoot Rift (Mississippi Valley Graben)
- Stratigraphy
- Geologic structure, faults and seismicity
- Sandblows
- **Attenuation**
- Local site alluvial soils
- Important Considerations

NATURAL HAZARDS MITIGATION INSTITUTE

UMR

Attenuation

Central & Eastern United States

- Low attenuation
- Ten to twenty times larger shaking intensity area
- Older, harder, dryer bedrock

Western United States

- High attenuation
- Relatively rapid decay of shaking intensity
- Younger, softer, more fractured bedrock

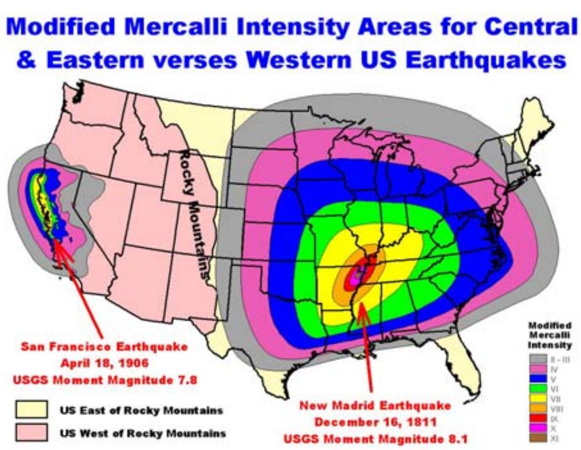

Low seismic wave attenuation properties of the bedrock in the Central and Eastern United States results in much larger areas experiencing any given level of shaking.

General Geologic Setting and Seismicity of the FHWA Project Site in the New Madrid Seismic Zone

- Central and Eastern United States Earthquake Hazard
- Regional geology, topography and seismicity
- Mississippi Embayment and Reelfoot Rift (Mississippi Valley Graben)
- Stratigraphy
- Geologic structure, faults and seismicity
- Sandblows
- Attenuation
- **Local site alluvial soils**
- Important Considerations

NATURAL HAZARDS MITIGATION INSTITUTE

UMR

Local site alluvial soils

Alluvial Geology

•Saucier (Corps of Engineers) mapping

•Airphoto interpretation

•Some soil boring

•Little or no field work

•Abandoned courses and meanders of the modern Mississippi River

•Glacial outwash terraces or the ancient Ohio and Mississippi Rivers

Seismicity

•Southwest segment of NMSZ at or near bridge sites

NATURAL HAZARDS MITIGATION INSTITUTE

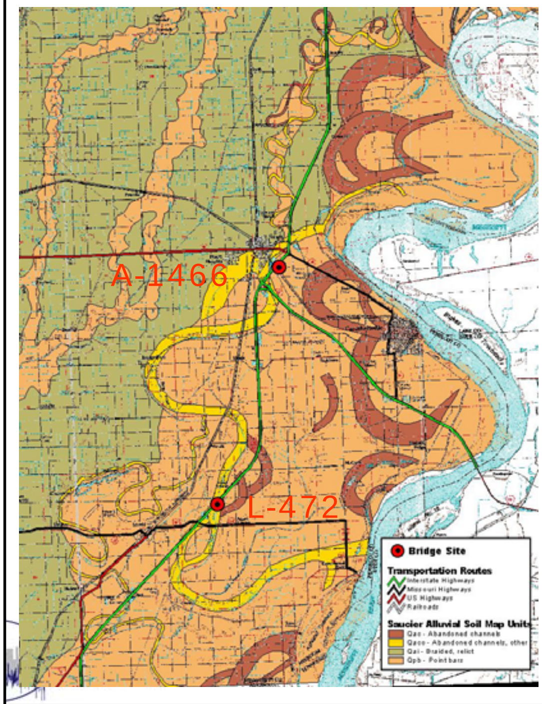

Bridge study sites (red circles) in Dunklin County, Missouri with local alluvial geology (Saucier, 1994) showing meander belt of modern Mississippi River system (brown, orange & yellow) and adjacent older glacial outwash terraces (tan).

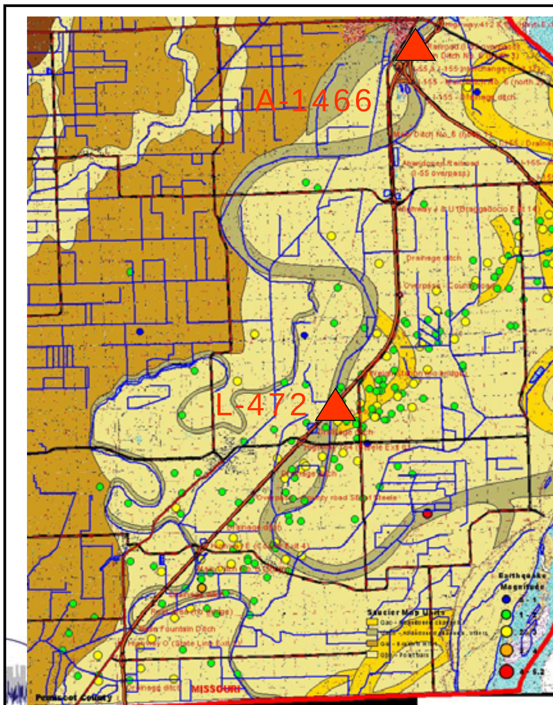

Bridge study sites (red triangles) in Dunklin County, Missouri with earthquake epicenters and local alluvial geology (Saucier, 1994) showing meander belt of modern Mississippi River system (light and dark yellow & gray) and adjacent older glacial outwash terraces (tan).

General Geologic Setting and Seismicity of the FHWA Project Site in the New Madrid Seismic Zone

- Central and Eastern United States Earthquake Hazard
- Regional geology, topography and seismicity
- Mississippi Embayment and Reelfoot Rift (Mississippi Valley Graben)
- Stratigraphy
- Geologic structure, faults and seismicity
- Sandblows
- Attenuation
- Local site alluvial soils
- **Important Considerations**

NATURAL HAZARDS MITIGATION INSTITUTE

UMR

Important Considerations

Past Large New Madrid Earthquakes

- Historic record
- Paleoseismic record

Future New Madrid Earthquake Probabilities

- Magnitude 7.5 to 8.0
- Magnitude larger than 6.0

NATURAL HAZARDS MITIGATION INSTITUTE

UMR

Prehistoric and Historic

Great New Madrid Earthquakes

(Based on paleosesimology and historic record)

DATE OF LARGE EARTHQUAKE	INTERVAL BETWEEN EARTHQUAKES
~300 AD	
	~600 years
~900 AD	
	~550 years
~1450 AD	
	~350 years
1811 -1812 AD	

NATURAL HAZARDS MITIGATION INSTITUTE

UMR

During a 50 year time period the New Madrid Seismic Zone has a

7 – 10% probability of a M 7.5 – 8.0 earthquake

(the size of the 1811-1812 earthquakes)

OR

25 – 40% probability of a M 6.0 or larger earthquake

(about the size of the 1895 Charleston, Missouri earthquake)

NATURAL HAZARDS MITIGATION INSTITUTE

UMR

PRESENTATION 7

SYNTHETIC NEAR-FIELD ROCK MOTIONS IN THE NEW MADRID SEISMIC ZONE

Synthetic Near-Field Rock Motions in the New Madrid Seismic Zone

Genda Chen*, Ph.D., P.E., and Mostafa El-Engebawy, Ph.D.
*Associate Professor of Civil Engineering
Department of Civil, Architecture and Environmental Engineering
University of Missouri-Rolla
gchen@umr.edu

Geotechnical and Bridge Seismic Design Workshop
New Madrid Seismic Zone Experience
October 28-29, 2004

Participants

Genda Chen, Ph.D., P.E. (team leader)
Mostafa El-Engebawy, Ph.D.
Yuehua Zeng, Ph.D. (seismologist)
David Hoffman (geologist)
David Rogers, Ph.D., P.E. (geologist)
Robert Hermann, Ph.D. (seismologist)

NATURAL HAZARDS MITIGATION INSTITUTE

UMR UNIVERSITY OF MISSOURI-ROLLA

Outline of Presentation

- Objectives
- Overview of Study Area
- Characteristics of Near-Field Motions
- Generation of Synthetic Near-Field Rock Motions
- Discussion of Results
- Simulated vs. AASHTO & NCHRP 12-49 Spectra
- Comparison with other Simulation Methods
- Concluding Remarks

NATURAL HAZARDS MITIGATION INSTITUTE

UMR UNIVERSITY OF MISSOURI-ROLLA

Objectives

- To provide rock motion time histories at three bridge sites within the NMSZ for various combinations of moment magnitude and fault mechanism
- To evaluate near-field characteristics in the NMSZ
- To compare the spectra of the simulated motions with those of the AASHTO and the NCHRP 12-49 project
- To compare the results of the composite-source method with those of the finite-fault and the point-source models

NATURAL HAZARDS MITIGATION INSTITUTE

UMR UNIVERSITY OF MISSOURI-ROLLA

Overview of Study Area

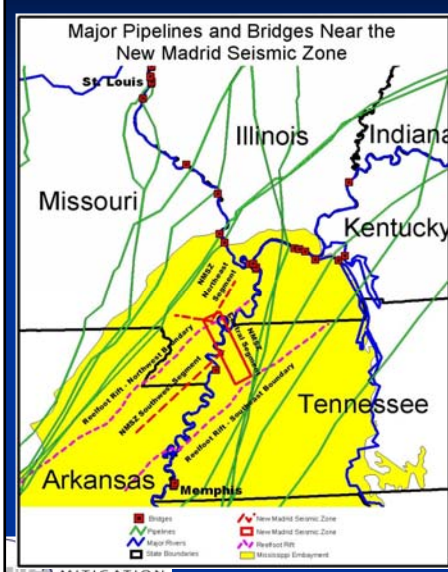

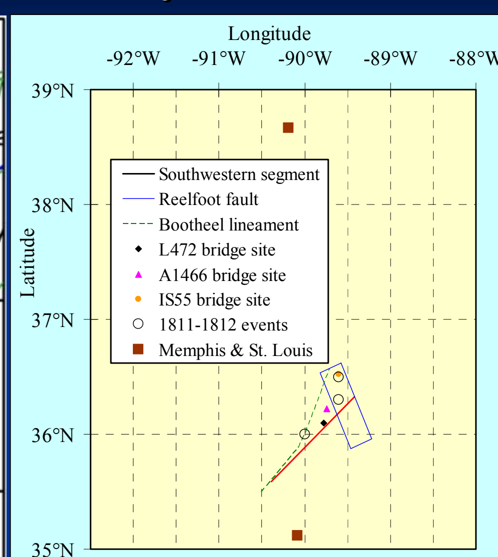

MITIGATION INSTITUTE

UMR UNIVERSITY OF MISSOURI-ROLLA

Characteristics of Near-Field Motions

- **Forward Directivity:** rupture towards the site and is characterized by a two-sided velocity pulse(s) in the fault-normal direction
- **Fling Step:** characterized by one-sided velocity pulse in the same direction as the slip on the fault

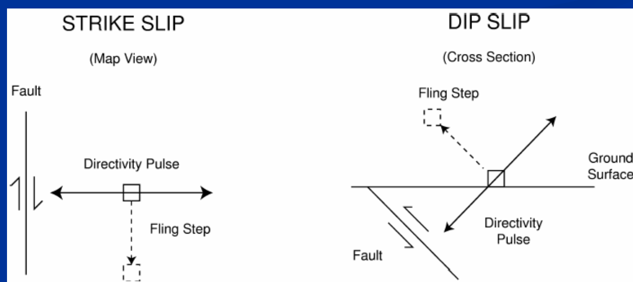

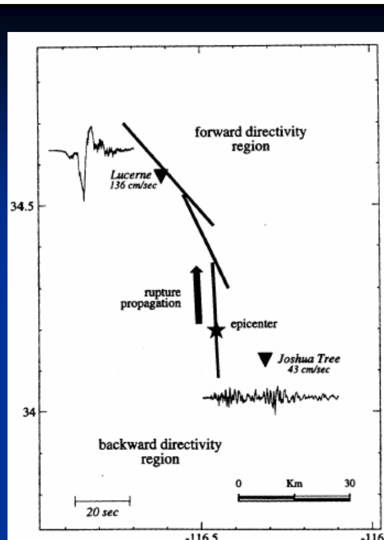

1992 Landers earthquake in Southern California (Strike-Slip Earthquake)

NATURAL HAZARDS MITIGATION INSTITUTE
UMR UNIVERSITY OF MISSOURI-ROLLA

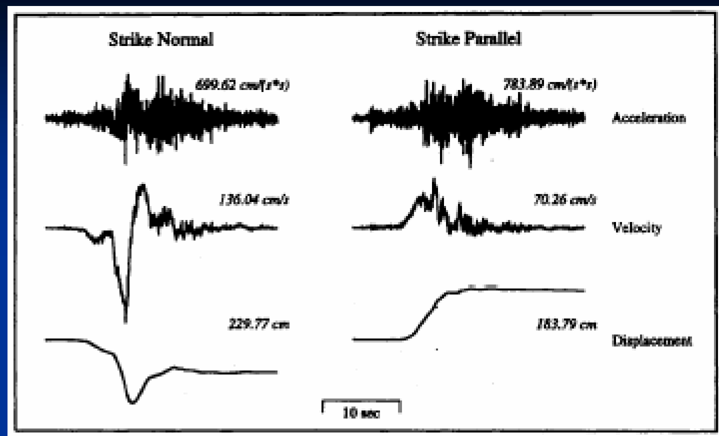

1992 Landers earthquake - Lucerne Records

Fault-normal: *double-sided velocity pulse; small permanent displacement*
Fault-parallel: *single-sided velocity pulse; large permanent displacements*

NATURAL HAZARDS MITIGATION INSTITUTE

UMR UNIVERSITY OF MISSOURI-ROLLA

Effects of Forward Rupture Directivity

- Increase the amplitude of intermediate and long period ground motion
- Fault-normal component is larger than fault-parallel component at intermediate and long periods

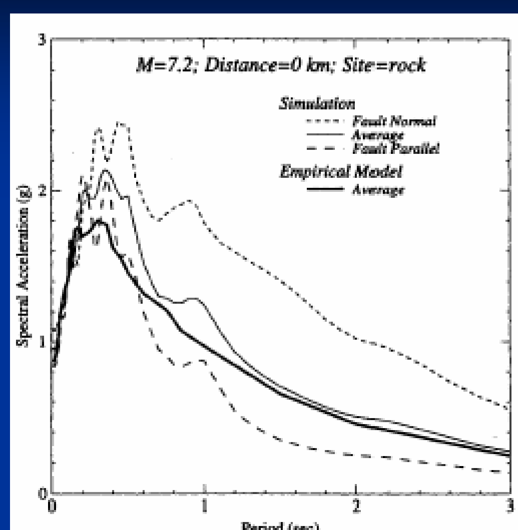

after Somerville et al. (1997)

NATURAL HAZARDS MITIGATION INSTITUTE

UMR UNIVERSITY OF MISSOURI-ROLLA

Parameters of Forward Rupture Directivity

after Somerville et al. (1997)

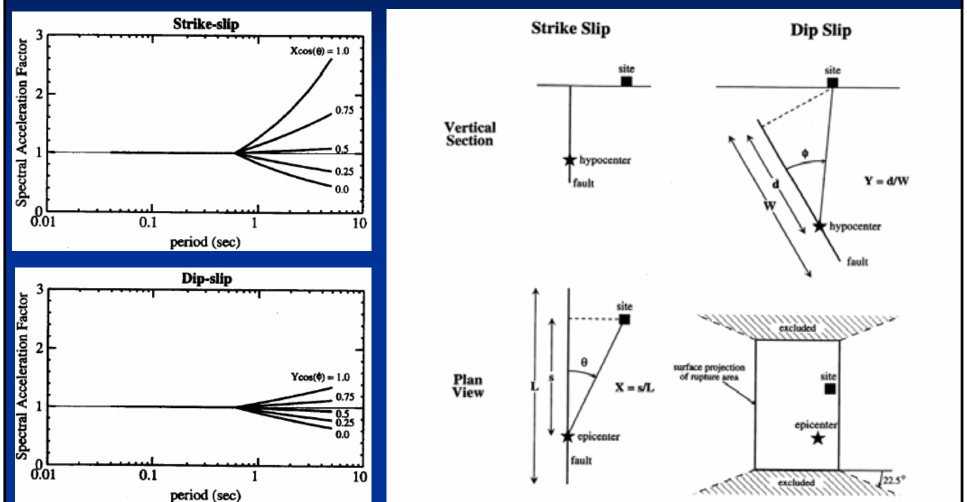

Directivity parameters: $X \cos \theta$ for strike-slip faults
$Y \cos \Phi$ for dip-slip faults

Generation of Synthetic Near-Field Ground Motions in the NMSZ

Earthquake Processes & Key Parameters

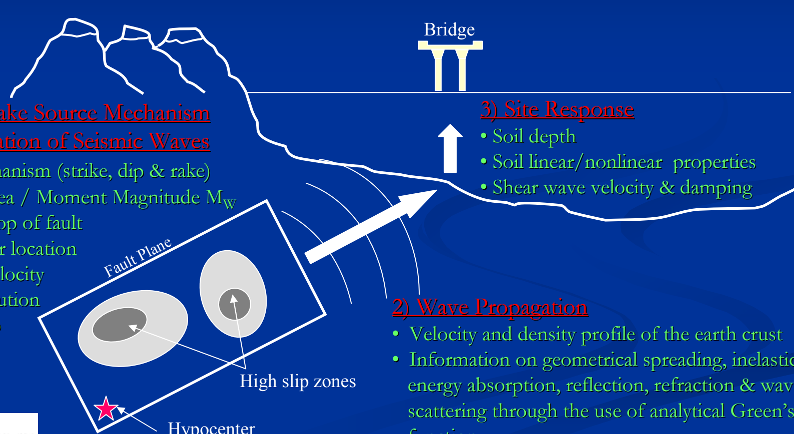

1) Earthquake Source Mechanism and Generation of Seismic Waves
- Fault mechanism (strike, dip & rake)
- Rupture area / Moment Magnitude M_W
- Depth to top of fault
- Hypocenter location
- Rupture velocity
- Slip distribution
- Stress drop

2) Wave Propagation
- Velocity and density profile of the earth crust
- Information on geometrical spreading, inelastic energy absorption, reflection, refraction & wave scattering through the use of analytical Green's function

3) Site Response
- Soil depth
- Soil linear/nonlinear properties
- Shear wave velocity & damping

Seismic Source Parameters

Best-estimates & uncertainties

Rupture Area

$\log A = -3.42 + 0.90\ M_W$ *s = 22% (26%)*

s is the standard deviation for strike-slip (reverse) faults

after Wells & Coppersmith (1994)

Fault	Best-estimate mechanism	Best-estimate rupture area
Southwestern segment (strike-slip fault)	Strike = 226.5° dip = 90° rake = 180°	L = 120 km, W = 18 km *for M_W 7.5,* L = 56 km, W = 13.6 km *for M_W 7.0,* L = 27 km, W = 10 km *for M_W 6.5*
Reelfoot fault (reverse fault)	Strike = 156.1° dip = 32° rake = 90°	L = 82 km, W = 28 km *for M_W 7.5,* L = 44 km, W = 18 km *for M_W 7.0,* L = 22 km, W = 11 km *for M_W 6.5*

NATURAL HAZARDS MITIGATION INSTITUTE

UMR UNIVERSITY OF MISSOURI-ROLLA

Seismic Source Parameters

Best-estimates & uncertainties

Depth to top of the fault

1 km or 5 km

Rake angle of slip on fault

150, 180 or -150 °

Stress drop

100, 150 or 200 bars

Rupture velocity

80% or 85% of V_S

NATURAL HAZARDS MITIGATION INSTITUTE

UMR UNIVERSITY OF MISSOURI-ROLLA

Wave Propagation Parameters

Best-estimates & uncertainties

Velocity model of the earth crust
Chiu et al. (1992)
20% variation

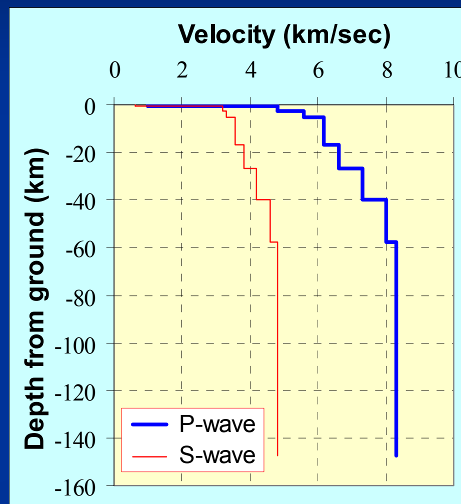

NATURAL HAZARDS MITIGATION INSTITUTE

UMR UNIVERSITY OF MISSOURI-ROLLA

Logic Tree of Uncertain Parameters

Increase fault length by σ — ***Weight 1/3***
Best-estimate rupture area — ***Weight 1/3***
Increase fault width by σ — ***Weight 1/3***

Depth to top of fault 1 km — ***Weight 1/2***
Depth to top of fault 5 km — ***Weight 1/2***

Hypocenter location along strike and dip — ***Equally-Distributed***

Rupture velocity = 80% shear wave velocity — ***Weight 1/2***
Rupture velocity = 85% shear wave velocity — ***Weight 1/2***

Reference rake angle – 30º — ***Weight 1/3***
Reference rake angle — ***Weight 1/3***
Reference rake angle + 30º — ***Weight 1/3***

20% decrease in velocity — ***Weight 1/3***
USGS' velocity model — ***Weight 1/3***
20% increase in velocity — ***Weight 1/3***

Stress drop = 100 bars — ***Weight 1/3***
Stress drop = 150 bars — ***Weight 1/3***
Stress drop = 200 bars — ***Weight 1/3***

NATURAL HAZARDS MITIGATION INSTITUTE

UMR UNIVERSITY OF MISSOURI-ROLLA

The Composite Source Model

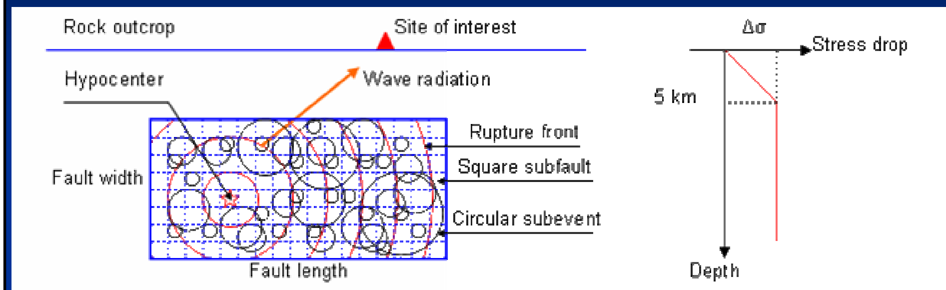

Earthquake Source

The source of a strong earthquake is taken as a superposition of the radiation from a significant number of circular subevents with a constant stress drop. Rupture initiates at the presumed hypocenter and propagates radially at a constant rupture velocity. Each subevent is triggered when the rupture front reaches the center of the subevent. The subevent then initiates the radiation of a displacement pulse.

NATURAL HAZARDS MITIGATION INSTITUTE

UMR UNIVERSITY OF MISSOURI-ROLLA

The Composite Source Model

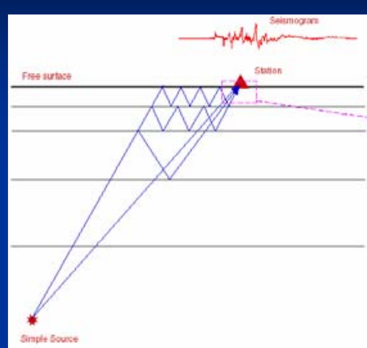

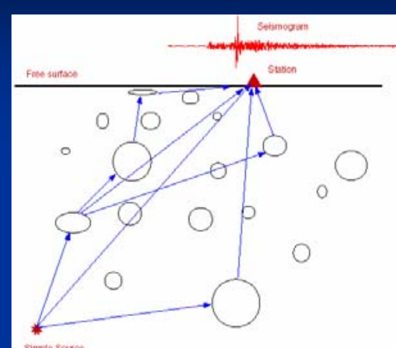

Wave Propagation & Wave Scattering

The generated displacement pulse propagates through a flat multi-layered earth crust. The wave propagation process is modeled with synthetic (analytical) Green's functions in both short- and long-period ranges. The short-period component is modified to account for the effects of random lateral heterogeneity of the earth by adding scattered waves.

NATURAL HAZARDS MITIGATION INSTITUTE

UMR UNIVERSITY OF MISSOURI-ROLLA

The Composite Source Model Validation

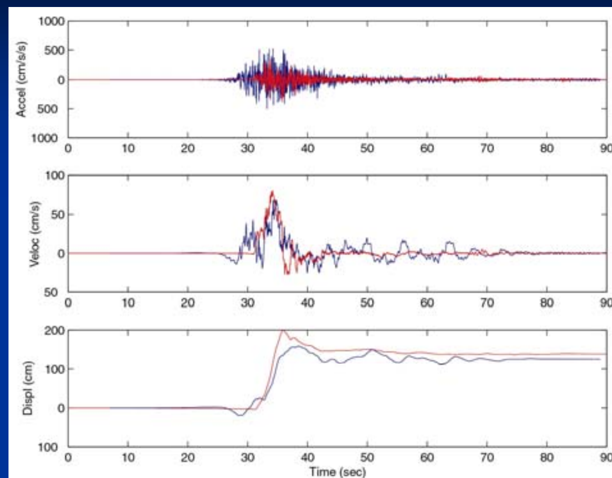

Observed (red) vs. synthetic (blue) ground motions at station SKR (east horizontal component) during 1999 Kocaeli earthquake (strike-slip)

NATURAL HAZARDS MITIGATION INSTITUTE

UMR UNIVERSITY OF MISSOURI-ROLLA

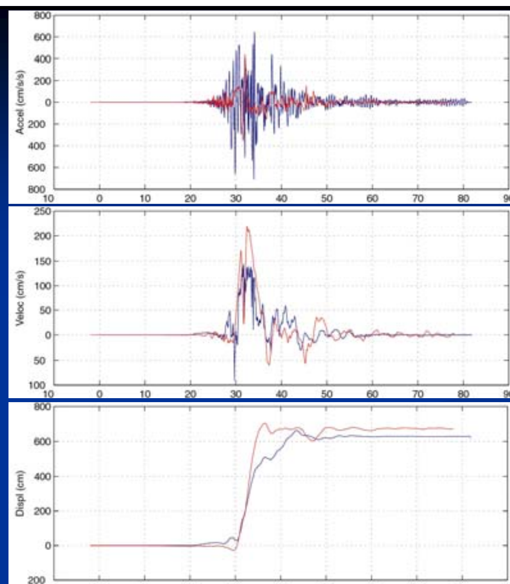

Observed (red) vs. synthetic (blue) ground motions at station T052 (NS component) during 1999 Chi-Chi earthquake (reverse)

NATURAL HAZARDS MITIGATION INSTITUTE

UMR UNIVERSITY OF MISSOURI-ROLLA

Discussion of Results of the Maximum Considered Earthquake (MCE) or M_W 7.5

NATURAL HAZARDS MITIGATION INSTITUTE

UMR UNIVERSITY OF MISSOURI-ROLLA

Total Uncertainty

Southwestern segment

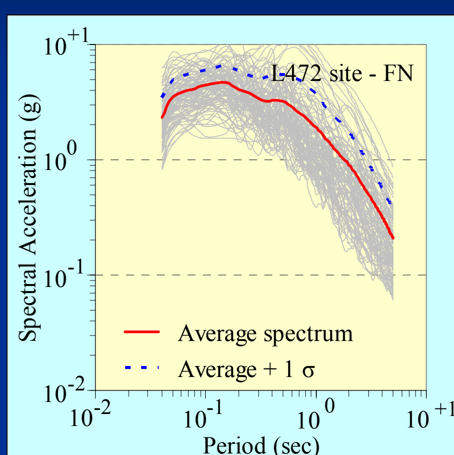

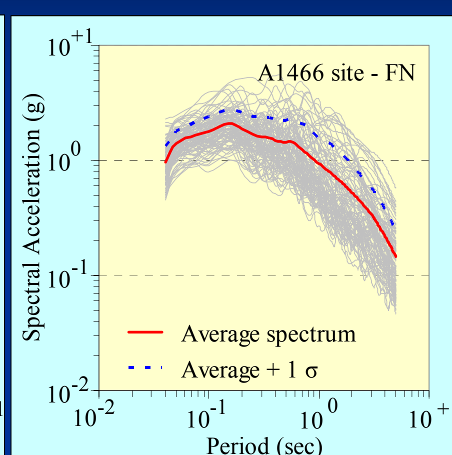

NATURAL HAZARDS MITIGATION INSTITUTE

UMR UNIVERSITY OF MISSOURI-ROLLA

Total Uncertainty

Reelfoot fault

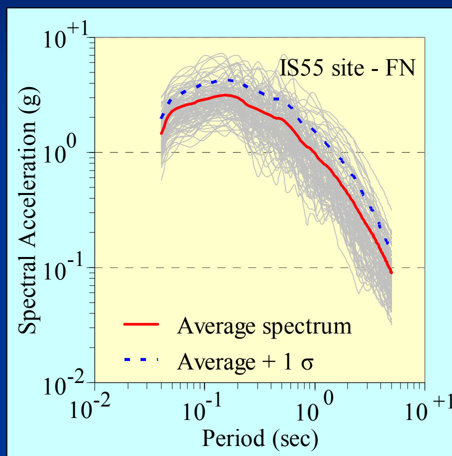

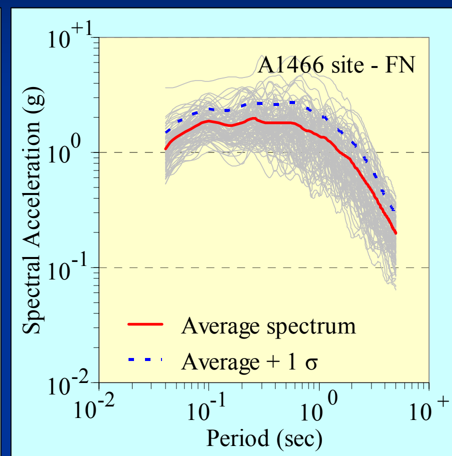

Average Response Spectra

Southwestern segment

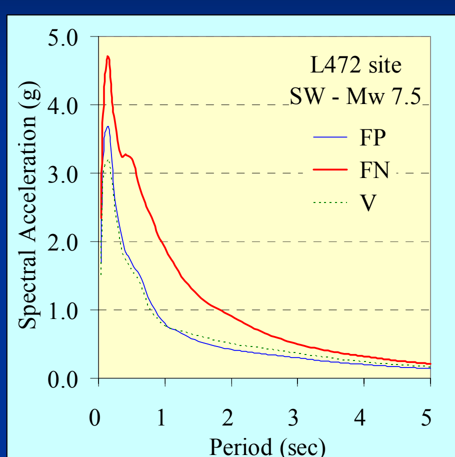

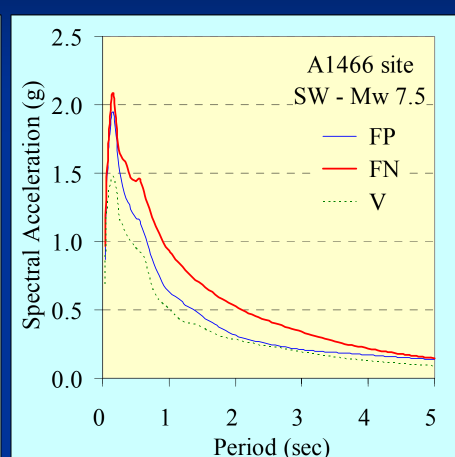

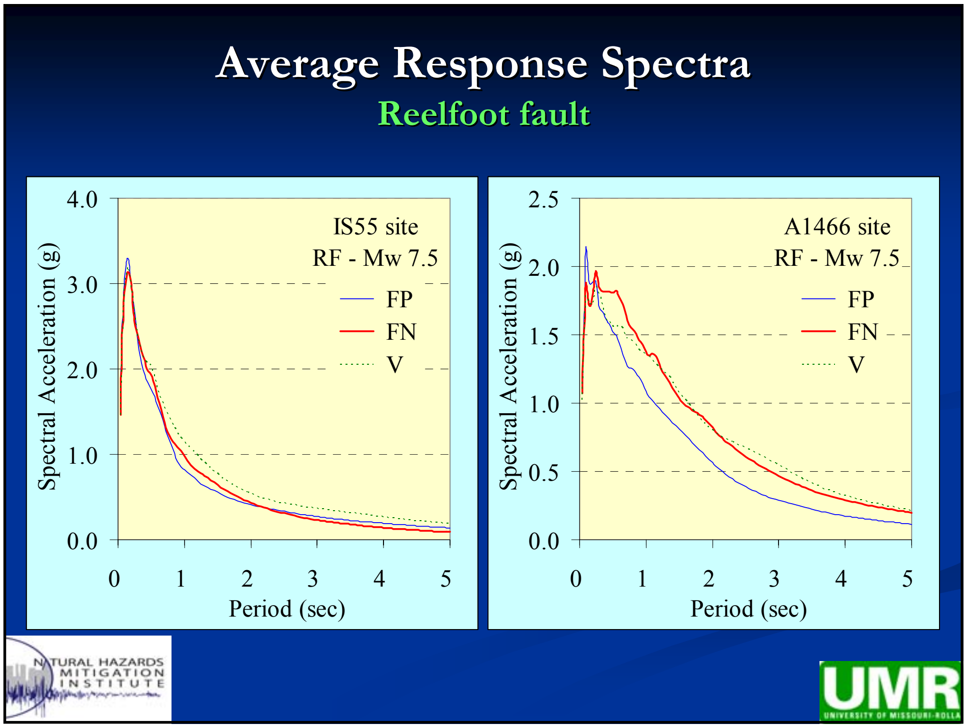
Average Response Spectra
Reelfoot fault
IS55 site
RF - Mw 7.5
FP
FN
V
Spectral Acceleration (g)
4.0
3.0
2.0
1.0
0.0
0
1
2
3
4
5
Period (sec)
A1466 site
RF - Mw 7.5
FP
FN
V
Spectral Acceleration (g)
2.5
2.0
1.5
1.0
0.5
0.0
0
1
2
3
4
5
Period (sec)
NATURAL HAZARDS
MITIGATION
INSTITUTE
UMR
UNIVERSITY OF MISSOURI-ROLLA

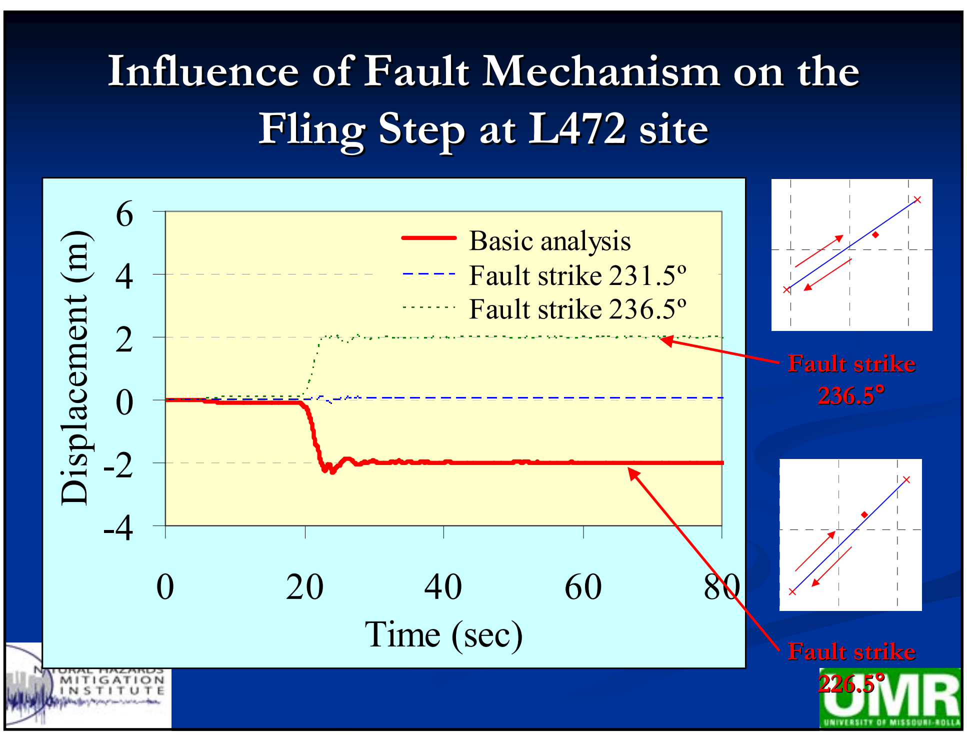
Influence of Fault Mechanism on the Fling Step at L472 site
Basic analysis
Fault strike 231.5º
Fault strike 236.5º
Displacement (m)
6
4
2
0
-2
-4
0
20
40
60
80
Time (sec)
Fault strike 236.5º
Fault strike 226.5º
MITIGATION
INSTITUTE
UMR
UNIVERSITY OF MISSOURI-ROLLA

Influence of Fault Mechanism on the Fling Step at L472 site

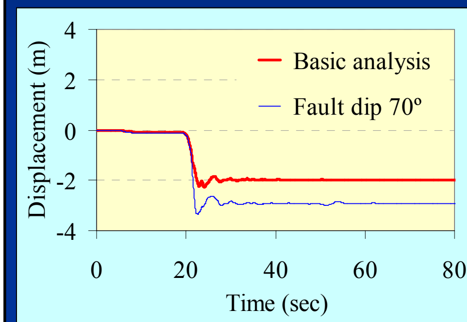

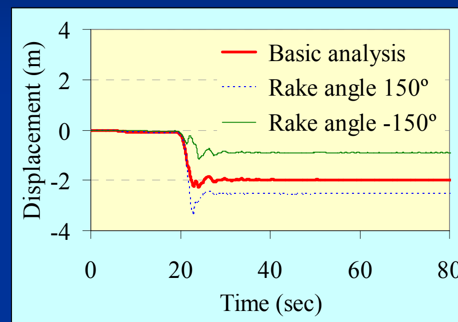

For basic analysis:
Fault dip 90°
Rake angle 180°

Influence of Depth to top of Fault and Stress Drop on the Fling Step at L472 site

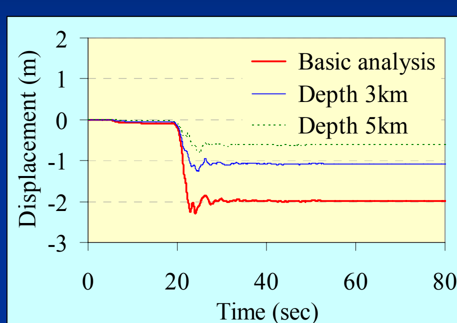

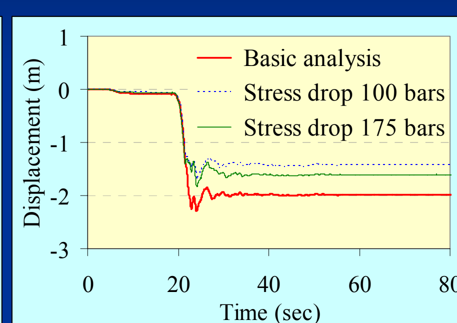

For basic analysis:
Depth 1km
Stress drop 150 bars

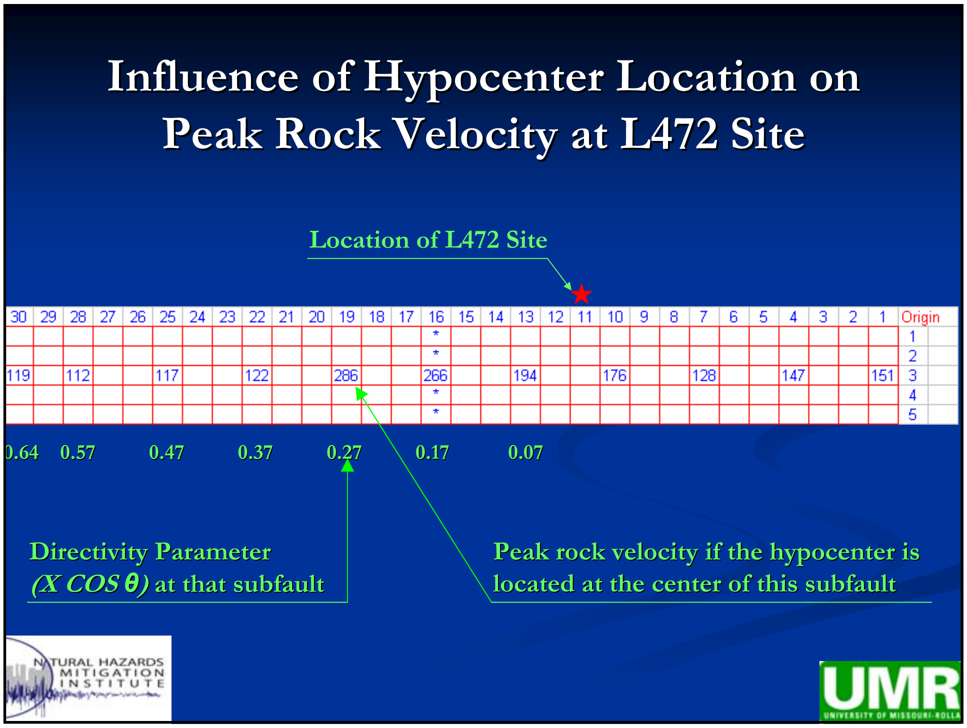
Influence of Hypocenter Location on Peak Rock Velocity at L472 Site
Location of L472 Site
30 29 28 27 26 25 24 23 22 21 20 19 18 17 16 15 14 13 12 11 10 9 8 7 6 5 4 3 2 1 Origin
1
2
119 112 117 122 286 266 194 176 128 147 151 3
4
5
0.64 0.57 0.47 0.37 0.27 0.17 0.07
Directivity Parameter (X COS θ) at that subfault
Peak rock velocity if the hypocenter is located at the center of this subfault
NATURAL HAZARDS MITIGATION INSTITUTE
UMR
UNIVERSITY OF MISSOURI-ROLLA

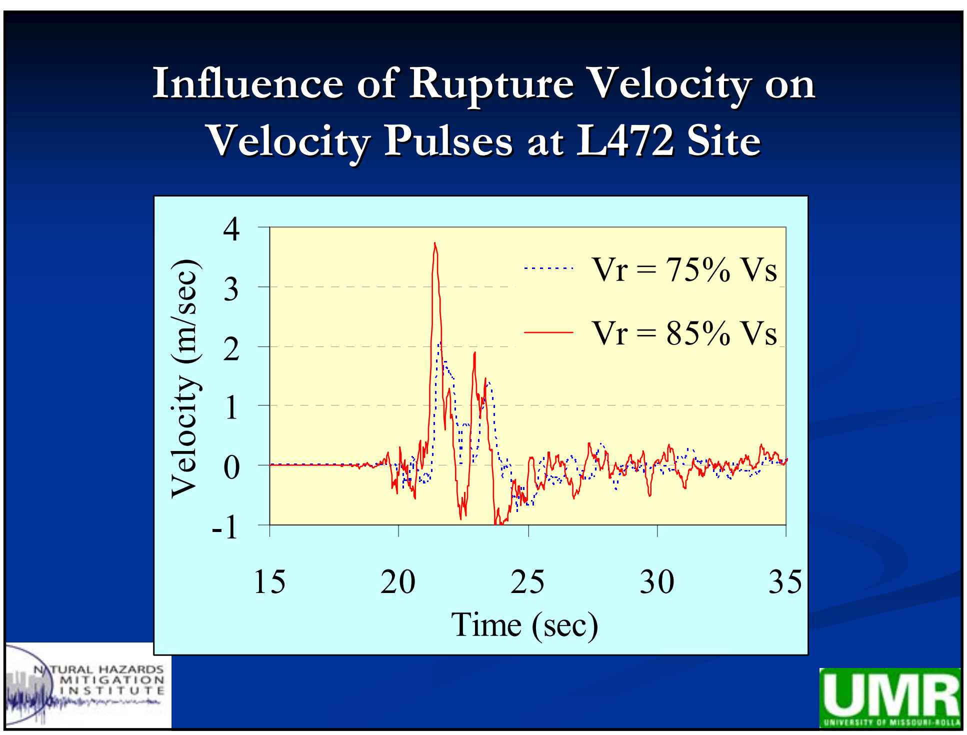
Influence of Rupture Velocity on Velocity Pulses at L472 Site
Velocity (m/sec)
4
3
2
1
0
-1
15 20 25 30 35
Time (sec)
Vr = 75% Vs
Vr = 85% Vs
NATURAL HAZARDS MITIGATION INSTITUTE
UMR
UNIVERSITY OF MISSOURI-ROLLA

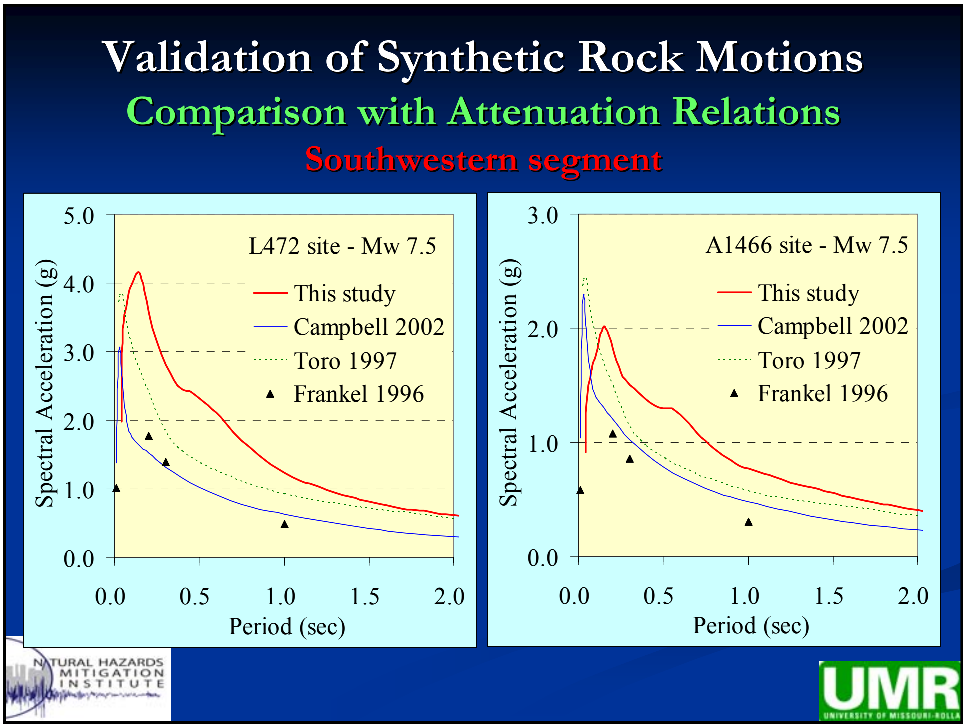
Validation of Synthetic Rock Motions
Comparison with Attenuation Relations
Southwestern segment
L472 site - Mw 7.5
This study
Campbell 2002
Toro 1997
Frankel 1996
Spectral Acceleration (g)
Period (sec)
A1466 site - Mw 7.5
This study
Campbell 2002
Toro 1997
Frankel 1996
Spectral Acceleration (g)
Period (sec)
NATURAL HAZARDS MITIGATION INSTITUTE
UMR
UNIVERSITY OF MISSOURI-ROLLA

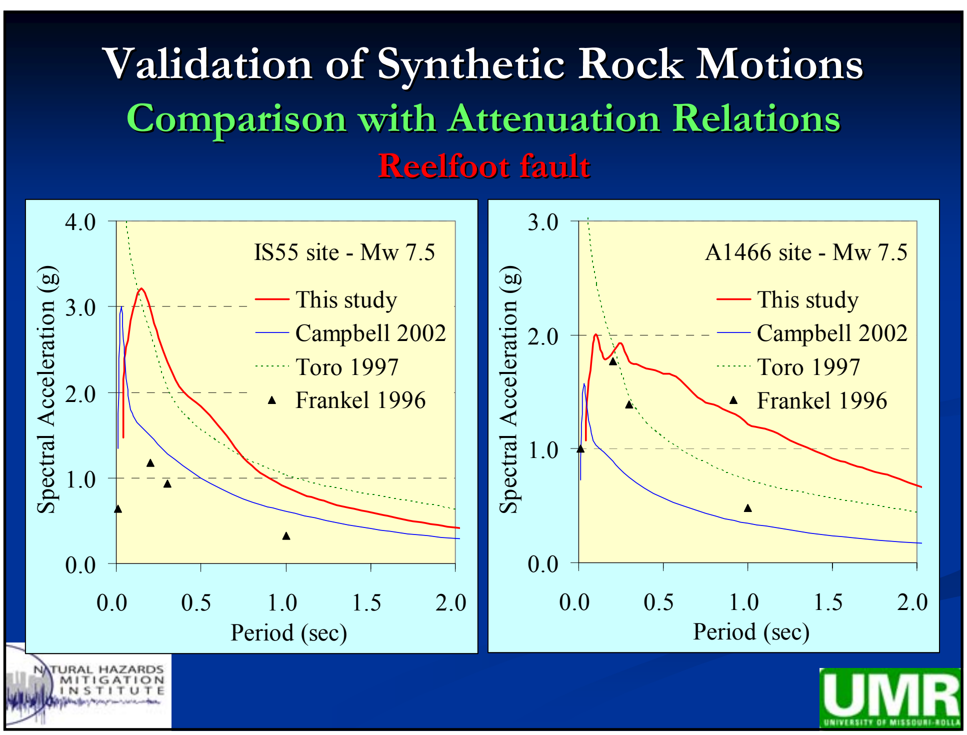
Validation of Synthetic Rock Motions
Comparison with Attenuation Relations
Reelfoot fault
IS55 site - Mw 7.5
This study
Campbell 2002
Toro 1997
Frankel 1996
Spectral Acceleration (g)
Period (sec)
A1466 site - Mw 7.5
This study
Campbell 2002
Toro 1997
Frankel 1996
Spectral Acceleration (g)
Period (sec)
NATURAL HAZARDS MITIGATION INSTITUTE
UMR
UNIVERSITY OF MISSOURI-ROLLA

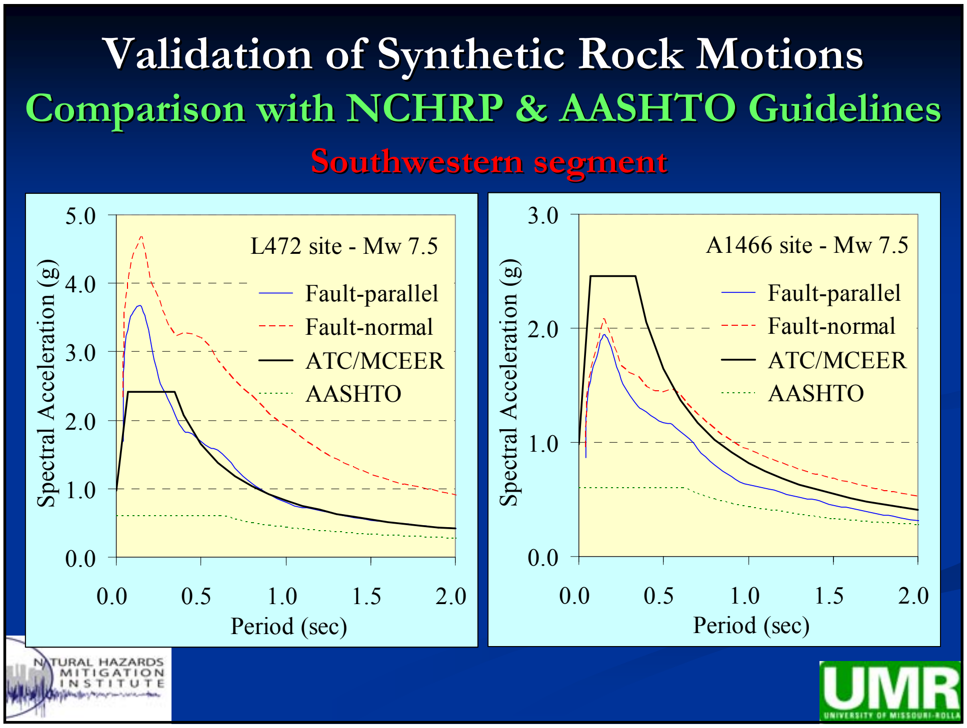
Validation of Synthetic Rock Motions
Comparison with NCHRP & AASHTO Guidelines
Southwestern segment
L472 site - Mw 7.5
Fault-parallel
Fault-normal
ATC/MCEER
AASHTO
Spectral Acceleration (g)
Period (sec)
0.0
1.0
2.0
3.0
4.0
5.0
0.5
1.5
A1466 site - Mw 7.5
Fault-parallel
Fault-normal
ATC/MCEER
AASHTO
Spectral Acceleration (g)
Period (sec)
NATURAL HAZARDS MITIGATION INSTITUTE
UMR
UNIVERSITY OF MISSOURI-ROLLA

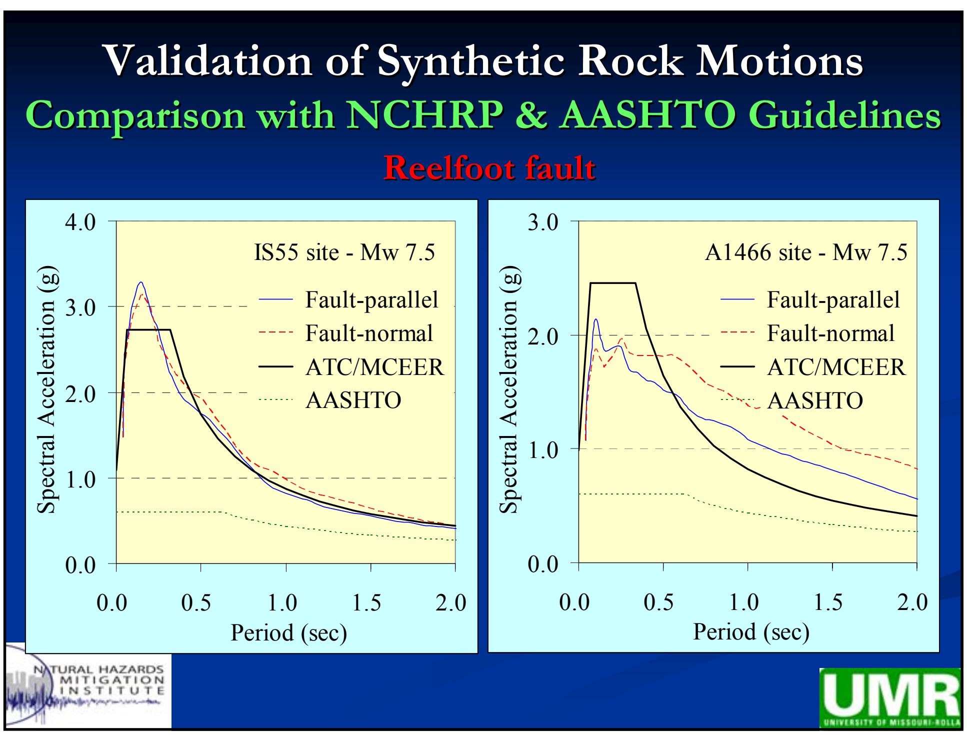
Validation of Synthetic Rock Motions
Comparison with NCHRP & AASHTO Guidelines
Reelfoot fault
IS55 site - Mw 7.5
Fault-parallel
Fault-normal
ATC/MCEER
AASHTO
Spectral Acceleration (g)
Period (sec)
A1466 site - Mw 7.5
Fault-parallel
Fault-normal
ATC/MCEER
AASHTO
Spectral Acceleration (g)
Period (sec)
NATURAL HAZARDS MITIGATION INSTITUTE
UMR
UNIVERSITY OF MISSOURI-ROLLA

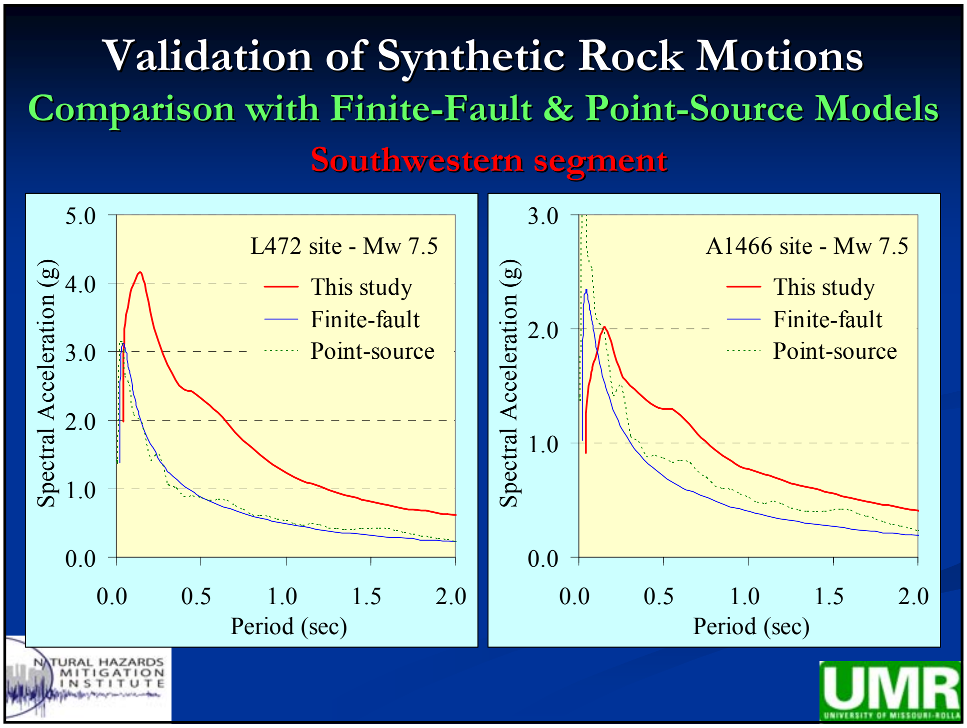
Validation of Synthetic Rock Motions
Comparison with Finite-Fault & Point-Source Models
Southwestern segment
L472 site - Mw 7.5
This study
Finite-fault
Point-source
Spectral Acceleration (g)
Period (sec)
A1466 site - Mw 7.5
This study
Finite-fault
Point-source
Spectral Acceleration (g)
Period (sec)
NATURAL HAZARDS MITIGATION INSTITUTE
UMR
UNIVERSITY OF MISSOURI-ROLLA

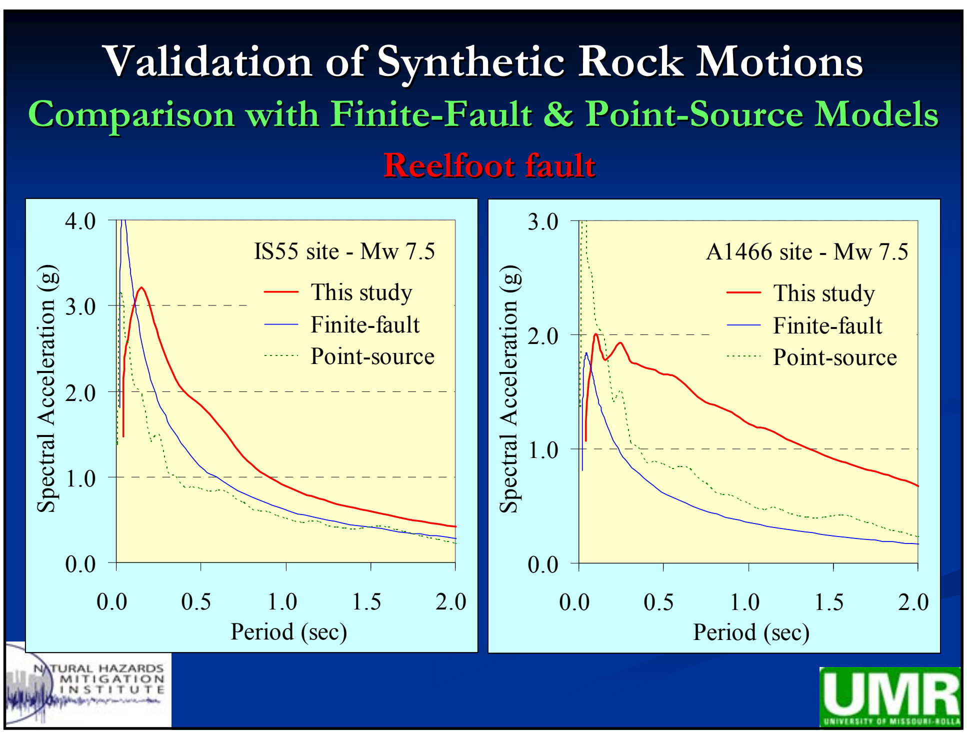
Validation of Synthetic Rock Motions
Comparison with Finite-Fault & Point-Source Models
Reelfoot fault
IS55 site - Mw 7.5
This study
Finite-fault
Point-source
Spectral Acceleration (g)
Period (sec)
A1466 site - Mw 7.5
This study
Finite-fault
Point-source
Spectral Acceleration (g)
Period (sec)
NATURAL HAZARDS MITIGATION INSTITUTE
UMR
UNIVERSITY OF MISSOURI-ROLLA

Near-Field Characteristics of the Selected Motions

Selection criteria of rock motions

1) Fit the average response spectra
2) Fling step in the direction of the slip on the fault
3) Velocity pulse in the fault-normal direction
4) Realistic peak rock accelerations
   (within 75%-125% of Toro et al., 1997)

Near-Field Characteristics of the Selected Motions

Fling step from the southwestern segment

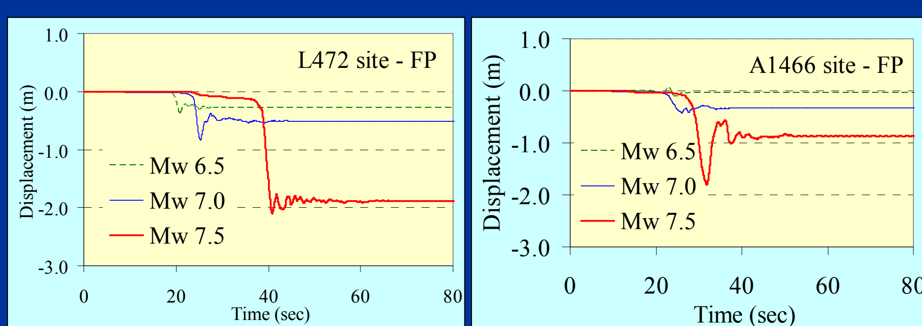

Near-Field Characteristics of the Selected Motions

Fling step from the Reelfoot fault

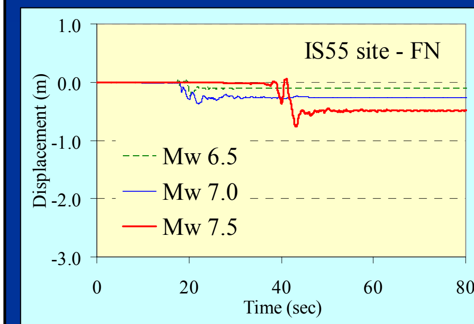

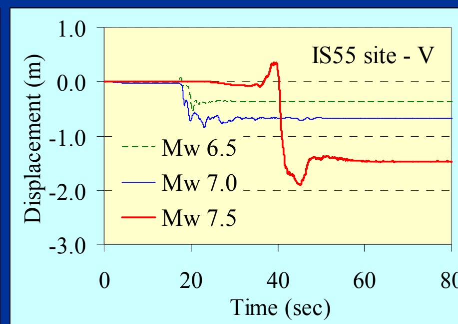

NATURAL HAZARDS MITIGATION INSTITUTE

UMR UNIVERSITY OF MISSOURI-ROLLA

Near-Field Characteristics of the Selected Motions

Velocity pulse from the southwestern segment

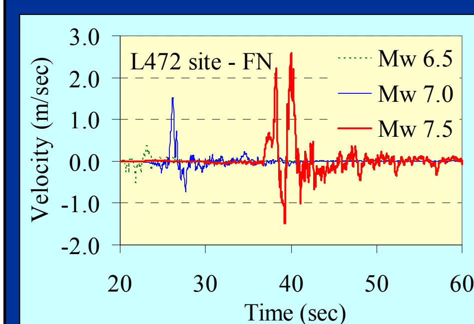

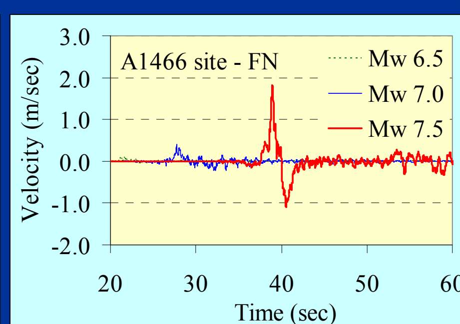

NATURAL HAZARDS MITIGATION INSTITUTE

UMR UNIVERSITY OF MISSOURI-ROLLA

Near-Field Characteristics of the Selected Motions

Velocity pulse from the Reelfoot fault

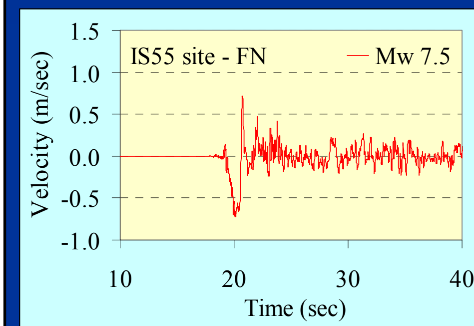

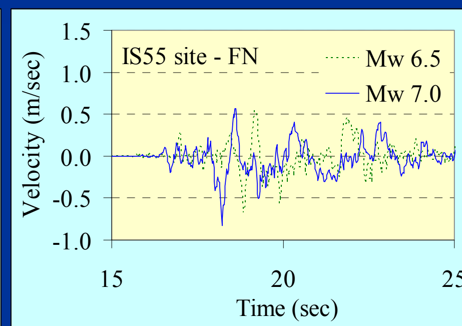

St. Francis River Site (Far-Field)

A3708 site is about 50km from the Reelfoot fault and 87km from the southwestern segment

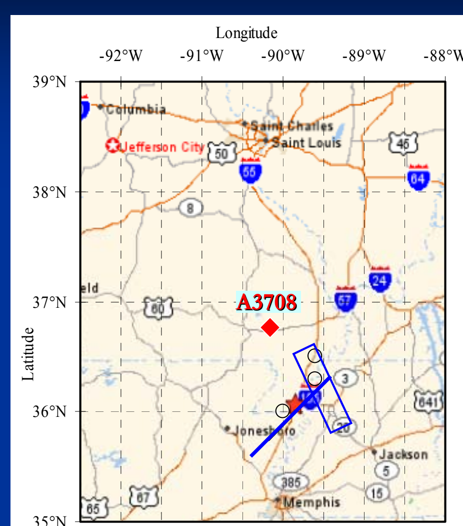

Far-Field Rock Motions

Comparison with NCHRP & AASHTO Guidelines

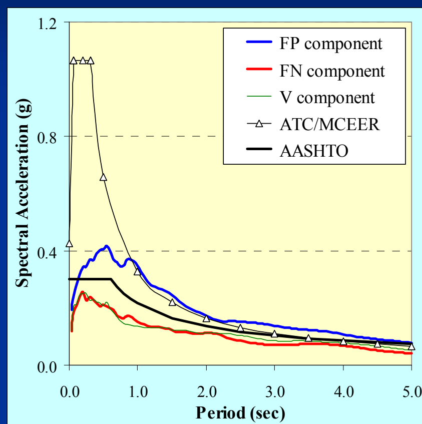

Southwestern segment

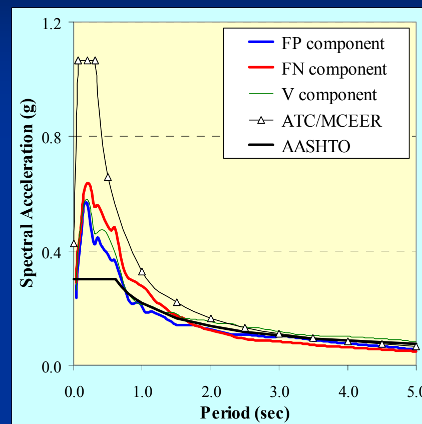

Reelfoot fault

Average of 20 simulations

Concluding Remarks

- The uncertainty of near-fault motions increases with moment magnitude and decreases with distance to fault
- The southwestern segment (strike-slip) contributes more to the total uncertainty than the Reelfoot fault (reverse) due to its forward rupture directivity effects
- The vertical component associated with the Reelfoot fault is stronger than that of the southwestern segment
- Fling step is dependent on the fault mechanism (strike, dip and rake), depth to top of the fault and stress drop

Concluding Remarks

- Velocity pulses are dependent on the hypocenter location along the strike and rupture velocity
- The simulated spectral accelerations are higher than those of the attenuation relations, point-source or finite-fault models due to forward rupture directivity effects, particularly for M_W 7.5 for strike-slip faults
- Velocity pulses associated with M_W 7.5 are very large as compared to M_W 7.0 or 6.5 that may impose special seismic demands for structures very close to active faults

NATURAL HAZARDS MITIGATION INSTITUTE

UMR
UNIVERSITY OF MISSOURI-ROLLA

Concluding Remarks

- In comparison with ATC/MCEER spectra, the near-field motions in the proximity of the faults (<5 km) are generally higher, and those around 10km are similar in long period components but smaller in short period components.
- The far-field rock motion is on the average less than what ATC/MCEER specified in their recommended guidelines.

NATURAL HAZARDS MITIGATION INSTITUTE

UMR
UNIVERSITY OF MISSOURI-ROLLA

PRESENTATION 8

GEOTECHNICAL SITE CHARACTERIZATION

GEOTECHNICAL SITE CHARACTERIZATION

Neil Anderson, Ph.D.
Professor of Geology and Geophysics
Richard W. Stephenson, P.E., Ph.D.
Professor of Civil, Architectural and Environmental Engineering
University of Missouri-Rolla (UMR)

Geotechnical and Bridge Seismic Design Workshop
New Madrid Seismic Zone Experience

October 28-29, 2004, Cape Girardeau, Missouri

Outline

- Objectives of exploration program
- Exploration Program
  - Drilling and sampling
  - Geophysical testing
- Results of exploration program
  - Subsurface stratigraphy
  - Soil properties
  - Shear wave velocity profiles
- Site Classification
- Strain-dependent shear modulus and damping functions
- Final Comments

OBJECTIVES

- Determine strain-dependent shear modulus and damping characteristics of subsoil
- Identify soil strata prone to liquefaction

Major Issues

- Deep unconsolidated soils
- High ground water levels
- High levels of ground motion

GEOTECHNICAL EXPLORATION PROGRAM

- Site

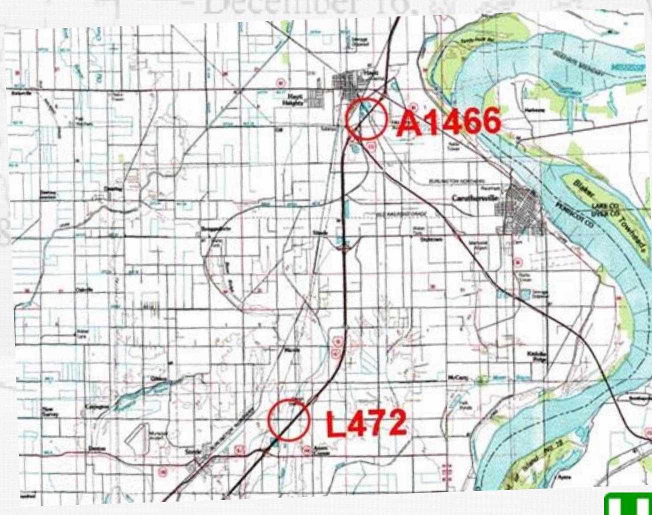

Field Exploration Program

Drilling – Failing 1500

- Rotary with mud
- Truck mounted
- Normal capacity
  - -1500 ft deep and 2-in to 13-in diameters
  - - 4.5 in for this project

- Hollow Stem Auger
  - 80 to 200 feet deep
- SPT Tests
  - Automatic safety hammer
- Sampling
  - Every 5 feet for first 25 feet
  - Every 10 feet below 25 foot depth
  - Cohesionless soils
    - Standard and oversize split spoon samples
  - Cohesive Soils
    - Seamless steel tubes (Shelby Tubes)

- Cone Penetration Testing
  - Continuous log of :
    - Tip Resistance
    - Side Sleeve Friction
    - Pore Water Pressures
- CPT & SCPT
  - Manufacturer: Hogentogler Co.
    - Electronic Subtraction Cone
      - Tip resistance
      - Local resistance
      - Pore pressure
      - Inclination
      - Downhole seismic velocity
      - Temperature

- Pushing Rigs - CME 850
- Cone tip saturated in vacuum with glycerin
  Push speed – 20 cm/s

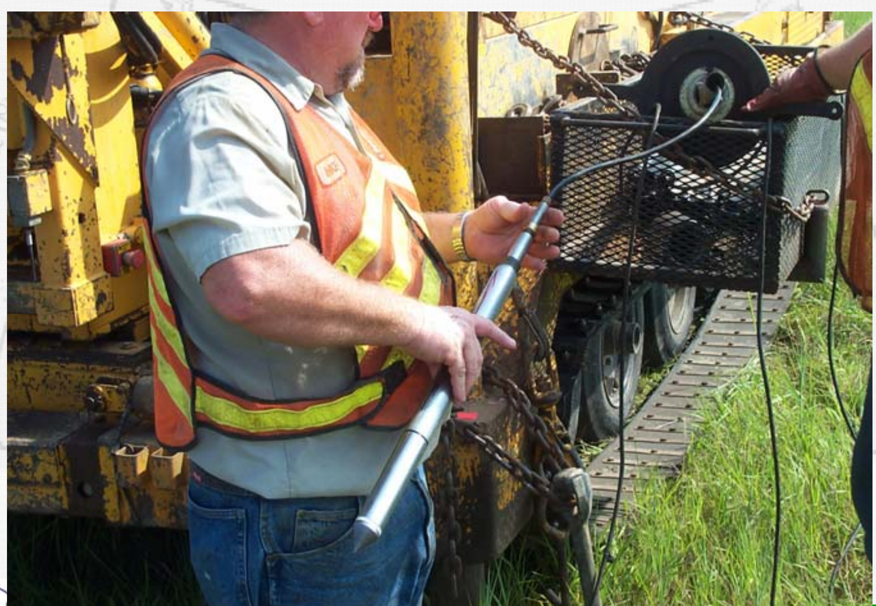

Typical Cone/SPT Data

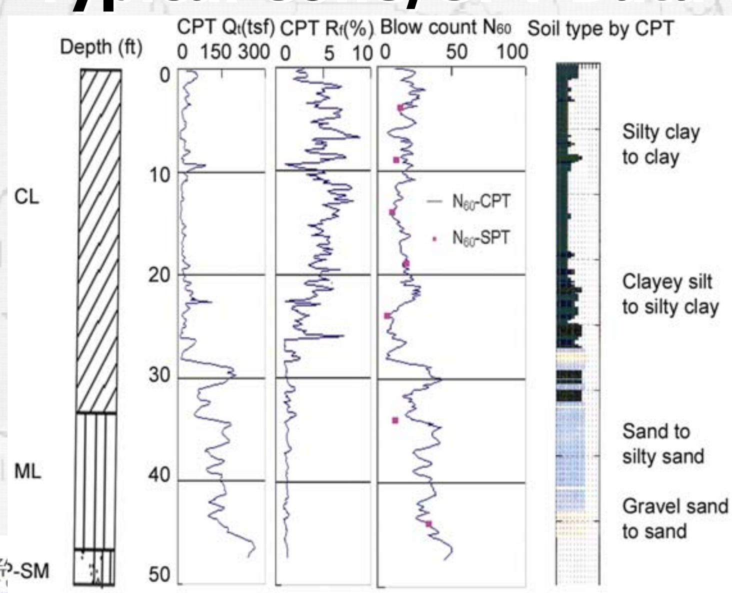

GEOPHYSICAL TESTING

- Seismic Cone Penetration
- Cross-Hole Seismic Velocity
- Spectral Analysis of Surface Waves (SASW)

CROSS-HOLE SEISMIC

Technique employs twinned (or tripled) boreholes completed at the base of the zone of interest and separated by surface distances on the order of 3 to 4 m. (Subsurface separ-ations are determined using a borehole inclinometer.)

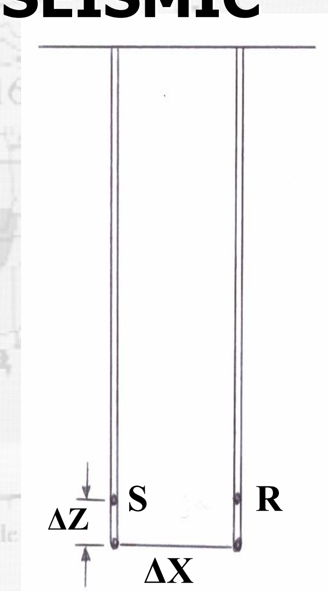

CH SEISMIC

Shear-wave source lowered to base of one borehole; triaxial geophone lowered to same depth in adjacent borehole.

Hammer source is discharged twice - with opposite directional impacts - thereby generating two opposite-polarity shear-wave records.

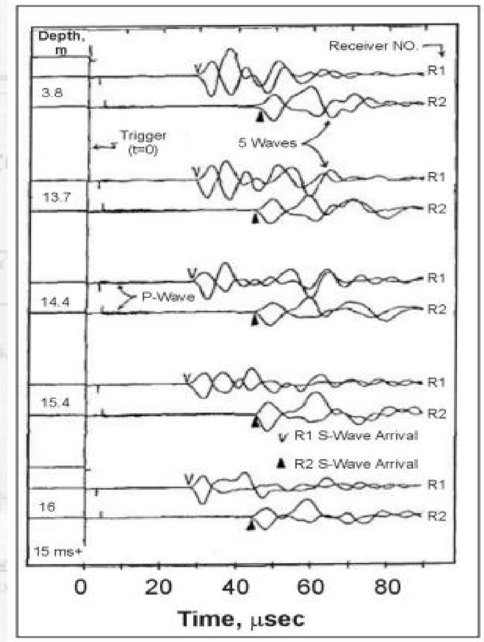

CROSS-HOLE SEISMIC

Source and geophone are raised (at regular intervals) to top of borehole. Interval shear-wave velocities (V_{int}) calculated for each layer tested on the basis of borehole separation (x) and shear-wave travel time (Δt).

$$Vint = \Delta x/\Delta t$$

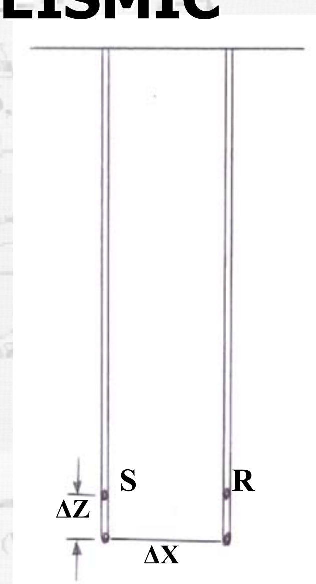

CROSS-HOLE SEISMIC

Strengths: Cross-borehole tool is "theoretically" capable of providing more accurate in-situ, shear-wave interval velocities than either the SCPT or MASW techniques.

Weaknesses: Related to cost and site accessibility, as twinned boreholes are required.

SEISMIC CONE PENETROMETER

Employs a down-hole geophone and surface source. As SCPT cone is pressed into the soil, it is halted at predetermined depths and surface shear-wave source is discharged. The travel time of the shear-wave energy (ΔT_n) is measured for each SCPT test depth (Z_n).

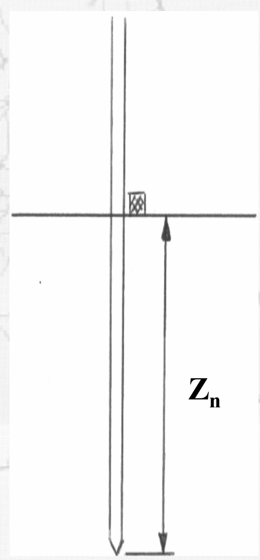

SEISMIC CONE PENETROMETER

An interval velocity is then calculated for each depth interval.

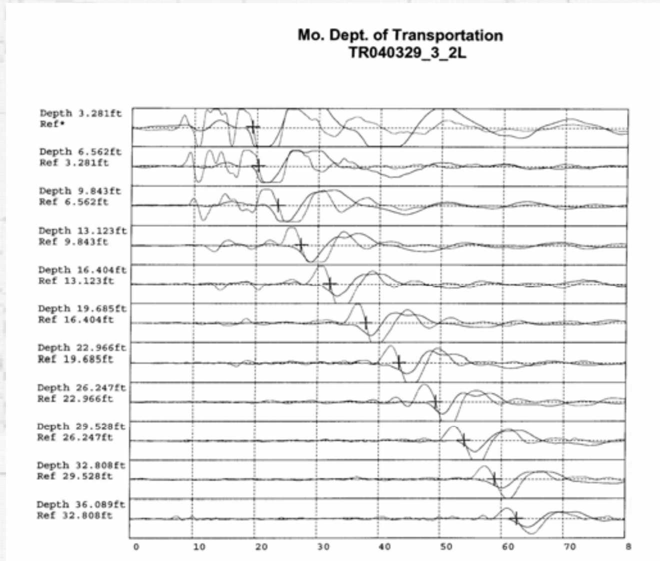

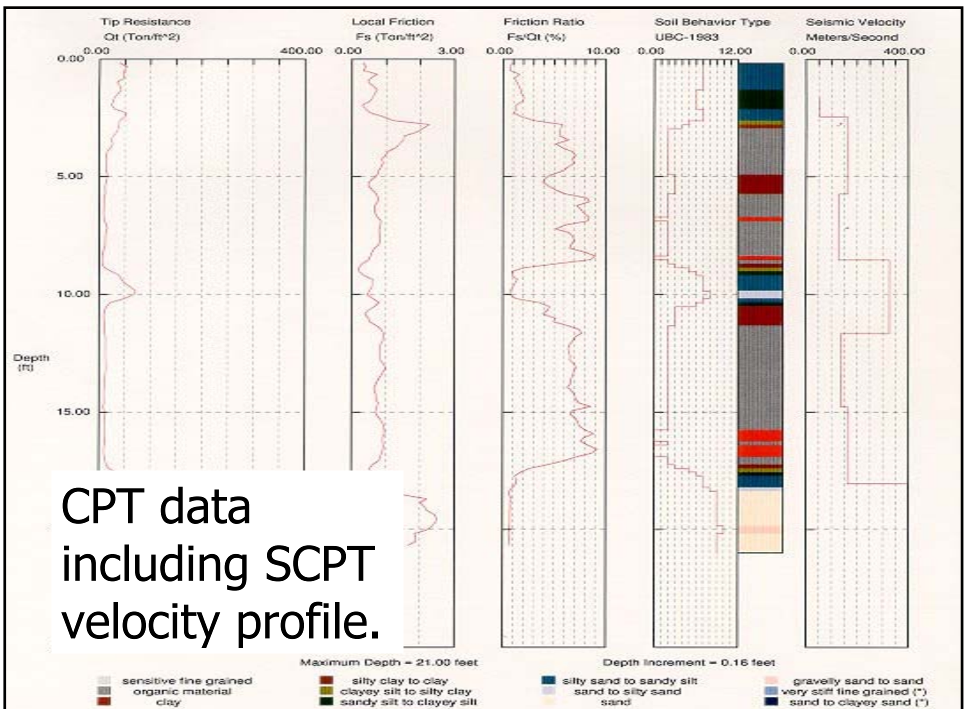

CPT data including SCPT velocity profile.

SEISMIC CONE PENETROMETER

Strengths: If all travel times are measured accurately, the SCPT tool is capable of providing accurate interval velocities for layers with thicknesses on the order of 1 m.

Weaknesses: If all travel times are not accurately measured, the output interval velocities will be inaccurate.

SASW TECHNIQUE

Rayleigh waves are generated using active and/or passive sources. In a heterogeneous earth, shear-wave and compressional-wave velocities vary with depth. Hence, the different component frequencies of Rayleigh waves exhibit different phase velocities.

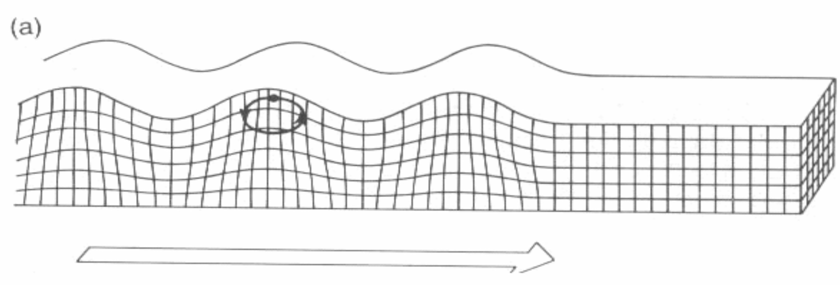

SASW TECHNIQUE

The phase velocity of each component frequency is a function of the variable body wave velocities over the vertical depth range of particle motion associated with that specific wavelength.

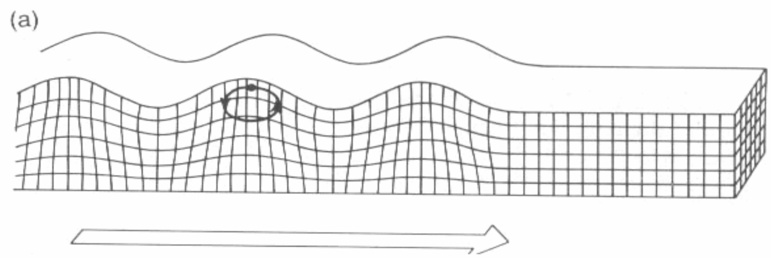

NATURAL HAZARDS MITIGATION INSTITUTE

UMR UNIVERSITY OF MISSOURI-ROLLA

SASW TECHNIQUE

During processing, phase velocities are calculated for each component frequency of the recorded Rayleigh waves.

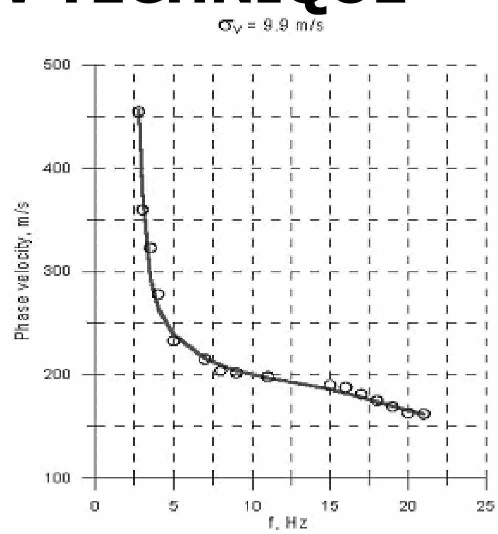

NATURAL HAZARDS MITIGATION INSTITUTE

UMR UNIVERSITY OF MISSOURI-ROLLA

Dispersion curve (phase velocity vs. frequency) is inverted and shear-wave velocity profile is generated.

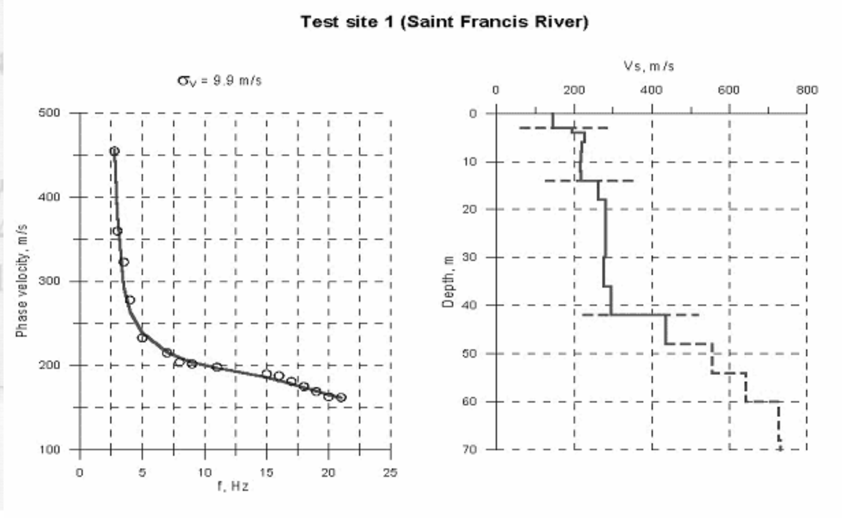

NATURAL HAZARDS MITIGATION INSTITUTE

UMR UNIVERSITY OF MISSOURI-ROLLA

SASW TECHNIQUE

Strength: The technique can be used in areas where the SCPT cannot be employed. SASW data are relatively inexpensive to acquire.

Weakness: Depth of investigation is limited by source. Vs/Vp ratios must be estimated during inversion.

NATURAL HAZARDS MITIGATION INSTITUTE

UMR UNIVERSITY OF MISSOURI-ROLLA

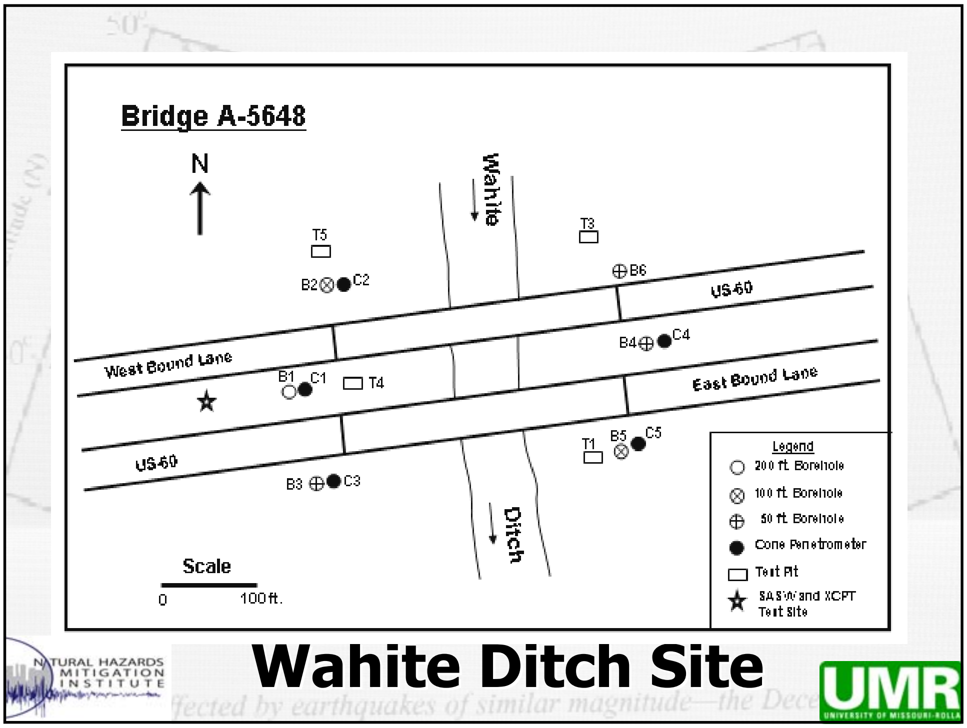

Bridge A-5648
N
Wahite
Ditch
T5
T3
T4
T1
B2
C2
B6
US 60
B4
C4
West Bound Lane
B1
C1
East Bound Lane
US 60
B5
C5
B3
C3
Legend
200 ft. Borehole
100 ft. Borehole
50 ft. Borehole
Cone Penetrometer
Test Pit
SASW and XCPT Test Site
Scale
0
100 ft.
NATURAL HAZARDS MITIGATION INSTITUTE
Wahite Ditch Site
UMR
UNIVERSITY OF MISSOURI-ROLLA

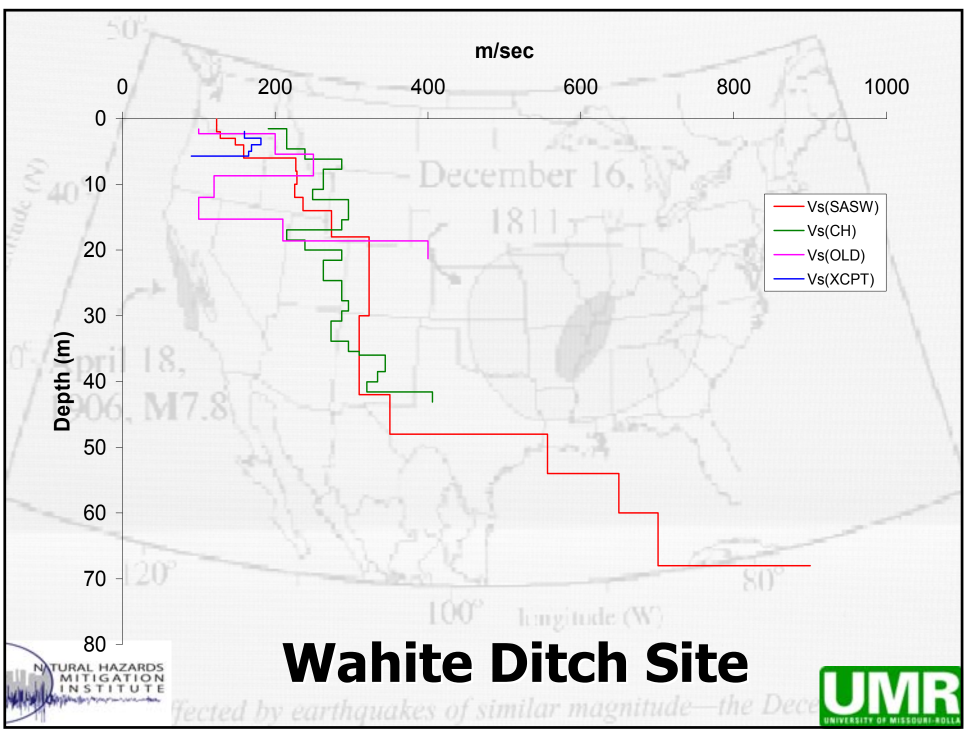

m/sec
0
200
400
600
800
1000
Depth (m)
0
10
20
30
40
50
60
70
80
Vs(SASW)
Vs(CH)
Vs(OLD)
Vs(XCPT)
NATURAL HAZARDS MITIGATION INSTITUTE
Wahite Ditch Site
UMR
UNIVERSITY OF MISSOURI-ROLLA

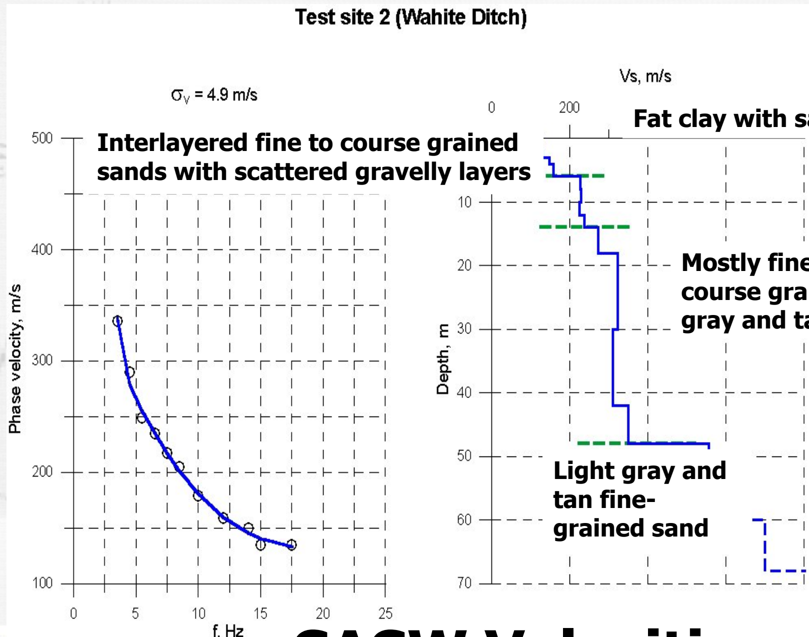

SASW Velocities

CH Velocities

CH velocities correlate well with SASW data. SASW velocities increase step-wise from ~130 m/s to ~350 m/s. Same interval on the BH profile is characterized by shear-wave velocities that increase gradually from about ~150 to ~380 m/s.

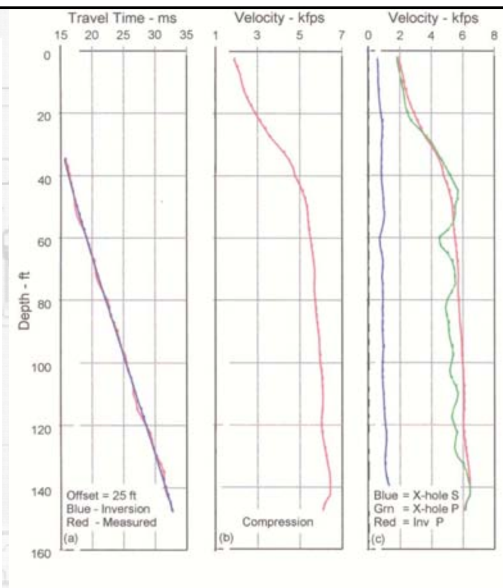

Figure 10. (a). Comparison of travel times from field measurements and inversion model. (b). Corresponding inversion velocity. (c). Comparison of inversion velocity with tomographic velocities.

SCPT Velocities

Near-surface (<6 m) clays characterized by SCPT shear-wave velocities ranging from ~100-240 m/s. Highest velocities are observed at depths of ~3 m. Underlying sands are characterized by velocities on the order of 400 m/s. Values are significantly higher than SASW and cross-borehole velocities over same lithology/ same depth intervals.

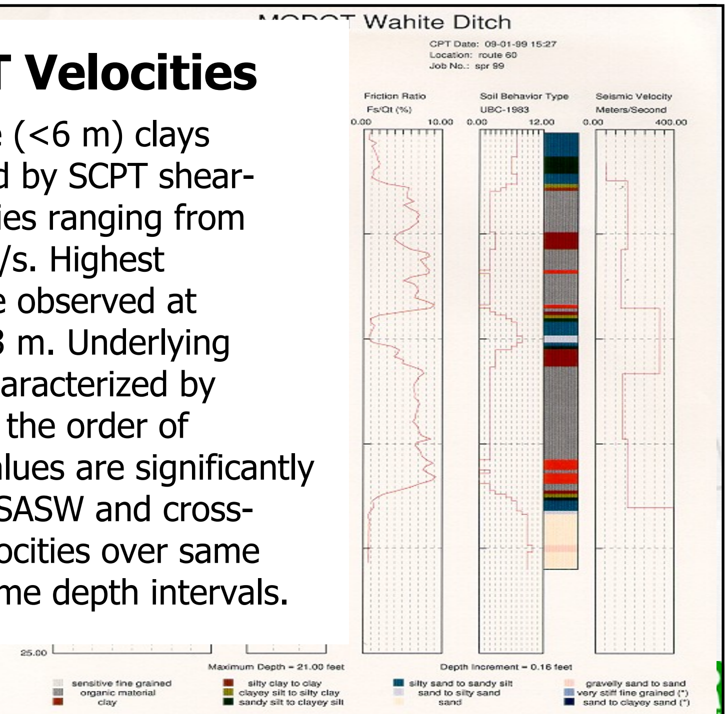

NATURAL HAZARDS MITIGATION INSTITUTE

Conclusions

- SASW-derived shear-wave velocity profiles correlate well with subsurface lithologic logs & available cross-borehole shear-wave velocity control.
- Clays, silts and sands exhibit relatively characteristic SASW-derived shear-wave velocities, which increase step-wise with depth of burial.
- The SASW and BH shear-wave velocity profiles and borehole lithologic data do not correlate particularly well with the SCPT shear-wave velocity profiles – particularly at shallow depths.

NATURAL HAZARDS MITIGATION INSTITUTE

UMR UNIVERSITY OF MISSOURI-ROLLA

Testing Program

Bridge A1466

Test type	CPT	SCPT	Borehole		
Number	4	3	2	1	2
Depth (ft)	23~65	40~66	80	100	200
Note	An observation well was installed at one 80′ borehole. Two 200′ boreholes were used for cross-hole geophysical test.				

Bridge L472

Test type	CPT	SCPT	Borehole	
Number	4	3	2	2
Depth (ft)	41~54	36~41	80	100
Note	P1 and P2 were moved from the bottom to the top of slope due to the soft soil after raining			

LAYOUT OF EXPLORATION

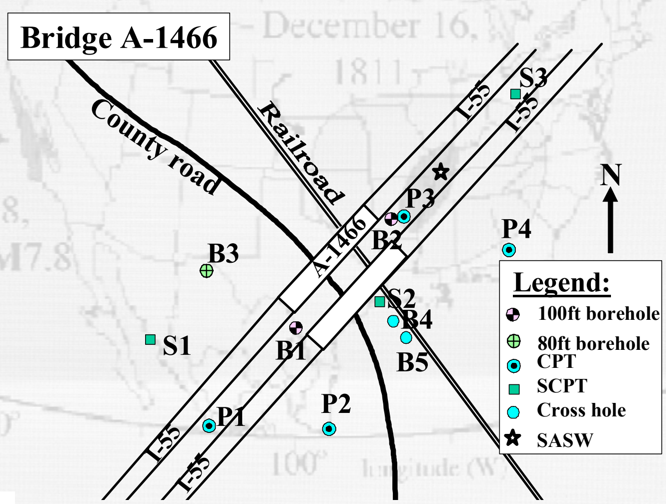

LAYOUT OF EXPLORATION

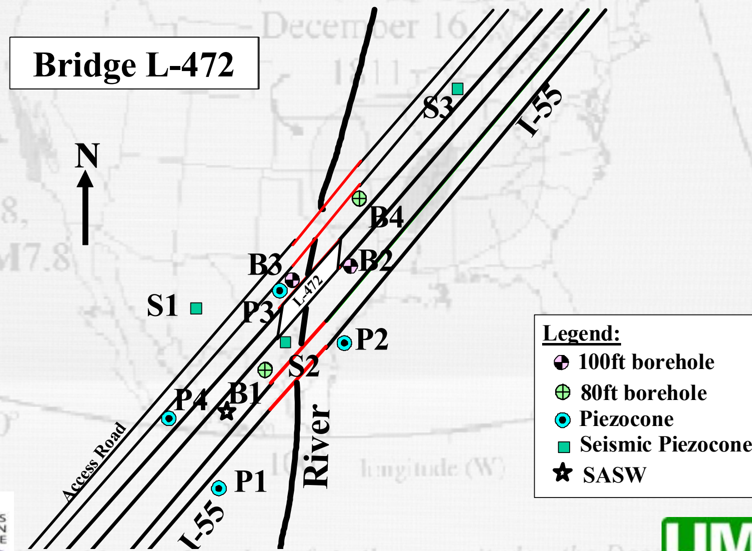

CPT CLASSIFICATION

- Based on UBC83
  - Tip resistance
  - Friction ratio
  - Laboratory classification tests

A1466

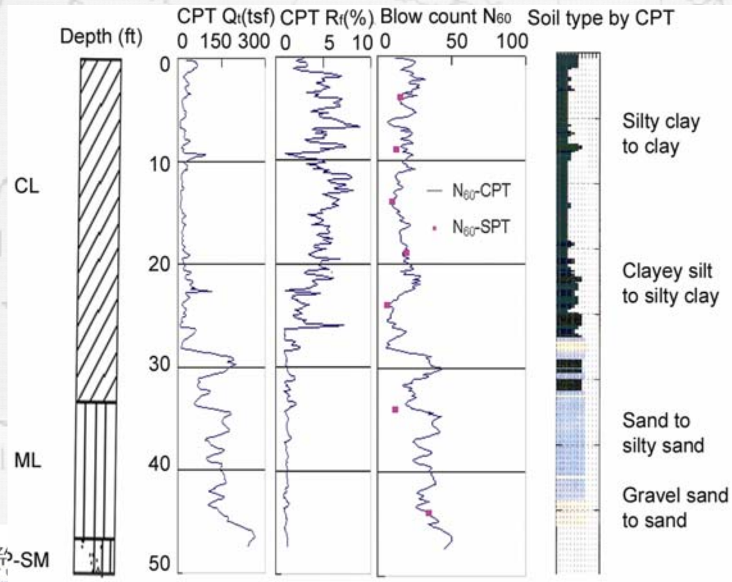
Depth (ft)
CPT Qt(tsf)
0 150 300
CPT Rf(%)
0 5 10
Blow count N60
0 50 100
Soil type by CPT
0
10
20
30
40
50
CL
ML
SP-SM
N60-CPT
N60-SPT
Silty clay
to clay
Clayey silt
to silty clay
Sand to
silty sand
Gravel sand
to sand

L472

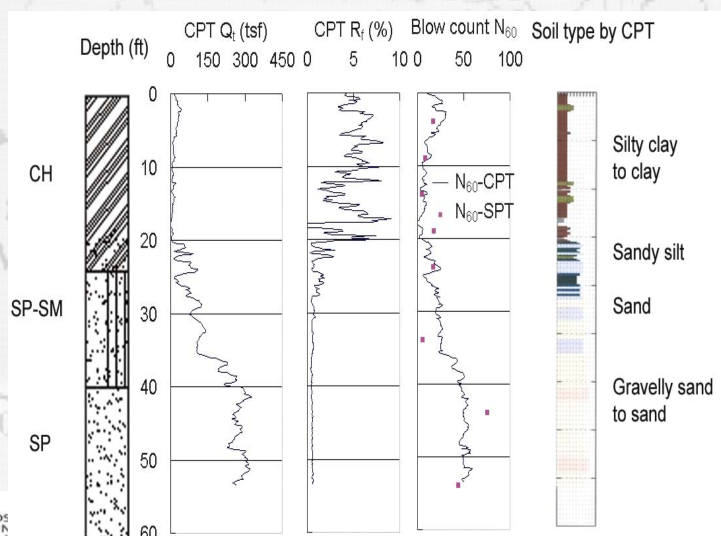
Depth (ft)
CPT Qt (tsf)
0 150 300 450
CPT Rf (%)
0 5 10
Blow count N60
0 50 100
Soil type by CPT
0
10
20
30
40
50
60
CH
SP-SM
SP
N60-CPT
N60-SPT
Silty clay
to clay
Sandy silt
Sand
Gravelly sand
to sand

DEEP SOIL PROPERTIES

- CPT maximum depth ~ 20 m (60 ft)
- SPT maximum depth ~ 60 m (200 ft)
- Depth of soil profile:
  - 650 to 720 m (2100-2400 ft)
- Must determine necessary soil properties from available correlations

---

- Soils at depth were classified from water well log descriptions
  - Well No. 2 was drilled in 1949 at Steele.
    - 720 m deep.
  - Well No. 4 was drilled in 1947 at Hayti
    - 650 m deep

CORRELATIONS

- Unit Weight (Mayne, 2001)

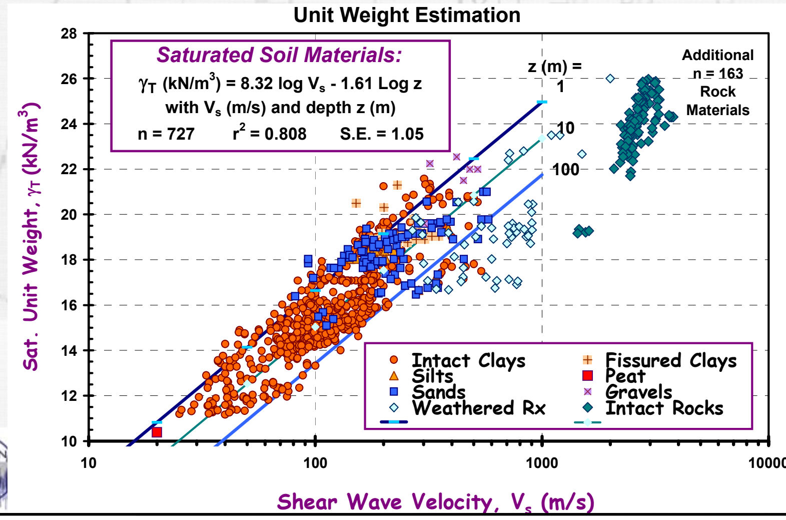

- Internal friction angle, Φ
  - Schmertmann, 1975)

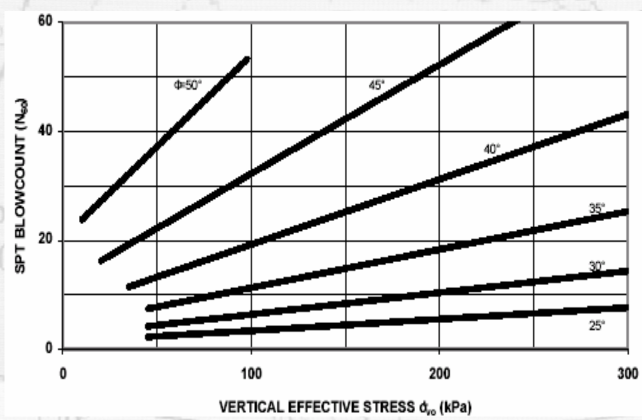

$$\phi' \approx \tan^{-1}\left[N_{60}/12.2 + 20.3\sigma'_{v0}/P_a\right]^{0.34}$$

- Deep soils without SPT N values:
  - Terzaghi, et al., 1996

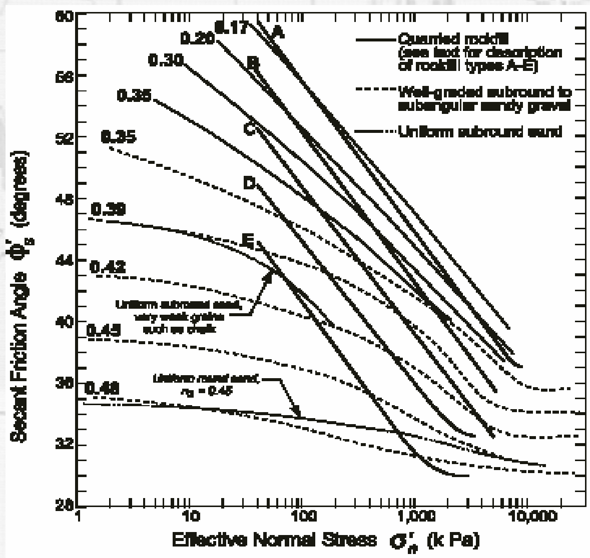

- Cohesive Soils
  - Mesri, 1993

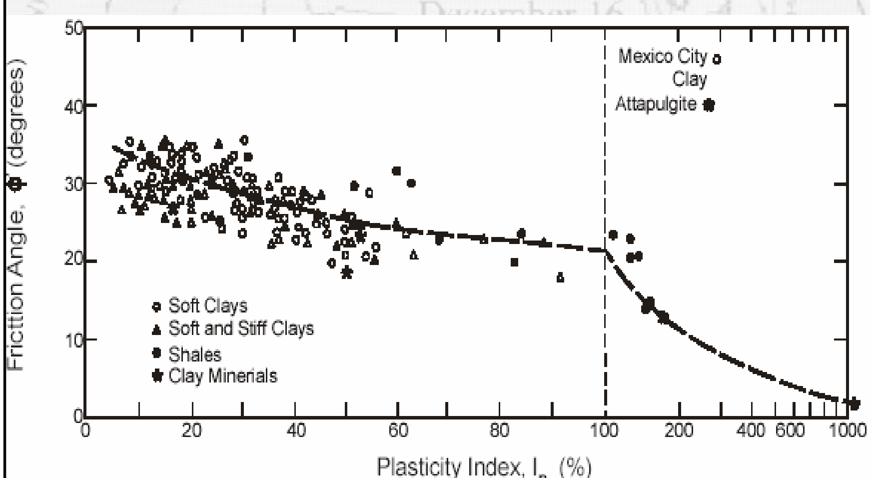

SHEAR WAVE VELOCITIES

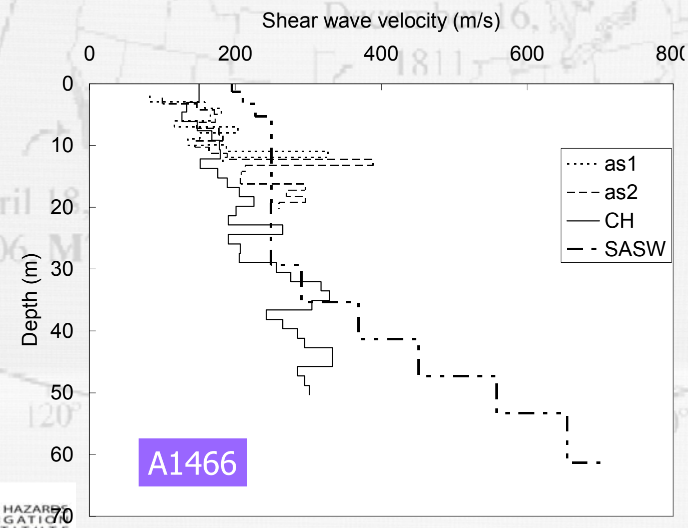

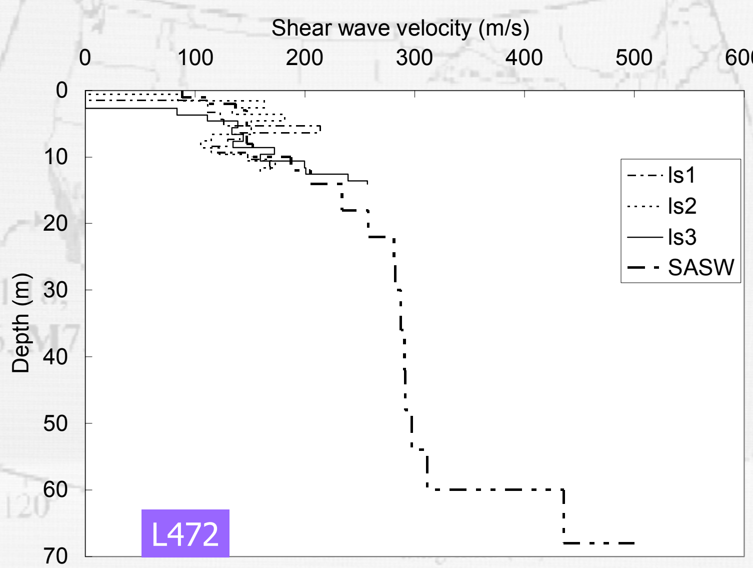

- Maximum Shear Modulus

$$G_{\max} = \rho v_s^2$$

ρ- mass density
v_s-shear wave velocity

$$G_{\max} = 1230 OCR^k \frac{(2.973 - e)^2}{1 + e} (\sigma'_0)^{0.5}$$

OCR-overconsolidation ratio
e-void ratio
σ'_0-mean principal effective stress
k-function of PI

Comparison of (Gmax)field/(Gmax)correlation at B3 of A1466

Ratio of G_{max}	SCPT/Hardin	SASW/Hardin	Cross-hole/Hardin
CL (0~5.5 m)	0.87	3.13	0.95
ML (5.5~9.1 m)	0.87	3.18	0.81
SM (9.1~13.2 m)	1.57	1.50	0.82
SP (13.2~21.3 m)	-	0.74	0.45
SP-SM (21.3~25.6 m)	-	0.70	0.66
Overall	1.06	1.30	0.68

Comparison of (Gmax)field/(Gmax)correlation at B1 of L472

Ratio of G_{max}	SCPT/Hardin	SASW/Hardin
CL (0~3.7 m)	0.58	0.56
OH (3.7~5.2 m)	1.41	1.18
CL (5.2~6.4 m)	0.70	0.71
CH (6.4~8.5 m)	0.35	0.67
SM (8.5~11.6 m)	0.37	0.47
SP-SM(11.6~25.6 m)	-	0.87
Overall	0.60	0.79

SHEAR WAVE VELOCITY FROM SPT TESTING

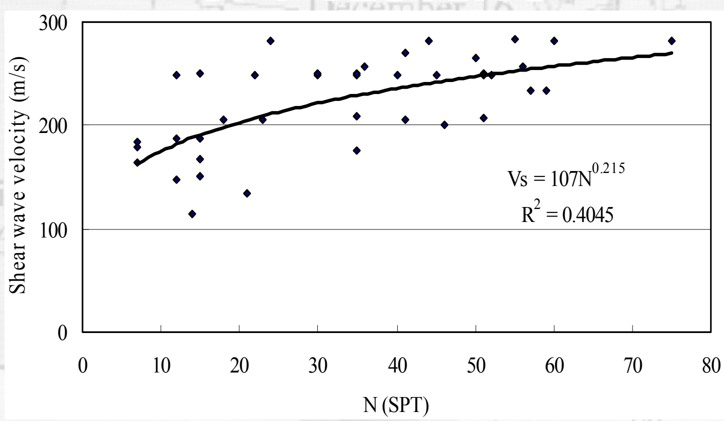

$$V_s = 107 N^{0.215}$$

COMPARISON TO PUBLISHED VALUES

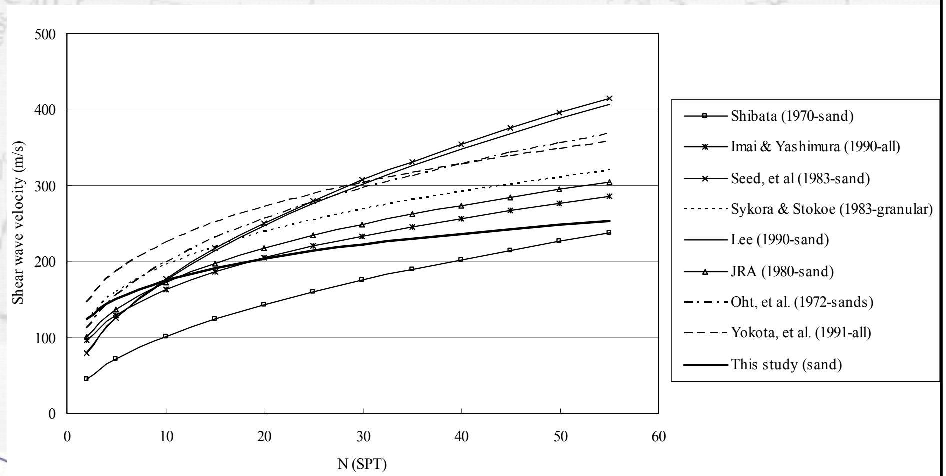

SOIL PROFILE AT BRIDGE SITE A1466

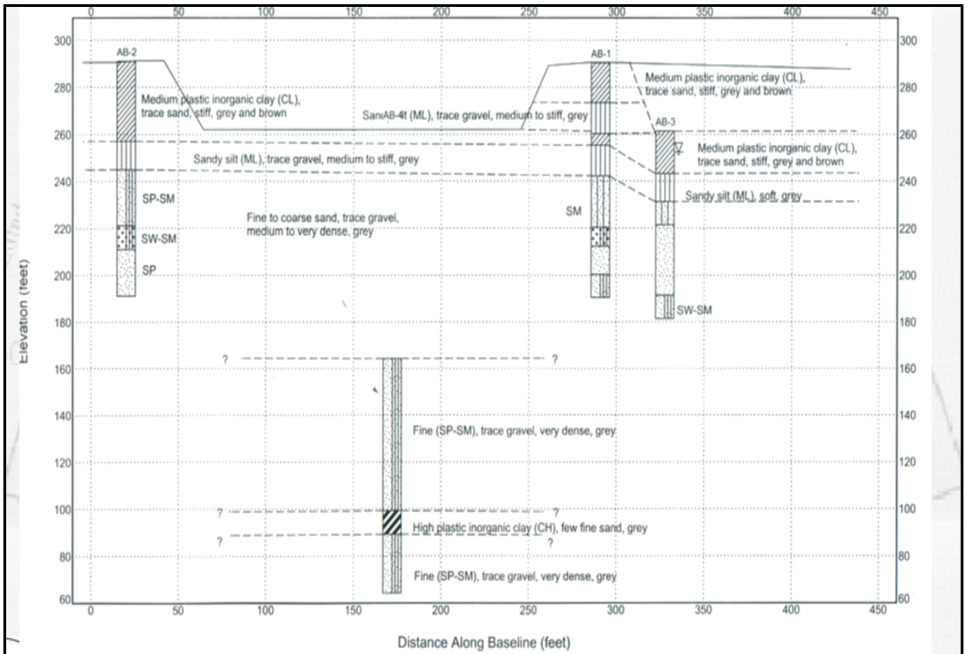

SOIL PROFILE AT BRIDGE SITE L472

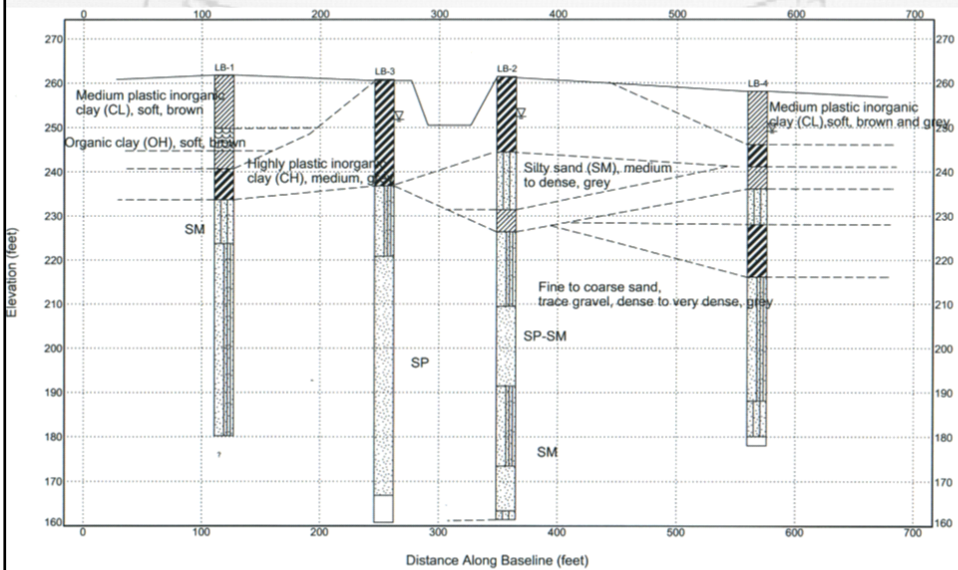

NATURAL HAZARDS MITIGATION INSTITUTE

UMR UNIVERSITY OF MISSOURI-ROLLA

SITE CLASSIFICATION

- Based on National Earthquake Hazards Reduction Program (NEHRP).

NATURAL HAZARDS MITIGATION INSTITUTE

UMR UNIVERSITY OF MISSOURI-ROLLA

Site Class	Description
A	Hard rock with $\bar{v}_s$ > 1500 m/s
B	Rock 760 m/s < $\bar{v}_s \le$ 1500 m/s
C	Very dense soil and soft rock with 360 m/s< $\bar{v}_s \le$ 760 m/s
D	Stiff soil with $\bar{v}_s$< 180 m/s or with 15≤N'≤50 or 50 kPa≤ $\bar{s}_u$ 180 m/s ≤ 100 kPa
E	A soil profile with $\bar{v}_s$ < 180 m/s or with either N ≤15, s_u<50 kPa or any profile with ore than 10 ft (3 m) of soft clay defined as soil with PI>20, w≥40 %, and s_u< 25 kPa
F	Soils requiring site-specific evaluations: 1. Soils vulnerable to potential failure or collapse under seismic loading such as liquefiable soils, quick and highly sensitive clays, and collapsible weakly cemented soils. 3. Peats and/or highly organic clays (*H* > 3 m of peat and/or highly organic clay where *H* = thickness of soil) 3. Very high plasticity clays (*H* > 8 m with PI > 75) 4. Very thick soft/medium stiff clays (*H* > 36 m)

Site Class	Maximum Considered Earthquake Spectral Response Acceleration at Short Periods				
	$S_s \le$ 0.25	S_s = 0.50	S_s = 0.75	S_s = 1.00	$S_s \ge$ 0.25
A	0.8	0.8	0.8	0.8	0.8
B	1.0	1.0	1.0	1.0	1.0
C	1.2	1.2	1.1	1.0	1.0
D	1.6	1.4	1.2	1.1	1.0
E	3.5	1.7	1.2	0.9	0.9
F	*a*	*a*	*a*	*a*	*A*

Site Class	Maximum Considered Earthquake Spectral Response Acceleration at long Periods				
	$S_l \leq 0.1$	$S_l = 0.2$	$S_l = 0.3$	$S_l = 0.4$	$S_l \geq 0.5$
A	0.8	0.8	0.8	0.8	0.8
B	1.0	1.0	1.0	1.0	1.0
C	1.7	1.6	1.5	1.4	1.3
D	3.4	3.0	1.8	1.6	1.5
E	3.5	3.2	3.8	3.4	3.4
F	*a*	*a*	*a*	*a*	*A*

BRIDGE SITE A1466

Geophysical tests	S1	S2	S3	Cross-hole	SASW
Depth (m)	13.92	20.23	6.55	30.50	29.28
V_S (m/s)	135.96	171.53	220.01	178.06	241.78
Borings	B1	B2		B3	
Depth (m)	21.65	23.56		25.6	
$\overline{N}$	22	20		8.56	

Site Class E-Based on average shear wave velocity from cross-hole test

Site Class D-Based on average shear wave velocity from SASW test

BRIDGE SITE L472

Geophysical tests	S1	S2	S3	SASW
Depth (m)	11.90	13.50	14.07	30
v_s(m/s)	133.02	130.45	128.54	193.10
Borings	B1	B2	B3	B4
Depth (m)	25.6	31.1	31.1	25.6
$\bar{N}$	11.54	17.63	13.88	8.59

Site Class D-Based on average shear wave velocity from SASW test

INCONSISTENCIES

- Maybe classified as:
  - D based on average shear wave velocity
  - E based on average SPT values
- Classification based on Western United States conditions
  - New Madrid zone is much different
  - Little data on deep soil properties

DYNAMIC SOIL PROPERTIES

SHEAR MODULUS AND DAMPING RATIO AT LOW STRAIN LEVELS

- Measured from:
  - Shear wave velocity measurements
    - Field (geophysical testing)
    - Laboratory
      - Resonant column
      - Ultrasonic velocity

Influencing parameters

- Soil type
- Density (void ratio)
- Overconsolidation ratio (OCR)
- Effective confining stresses

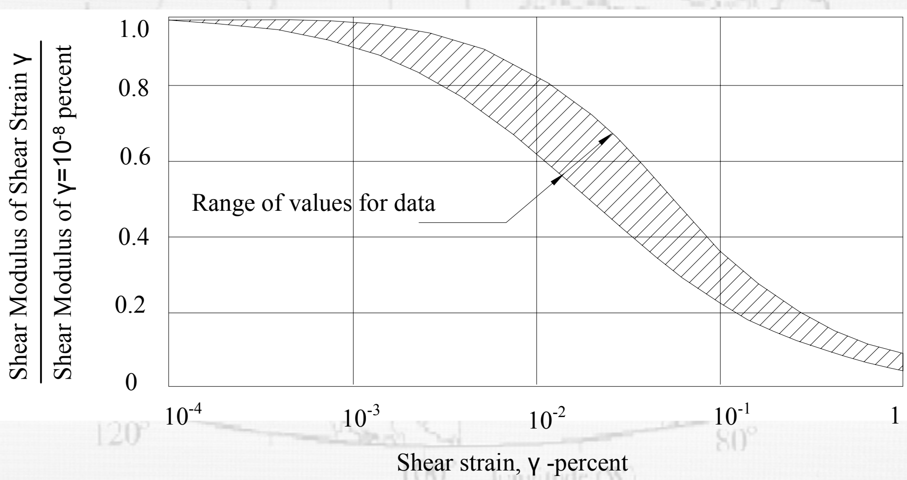

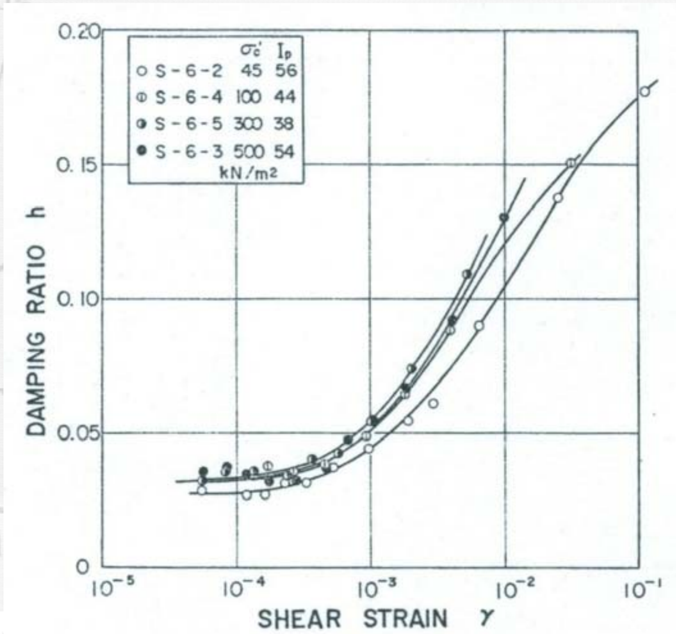

We found more than two dozen published correlation equations for strain-dependent shear modulus and damping.

Conclusions

- Gmax increases with PI and time increasing for cohesive soil. Gmax is not sensitive to confining duration time for sandy soil.
- Gmax increases and damping ratio at small strain decreases with confining pressure increasing and Gmax is independent of loading frequency.
- Grain size, grain shape, gradation, degree of saturation, and frequency of vibration introduce insignificant effects on shear modulus of sands.
- G/Gmax and D are not sensitive to confining pressure and OCR but highly dependent on PI for cohesive soils. It increases with PI decreasing.

- The effect of loading frequency on G/Gmax reduction curves can be negligible.
- G/Gmax increases and D decreases with confining pressure increasing for sand.
- G/G_0' and D is relatively confining pressure independent for clayey sands.

Relationships used for this study:

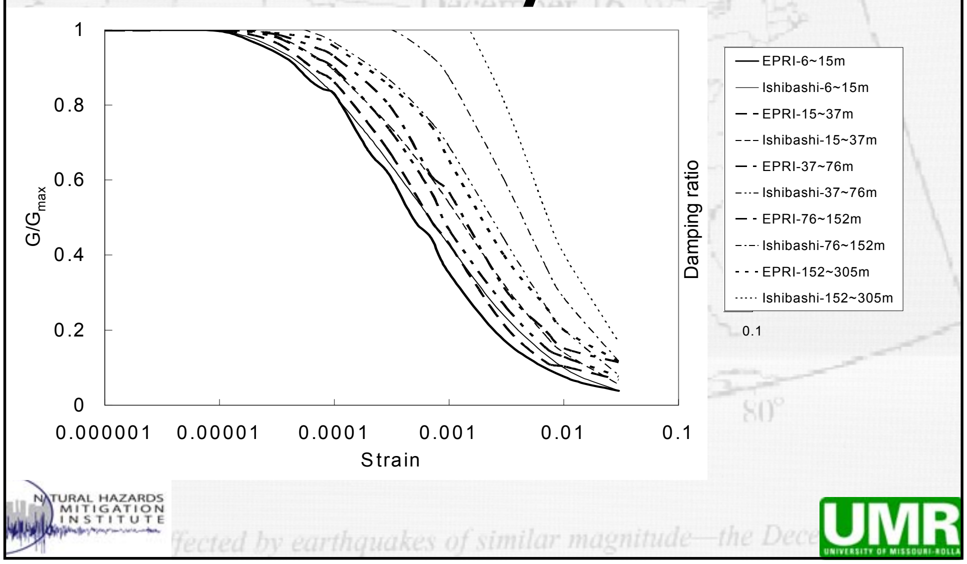

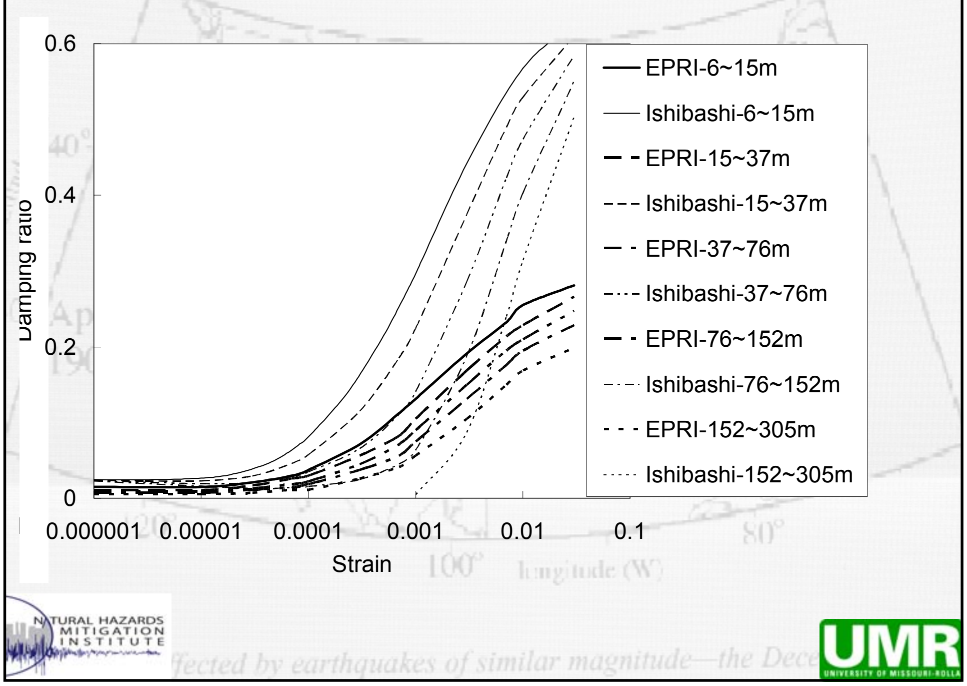

Final Comments

- Hampered by lack of deep exploration boreholes in the NMSZ
- Lack of information on the effect of high confining pressures on soil properties
- Lack of information on the behavior of silty soils, i.e., ML,SM, etc.

NATURAL HAZARDS MITIGATION INSTITUTE

UMR UNIVERSITY OF MISSOURI-ROLLA

Future Work

- Comprehensive Laboratory Study of silts, silty clays

NATURAL HAZARDS MITIGATION INSTITUTE

UMR UNIVERSITY OF MISSOURI-ROLLA

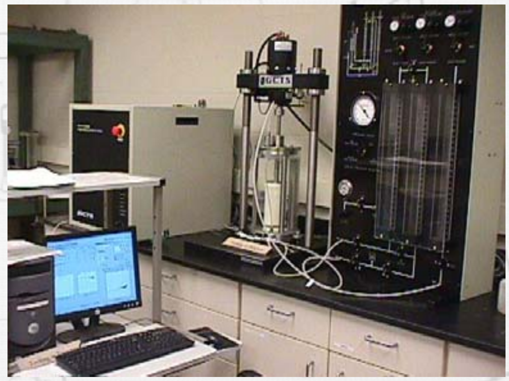

Stress path Triaxial

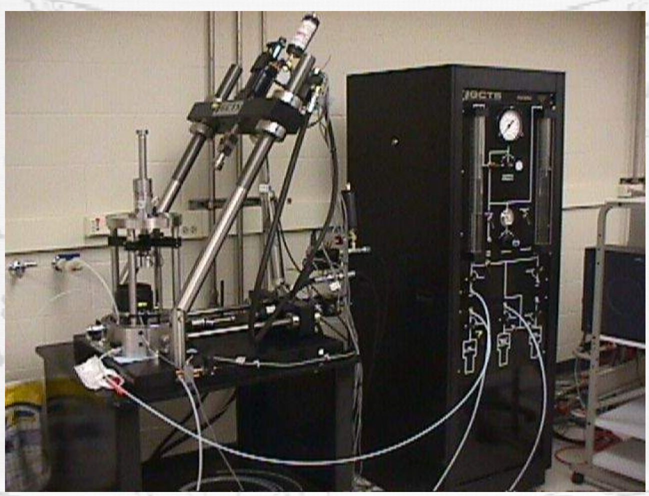

Cyclic Simple Shear

Ultrasonic Velocity

NATURAL HAZARDS MITIGATION INSTITUTE

UMR UNIVERSITY OF MISSOURI-ROLLA

Resonant Column

NATURAL HAZARDS MITIGATION INSTITUTE

UMR UNIVERSITY OF MISSOURI-ROLLA

PRESENTATION 9

SITE RESPONSE ANALYSIS
INCLUDING LIQUEFACTION

SITE RESPONSE ANALYSIS INCLUDING LIQUEFACTION

Ronaldo Luna, Ph.D., P.E.
Associate Professor of Civil Engineering
University of Missouri-Rolla (UMR)

Geotechnical and Bridge Seismic Design Workshop
New Madrid Seismic Zone Experience

October 28-29, 2004, Cape Girardeau, Missouri

SITE RESPONSE ANALYSIS INCLUDING LIQUEFACTION

Investigators:

Mr. Wanxing Liu
Dr. Ronaldo Luna (Lead)
Dr. Richard Stephenson
Dr. Wei Zheng

NATURAL HAZARDS MITIGATION INSTITUTE

UMR UNIVERSITY OF MISSOURI-ROLLA

Presentation Outline

- Presentation Objectives
- Seismic Response Methodology
- Site Response Analysis for this study
- Application to NMSZ Bridge Sites
- Simulated vs. Observed Near-Field Ground Motions
- Summary & Conclusions

NATURAL HAZARDS MITIGATION INSTITUTE

UMR UNIVERSITY OF MISSOURI-ROLLA

Objectives

- Define the required dynamic soil properties for site response
- Obtain ground motions at ground surface in time domain modeling
- Study effects of deep Soils – high confinement
- Examine the liquefaction potential at the sites

Properties of Earthquakes

- Anomalously high frequency and long duration
- Large influenced area
- Long recurrence interval, but the probability of recurrence is high in next 50 years

Source :The Center for Earthquake Research and Information (CERI) at The University of Memphis

Magnitude	Recurrence Interval	Probability of Recurrence in the years 2000-2015	Probability of Recurrence in the years 2000-2050
>= 6.0	70+/-15 years	40 - 70%	88 - 98%
>= 7.5	250+/-60 years	6.0 - 9.5%	21 - 33%
>= 8.0	550+/-125 years	0.4 - 1.1%	1.6 - 4.3%

Bridge Foundation Damage

- A large amount of bridge foundation (pile foundations) damage and failure were observed in the 1964 Alaska, 1989 Loma Prieta, 1995 Kobe, 1999 Chi-Chi, 1999 Izmit earthquakes (Magnitude ranging from 6.4 to 8.3).
- These failures have been found primarily due to two factors:
  – Loss of lateral soil support may occur due to liquefaction of cohesionless soils or strain softening of cohesive soils near the pile head, and
  – Large loads and displacements due to laterally spreading soil deposit after liquefaction.

Shi-Wei Bridge Collapse

Shi-wei Bridge Collapse during the Chi-Chi Earthquake

Bridges in the NMSZ

- Similar sub structure and foundation conditions as the Shi-wei Bridge.
- Bridge decks supported on steel rocker bearings with multiple expansion joints.

- It is necessary to study SPSI to understand the seismic behavior of highway bridges.
- The purpose of this research is to study the dynamic soil properties in the NMSZ and the current analytical methods for SPSI and develop a sound approach for the fully-coupled SPSI analysis in the NMSZ.

NATURAL HAZARDS MITIGATION INSTITUTE

UMR UNIVERSITY OF MISSOURI-ROLLA

Earthquake Ground Motion Simulation

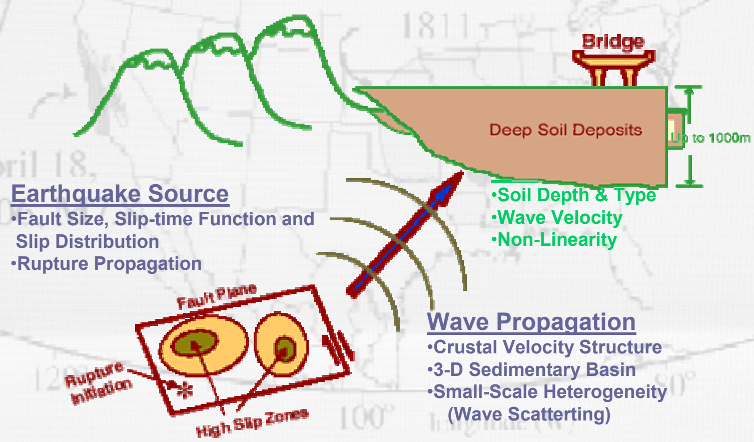

NATURAL HAZARDS MITIGATION INSTITUTE

UMR UNIVERSITY OF MISSOURI-ROLLA

Two-Step Approach

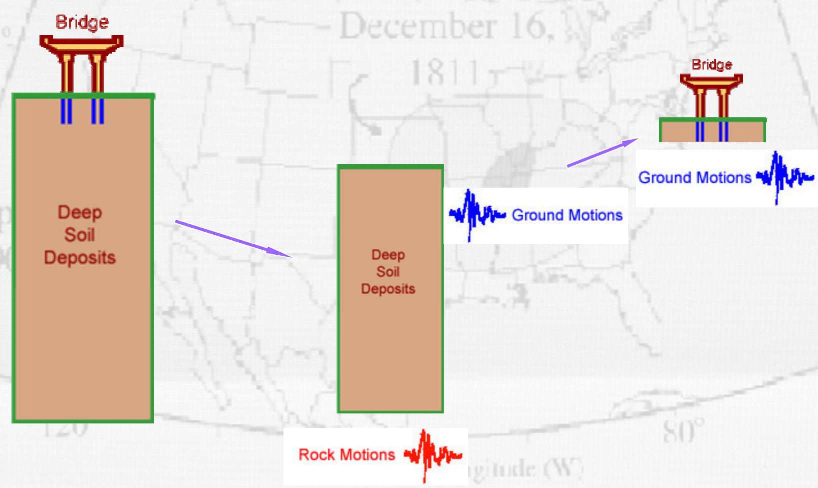

Seismic Site Response

- Seismic site response is usually referred to as the propagation of seismic waves from an input base rock to the ground surface through the local site soils.
- Since the 1970's methodologies have been developed to analyze this process using equivalent-linear or nonlinear methods.

Seismic Site Response

Equivalent linear methods in the Frequency Domain:

- SHAKE (Schnabel et al., 1972) → 1D
- FLUSH (Lysmer et al. 1975) → 2-D
- RASCALS, Silva (1992) → deep soils
- Assimaki (2001) introduced frequency-dependent soil parameters.

Seismic Site Response

1D Nonlinear Methods in the Time Domain:

Program	Soil model	Method	Stress	Reference
CHARSOIL	Ramberg-Osgood	Characteristics	Total	Streeter et al. (1973)
DESRA-2	Hyperbolic	Finite element	Effective	Lee and Finn (1978, 1991)
DESRAMOD2	Hyperbolic	Finite element	Effective	Vucetic (1998)
DESRA-MUSC	Hyperbolic	Finite element	Effective	Qiu(1998)
D-MOD(derived from DESRA-2)	M-K-Z (Matasovic, Konder, and Zelasko)	Finite element	Effective	Matasovic (1993)
MASH	Martin-Davidenkov	Finite element	Effective	Martin and Seed (1978)
DYNA1D	Nested yield surface	Finite element	Effective	Prevost (1989)
TESS	HDCP (Hardin-Drnevich-Cundall-Pyke)	Finite difference	Effective	Pyke (1979, 1985, 1992)
SUMDES	Hypoplasticity	Finite element	Effective	Li et al. (1992)
DEEPSOIL (derived from D-MOD)	Modified hyperbolic with extended Masing criteria	Finite element	Total	Hashash and Park (2001)

Seismic Site Response

1D Nonlinear Methods in the Time Domain:

- There are many nonlinear, 1D ground response analysis computer programs using direct numerical integration in the time domain.

Seismic Site Response

2D Nonlinear Methods in the Time Domain:

- 1D methods are useful for level or gently sloping sites with parallel material boundaries. However, problems such as sloping or irregular ground surfaces, the presence of heavy, stiff, or embedded structures, or walls and tunnels all require 2D or even 3D analysis.

Seismic Site Response

2D Nonlinear Methods in the Time Domain:

Program	Soil model	Method	Stress	Reference
TARA-3	Hyperbolic	Finite element	Effective	Finn et al. (1986)
DYNAFLOW	Multiple yield surface	Finite element	Effective	Prevost (1986)
DIANA	Different advanced models	Finite element	Effective	Kawai (1985)
FLAC	Hyperbolic (Finn and Byrne model)	Finite difference	Effective	Commercial
DYSAC2	Hypoplasticity	Finite element	Effective	-

NATURAL HAZARDS MITIGATION INSTITUTE

UMR UNIVERSITY OF MISSOURI-ROLLA

Recent Use of Site Response Methods

- Yu et al. (1993) studied the nonlinear behavior of soil using DESRA2 (Lee and Finn, 1978)
- Ni et al. (1997) extended this work to include deep saturated soil deposits accounting for the influence of pore pressure and stress-dependent damping and shear modulus ratio variations with shear strain (EPRI, 1993).

NATURAL HAZARDS MITIGATION INSTITUTE

UMR UNIVERSITY OF MISSOURI-ROLLA

Recent Use of Site Response Methods

- Ni et al. (2000) studied the nonlinearity of soil properties of shallow soil (upper 30 m).
- Assimaki et al. (2000) developed a simple four-parameter model to do site response of deep cohesionless soil (1 km deep) accounting for the stress-dependent modulus and damping ratio

Recent Use of Site Response Methods

- Romero and Rix (2001) studied the site response in the Central United States using the equivalent method RASCALS.
- Hashash et al. (2001) developed a new model accounting for the effect of high confining pressure on modulus degradation and damping ratio of deep soil.
- In 2002 this method used full Rayleigh damping formulation to represent the viscous damping of soils.

Development of New Deep Ground Response Analysis

Nonlinear Soil Properties

- Quite nonlinear Soil properties under seismic loading condition.
- In Vucetic & Dobry 's curves, for a given shear strain g, PI increases, G/G_{max} rises and l reduced.

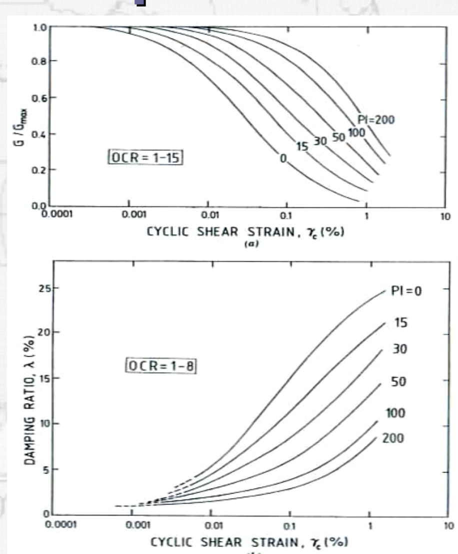

(Vucetic and Dobry, 1991)

Effect of Confining Pressure

Ishibashi (1992) pointed out that the method of Vucetic & Dobry didn't include one of the significant parameters, the effective mean normal stress.

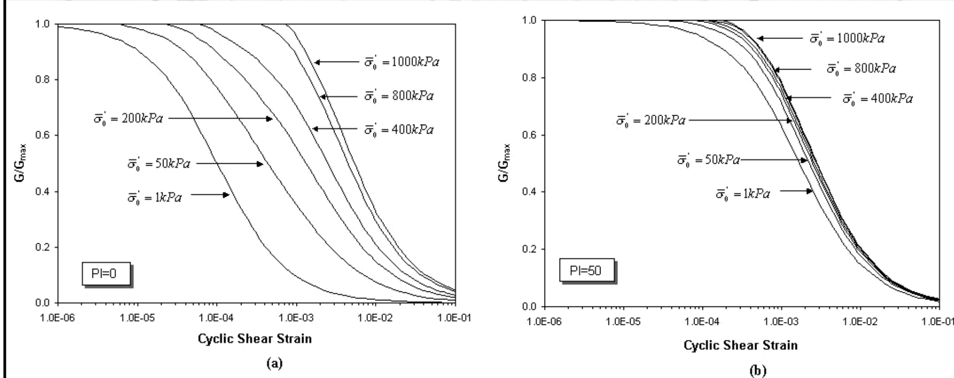

Unified Formula

Shear Modulus

$$\frac{G}{G_{\max}} = K(\gamma, PI)(\sigma_m')^{m(\gamma, PI)}$$

$$K(\gamma, PI) = 0.5\left\{1 + \tanh\left[\ln\left(\left(\frac{0.000101 + n(PI)}{\gamma}\right)^{0.492}\right)\right]\right\}$$

$$m(\gamma, PI) = 0.272\left\{1 - \tanh\left[\ln\left(\left(\frac{0.000556}{\gamma}\right)^{0.4}\right)\right]\right\}\exp(-0.0145\, PI^{1.3})$$

$$n(PI) = \begin{cases} 0.0 & for \quad PI = 0 \\ 3.37 \times 10^{-6} PI^{1.404} & for \quad 0 < PI \le 15 \\ 7.0 \times 10^{-7} PI^{1.976} & for \quad 15 < PI \le 70 \\ 2.7 \times 10^{-5} PI^{1.115} & for \quad PI > 70 \end{cases}$$

Unified Formula (contd.)

Damping Ratio

$$\lambda = \frac{0.333\,(1+\exp(-0.0145\,PI^{1.3}))}{2}\left\{0.586\left(\frac{G}{G_{max}}\right)^2 - 1.547\left(\frac{G}{G_{max}}\right) + 1\right\}$$

Backbone Curve

- **The shear modulus degradation curve presented in previous slide can be described as the backbone curve in stress-strain field.**

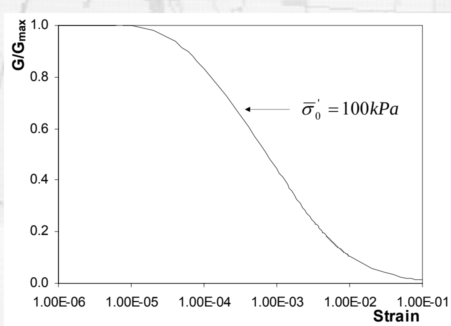

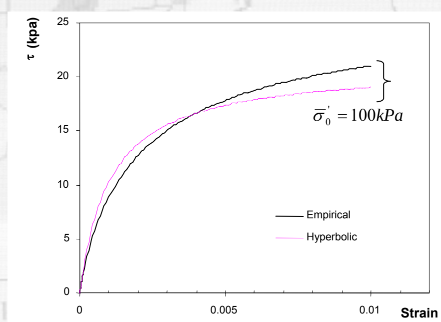

Extended Masing Criteria

- The extended Masing criteria (1926) are used to govern the unloading-reloading behavior of soil.

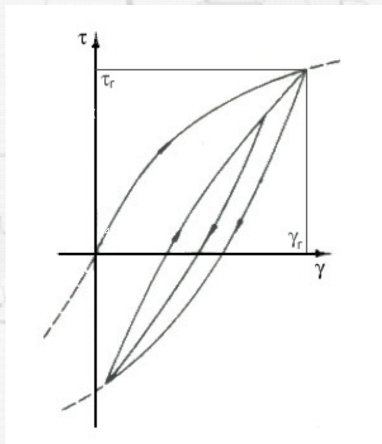

Extended Masing Criteria

Finite Element Approach

Global Dynamic Equation

$$[M]\{\ddot{u}\}+[C]\{\dot{u}\}+[K]\{u\}=P(t)$$

where

$$P(t)=-[M]\{I\}\ddot{u}_g(t)$$

Rayleigh Damping Formulation

$$[c]_{el}=\alpha[m]_{el}+\beta[k]_{el}$$

$$\alpha=2\lambda\omega_1\omega_2/(\omega_1+\omega_2)$$

$$\beta=2\lambda/(\omega_1+\omega_2)$$

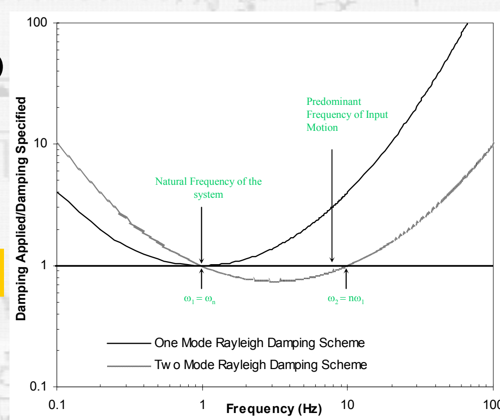

OpenSees Framework

- OpenSees - Open System for Earthquake Engineering Simulation
- OpenSees developed by PEER is a software framework to create models and analysis methods to simulate structural and geotechnical systems under earthquake loading.
- C++ language is used as compiler and finite element method is used for analysis.
- Tool Command Language (TCL) is used as interpreter to create commands.

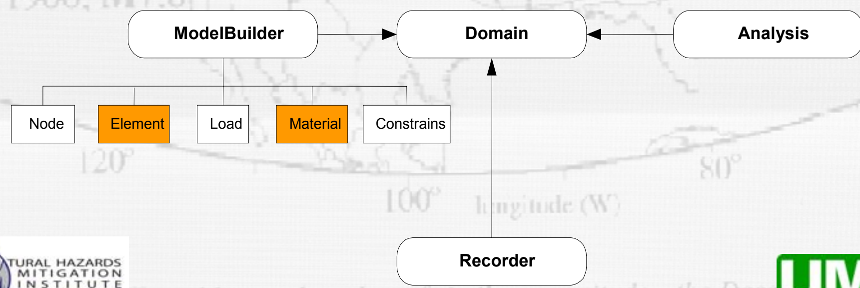

Work Chart of Programming

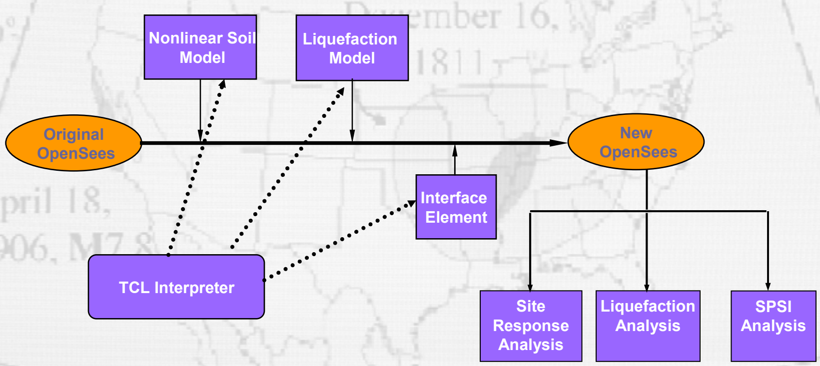

Site for Validation

- **Treasure Island** (TRI) man-made island
- Yerba Buena Island (YBI) – large base rock output, 2 km away from Treasure Island.
- Both islands are located 70~75 km northwest of the epicenter

Treasure Island Soil Profile

Treasure Island site consists of about 13m sandy fill, underlain by about 16 m thick of Young Bay Mud. Underlying the Young Bay Mud are alternating layers of dense sand and Old Bay Mud to a depth of about 89 m.

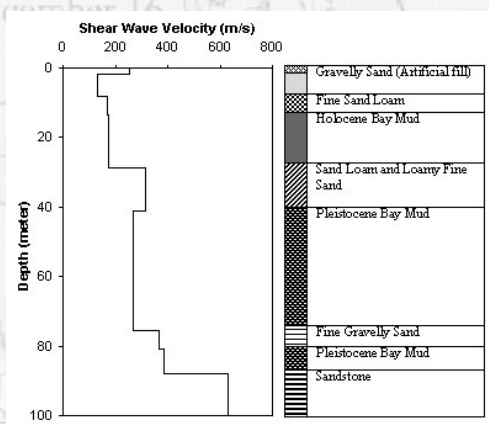

(Gibbs et al. 1992)

Response Spectra Comparison (90°)

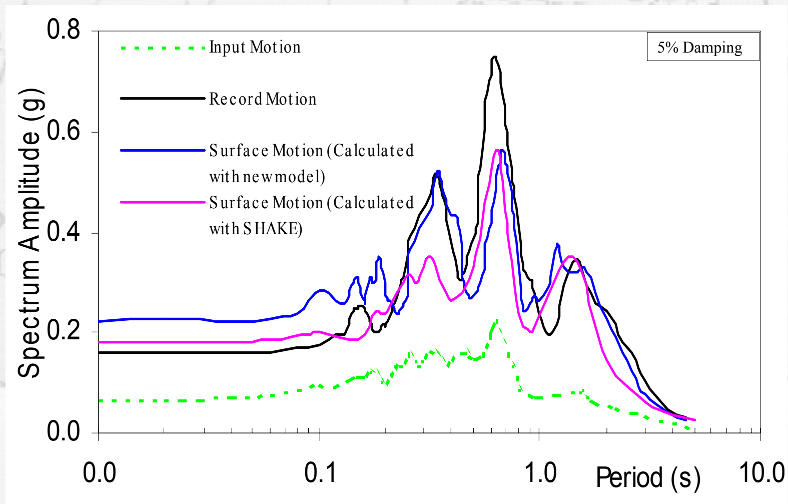

Response Spectra Comparison (00°)

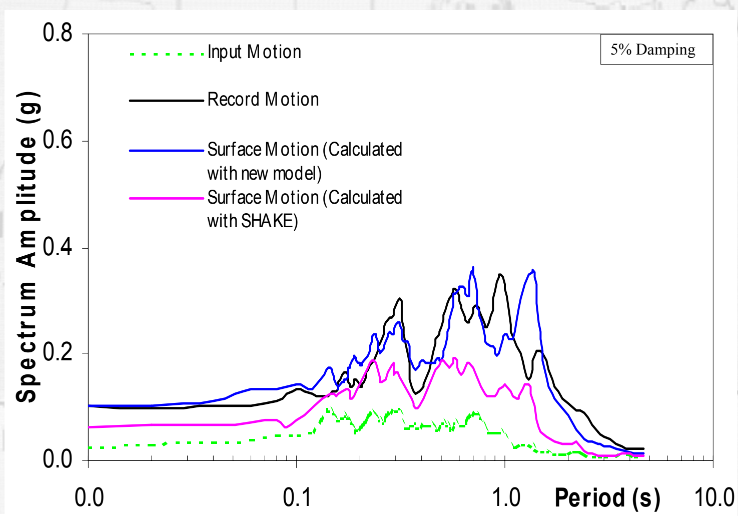

Application in the NMSZ

- The new soil model is applied a highway bridge site near Hayti, Missouri in the NMSZ.
- The thickness of the sediment at the study site is estimated at about 600 m.
- The shallow shear wave velocity profile was based on cross-hole testing data measure at the study site. The deeper soil profile was inferred to the several deep wells in Mississippi Embayment area.

NATURAL HAZARDS MITIGATION INSTITUTE

UMR UNIVERSITY OF MISSOURI-ROLLA

Shear Wave Velocity Profile

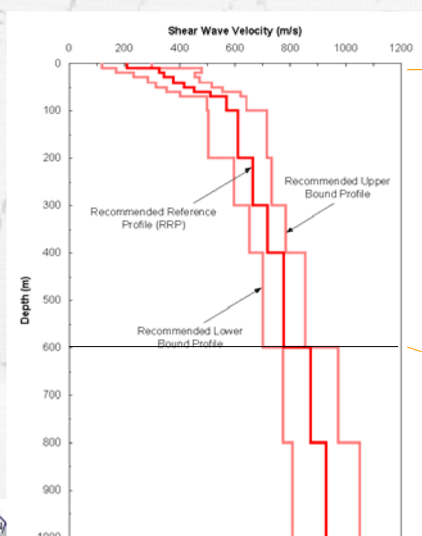

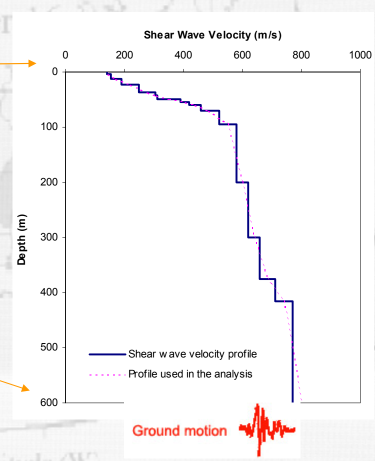

M=6.5, PGA=0.148g

UMR UNIVERSITY OF MISSOURI-ROLLA

Site Response Analysis

- The composite source model program was used to develop the synthetic ground motions.
- Three cases were studied for the site response analysis. One is in the new model and two are in SHAKE.
  - New model.
  - SHAKE1. Vucetic and Dobry's curves developed in the database of SHAKE are used for the whole soil profile.
  - SHAKE2. Modified modulus degradation curve and damping curves for the deep soil layers (Ishibashi and Zhang, 1993).

NATURAL HAZARDS MITIGATION INSTITUTE

UMR UNIVERSITY OF MISSOURI-ROLLA

Comparison of PGA

Ground Motions	PGA (g)
Synthetic Input Motion (rock)	0.148
Computed at Surface (New Model)	0.259
Computed at Surface (SHAKE1)	0.133
Computed at Surface (SHAKE2)	0.374

NATURAL HAZARDS MITIGATION INSTITUTE

UMR UNIVERSITY OF MISSOURI-ROLLA

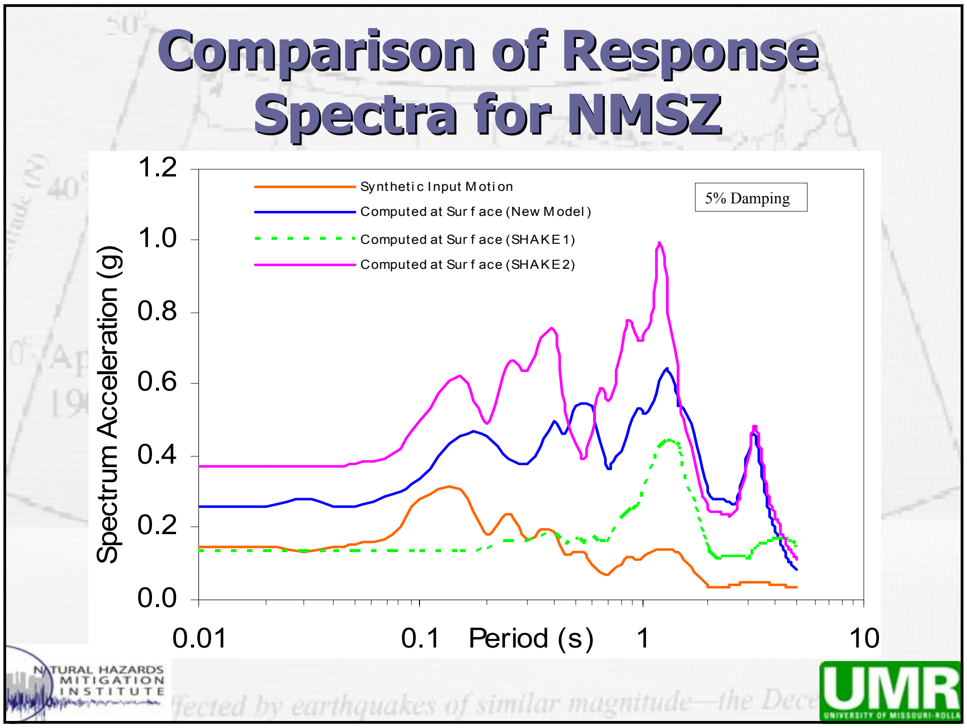

Comparison of Response Spectra for NMSZ
Synthetic Input Motion
Computed at Surface (New Model)
Computed at Surface (SHAKE1)
Computed at Surface (SHAKE2)
5% Damping
Spectrum Acceleration (g)
Period (s)
NATURAL HAZARDS MITIGATION INSTITUTE
UMR
UNIVERSITY OF MISSOURI-ROLLA

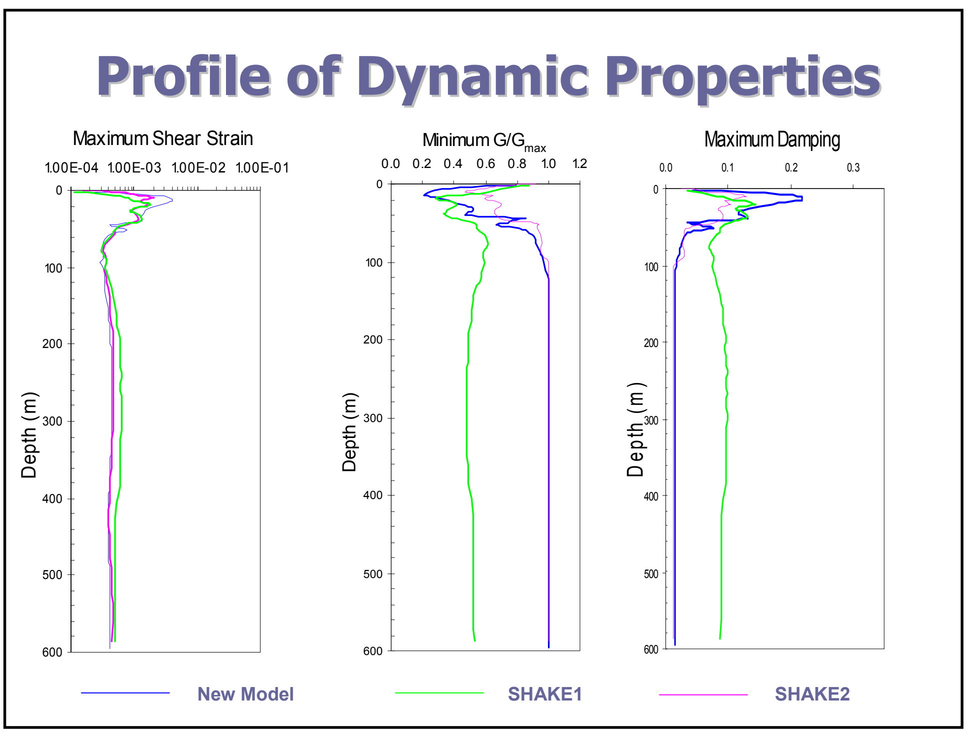

Profile of Dynamic Properties
Maximum Shear Strain
Minimum G/Gmax
Maximum Damping
Depth (m)
New Model
SHAKE1
SHAKE2

Near Field Study

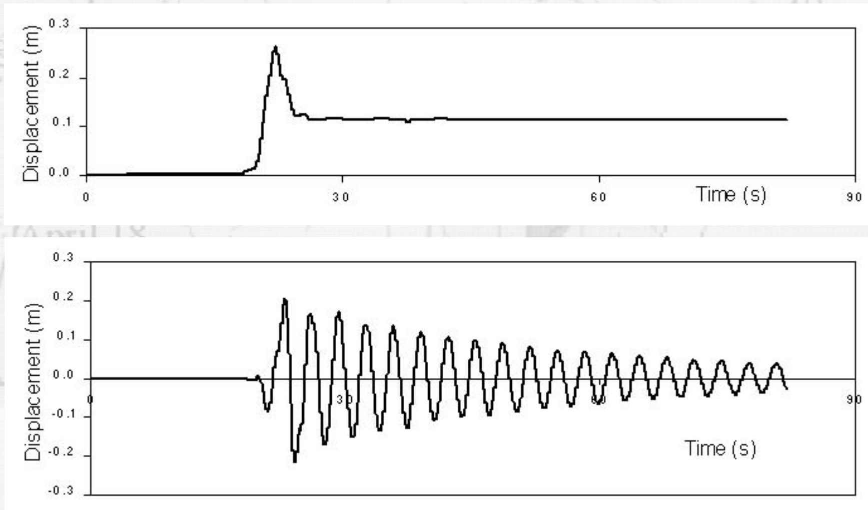

Displacement Time Histories at A1466 M=6.5 (Composite Source) (a) Input (b) Surface

Liquefaction Considerations in the NMSZ

Liquefaction Considerations - NMSZ-

- Shallow sediments in the NMSZ consist of silts, sands and low plastic soil that have high potential for liquefaction.
- Lots of liquefaction vestige, such as sand boiling and landslides, can be still found today for 1811-1812 earthquakes.
- Computational techniques that include liquefaction modeling are important for the performance evaluation of infrastructure built on these foundation soils.

Pore Water Pressure Generation Model

- Martin et al. (1975)'s four-parameter pore water pressure generation model.

$$\Delta\varepsilon_v = C_1(\gamma - C_2\varepsilon_v) + \frac{C_3\varepsilon_v^2}{\gamma + C_4\varepsilon_v}$$

- Byrne (1991)'s two-parameter pore water pressure generation model.

$$\Delta\varepsilon_v = C_1\gamma\exp(-C_2(\frac{\varepsilon_v}{\gamma}))$$

Parameters for Byrne's Model

- The value of C_1 and C_2 can be empirically determined from the relative density or the normalized penetration value.

$$C_1 = 7600(D_r)^{-2.5} \quad \text{or} \quad C_1 = 8.7(N_1)_{60}^{-1.25}$$

- The parameter C_2 has been found to be a constant fraction of C_1 as follows .

$$C_2 = 0.4 / C_1$$

Application in Earthquake Problem

- The equation can be written in the incremental form by assuming that the volumetric strain develops linearly with shear strain during any half cycle (Byrne & Mclintyre, 1995).

$$d\varepsilon_v = 0.25 C_1 d\gamma \exp(-C_2(\frac{\varepsilon_v}{\gamma}))$$

- After the incremental change in volumetric strain is determined, the incremental change in pore water pressure can be obtained as follows:

$$du = Md\varepsilon_v$$

- The model is loosely coupled into the nonlinear soil model. At the end of each time step, the pore water pressure is updated based on the increment of shear strain of this step.

Field Verification

The pore water pressure generation model described above was verified using the records at the Wildlife site during the 1987 Superstition Hills Earthquake (M_s =6.6). The site stratigraphy consists of a silt layer approximately 2.5m thick underlain by a 4.3 m thick layer of loose silty-sand, underlain by a stiff to very stiff clay.

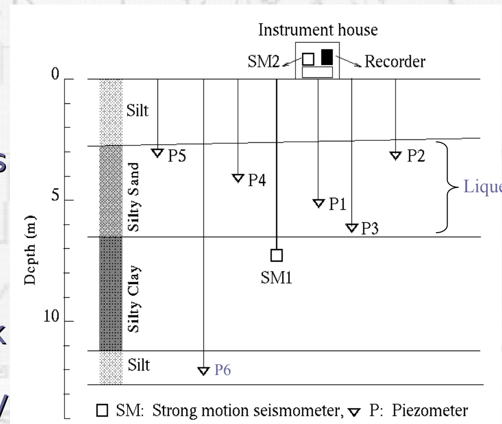

Acceleration Time Series

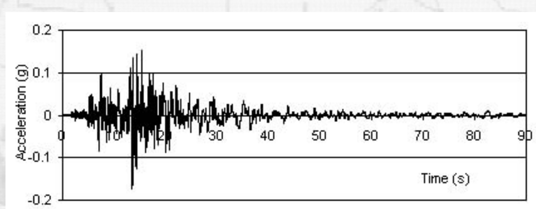

Downhole Acceleration Time Series

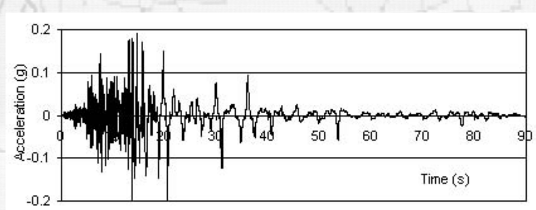

Uphole Acceleration Time Series

Comparison for Relative Displacement

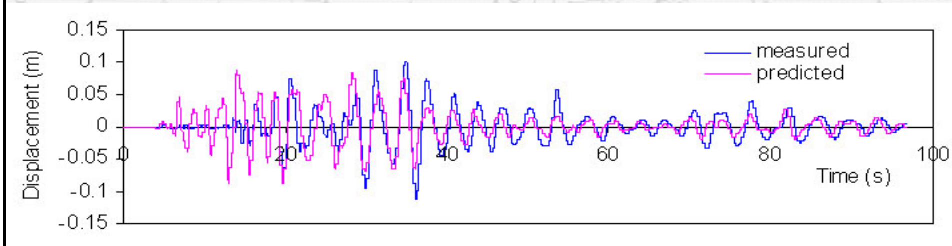

Comparison of Measured and Predicted Relative Displacement Time Histories

Comparison for Pore Water Pressure Ratios

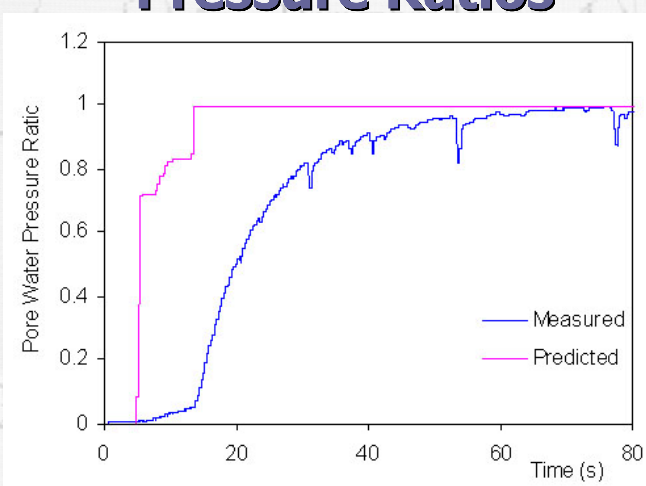

Comparison for Response Spectra at Surface

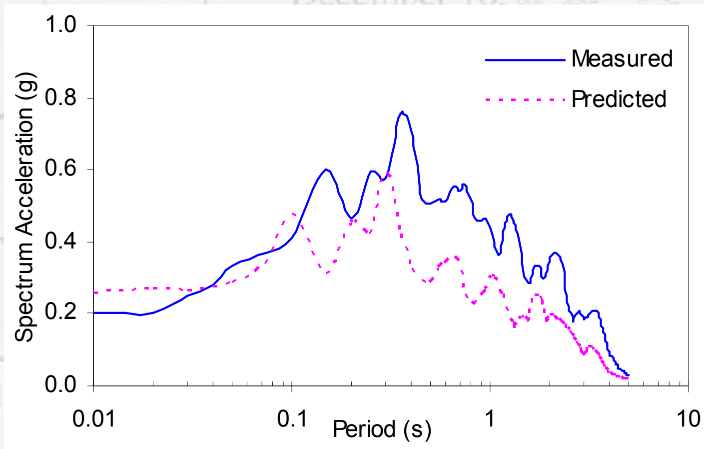

Liquefaction Analysis in the NMSZ

Liquefaction Analysis in the NMSZ

- Liquefaction analysis was performed at the same bridge site and the same soil profile was used.
- The synthetic motions with different energy levels were used.
- The pore water pressure generation model was used to examine the liquefaction performance of the near surface soil layers (around 60m).
- The parameters for the pore water pressure generation model were estimated from the SPT and CPT test data.

Synthetic Input Motions

Summary of the Synthetic Motions

Magnitude	M =6.5					M =7.0					M =7.5				
Series No.	1	2	3	4	5	6	7	8	9	10	11	12	13	14	15
a_{max} (g) FP	0.18	0.27	0.23	0.18	0.13	0.45	0.54	0.39	0.47	0.31	0.78	0.55	0.85	1.03	0.68
a_{max} (g) FN	0.15	0.24	0.27	0.20	0.12	0.42	0.47	0.32	0.41	0.35	1.10	0.73	0.94	1.02	0.79

Results for M=6.5 Earthquakes

Layer No.	Depth (m)	Soil Type	Max Pore Water Pressure Ratio									
			FP Direction					FN Direction				
Series No.			1	2	3	4	5	1	2	3	4	5
1	5.5~7.4	Sandy Silt	0.18	0.56	0.16	0.15	0.13	0.18	0.63	0.84	0.96	0.19
2	7.4~11.8	Loose Sandy Silt	0.30	0.68	0.24	0.25	0.22	0.37	0.76	**1.00**	**1.00**	0.31
3	11.8~18.2	Medium Dense Sand	0.13	0.27	0.11	0.11	0.10	0.13	0.30	0.40	0.46	0.13
4	18.2~22.5	Dense Sand	0.05	0.16	0.06	0.07	0.06	0.10	0.18	0.23	0.27	0.08
5	22.5~39.3	Dense Sand	0.03	0.06	0.02	0.03	0.02	0.04	0.07	0.09	0.09	0.03

Results for M=7.0 Earthquakes

Layer No.	Depth (m)	Soil Type	Max Pore Water Pressure Ratio									
			FP Direction					FN Direction				
Series No.			6	7	8	9	10	6	7	8	9	10
1	5.5~7.4	Sandy Silt	0.93	**0.98**	0.87	**1.00**	0.38	**0.98**	0.84	0.97	0.92	**1.00**
2	7.4~11.8	Loose Sandy Silt	**1.00**	**1.00**	**1.00**	**1.00**	0.49	**1.00**	**1.00**	**1.00**	**1.00**	**1.00**
3	11.8~18.2	Medium Dense Sand	0.50	0.56	0.42	0.64	0.21	0.48	0.41	0.49	0.50	0.55
4	18.2~22.5	Dense Sand	0.33	0.37	0.26	0.48	0.14	0.31	0.26	0.32	0.31	0.38
5	22.5~39.3	Dense Sand	0.14	0.17	0.10	0.20	0.06	0.13	0.12	0.13	0.12	0.14

Results for M=7.5 Earthquakes

Layer No.	Depth (m)	Soil Type	Max Pore Water Pressure Ratio									
			FP Direction					FN Direction				
Series No.			11	12	13	14	15	11	12	13	14	15
1	5.5~7.4	Sandy Silt	1.00	1.00	1.00	1.00	1.00	1.00	1.00	1.00	1.00	1.00
2	7.4~11.8	Loose Sandy Silt	1.00	1.00	1.00	1.00	1.00	1.00	1.00	1.00	1.00	1.00
3	11.8~18.2	Medium Dense Sand	0.85	0.50	0.59	0.55	0.66	1.00	0.60	0.93	0.92	0.66
4	18.2~22.5	Dense Sand	0.64	0.36	0.44	0.39	0.48	0.84	0.64	0.67	0.65	0.48
5	22.5~39.3	Dense Sand	0.28	0.19	0.21	0.20	0.22	0.36	0.33	0.32	0.21	0.24

Comparison: Response Spectra

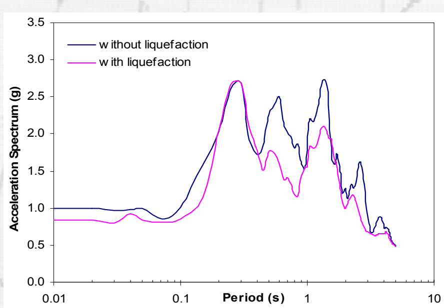

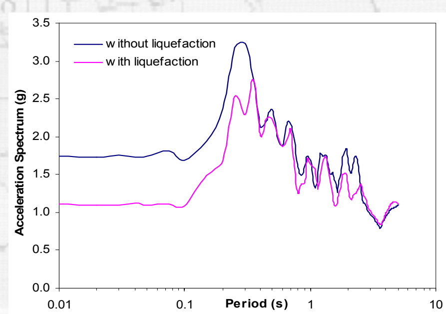

Comparisons of the Computed Response Spectra for Motion No. 11
(a) in Parallel Direction (b) in Normal Direction

Comparison: Displacement Histories

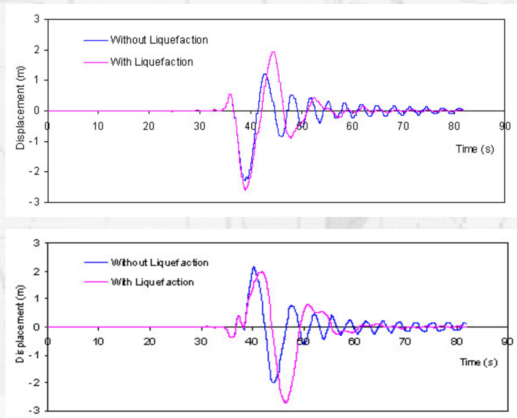

Comparison of the Displacement Time Histories at Ground Surface for Motion No. 11 (a) in Parallel Direction (b) in Normal Direction

Summary & Conclusions

Summary of Findings

- A new nonlinear soil model was developed to take into account the influence of the confining pressure on the site response analysis of deep soil deposits.
- Results from the site response analysis indicates that ignoring the influence of confining pressure on site response analysis will significantly underestimate the ground response in deep soil sites.

Summary of Findings

- A two-parameter pore water pressure generation model is loosely coupled into the nonlinear soil model. Preliminary results show that the liquefaction could happen for M=6.5 or larger earthquakes in this area.
- Near field effects have been studied. After the seismic waves propagate through the deep soil deposit, the fling effect is not present while the pulse is still found in the surface motions. These preliminary findings are in agreement with the lack of evidence of surface ground rupture due to previous earthquakes in the NMSZ.

Summary of Findings

- Near field energy pulse could be transmitted to the piles and other bridge components after propagating through the inelastic behavior of pile-soil interaction. However, near-field properties in the superstructure are not as significant as when the degradation of soil springs due to the pore water pressure is considered.

PRESENTATION 10

SEISMIC PERFORMANCE OF EMBANKMENTS

SEISMIC PERFORMANCE OF EMBANKMENTS

Richard W. Stephenson, Ph.D., P.E.
Professor of Civil, Architectural and Environmental Engineering
Wanxing Liu
Graduate Student
University of Missouri-Rolla (UMR)

Geotechnical and Bridge Seismic Design Workshop
New Madrid Seismic Zone Experience

October 28-29, 2004, Cape Girardeau, Missouri

FAILURE MODES

- Slope failure
  - Rotational Slide
  - Block Slide
- Lateral Spreading and Associated Settlement

METHODS OF ANALYSIS

- Pseudostatic analysis,
- Newmark sliding block analysis,
- Makdisi-Seed analysis,
- Stress-deformation analysis,
- Physical modeling (shaking table testing, etc.).

PSEUDOSTATIC ANALYSIS

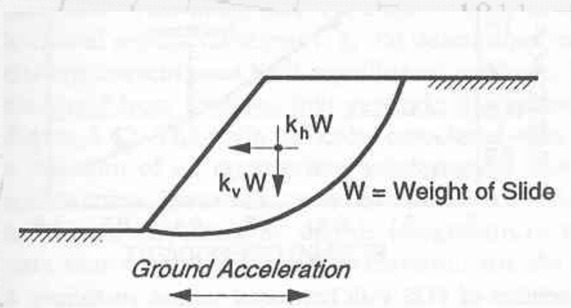

- A horizontal, down-slope inertia force (M*a) is applied to the sliding mass.
- $a=k_h W$
- Routine slope stability analyses conducted
  - Bishop
  - Method of slices,
  - Etc.

- Advantages
  - Relatively simple
  - Produces and index of stability (FS)
- Disadvantages
  - Rigid body analysis
  - Cannot simulate complex dynamic effects
  - Cannot evaluate influence of porewater pressure buildup
  - Cannot evaluate effect of degradation of shear strength.

Newmark Sliding Block Analysis

- First method to assess stability in terms of deformations rather than factor of safety.
- Assumes rigid-plastic materials
- Assumes knowledge of the time history of the acceleration acting on the embankment.

- Advantages
  - Estimates deformations
  - Relatively easy to use.
- Disadvantages
  - Potential failure mass and embankment are assumed to be rigid
  - Lateral displacements may be out of phase with the inertial forces at different points .
  - Can significantly over predict deformations

Makdisi-Seed Analysis

- Based on the sliding block method
- Uses average accelerations and the shear beam method.
  - Plot of average maximum acceleration with depth of the potential failure surface
  - Plot of normalized permanent displacement with yield acceleration.

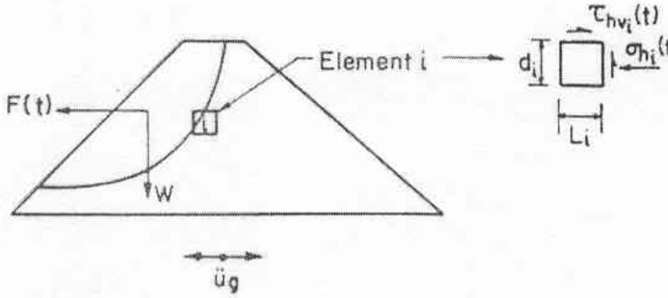

$$F(t) = \sum_{i=1}^{n} \tau_{hv_i}(t)\,L_i + \sigma_{h_i}(t)\,d_i$$

n = number of elements along the sliding surface

$$k_{av}(t) = F(t)/W$$

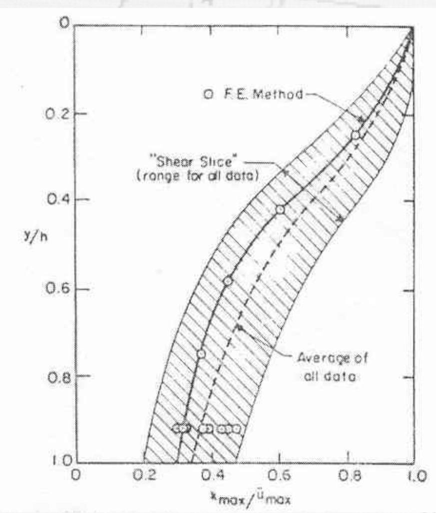

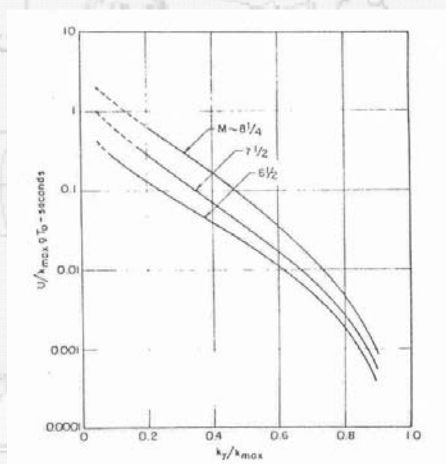

STRESS-DEFORMATION

- Dynamic computer programs
  - Strain potential approach
    - TARA-3
  - Stiffness reduction approach
    - DYNAFLOW
  - Nonlinear analysis approach
    - Finn Models (FLAC)
    - Hyperbolic model

NATURAL HAZARDS MITIGATION INSTITUTE

UMR UNIVERSITY OF MISSOURI-ROLLA

Finn Model

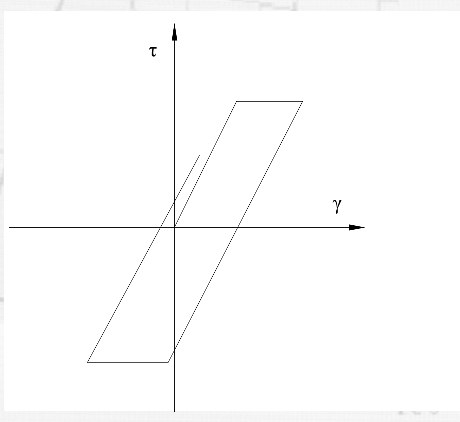

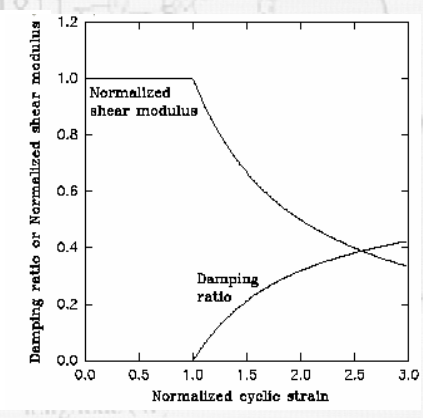

NATURAL HAZARDS MITIGATION INSTITUTE

UMR UNIVERSITY OF MISSOURI-ROLLA

Hyperbolic-Martin/Byrne Model

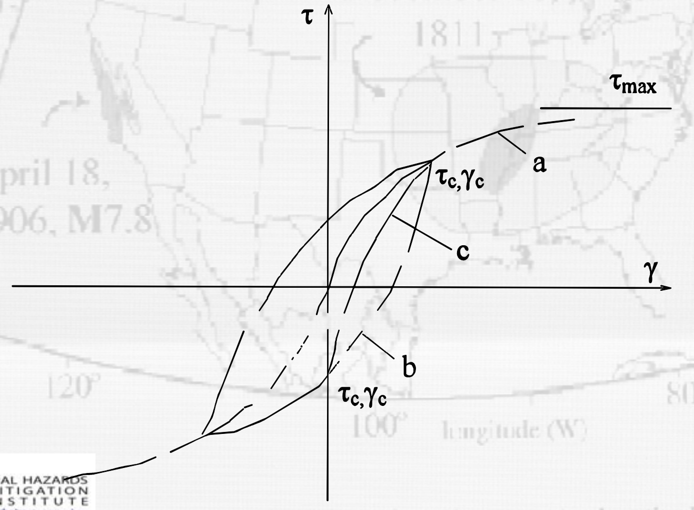

Pore Pressure Calculation

$$\Delta p = -\frac{k_w}{n}\Delta\varepsilon_{ii}$$

$$\Delta\sigma_{ij} = 2G\Delta\varepsilon_{ij}$$

$$\frac{1}{3}\Delta\sigma_{ii} = (k + \frac{k_w}{n})\Delta\varepsilon_{ii}$$

EMBANKMENT MODELING

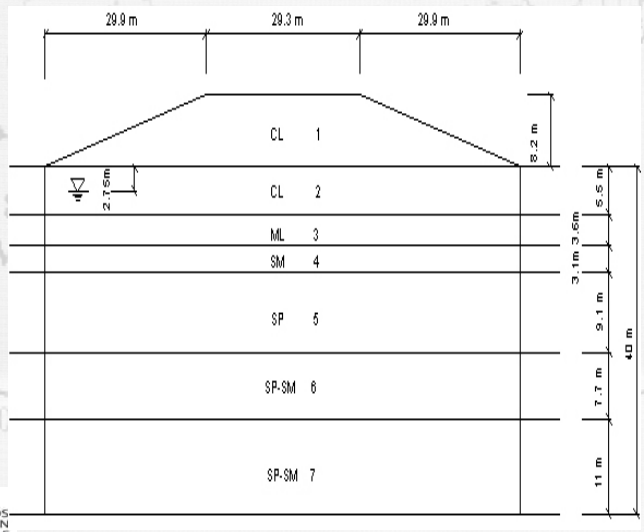

Soil unit	Soil Material	Density (Mg/m^3)	(kPa)	(º)	Shear modulus G (kPa)	Porosity n	$(N_1)_{60}$
1	CL	2023	10.8	25	59848	0.4	19
2	CL	1947	34.5	25	44393	0.44	11
3	ML	1876	0	32	56136	0.48	9
4	SM	2161	0	31	89935	0.3	8
5	SP	2181	0	45	118429	0.28	40
6	SP-SM	2120	0	44	112163	0.32	36
7	SP-SM	1916	0	44	179445	0.44	36

Embankment modeling

- Two cases studied
  - Embankment alone
  - Embankment with soil beneath
- Two source ground motions
  - motion at the ground surface
  - motion at 40 m below the ground surface.

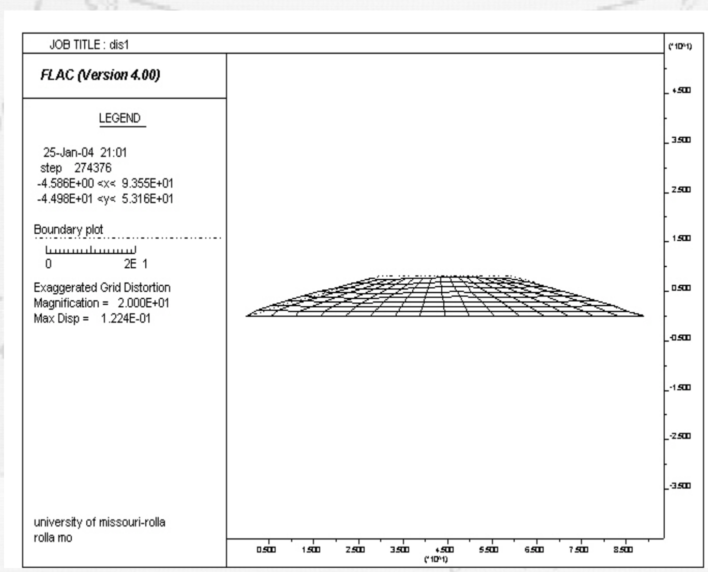

Finn Model

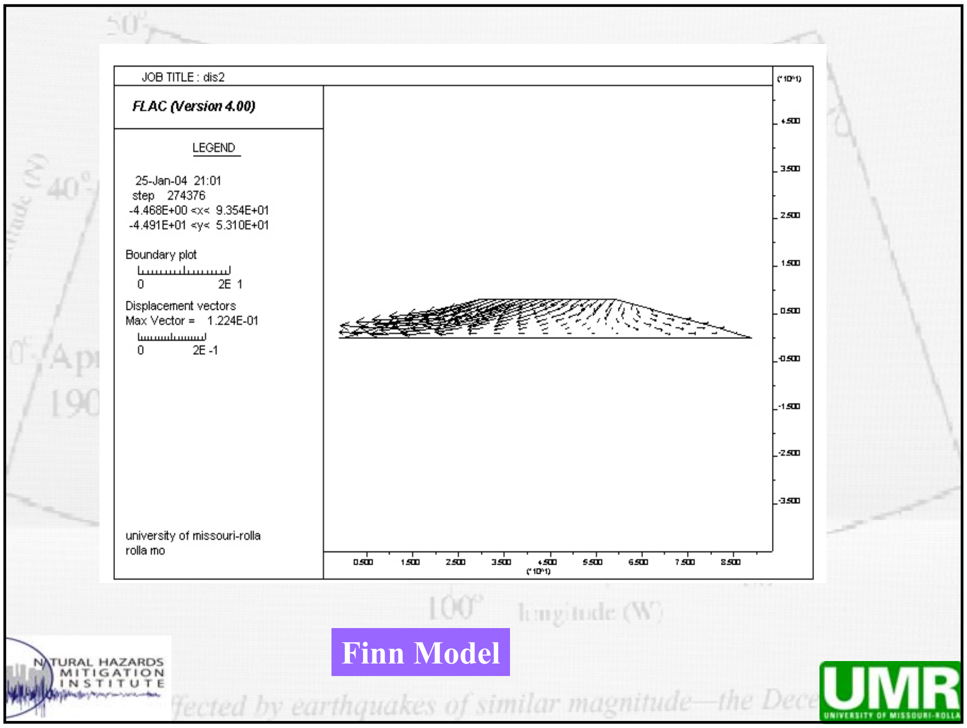
JOB TITLE : dis2
FLAC (Version 4.00)
LEGEND
25-Jan-04 21:01
step 274376
-4.468E+00 <x< 9.354E+01
-4.491E+01 <y< 5.310E+01
Boundary plot
0 2E 1
Displacement vectors
Max Vector = 1.224E-01
0 2E -1
university of missouri-rolla
rolla mo
NATURAL HAZARDS
MITIGATION
INSTITUTE
Finn Model
UMR
UNIVERSITY OF MISSOURI-ROLLA

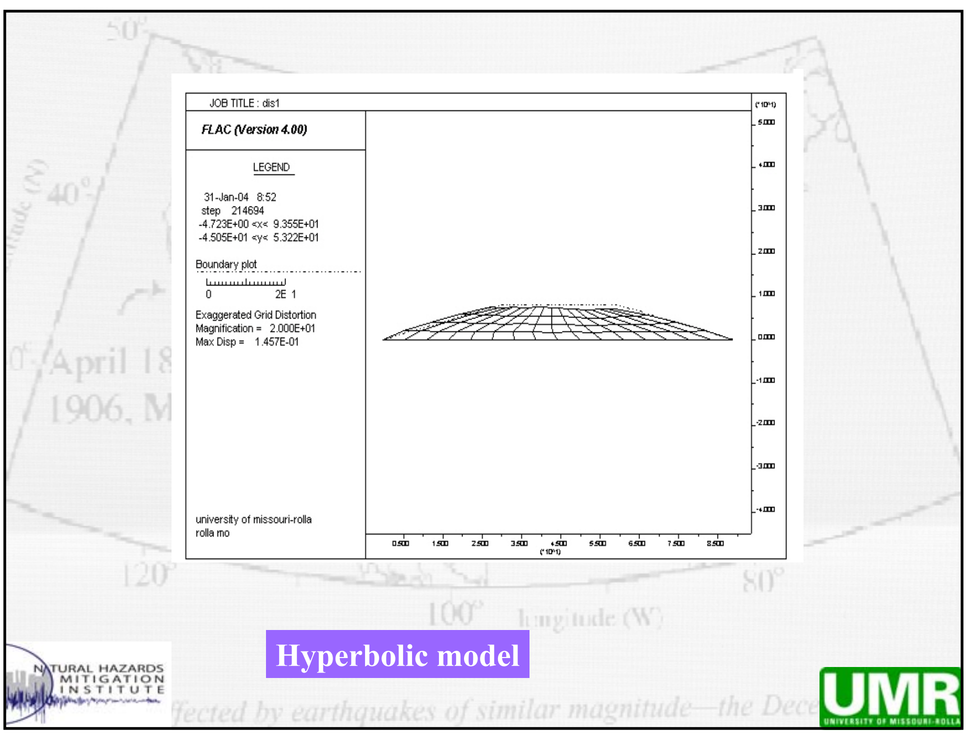
JOB TITLE : dis1
FLAC (Version 4.00)
LEGEND
31-Jan-04 8:52
step 214694
-4.723E+00 <x< 9.355E+01
-4.505E+01 <y< 5.322E+01
Boundary plot
0 2E 1
Exaggerated Grid Distortion
Magnification = 2.000E+01
Max Disp = 1.457E-01
university of missouri-rolla
rolla mo
NATURAL HAZARDS
MITIGATION
INSTITUTE
Hyperbolic model
UMR
UNIVERSITY OF MISSOURI-ROLLA

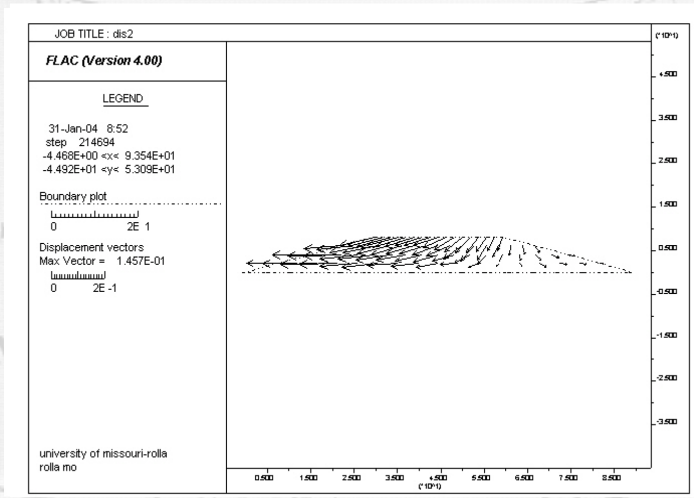

Hyperbolic model

LIQUEFACTION EFFECT ON THE DEFORMATIONS OF THE EMBANKMENTS

Two cases studied:

- Input motion without accounting for liquefaction of the subsoils.
- Input motion accounting for liquefaction of the subsoils.
  - Free-field site response analyses were performed to obtain acceleration-time histories at the level ground surface as input motions for the dynamic analysis of the approach embankments.

Response Spectra

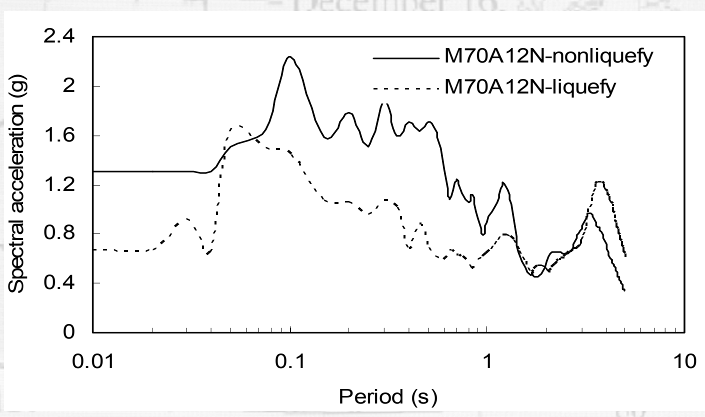

Normal Direction

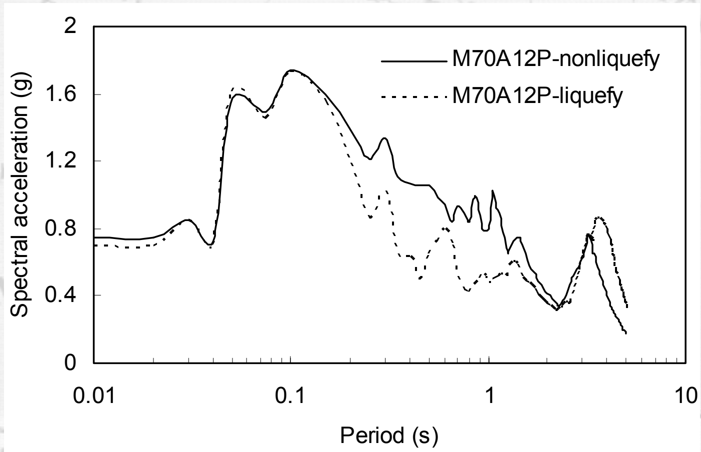

Parallel direction

Results

- Spectral accelerations for the cases accounting for liquefaction are smaller than those without accounting for liquefaction.
- Predominant period shift to a shorter period in the normal direction.

DEFORMATIONS

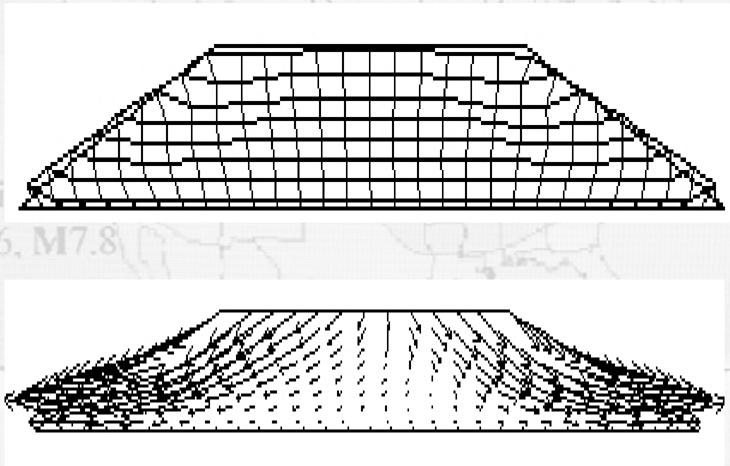

Normal direction w/o liquefaction

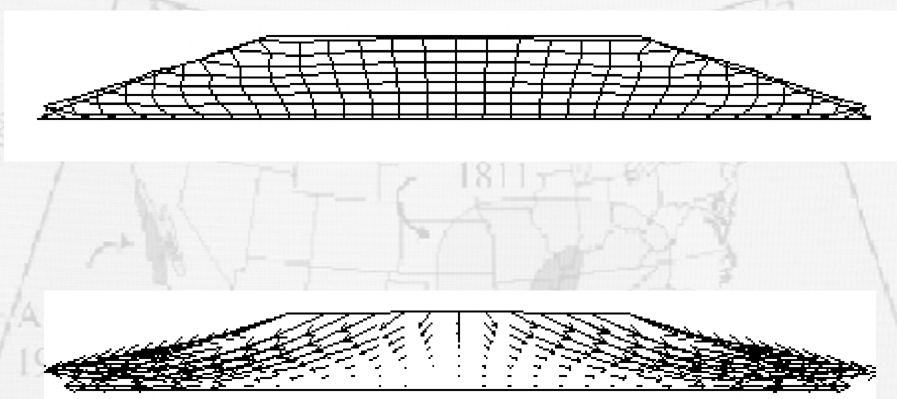

Normal direction with liquefaction

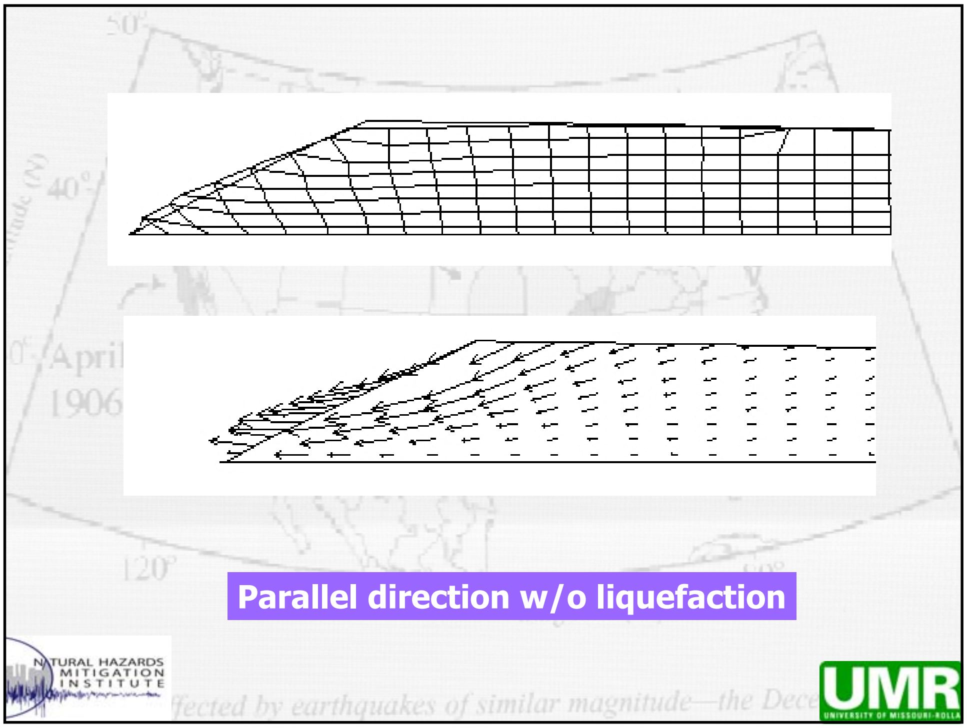
Parallel direction w/o liquefaction
NATURAL HAZARDS
MITIGATION
INSTITUTE
UMR
UNIVERSITY OF MISSOURI-ROLLA

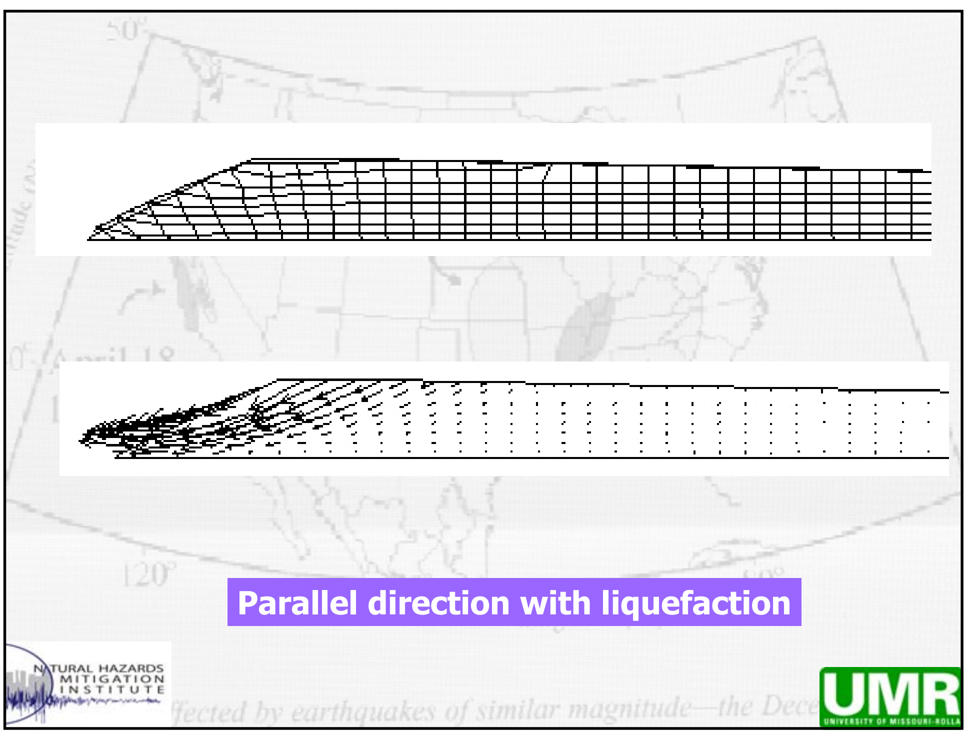
Parallel direction with liquefaction
NATURAL HAZARDS
MITIGATION
INSTITUTE
UMR
UNIVERSITY OF MISSOURI-ROLLA

Displacements along embankment profile Normal Direction

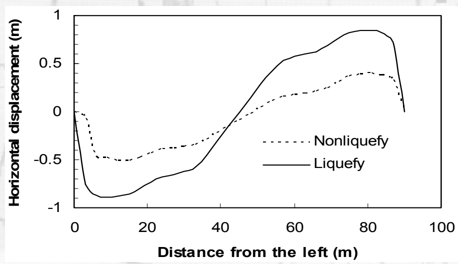

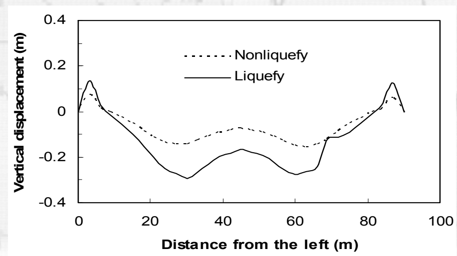

Horizontal **Vertical**

NATURAL HAZARDS MITIGATION INSTITUTE

UMR UNIVERSITY OF MISSOURI-ROLLA

CONCLUSIONS

- Large deformations will occur with a large earthquake.
- Deformations mainly due to foundation soil movement.
- Lateral spreading may occur.

NATURAL HAZARDS MITIGATION INSTITUTE

UMR UNIVERSITY OF MISSOURI-ROLLA

Displacements along embankment profile Parallel Direction

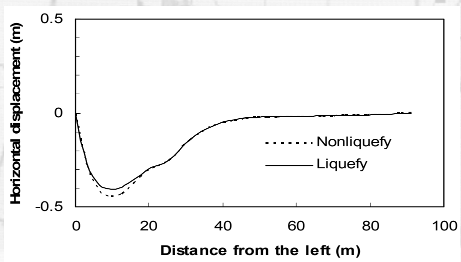

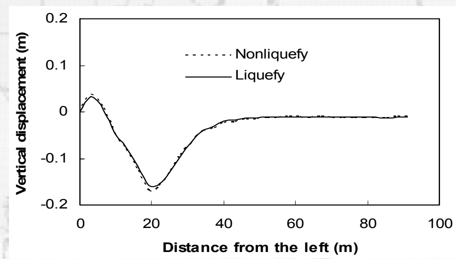

Horizontal

Vertical

NATURAL HAZARDS MITIGATION INSTITUTE

UMR UNIVERSITY OF MISSOURI-ROLLA

Shake Table Testing

NATURAL HAZARDS MITIGATION INSTITUTE

UMR UNIVERSITY OF MISSOURI-ROLLA

Purpose

- Determine the shaking-induced displacement and dynamic response of a model of the A1466 embankment and to compare it to the numerical model.

Scaling Laws

Mass Density	1	Acceleration	1	Length	λ
Force	λ^3	Shear Wave Velocity	$\lambda^{1/2}$	Stress	λ
Stiffness	λ^2	Time	$\lambda^{1/2}$	Strain	1
Modulus	λ	Frequency	$\lambda^{-1/2}$	-	-

CONTAINER

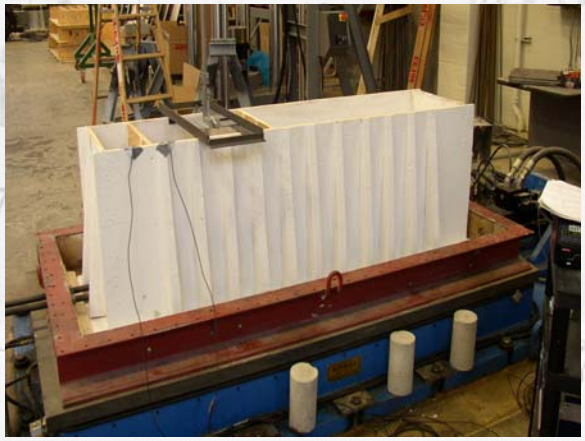

NATURAL HAZARDS MITIGATION INSTITUTE

UMR UNIVERSITY OF MISSOURI-ROLLA

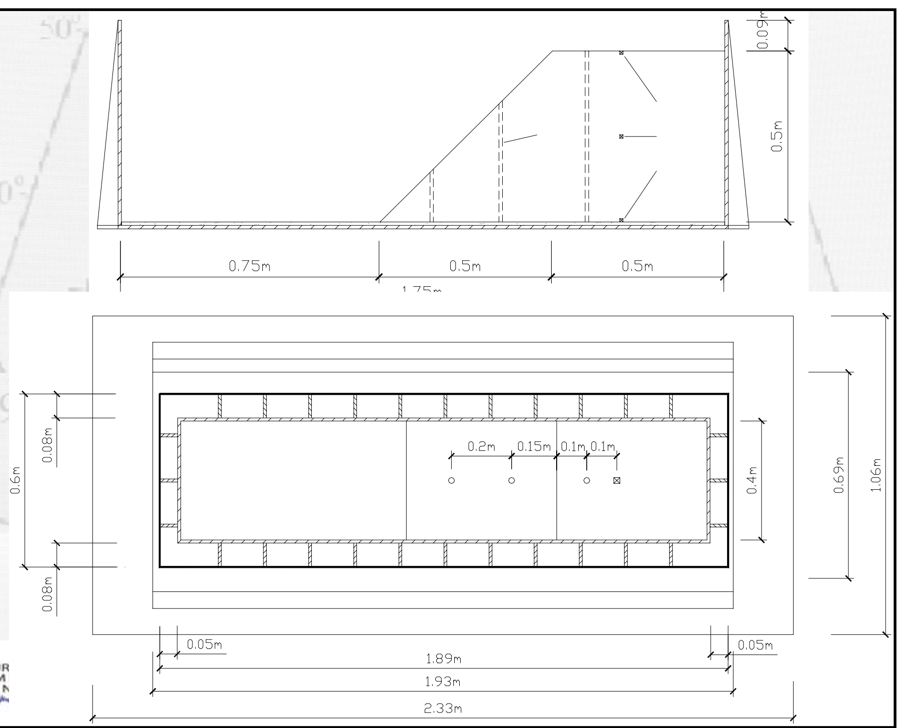

Deformations

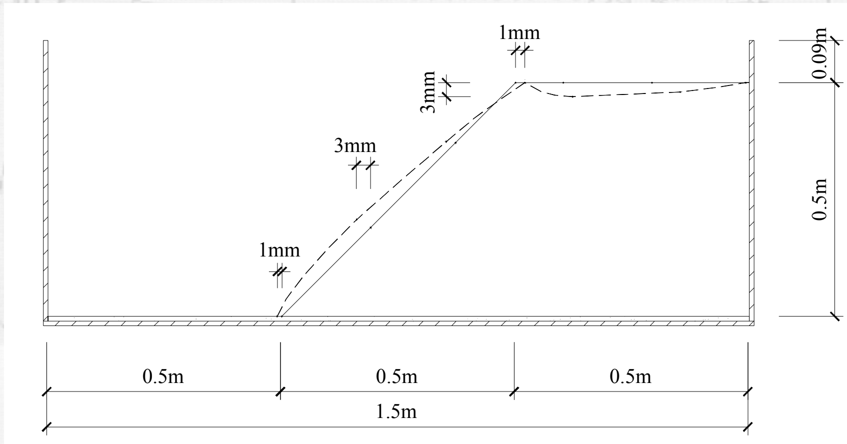

PRESENTATION 11

BRIEF OVERVIEW OF SEISMIC HAZARD POSTED BY THE NEW MADRID SEISMIC ZONE

BRIEF OVERVIEW OF

SEISMIC THREAT POSED BY THE NEW MADRID SEISMIC ZONE

J. David Rogers, Ph.D., P.E., R.G., C.E.G.

Karl F. Hasselmann Chair in Geological Engineering

Natural Hazards Mitigation Institute

University of Missouri-Rolla

rogersda@umr.edu

UMR

EARTHQUAKES

- 4 million earthquakes occur every year; or about 11,000 each day
- About 6,200 quakes are strong enough for people to notice
- About 800 damaging quakes between Magnitude 5.0 and 5.9 each year
- About 120 destructive quakes with Magnitudes 6.0 to 6.9 each year
- Despite improved building codes, about 15,000 people are killed each year

UMR

QUAKES KILL PEOPLE

- In 1556, 830,000 people were killed in Shensi, China
- 180,000 killed near Kansou, China in 1920 quake
- 9,500 people were killed and 30,000 injured in Mexico City in September 1985 by a M8.1 earthquake 350 km away!
- In 2003, 43,819 people were killed by earthquakes worldwide
- Geology beneath site is just as important as quake magnitude

UMR

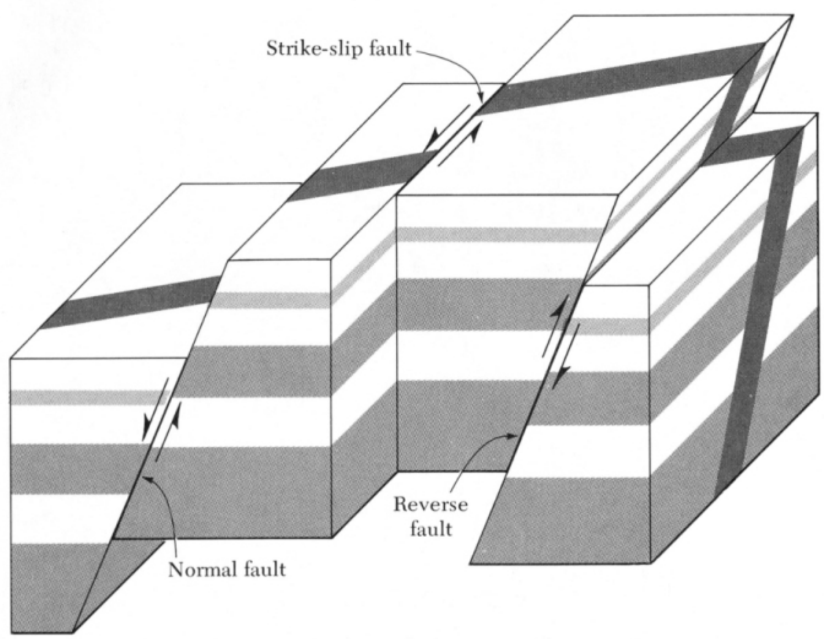

Diagram showing the three main types of fault motion.

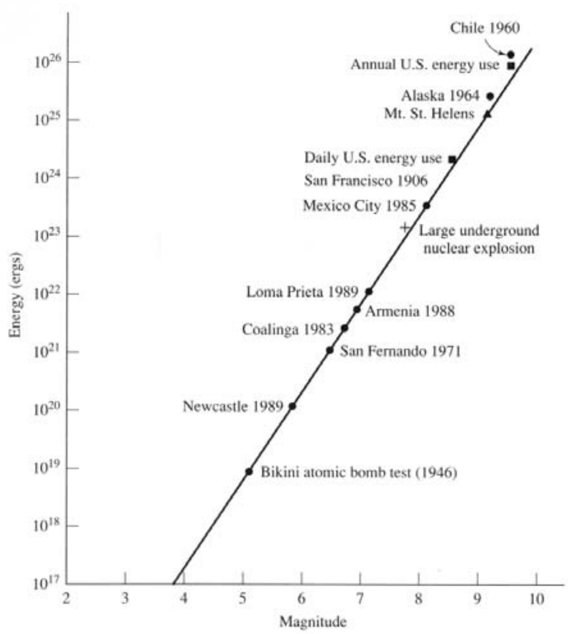

Earthquake Magnitude versus Energy Release

- Modern earthquake magnitudes are based on energy release using a logarithmic scale
- Each numerical magnitude is about 33X the energy release of preceding numerical value

UMR

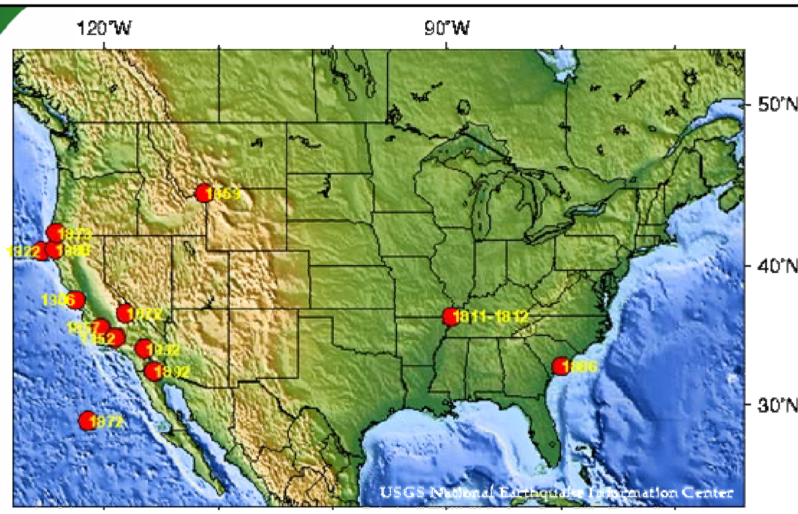

- In 1663 the European settlers experienced their first earthquake in America. From 1975-1995 there were only four states that did not have any earthquakes: Florida, Iowa, North Dakota, and Wisconsin. The most damaging earthquakes have occurred in California, Nevada and Alaska. Should we be concerned in the Midwest?

UMR

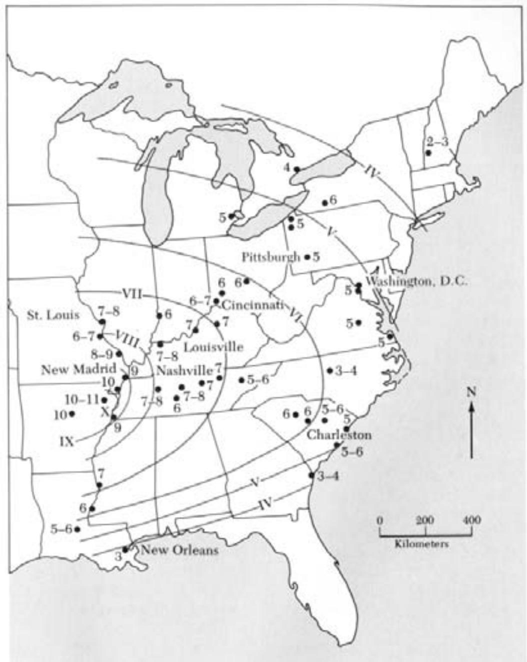

- Isoseismal lines for the December 16, 1811 M_s 8.6 New Madrid earthquake
- Felt over an area greater than 1 million square miles
- Extensive damage to masonry in Cincinnati
- Rang church bells in Boston
- Most people lived along rivers in Midwest and no inhabitants west of the Mississippi

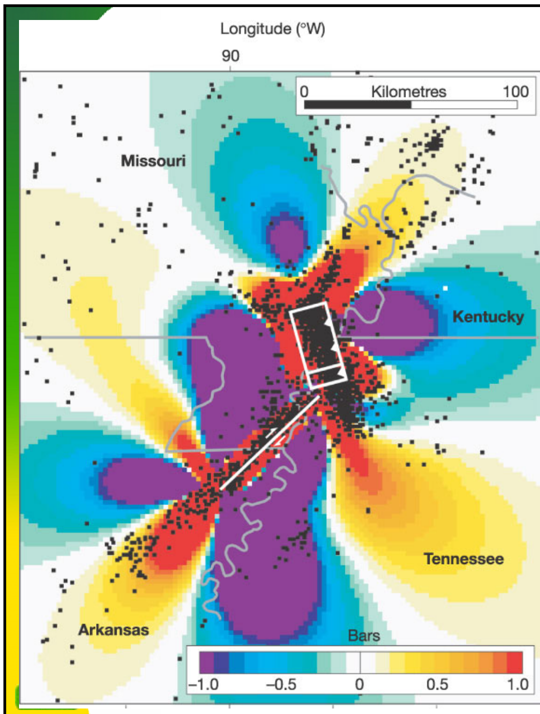

NEW MADRID STRESS FIELD

- Solution for distribution of the elastic stress field in the crustal basement at a depth of 12 km for earthquakes felt in late1811 and early 1812

NEW MADRID SEISMIC ZONE

- 2000 quakes in New Madrid Seismic Zone in 1811-12; four with M> 7.5
- Felt over 1 million square miles!
- Chimneys toppled in Cincinnati, Ohio, 560 km away
- Raised and lowered vast tracts of land as much as 20 feet, temporarily reversing flow of Mississippi River
- Ground fissures and massive liquefaction over a zone measuring 240 x 80 km!

UMR

POST 1812 SEISMICITY in NEW MADRID SEISMIC ZONE

- M6.3 quake in Marked Tree, AR in 1843; did considerable damage to Memphis, 60-70 km east
- M6.6 quake in Charleston, MO in 1895; Felt in 23 states, 30 km of sand blows
- M5.4 in Wabash Valley (Dale, IL) in 1968; also felt in 23 states; light damage in St. Louis
- M5.0 in Wabash Valley west of Vincennes, IN (Olney, IL) in 1987
- M4.6 near Evansville, IN in 2002

UMR

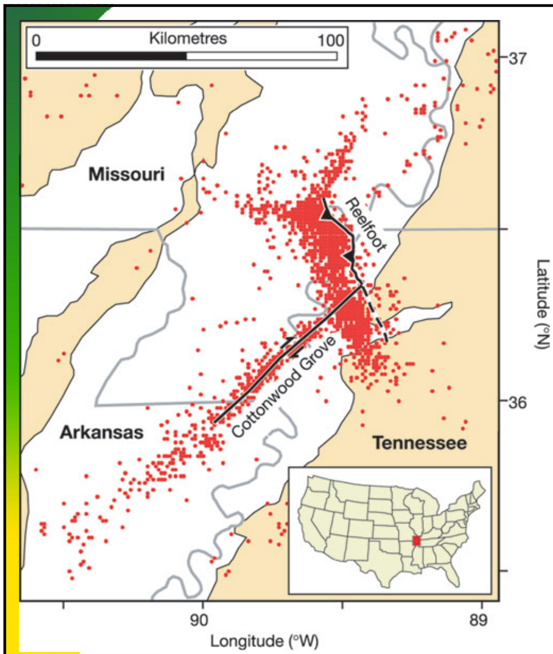

ACTIVE SEISMICITY

- Epicenters recorded between 1974-96 describe a seismically active zone of complex intraplate tectonics
- Right lateral strike slip and blind thrust faulting occur in the same region

UMR

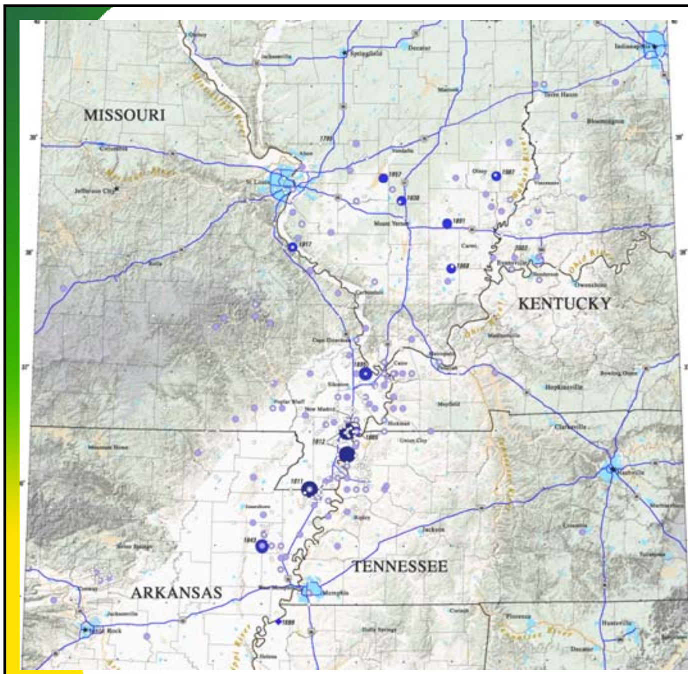

OTHER SEISMIC SOURCES

- Not all of the region's quakes emanate from the recognized New Madrid Zone
- Other sources likely

UMR

DAMAGE POTENTIAL

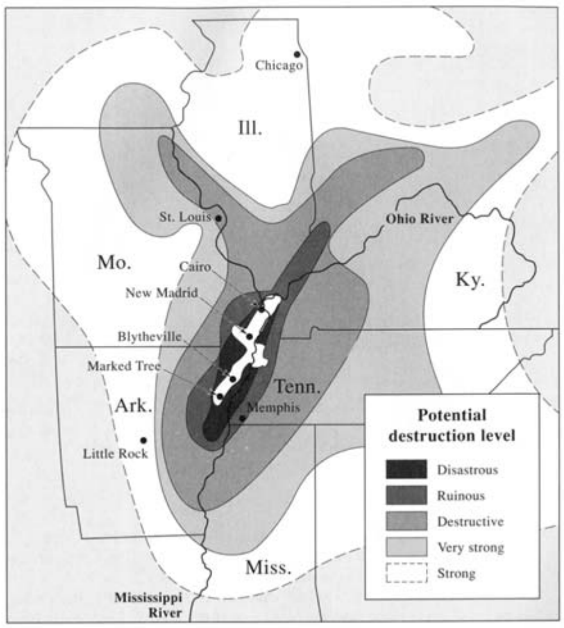

Published damage predictions for the New Madrid Seismic Zone have focused on the near field area, in the upper Mississippi Valley

These are based on synthetic motion time histories with assumed soil cover; not on site specific characteristics or dynamic properties of structures.

UMR

EARTHQUAKE MECHANISMS THAT COMMONLY IMPACT STRUCTURES

- Surface fault rupture hazards
- Ground waves and fling effects
- Topographic enhancement of seismic energy
- Dynamic consolidation of soils
- Liquefaction and lateral spreading
- Site amplification effects
- Long period motion and resonant frequency effects
- Out-of-phase structural response

UMR

SURFACE FAULT RUPTURE HAZARDS

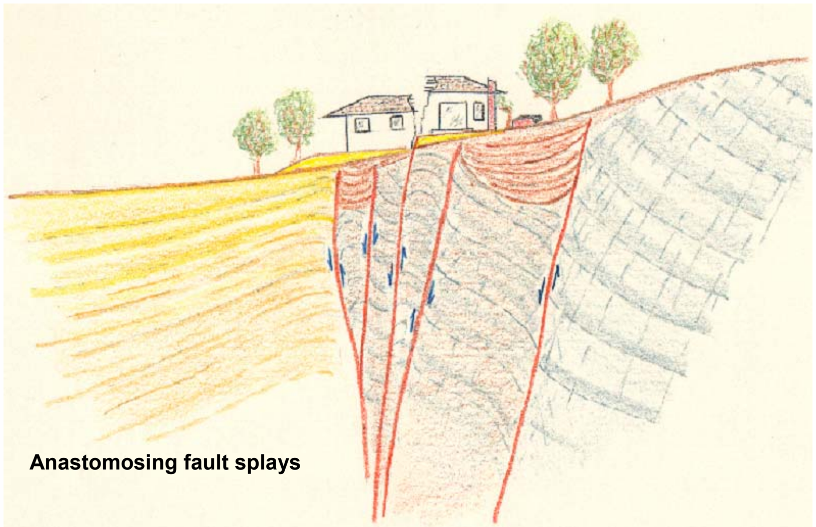

Anastomosing fault splays

- Major active faults usually extend up to the ground surface, where they can pose a threat to structures. Only about 2% of earthquake-induced structural damage is caused by surface fault rupture. Various fault strands identified near the ground surface may be active, dormant or ancient, as shown above.

UMR

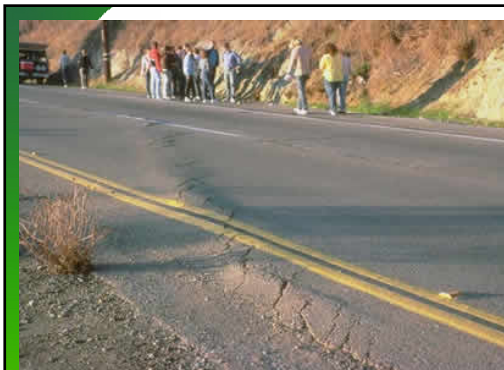

SURFACE RUPTURE

- Only a small percentage of earthquakes actually cause noticeable surface fault rupture
- Sometimes it is rather discrete (upper left)
- On other occasions it can be very abrupt and graphic (lower left)

UMR

FREE BOUNDARY/ GROUND WAVE EFFECT

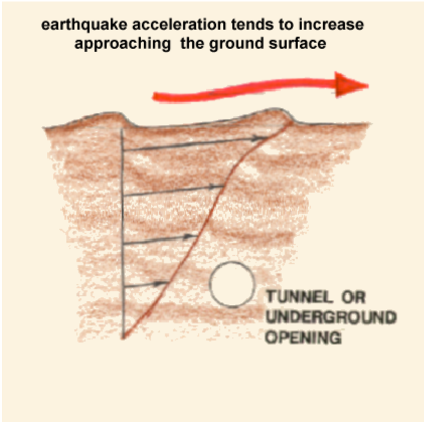

- As the seismic wave train propagates upward and along the Earth's surface, the peak ground accelerations will tend to increase at the ground surface because there is no confinement. Tunnels and underground openings usually record much lower values of acceleration due to their increased confinement.

UMR

TOPOGRAPHIC INFLUENCE ON SITE RESPONSE

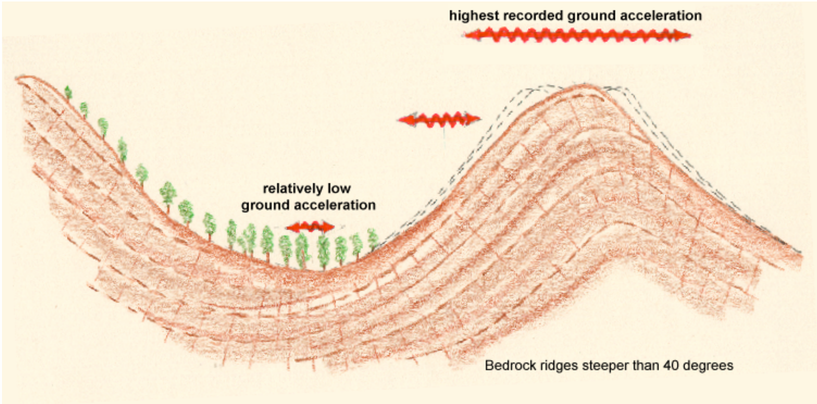

- Steep-sided bedrock ridges usually experience much higher accelerations during earthquakes because they are less laterally constrained. In the October 1989 Loma Prieta earthquake the PGA of 0.77g was recorded in the valley bottom at Corralitos. Estimates of PGA values for the adjoining ridges were in excess of 1.30g.

UMR

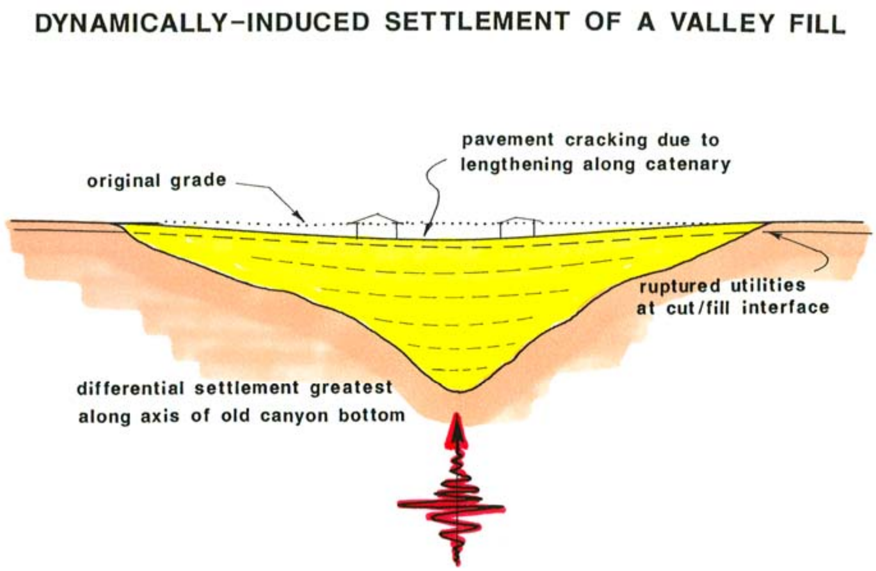

- **Fill embankments tend to consolidate and settle under dynamic loading in the near-field zone**

UMR

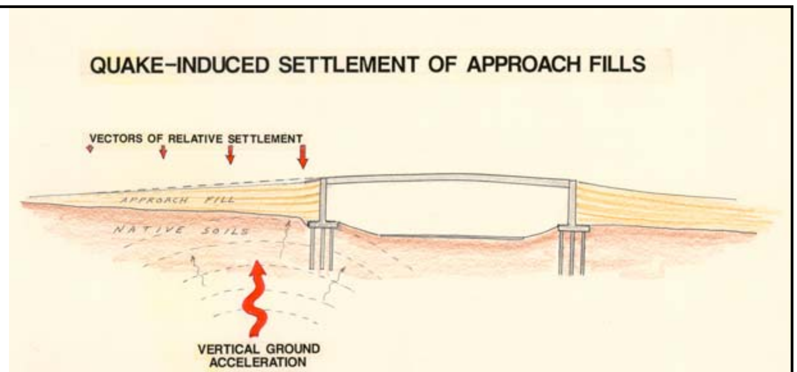

- **Regardless of the compactive effort engendered to filled ground during placement, these materials tend to compress during earthquake-induced shaking, often causing abrupt settlement of the approach fills at the abutments.**

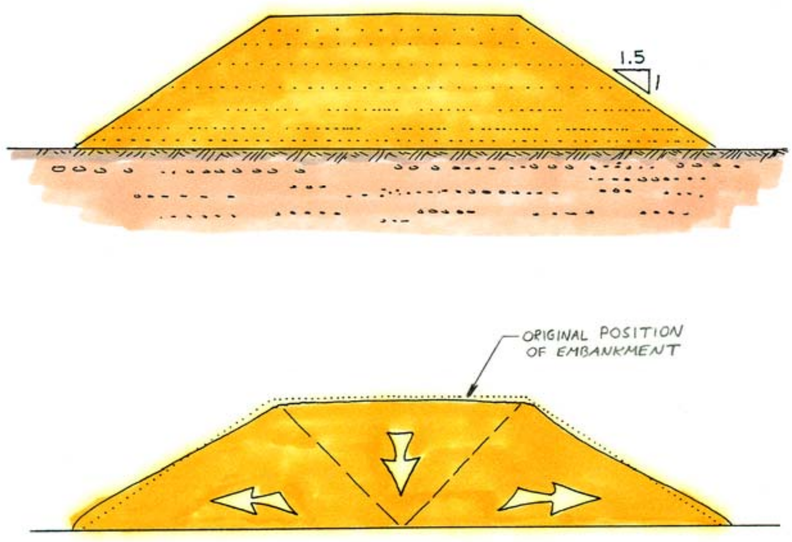

- Mechanism of seismically-induced settlement of bridge approach fill prisms

QUAKE-INDUCED SETTLEMENT

- Approach fills for pile supported bridges commonly exhibit grievous differential settlement
- Impacts traffic flow and any entrained utilities, like fire mains
- These examples are from Aug 1999 Chi Chi earthquake in Taiwan

APPROACH FILL SETTLEMENT

- Seismically-induced settlement and lurching of approach fills for the Cayumapa River Bridge near Valdivia, Chile, which occurred during the M9.5 May 1960 earthquake
- Replacement structure being constructed in lower view, using Geofoam

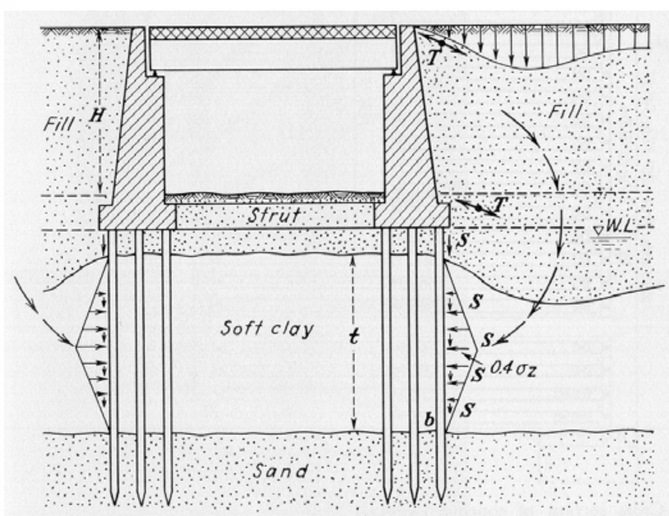

- Tschebotarioff (1973) presented case studies of pile supported bridges that failed because of approach fill settlement.

SETTLEMENT OF APPROACH FILL

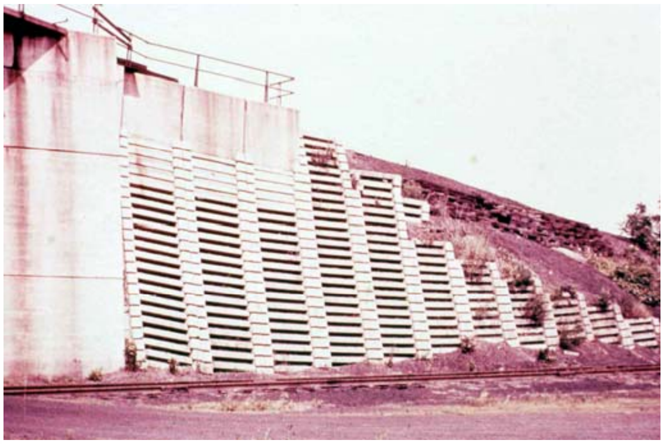

- Crib wall supported approach fill for pile supported bridge. As fill consolidated, crib wall deformed and supporting piles deflected inward, towards channel. Taken from Tschetarioff (1973).

UMR

LIQUEFACTION

- Bridge failures during April 1991 M7.5 Costa Rica earthquake
- Though supported on steel and concrete piles respectively, these bridges both failed due to liquefaction of foundation materials, which tilted the piles

LIQUEFACTION

Liquefaction is a failure mechanism by which cohesionless materials lose shear strength when the pore pressure is excited to a level equal to the effective confining stress. Usually limited to the upper 50 feet and typically occurs in silt, sand and fine gravel.

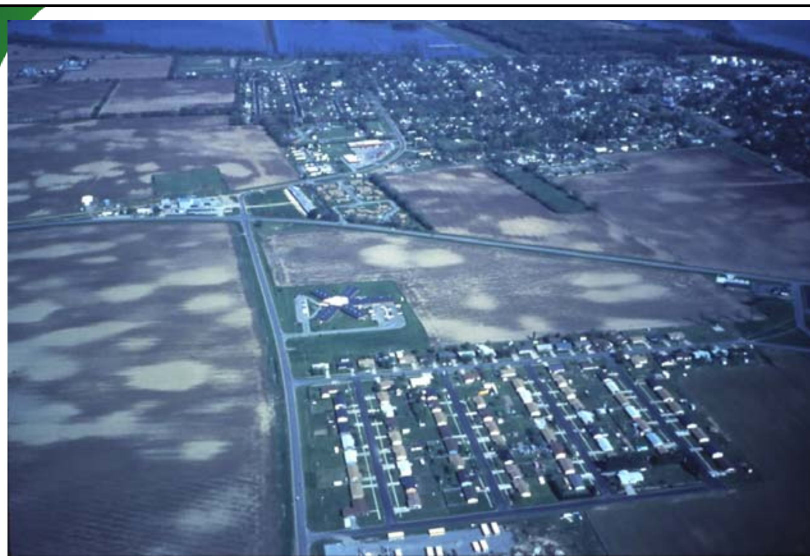

- Recent sand blows dot the landscape surrounding New Madrid, MO, testifying to massive liquefaction

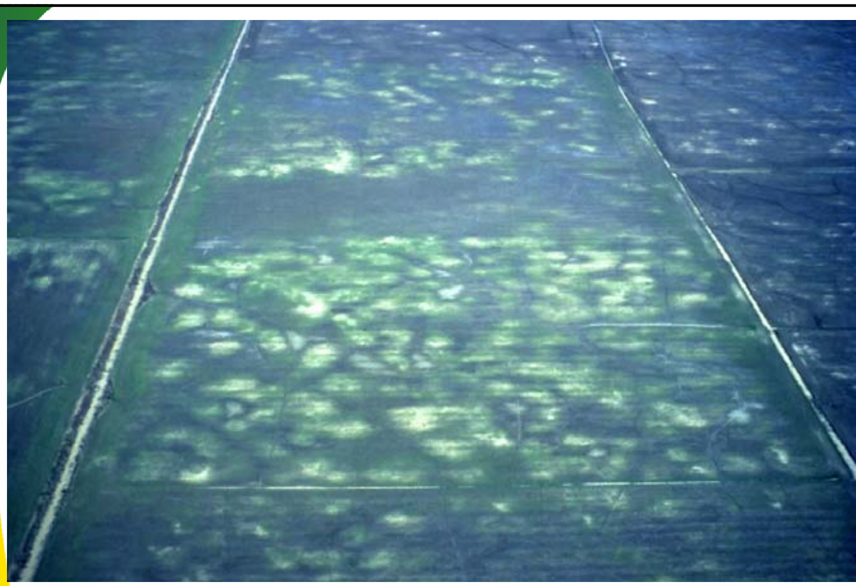

- Enormous tracts of land exhibit evidence of paleoliquefaction – on a grandiose scale

- Farm lands west of Big Lake, AR reveal a series of linear fissures which disgorged liquefied sand from beneath a silt cover.

PALEOLIQUEFACTION STUDIES

- C14 dating of organics caught in sand boils and dikes are used to date past earthquakes. Three M7.5 to M8 paleoevents have been conclusively dated: ~1450, ~900 and ~550 AD.

UMR

Paleoliquefaction Assessments

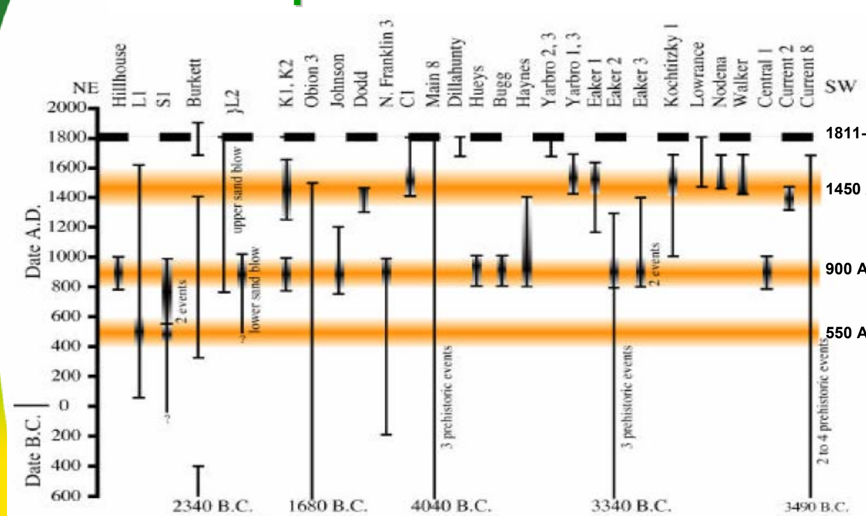

Shaded orange lines show most probable ages of major earthquakes in the NMSZ prior to 1811-12 (shown as dashed line)

UMR

Liquefaction of Confined Horizons Causes Lateral Spreads

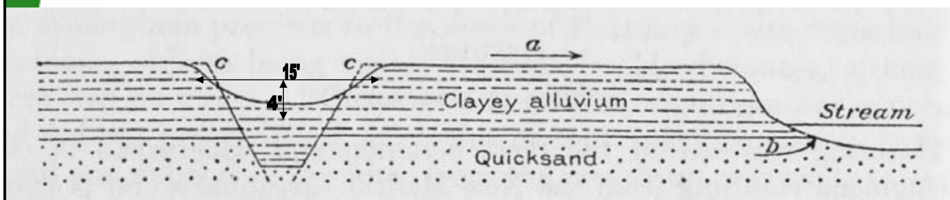

- **Lateral spreads** were initially recognized and identified by USGS geologist Myron Fuller while studying the effects of the 1811-12 New Madrid earthquakes between 1905-12. Fuller made the sketch above, noting that: ***"The depth of the openings was not usually very great, probably being in most cases limited to the hard clayey zone extending from the surface down to the quicksand which usually underlies the surface soil at depths of from 10 to 20 feet."***

UMR

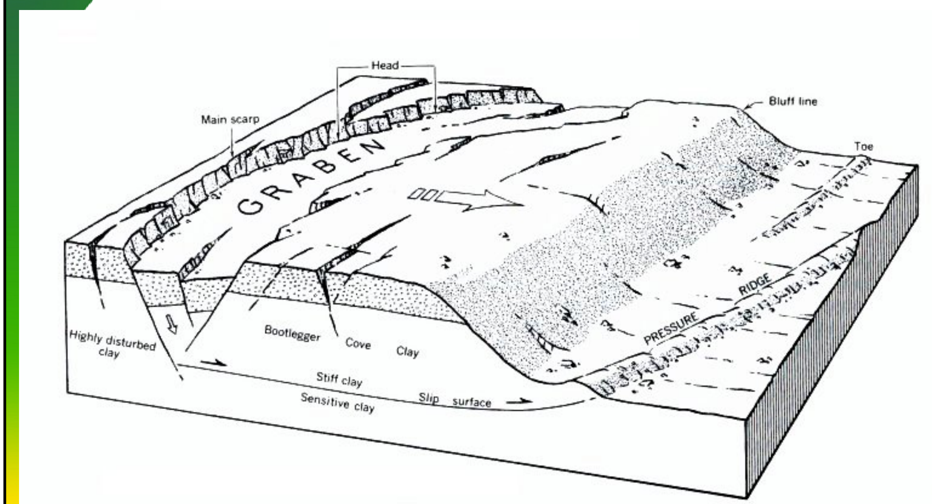

Block diagram of a lateral spread which evolved from post-1964 earthquake evaluations in Alaska by Walt Hansen in USGS Professional Paper 542-A (1966)

UMR

LATERAL SPREADING

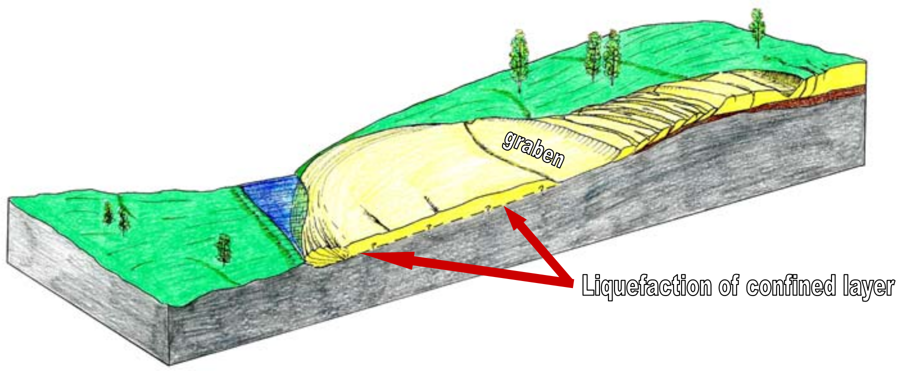

- Lateral spreads can exhibit different length-to-depth ratios, depending on soil sensitivity. Liquefaction occurs along discrete horizons which are confined, allowing lateral translation of rafted material, usually towards open channels or depressions.

UMR

Topographic Expression of Lateral Spreads Near Helena, Arkansas

- Divergent contours
- Stepped topography
- Headscarp evacuation grabens
- Arcuate headscarps

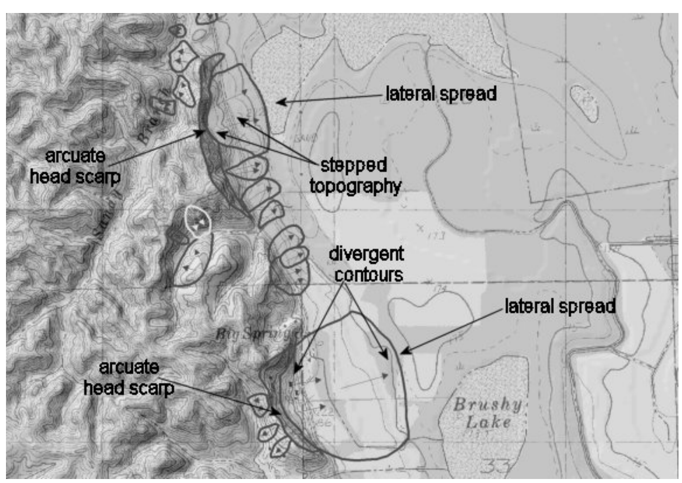

UMR

Jeffersonville Lateral Spread Along Crowley's Ridge ~ 25 km north of Helena, Arkansas

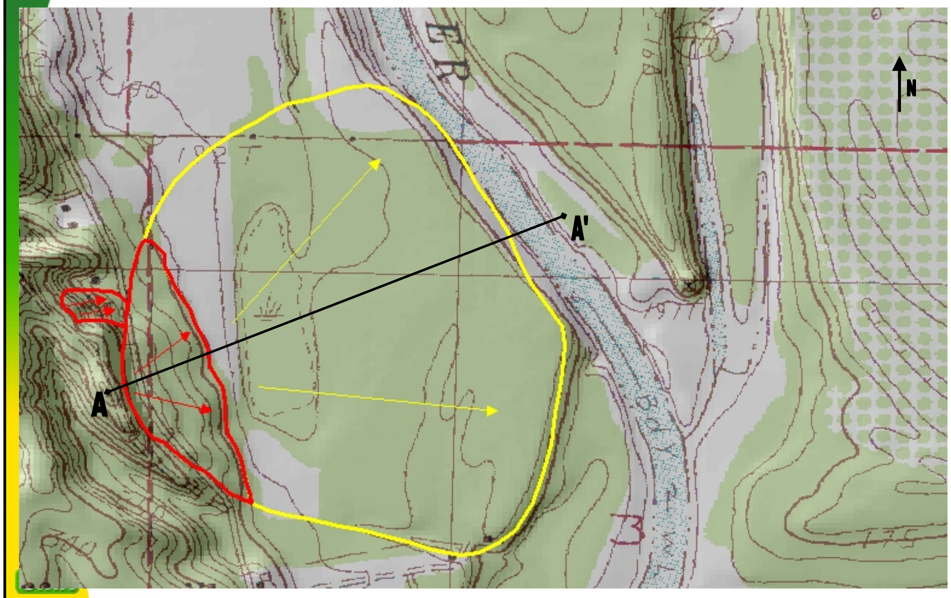

Cross-section through Jeffersonville Lateral Spread and Crowley's Ridge

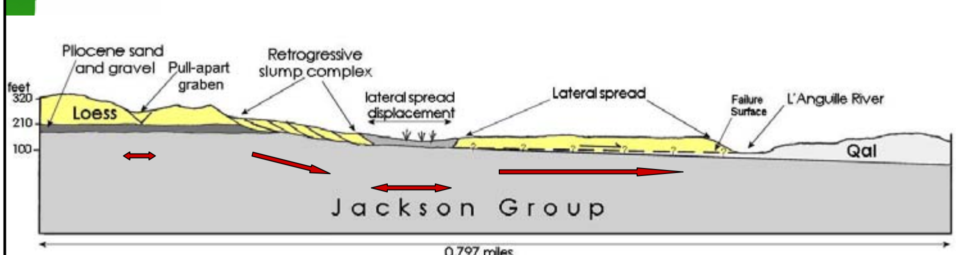

The Jeffersonville Lateral Spread feature appears to have been triggered by the 1811-12 New Madrid earthquake sequence, with the ground translating easterly into the L'Anguille River, near its mouth with the St. Francis River. The eastern escarpment of Crowley's Ridge is peppered with similar features.

UMR

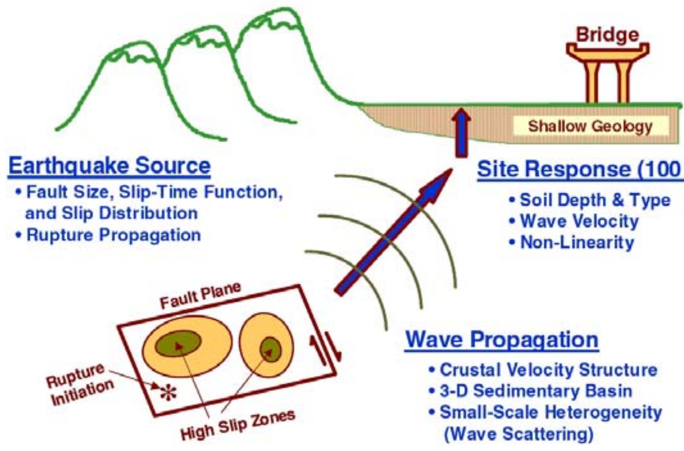

- The type, depth and size of earthquake combine with geophysical properties of the underlying geology to affect <u>seismic site response</u>

UMR

WHAT IS SITE RESPONSE ?

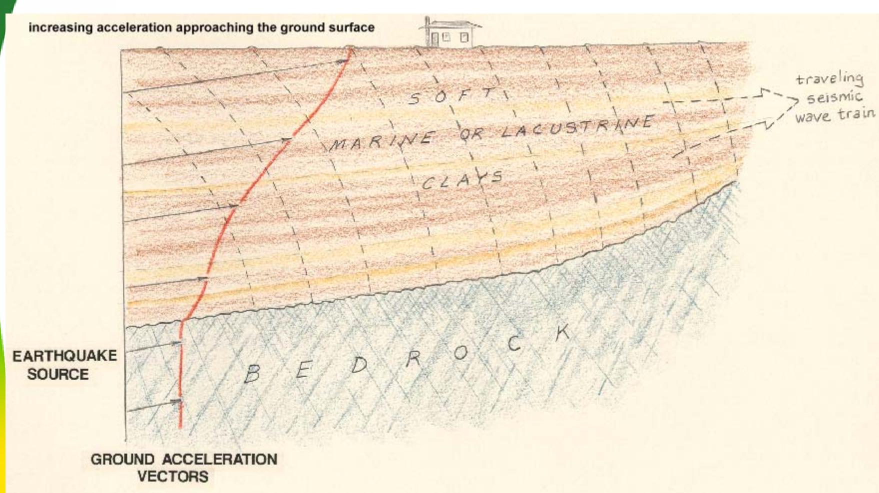

- Site response is used to describe the fundamental period of vibration generated by a typical earthquake at any particular site. If soft unconsolidated sediments overlie resistant bedrock an impedance contrast develops at this boundary which causes incoming seismic energy to be absorbed at a rate faster than it can be transferred through the upper layers, causing significant amplification of ground motions.

UMR

SOFT SEDIMENTS UNDERLYING MEXICO CITY

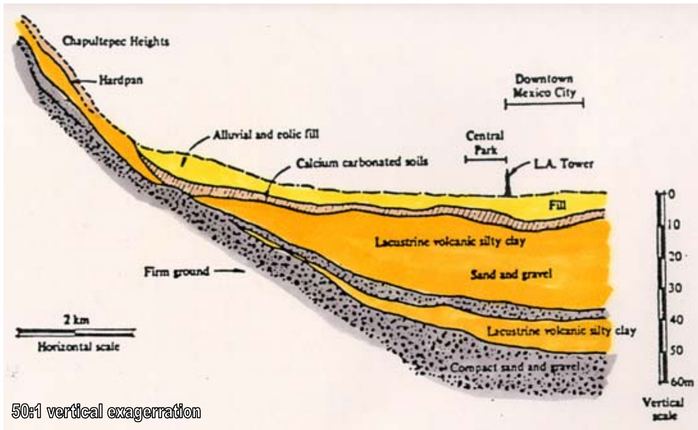

- **Generalized geologic cross section of the southern margins of the lacustrine basin underlying Mexico City. The lacustrine sediments were covered with fill as the city developed. These soft materials amplified the incoming seismic wave train from a M.8.1 earthquake located 52 km off the coast of Michoacan Province, some 350 km from Mexico City!**

ZONE OF HEAVIEST DAMAGE DURING 1985 MEXICO CITY EARTHQUAKE

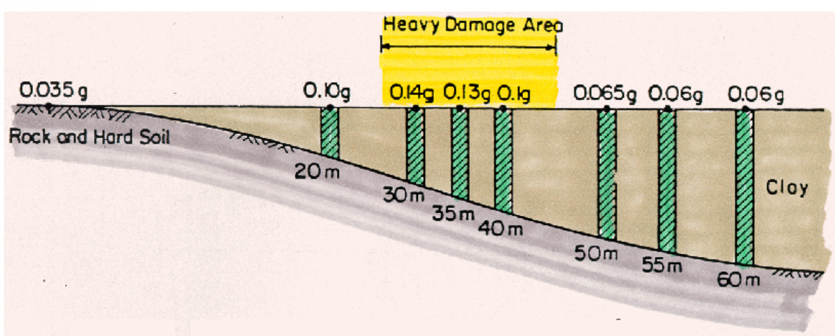

- **Computed distribution of peak ground surface accelerations for typical soil profiles in Mexico City, bounding the zone that experienced severe damage during the 1985 M. 8.1 Michoacan earthquake. The earthquake epicenter was 350 km from Mexico City and lasted close to 3 minutes. More than 500 buildings within the highlighted zone were severely damaged and 100 buildings between 6 and 22 stories high actually collapsed; killing 9,500, injuring 30,000 and leaving 100,000 homeless.**

VARIANCE OF RESPONSE SPECTRA WITH SEDIMENT THICKNESS IN MEXICO CITY

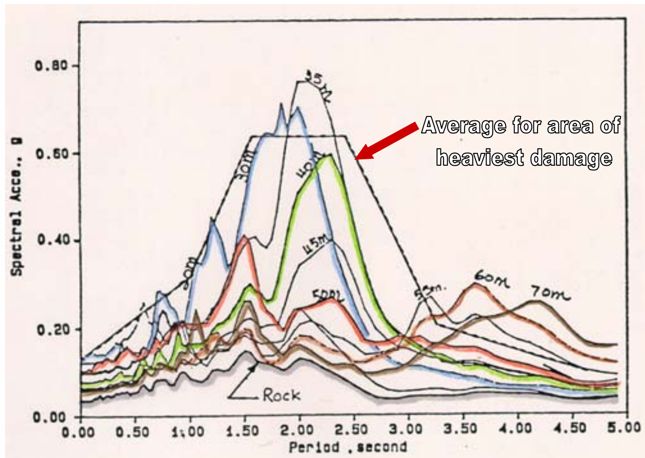

- **Response spectra calculated for different thicknesses of soft sediments in southern Mexico City, between downtown and Chapultepec Heights. Note impact of 30 to 45 m thickness.**

UMR

MODES OF VIBRATION

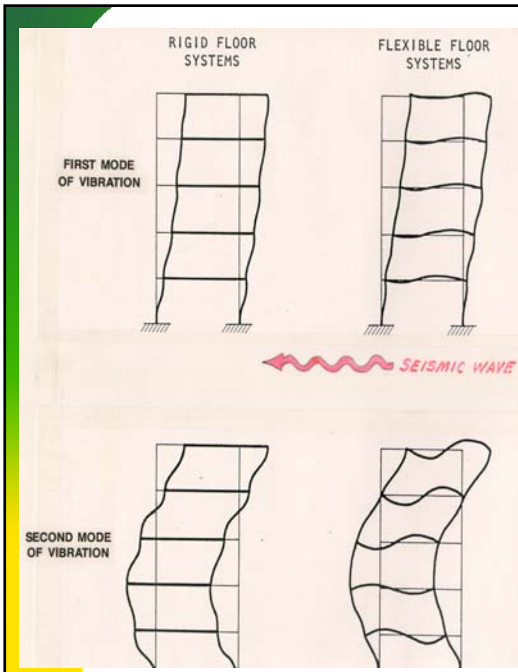

- **All structures posses fundamental modes of vibration which depend on their skeletal make-up: including material type, shear panels, connections, span distances and symmetry.**
- **This fundamental mode is known as the "first mode of vibration" and it generally controls the seismic design of most symmetrical structures.**
- **Secondary modes of vibration become increasingly important in complex structures with asymmetrical form or stiffness, or structures with damaged frames.**

UMR

SITE RESPONSE VERSUS STRUCTURAL RESPONSE

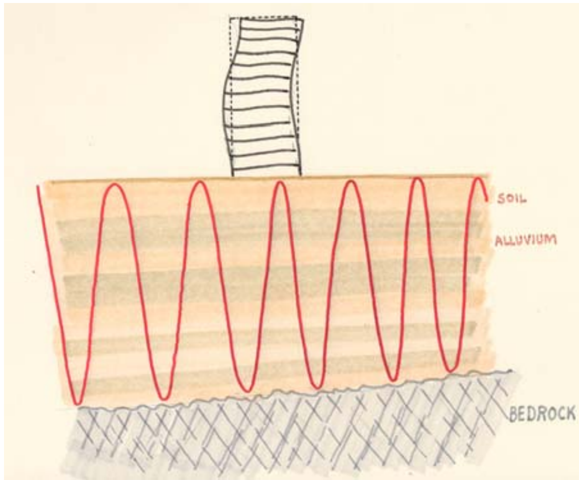

- The fundamental period of vibration of any structure depends on its design and construction details. If the site period and structural period converge, a resonant frequency results which may be an order of magnitude greater than the natural site period, and the structure will be severely damaged or destroyed.

UMR

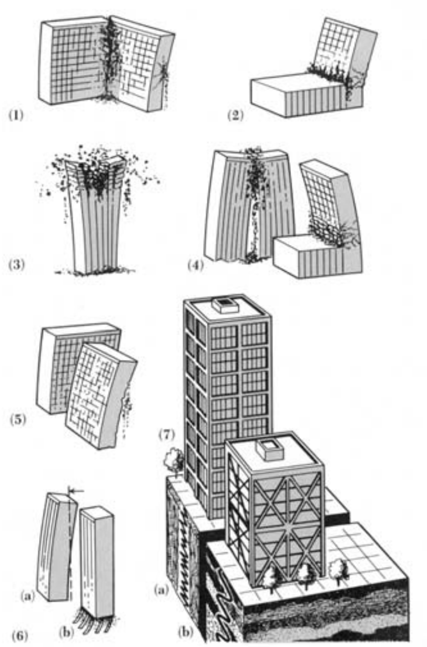

OUT-OF-PHASE MOTION

- Adjacent structures can react differently to seismic excitation, depending on focal aspects of incoming energy, long period motion, site amplification, and degrading structural response as frames become damaged

UMR

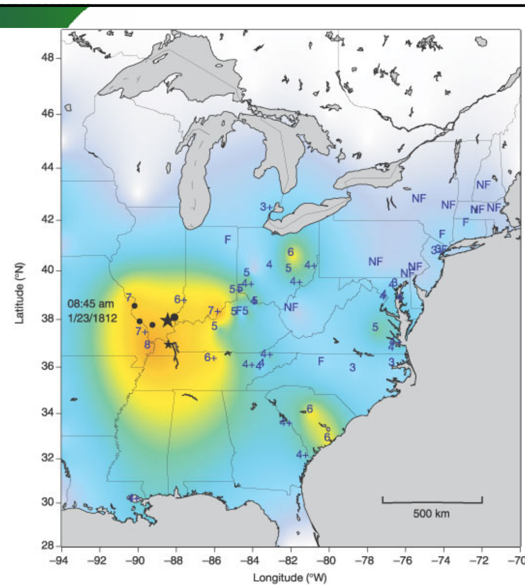

Perceived shaking	Not felt	Weak	Light	Moderate	Strong	Very strong	Severe	Violent	Extreme
Potential damage	None	None	None	Very light	Light	Moderate	Moderate/heavy	Heavy	Very heavy
Peak acceleration (% of *g*)	<0.17	0.17–1.4	1.4–3.9	3.9–9. 2	9.2–18	18–34	34–65	65–124	>124
Peak velocity ($cm\ s^{-1}$)	<0. 1	0.1–1. 1	1.1–3. 4	3.4–8. 1	8.1–16	16–31	31–60	60–116	>116
Instrumental intensity	I	II–III	IV	V	VI	VII	VIII	IX	X+

- **Recently, the destructive effects of the 1811-12 New Madrid events has been attributed to site amplification effects, since most of the inhabited areas were in Holocene channels along major drainages.**
- **This is a revised map illustrating shaking severity for the January 23, 1812 event, thought to have been something between M7.5 and M8.0**

Geology Northern Mississippi Embayment

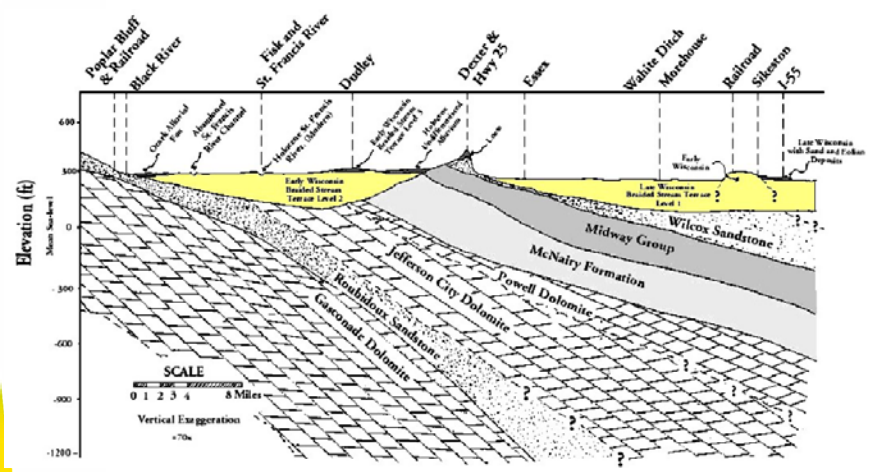

Impedance contrasts within the Wisconsin age river channels (yellow) likely pose the greatest seismic threat to highway infrastructure in the Midwest.

UMR

WHAT IS THE DESIGN EARTHQUAKE?

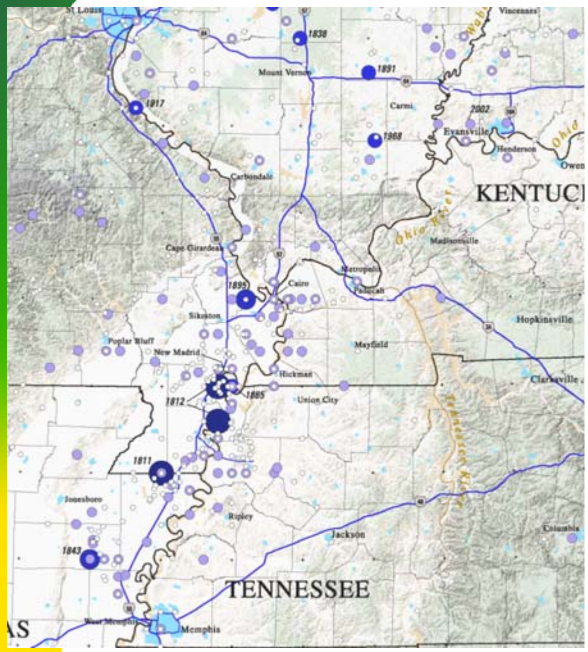

- >M7.5 in ~550
- >M7.5 in ~900
- >M7.5 in ~1450
- M7.5+ in 1811
- M8.0 in 1812
- M6.3 in 1843
- M6.6 in 1895
- M5.4 in 1968
- M5.0 in 1987
- M4.6 in 2002

Recurrence Intervals for New Madrid Earthquake Events*

Magnitude	Recurrence Interval
4.0	14 Months
5.0	10 – 12 Years
6.0	70 – 90 Years
7.0	254 – 500 Years
8.0	550 – 1200 Years

* based on existing data; always subject to update and revision

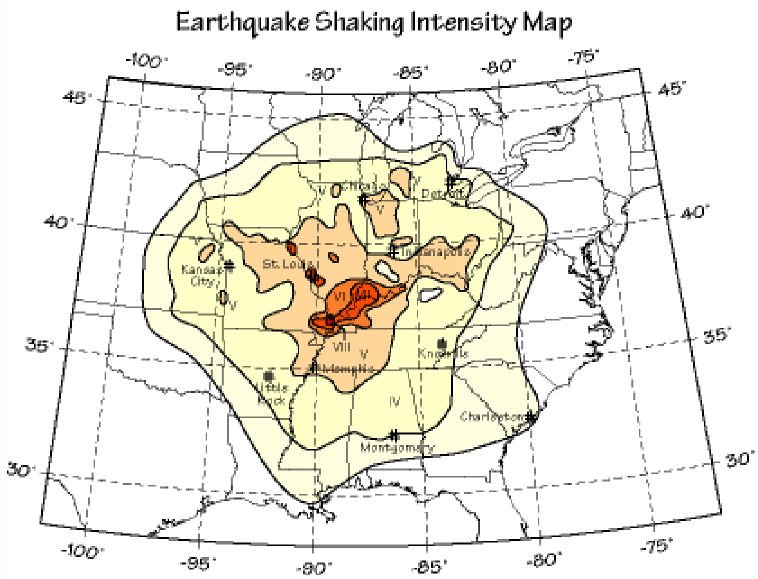

- 1895 M6.6 Charleston, MO earthquake

UMR

1895 M6.6 Charleston, MO Quake

- October 31, 1895 Magnitude 6.6 Earthquake near Charleston Missouri. Modified Mercalli Intensity VIII
- Largest earthquake to occur in the Mississippi Valley region since the 1811-1812 New Madrid earthquake sequence. The estimated body-wave magnitude of this event is 5.9 and the surface-wave magnitude estimate is 6.7.
- People in 23 states felt this earthquake which caused extensive damage. to a number of structures in the Charleston region, including schools, churches, and homes. Structural damage and liquefaction were reported along a line from Bertrand, MO to Cairo, IL. The most severe damage occurred in Charleston, Puxico, and Taylor, Missouri; Alton, and Cairo, Illinois; Princeton, Indiana; and Paducah, Kentucky.
- The earthquake caused extensive damage (including downed chimneys, cracked walls, shattered windows, and broken plaster) to school buildings, churches, private houses, and to almost all the buildings in the commercial section of Charleston, MO. That's the reason the epicenter was assumed to be near Charleston.

UMR

Illinois Central Bridge at Cairo, IL

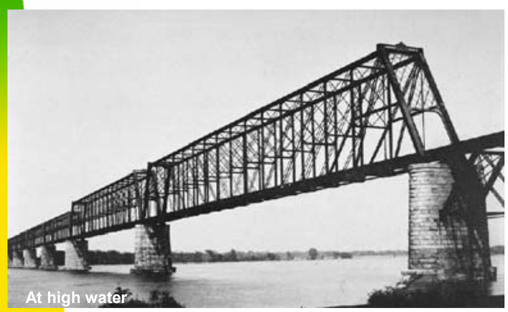

- The Illinois Central Railroad bridge across the Ohio River at Cairo, IL was the longest iron or steel bridge in world when completed in 1889 (4 miles).
- One of its masonry bents was cracked and severely damaged during Oct 1895 Charleston, MO quake

SHAKING INTENSITY versus DISTANCE

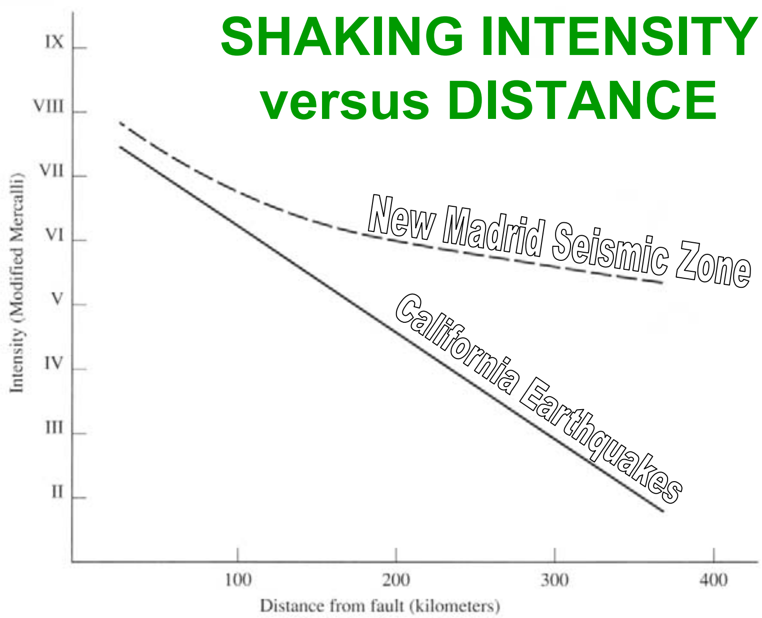

Midwest quakes are less frequent, but much more lethal than California quakes because there is <u>less damping</u> of seismic energy.

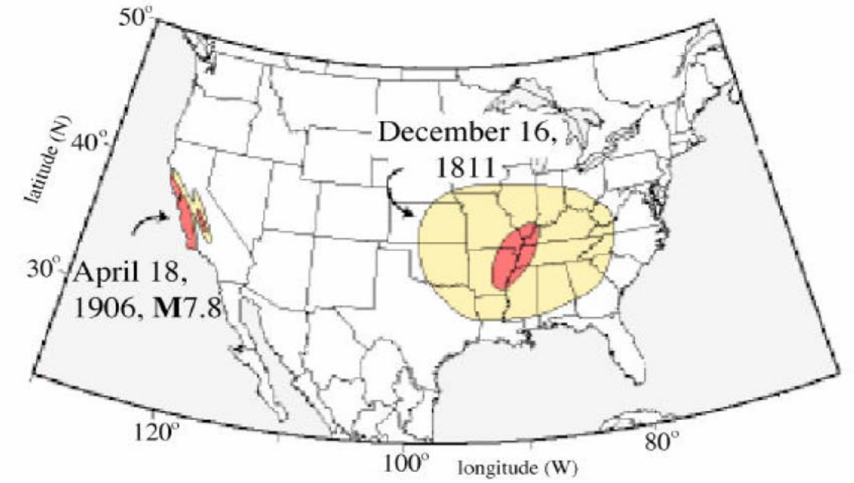

Areas affected by earthquakes of similar magnitude - the December 1811 M_s8.0 New Madrid and M_s8.3 1906 San Francisco earthquakes. The red zones denote areas of minor to major damage. The three largest New Madrid quakes affected more than 10X area San Francisco quake, deadliest in US history.

UMR

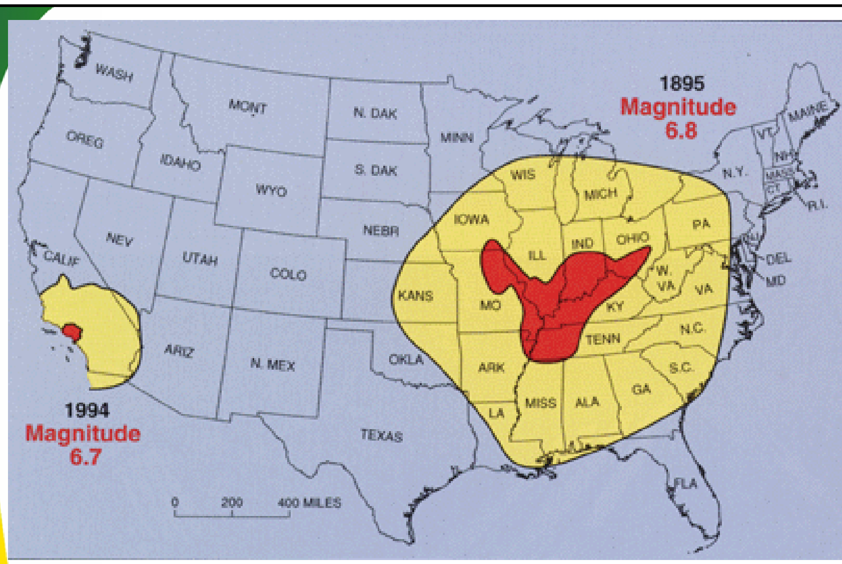

- Areas affected by earthquakes of similar magnitude – the M6.8 1895 Charleston, MO and M6.7 1994 Northridge earthquakes.

UMR

Current and Proposed MODOT Standards for Seismic Design

- **Green lines** are current ASSHTO design parameters using USGS 10% PE (1988)
- **Red lines** are proposed design parameters using USGS 2% PE (1996)

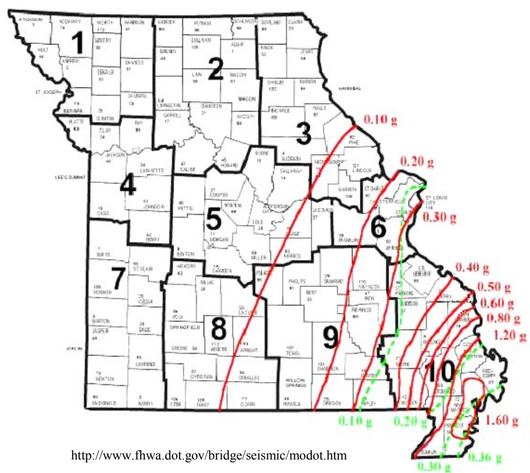

UMR

SCREENING ANALYSES

- **Risk assessment** is perhaps the most nefarious aspect of our profession. If we wanted to know the 100 year recurrence frequency flood, we would need 1000 years of flow records.
- We have a significant risk of future destructive earthquakes in the Midwest. But, our probabalistic models are based solely on data gathered from the New Madrid Seismic Zone, ignoring other likely sources.
- **Screening analyses** allow us to identify the structures with the greatest risk-consequence of failure and prioritize bridges based on seismic vulnerability.

UMR

EXAMPLE SCREENING ANALYSIS

- A preliminary site response evaluation was undertaken on three bridge sites along the Missouri River, located between 215 and 257 km from the New Madrid Seismic Zone.
- In our lifetimes, the most likely earthquake to impact these structures would be a repeat of the M6.6 Charleston, MO quake of 1895, which has a recurrence frequency of 70+/- 15 years (overdue since 1980).

UMR

TECHNICAL APPROACH

- Model one-dimensional equivalent linear site response and liquefaction susceptibility at the bridge sites.
- Liquefaction potential assessed through a two part qualitative and quantitative analysis.
- Generate artificial time histories using Boore's (2001) SMSIM code for base rock input motions.
- Simulation of seismic wave propagation through the surficial materials using the program DEEPSOIL by Park and Hashash (2003).

UMR

Missouri River Bridges with High Quality Geotechnical Data

- Page Extension Missouri River Bridge explored in 1996. 215 km from NMSZ
- Page Extension Creve Coeur Lake Memorial Park Bridge explored in 1996. 215 km from NMSZ
- Proposed State Route 19 replacement for Hermann, Missouri Bridge explored in 1999. 257 km from the NMSZ

UMR

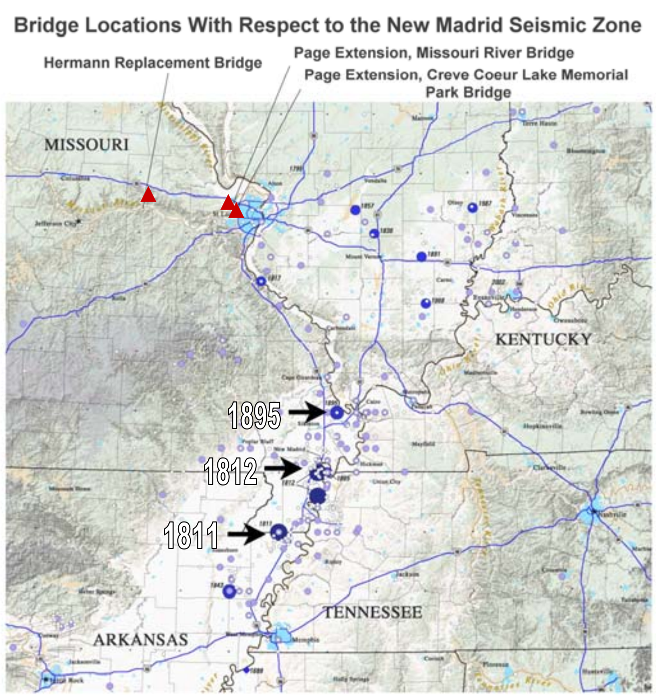

UMR

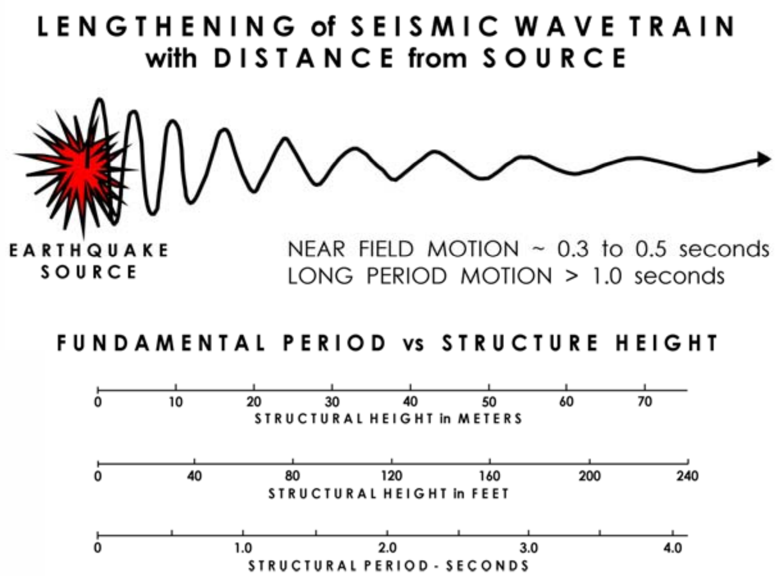

- Long period motions (T > 1.0 second) of great import when evaluating structures > 160 km from the quake hypocenter

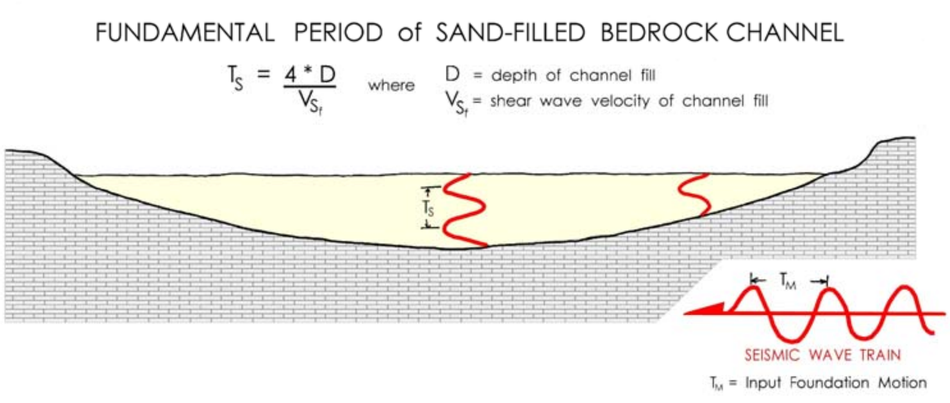

- **We can estimate the fundamental site period with some basic data. The period will change with location in a parabolic shaped channel.**

IMPEDANCE

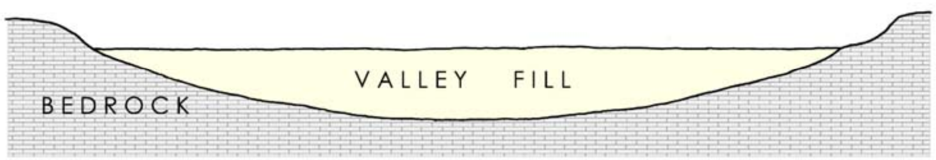

$$\text{IMPEDANCE RATIO} = \frac{\rho_{FOUNDATION} * V_{S\ BEDROCK}}{\rho_{VALLEY\ FILL} * V_{S\ VALLEY\ FILL}}$$

- **Site amplification is a function of the Impedance Ratio between the valley fill and the underlying basement rock. Impedance Ratios in Midwestern US channels are among the most excessive examples identified anywhere in the world.**

UMR

Estimating V_s from $(N_1)_{60}$

Regression Equation for Predicting V_S (m/s)	
FC < 10 %	$V_S = 95.5(N_1)_{60}^{0.226}$
FC = 10-35 %	$V_S = 103.4(N_1)_{60}^{0.205}$
FC = 0-40 %	$V_S = 101.8(N_1)_{60}^{0.205}$

$(N_1)_{60}$ in blows/0.3 meter

Andrus et al., 2004

UMR

SHEAR WAVE VELOCITY CORRELATIONS

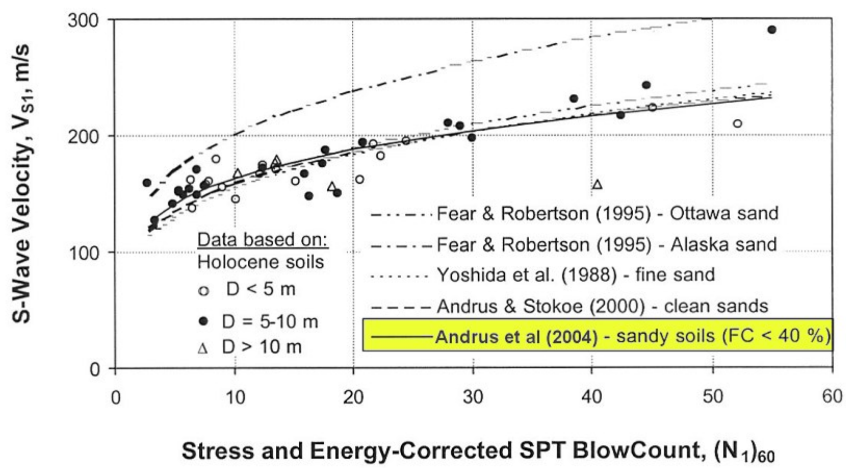

Andrus et al., 2004

UMR

LATERAL INCOHERENCE

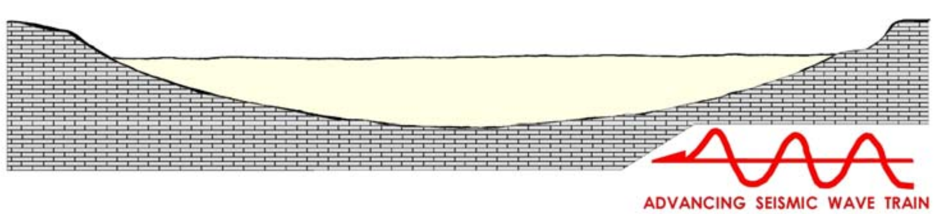

- **If we attempted to model the dynamic system created by the channel's interaction with an extremely long bridge structure, we would have to consider lateral and vertical incoherence of the foundations. This is usually performed in a full-blown dynamic analysis, not in a screening analysis.**

UMR

UNDERLYING GEOLOGY

- **The Missouri River bridges are founded on up to 31 m of unconsolidated loess, channel sands, silts, and oxbow clays/silts.**
- **Channel fill is unconsolidated Holocene age material; mostly saturated channel sands with low relative density**
- **Underlying bedrock is stiff Paleozoic age limestone, dolomite, and shale.**
- **All three bridges cross asymmetric channels, with bedrock on one abutment and unconsolidated sediment beneath the other.**

Page Extension, Missouri River

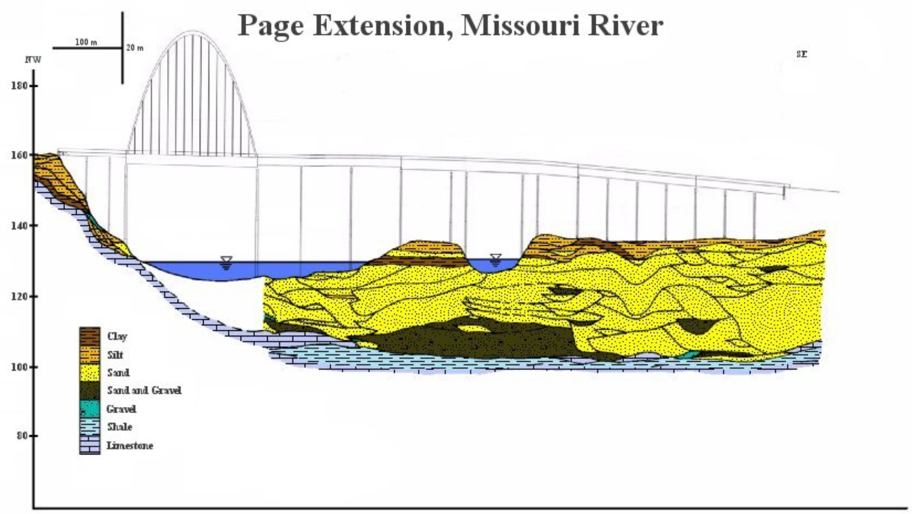

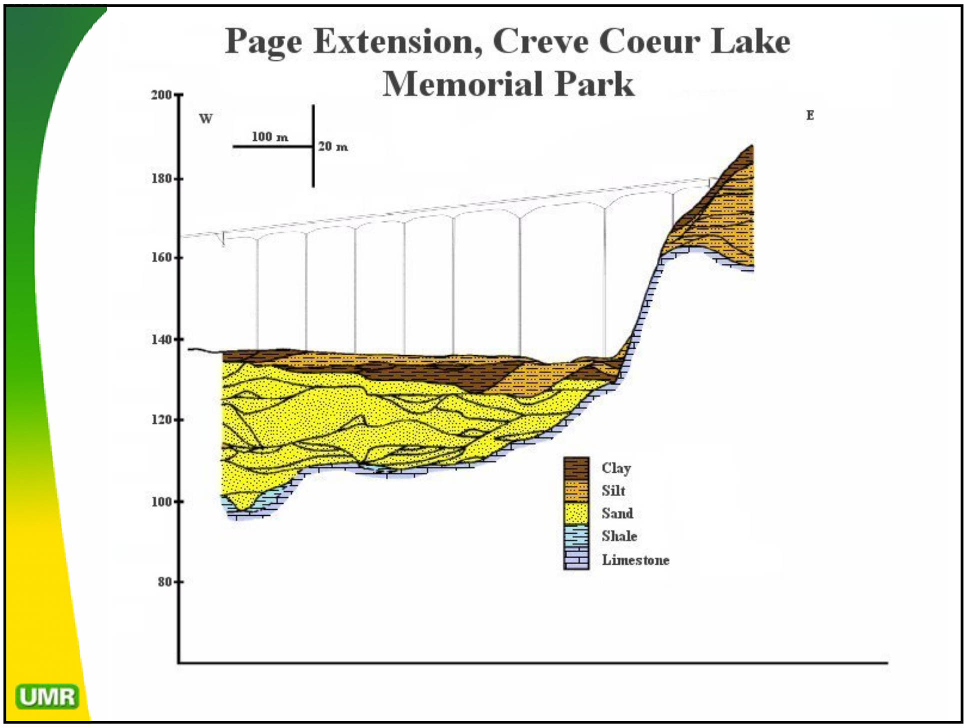
Page Extension, Creve Coeur Lake Memorial Park
200
180
160
140
120
100
80
W
E
100 m
20 m
Clay
Silt
Sand
Shale
Limestone
UMR

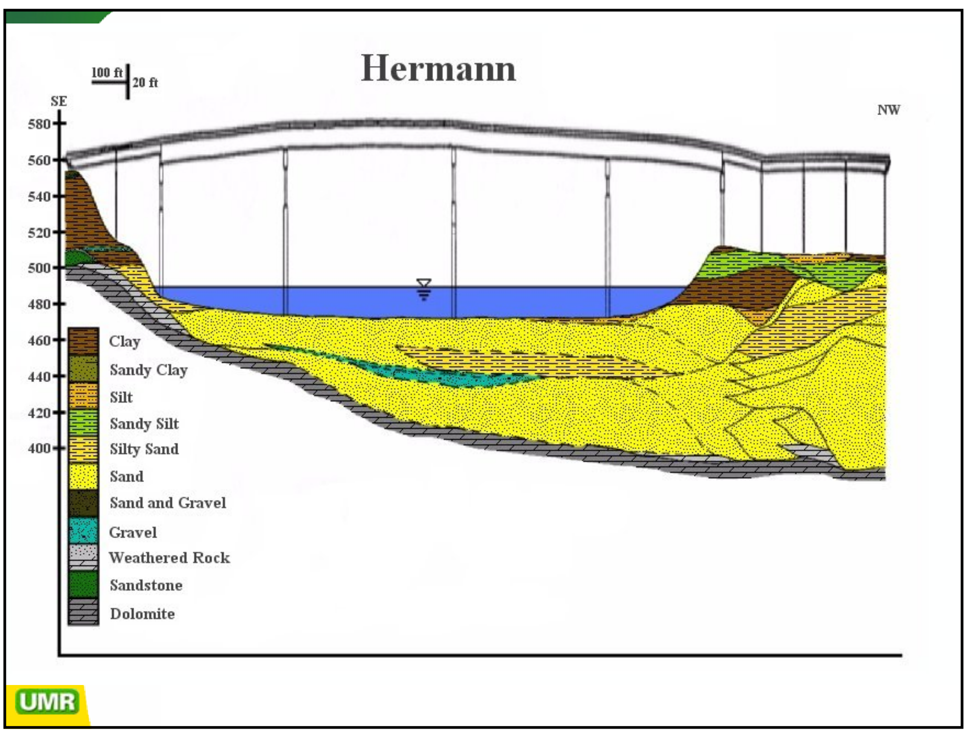
Hermann
100 ft
20 ft
SE
NW
580
560
540
520
500
480
460
440
420
400
Clay
Sandy Clay
Silt
Sandy Silt
Silty Sand
Sand
Sand and Gravel
Gravel
Weathered Rock
Sandstone
Dolomite
UMR

Generation of Artificial Time Histories

- Artificial time histories were generated using SMSIM code developed by Dave Boore of the USGS and modified by Bob Herrmann at St. Louis University for Midwest deep soil sites.

Model	NAME	SITE EFFECT
1	Atkinson-Boore 1995 (AB95)	ENA Hard Rock
2	USGS 1996	Generic B-C Boundary
3	USGS 1996 (modified)	Mid-Continent Deep Soil (new)
4	Mid-America Deep Soil AB95 source (modified)	Mid-Continent Deep Soil (new)
5	Mid-America Deep Soil USGS 96 source (modified)	Mid-Continent Deep Soil (new)

UMR

ARTIFICIAL TIME HISTORIES FOR SCREENING ANALYSES GENERATED FOR THREE HISTORIC EVENTS EMANATING FROM THE NEW MADRID SEISMIC ZONE:

- 16 Dec 1811 M_s8.6 = M7.3 event
- 7 Feb 1812 M_s 8.0 = M7.5 event
- 31 Oct 1895 M_s 6.8 = M6.6 event

UMR

Page Avenue Missouri River Bridge Artificial Time Histories

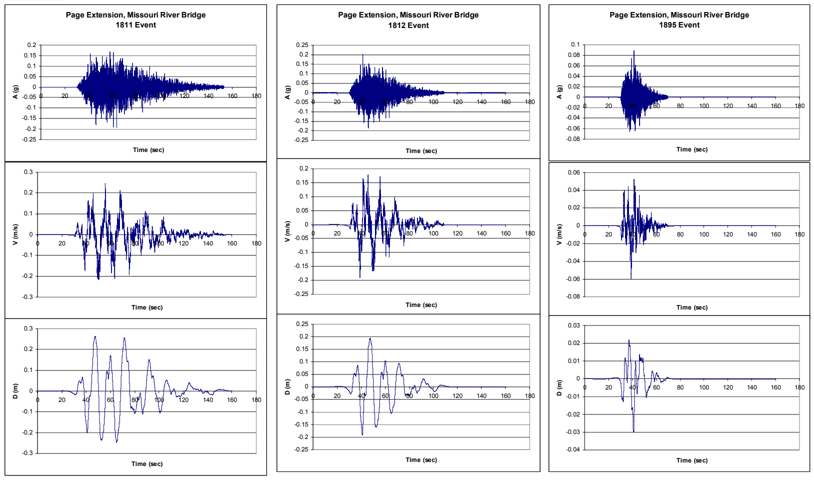

1811 1812 1895

UMR

Creve Coeur Lake Bridge Artificial Time Histories

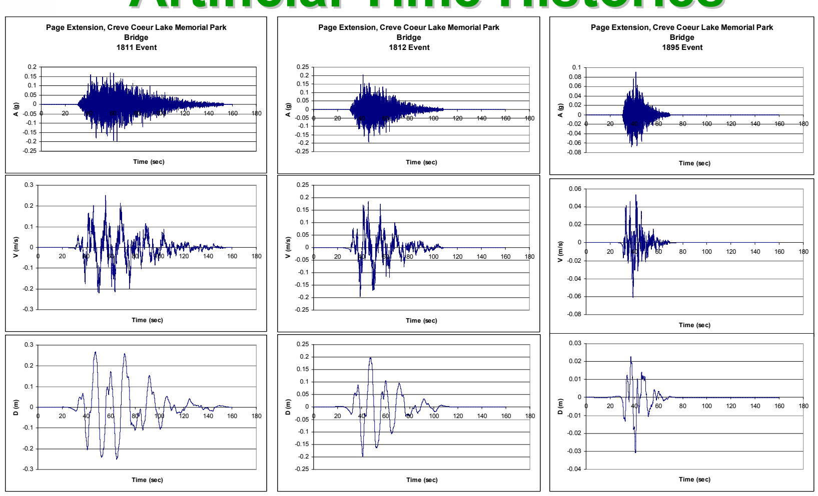

1811 1812 1895

UMR

Hermann Bridge Site Artificial Time Histories

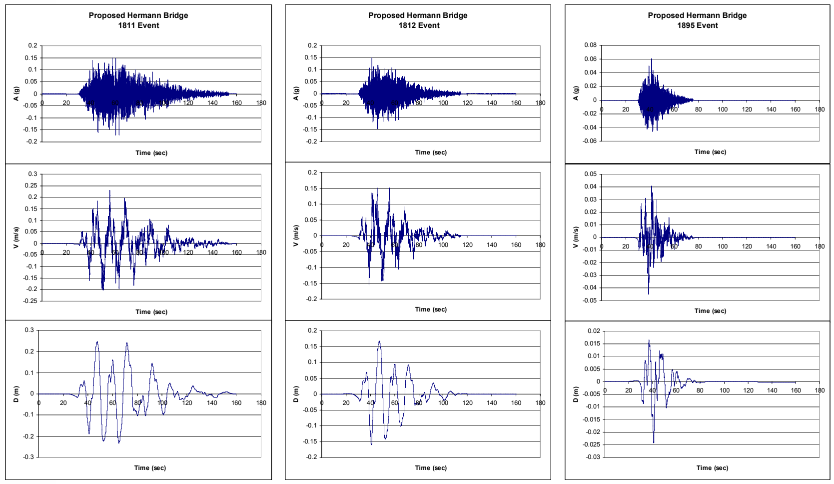

1811 1812 1895

Screening Analysis for Liquefaction Potential

- **Recommend using:**

  T. L. Youd,1998, *Screening Guide for Rapid Assessment of Liquefaction Hazard at Highway Bridge Sites*: Technical Report MCEER-98-0005
- **It employs a Qualitative Analysis; and**
- **A Quantitative Analysis**
- **Good idea to include both**

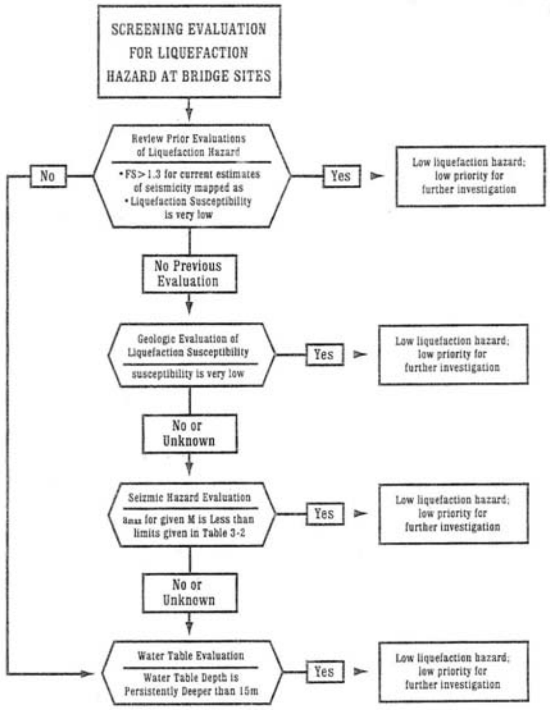

Qualitative Liquefaction Analysis Flow Chart from MCEER 98-05

GEOLOGIC EVALUATION

Type of Deposit	<500 yr	Holocene	Pleistocene	Pre-Pleistocene
River Channel	Very High	High	Low	Very Low
Flood Plain	High	Moderate	Low	Very Low
Alluvial Fan	Moderate	Low	Very Low	Very Low
Delta	High	Moderate	Low	Very Low
Lacustrine	High	Moderate	Low	Very Low
Colluvium	High	Moderate	Low	Very Low
Glacial Till	Low	Low	Very Low	Very Low

Youd (1998)

SEISMIC EVALUATION

Earthquake Magnitude	Soil Profile Type I and II (Stiff Sites)	Soil Profile Type III and IV (Soft Sites)
	Very Low Hazard for	
M < 5.2	Amax < 0.4g	Amax < 0.1g
5.2 < M < 6.4	Amax < 0.1g	Amax < 0.05g
6.4 < M < 7.6	Amax < 0.05g	Amax < 0.025g
7.6 < M	Amax < 0.025	Amax < 0.025

Youd (1998) Soil Profile Descriptions from AASHTO (1996)

UMR

WATER TABLE EVALUATION

Groundwater Table Depth	Relative Liquefaction Susceptibility
< 3 m	Very High
3 m to 6 m	High
6 m to 10 m	Moderate
10 m to 15 m	Low
> 15 m	Very Low

Youd (1998)

UMR

QUANTITATIVE ANALYSIS
Youd et al. (2001)

- Based on T. L. Youd et al., 2001, *Liquefaction Resistance of Soils: Summary Report from the 1996 NCEER and 1998 NCEER/NSF Workshops on Evaluation of Liquefaction Resistance of Soils*: ASCE Journal of Geotechnical and Geoenvironmental Engineering
- Cyclic Stress Ratio (CSR) vs. Cyclic Resistance Ratio (CRR) (normalized for M 7.5)
- Factor of Safety (includes a magnitude scaling factor)

UMR

MAGNITUDE SCALING FACTORS for calculating liquefaction factor of safety can be estimated from published charts

Magnitude, M	Seed and Idriss (1982)	Idriss[a]	Ambraseys (1988)	Arango (1996) Distance based	Arango (1996) Energy based	Andrus and Stokoe (1997)	Youd and Noble (1997b) $P_L < 20\%$	Youd and Noble (1997b) $P_L < 32\%$	Youd and Noble (1997b) $P_L < 50\%$
5.5	1.43	2.20	2.86	3.00	2.20	2.8	2.86	3.42	4.44
6.0	1.32	1.76	2.20	2.00	1.65	2.1	1.93	2.35	2.92
6.5	1.19	1.44	1.69	1.60	1.40	1.6	1.34	1.66	1.99
7.0	1.08	1.19	1.30	1.25	1.10	1.25	1.00	1.20	1.39
7.5	1.00	1.00	1.00	1.00	1.00	1.00	—	—	1.00
8.0	0.94	0.84	0.67	0.75	0.85	0.8?	—	—	0.73?
8.5	0.89	0.72	0.44	—	—	0.65?	—	—	0.56?

Note: ? = Very uncertain values.
[a]1995 Seed Memorial Lecture, University of California at Berkeley (I. M. Idriss, personal communication to T. L. Youd, 1997).

taken from Youd et al. (2001)

UMR

Page Ave. Missouri River Bridge CSR vs. CRR

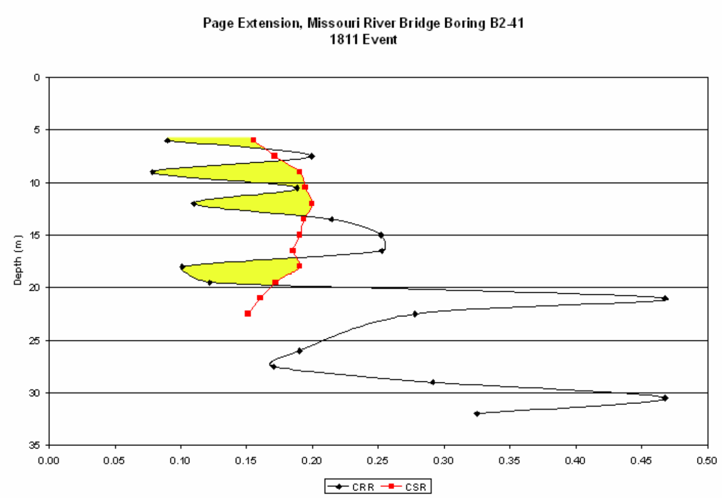

UMR

$M8_s.6$

Page Ave. Missouri River Bridge Liquefaction Factor of Safety

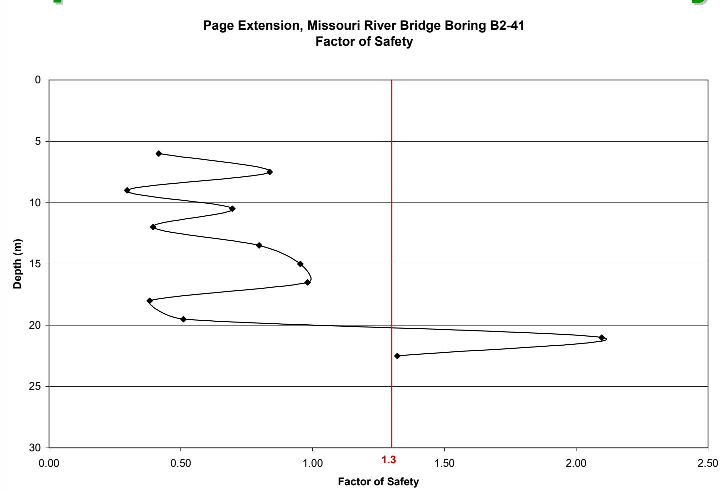

UMR

$M8_s.6$

Page Ave. Missouri River Bridge
CSR vs. CRR

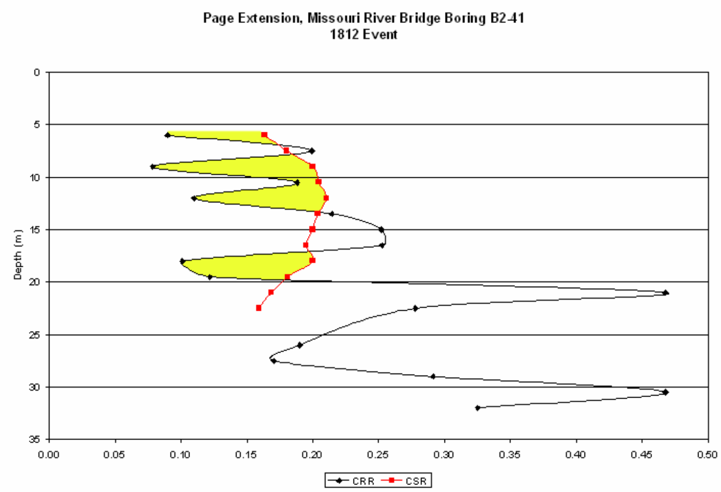

UMR

$M_s 8.6$

Page Ave. Missouri River Bridge
Liquefaction Factor of Safety

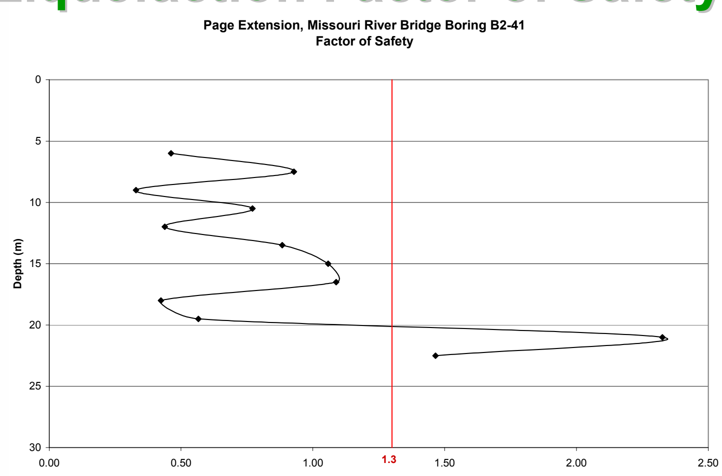

UMR

$M8_s.6$

Page Ave. Missouri River Bridge CSR vs. CRR

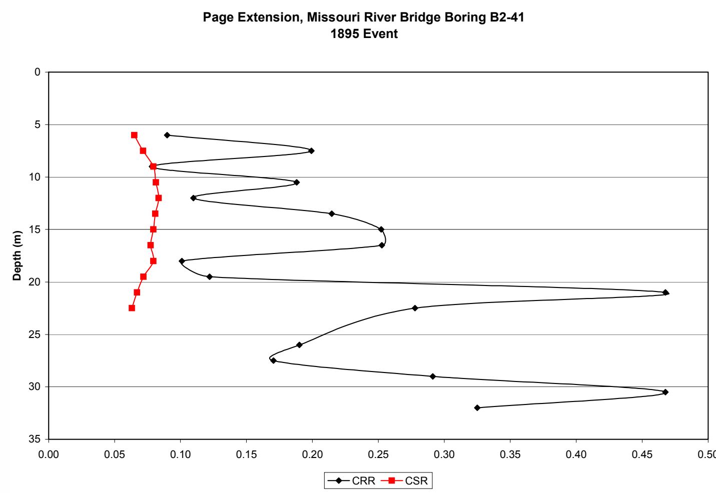

M8$_s$.6

Page Ave. Missouri River Bridge Liquefaction Factor of Safety

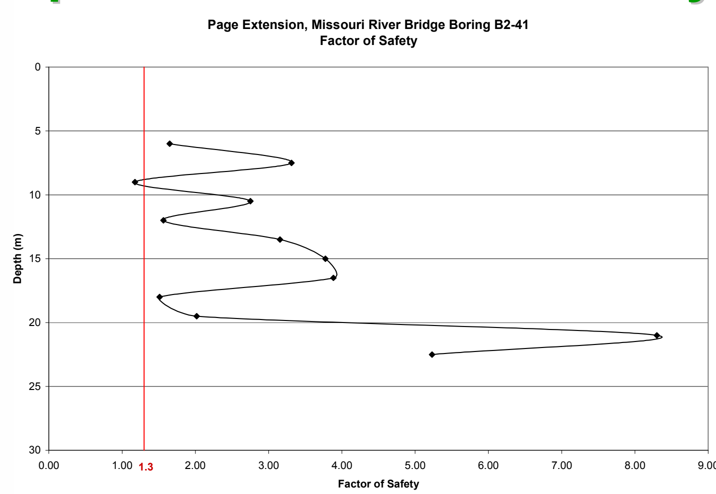

M_s8.6

1D Seismic Site Response Equivalent Linear Approach

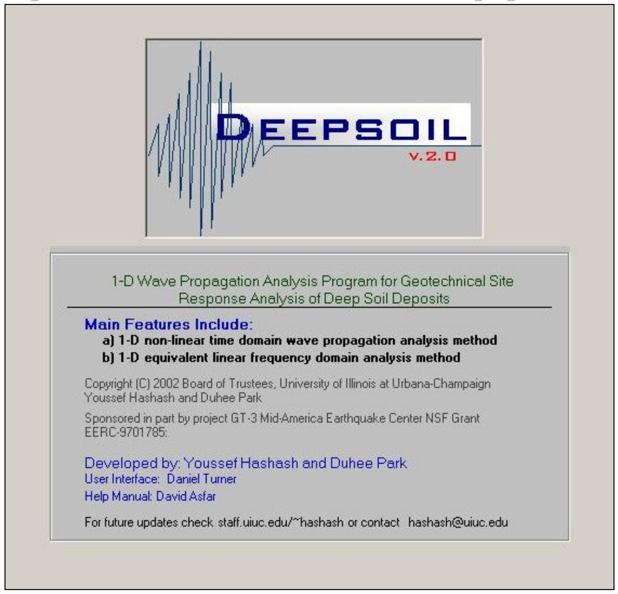

UMR

EPRI GENERIC MODULUS REDUCTION CURVES

- Soil parameters correlated from Corrected SPT blow counts.
- Dynamic soil parameters estimated to fit modulus reduction and damping curves recommended by EPRI (1993)

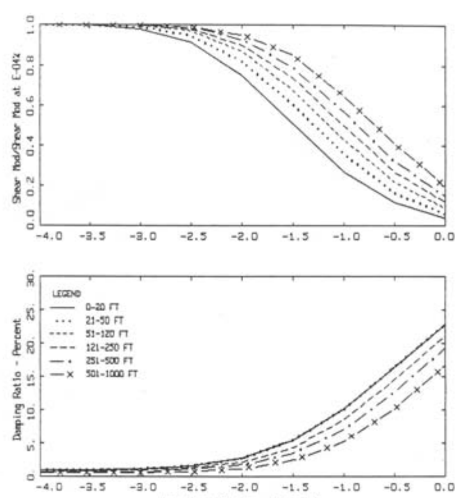

EPRI (1993)

UMR

EPRI Curves Approximated

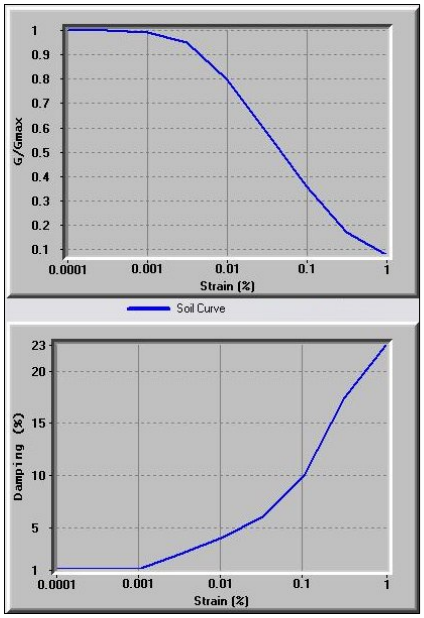

UMR

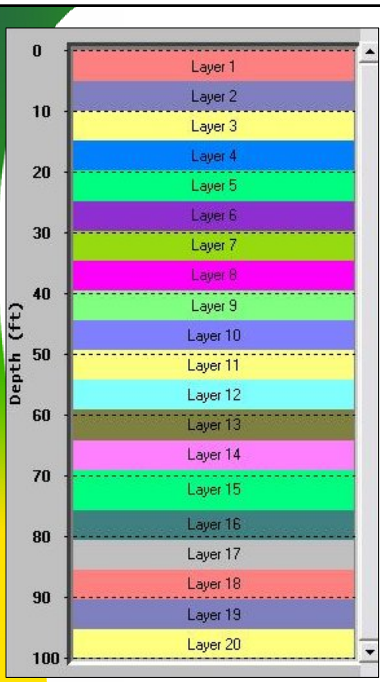

Soil Parameter Input Interface using DEEPSOIL 1-D wave propagation analysis

UMR

Page Ave. Missouri River Bridge M8.6 1811 NMSZ Event

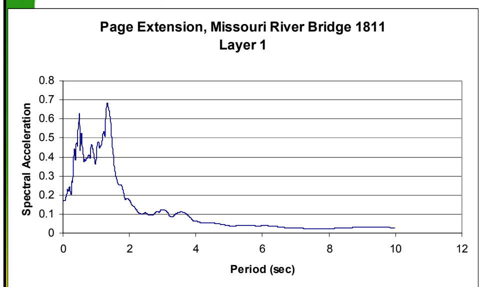

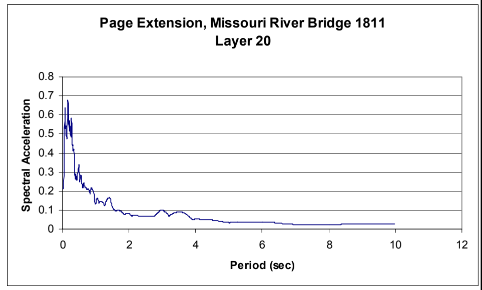

At ground surface

At bedrock interface

UMR

Page Ave. Missouri River Bridge M8.0 1812 NMSZ Event

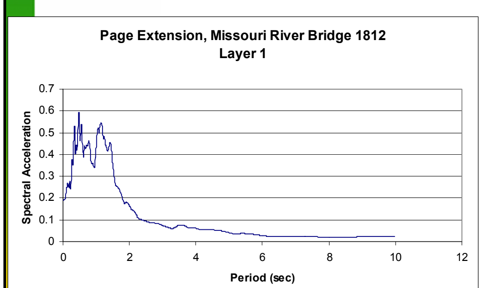

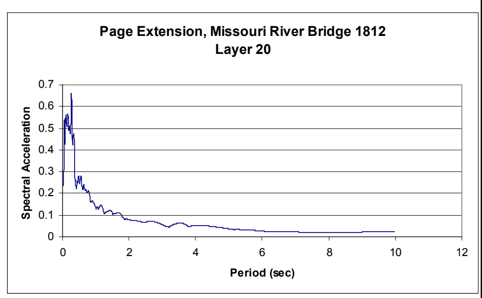

At ground surface

At bedrock interface

UMR

Page Ave. Missouri River Bridge M6.6 1895 NMSZ Event

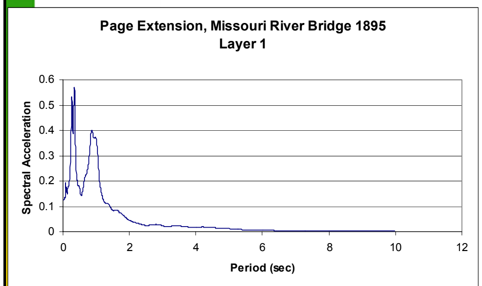

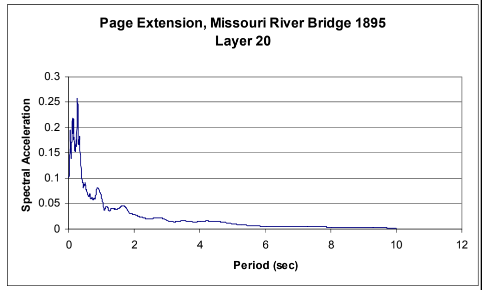

At ground surface

Increases to 0.58 g

At bedrock interface

a_{max} = 0.22g

UMR

Page Ave. Creve Coeur Lake Memorial Park Bridge M8.6 1811 Event

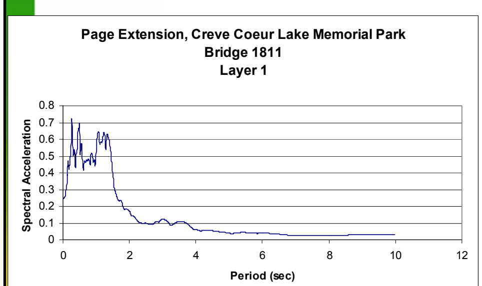

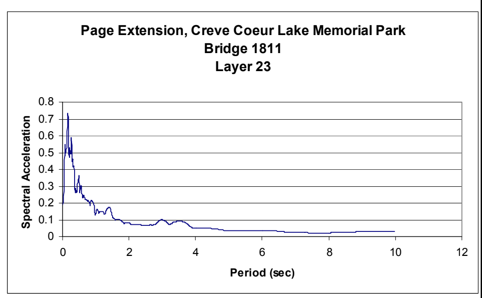

At ground surface

At bedrock interface

UMR

Page Ave. Creve Coeur Lake Memorial Park Bridge M8.0 1812 Event

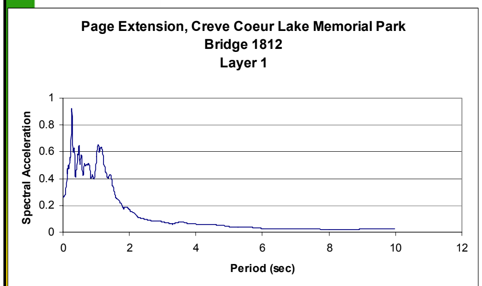

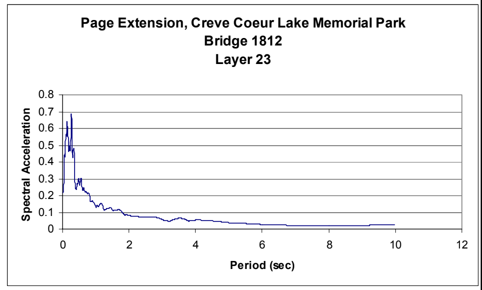

At ground surface

Increases to 0.90 g

At bedrock interface

a_{max} = 0.70g

UMR

Page Ave. Creve Coeur Lake Memorial Park Bridge M6.6 1895 Event

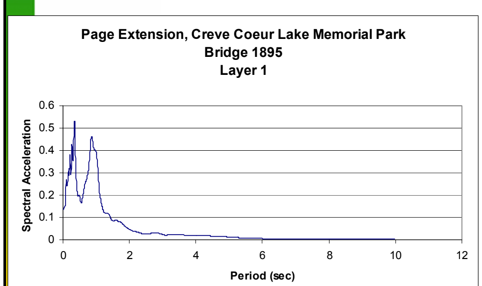

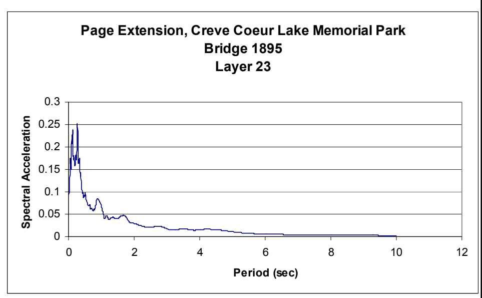

At ground surface

Increases to 0.53 g

At bedrock interface

a_{max} = 0.24g

UMR

Hermann Bridge Site
M8.6 1811 Event

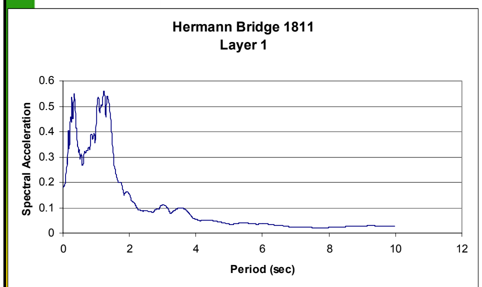

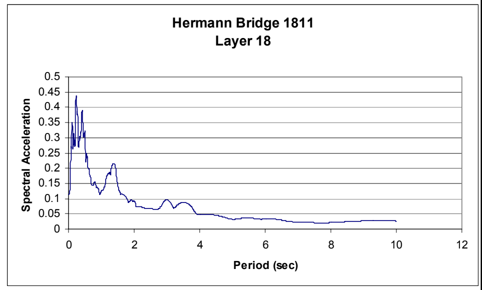

At ground surface

Increases to 0.56 g

At bedrock interface

a_{max} = 0.44g

UMR

Hermann Bridge Site
M8.0 1812 Event

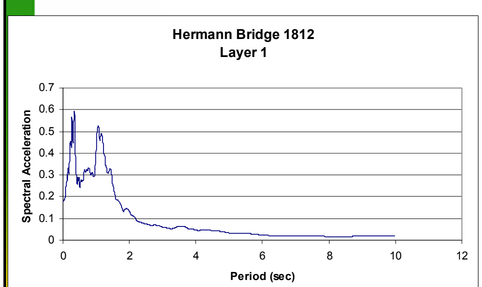

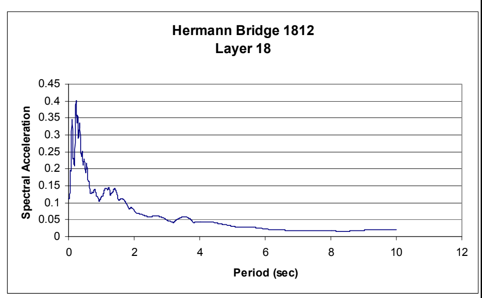

At ground surface

Increases to 0.60g

At bedrock interface

a_{max} = 0.39g

UMR

Hermann Bridge Site
M6.6 1895 Event

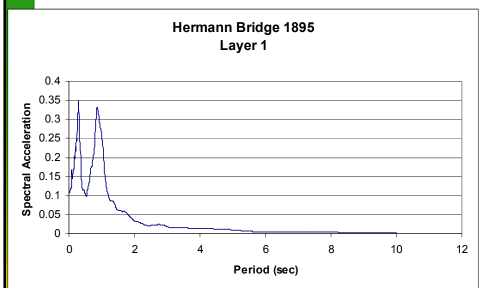

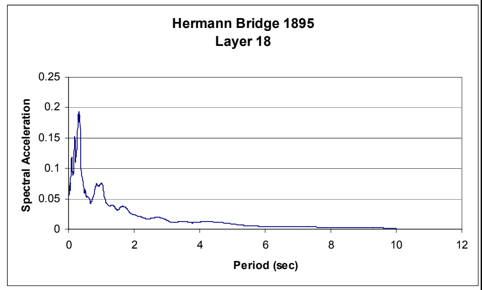

At ground surface
Increases to 0.35g

At bedrock interface
a_{max} = 0.19g

UMR

ELEMENTS of a TYPICAL CHANNEL CROSSING

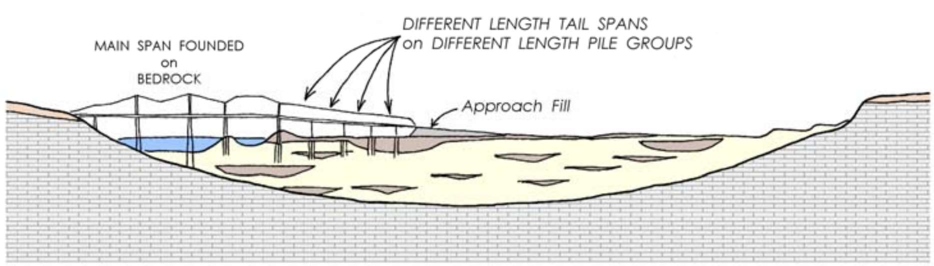

- Asymmetric channel section; Missouri river on far south side of parabolic shaped channel
- Main spans supported on stiff caissons to rock
- Tail spans supported on pile groups of differing length
- Soft pockets on old oxbows can be problematic
- Widespread liquefaction and lateral spreads likely near channels

UMR

ZONES COMMONLY SUSCEPTIBLE to LIQUEFACTION

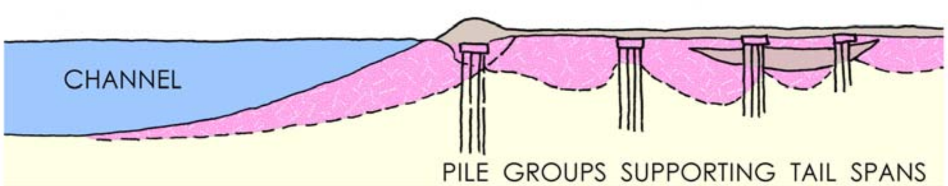

- Simply supported tail spans would appear to be most vulnerable part of existing highway bridges
- Site amplification causes long period motions to peak between 1.0 and 1.5 seconds
- We can expect liquefaction of foundations (areas shown in pink)

UMR

CONCLUSIONS

- Widespread liquefaction likely in M6.6 or greater events at great range (~250 km)
- Liquefaction so severe (deep) and continuous in M7.5+ events that localized failure/tilt of supporting pile groups can be expected
- Lateral spreads can be expected near channels in those areas subject to severe liquefaction. These would destroy any pile supported structures
- Long period motions will cause significant site amplification locally, which could trigger collapse of simply supported spans at great range (~250 km)
- Two-dimensional effect of bedrock channels not considered in these screening analyses. This could make matters worse locally.

UMR

PRESENTATION 12

SOIL-PILE-STRUCTURE INTERACTION – GEOTECHNICAL ASPECTS

NATURAL HAZARDS MITIGATION INSTITUTE

UMR
UNIVERSITY OF MISSOURI-ROLLA

SOIL-PILE-STRUCTURE INTERACTION - Geotechnical

Ronaldo Luna, Ph.D., P.E.
Associate Professor of Civil Engineering
University of Missouri-Rolla (UMR)

Geotechnical and Bridge Seismic Design Workshop
New Madrid Seismic Zone Experience

October 28-29, 2004, Cape Girardeau, Missouri

NATURAL HAZARDS MITIGATION INSTITUTE

UMR
UNIVERSITY OF MISSOURI-ROLLA

SOIL-PILE-STRUCTURE INTERACTION - Geotechnical

Investigators:

Dr. Genda Chen
Dr. Mostafa El-Engebawy
Dr. Ronaldo Luna (Lead)
Mr. Wanxing Liu
Dr. Wei Zheng

Presentation Outline

- Presentation Objectives
- Considerations of the soil-structure
- Framework of Development
- Soil-structure Modeling
- Validation of Model
- Application to the NMSZ
- Summary & Conclusions

Objectives

- Obtain ground motions at ground surface in time domain modeling
- Develop soil-pile interface elements and springs to model soil behavior.
- Examine the effect of liquefaction on foundations systems.

Development of Simulation System

- **Research Outline**
  1. Deep Ground Response Analysis
  2. Liquefaction Analysis in the NMSZ
  3. **SPSI Analysis in the NMSZ**
- OpenSees is used as a numerical simulation tool.

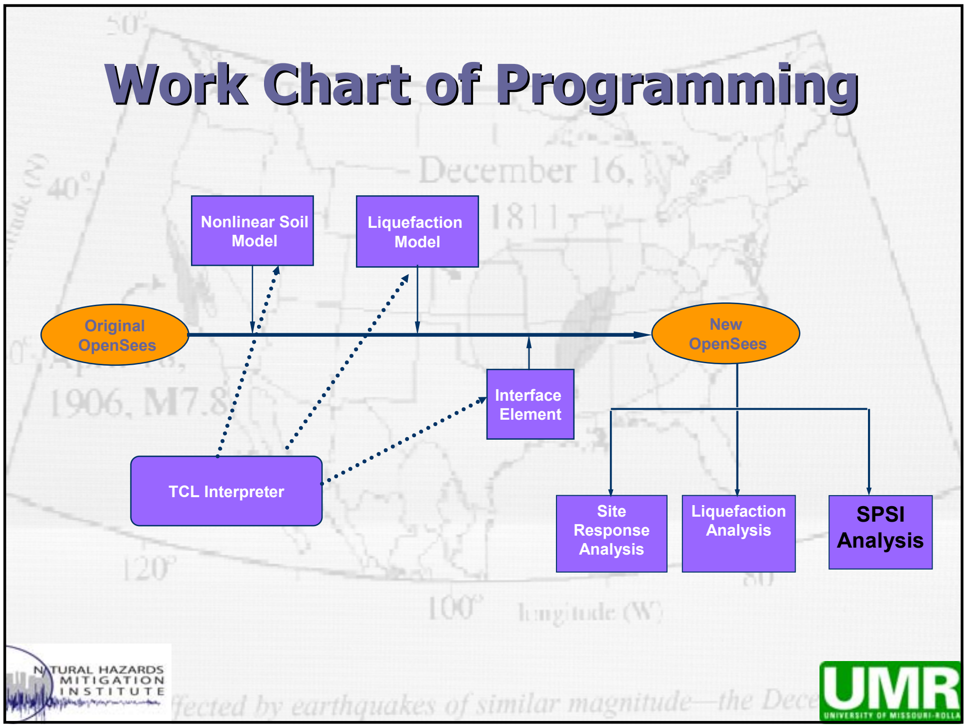
Work Chart of Programming
Nonlinear Soil Model
Liquefaction Model
Original OpenSees
New OpenSees
Interface Element
TCL Interpreter
Site Response Analysis
Liquefaction Analysis
SPSI Analysis
NATURAL HAZARDS MITIGATION INSTITUTE
UMR
UNIVERSITY OF MISSOURI-ROLLA

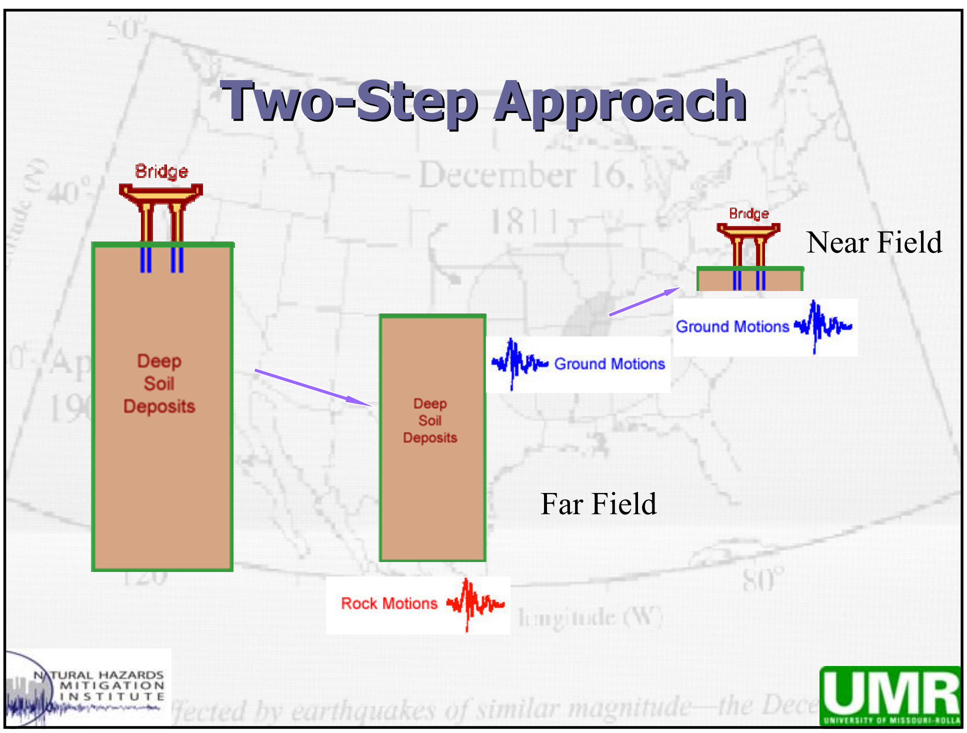
Two-Step Approach
Bridge
Deep Soil Deposits
Bridge
Near Field
Ground Motions
Ground Motions
Deep Soil Deposits
Far Field
Rock Motions
NATURAL HAZARDS MITIGATION INSTITUTE
UMR
UNIVERSITY OF MISSOURI-ROLLA

Considerations for Single Pile Seismic Response

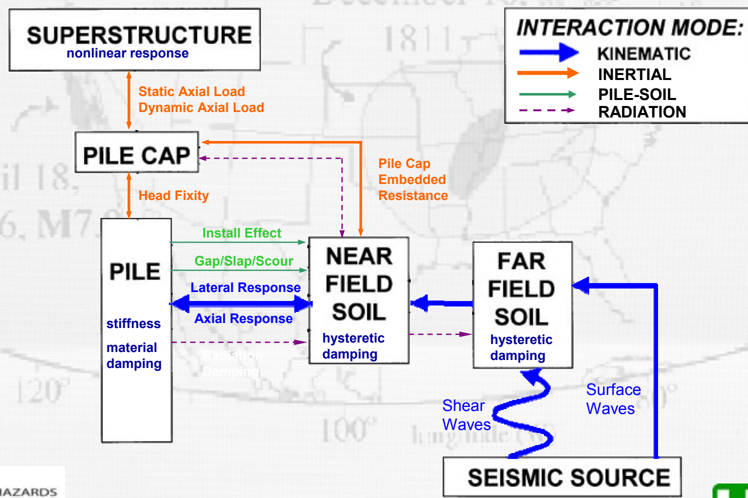

Methods for SPSI Analysis

- Existing methods for SPSI analysis:
  - Simplified substructure methods that uncouples the superstructure and foundation portions of the analysis.
  - Dynamic beam on Winkler foundation (dynamic p-y curve) method.
  - 2D and 3D modeling of the pile and soil continuum using finite element or finite difference method.
- Dynamic p-y curve methods are considerably less complex than finite element or finite difference modeling and provide several potential advantages over the simplified substructure method.

What is p-y curve?

- p – lateral soil resistance
- y – lateral pile deflection
- Stiffness derived from field test and normally stiffer with depth
- Nonlinear p-y spring components
  - Elastic component
  - Plastic component
  - Soil-pile gap

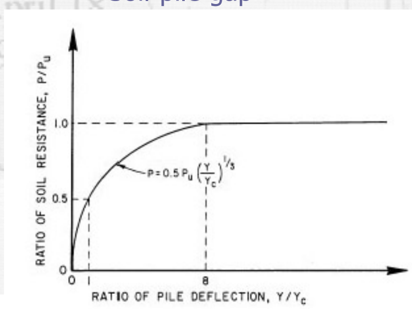

Clay (Matlock,1970)

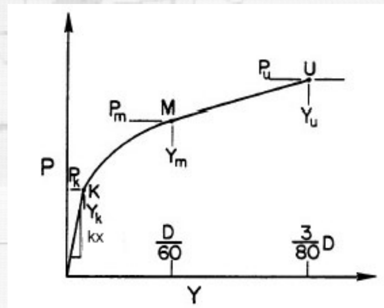

Sand (Reese et al.,1984)

Dynamic nonlinear *p-y* Curves

- Boulanger et al. (1999) presented a nonlinear *p-y* element.
- The nonlinear *p-y* behavior is conceptualized as consisting of elastic, plastic, and gap components in series.

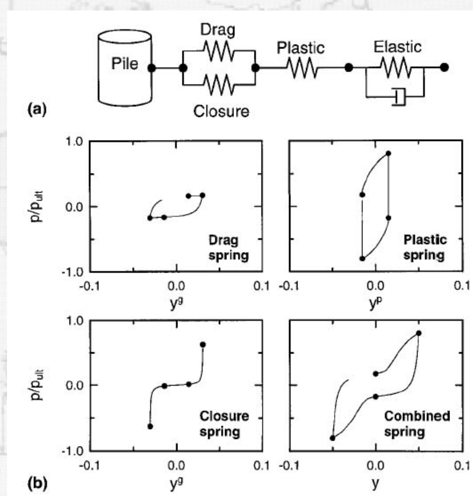

Coupled SPSI Approach

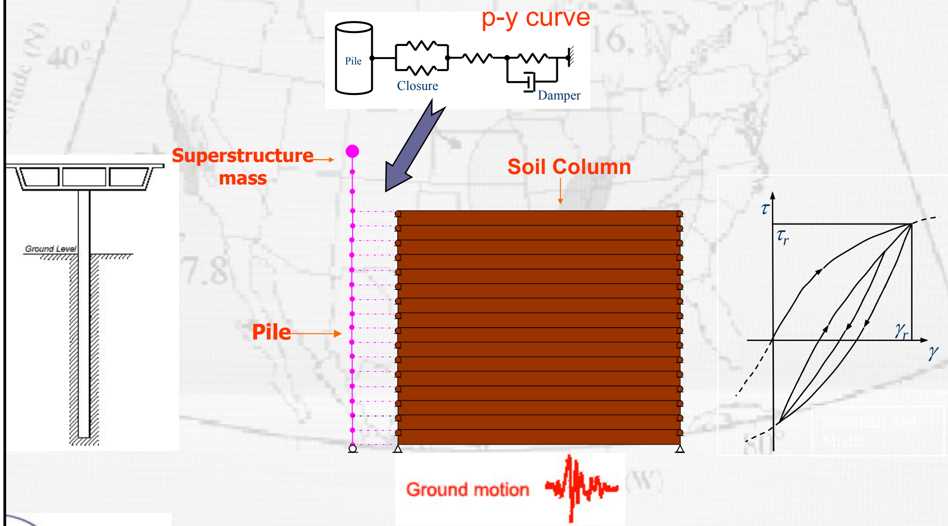

Liquefaction Consideration

- Softening of p-y relationship with increasing pore water pressure was found in lots of centrifuge tests. A degradation parameter C_u is determined and applied to the ultimate soil resistance P_u.

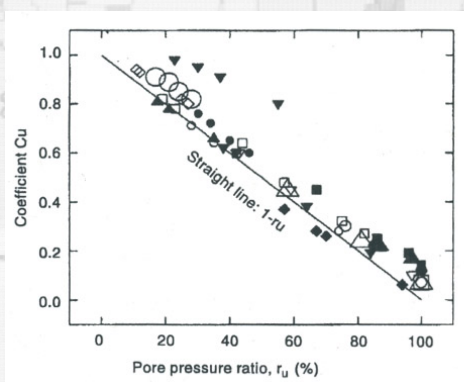

Dobry and Liu (1995)

Liquefaction Consideration

- When considering loading rate, Wilson (1998) found an appropriate multiplier for peak loads during an earthquake in a pseudo-static analysis in liquefying sand would be 0.25-0.35 for Dr = 55%, and 0.10 for Dr = 35%.

Loose sand

$$C_u = 1 - 0.9 r_u$$

Medium dense sand

$$Cu = 1 - 0.65 r_u$$

Model Calibration

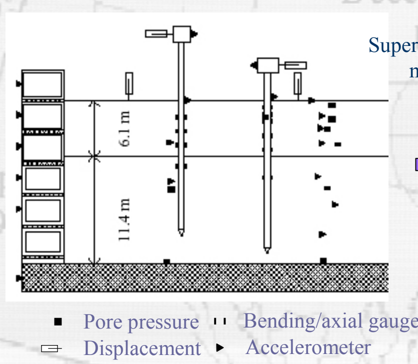

Centrifuge Tests (UC, Davis)

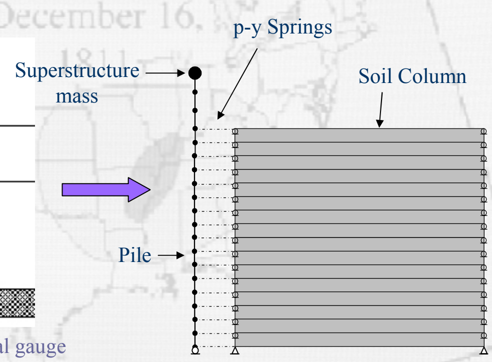

UMR Model

Earthquake Events

Earthquake Events for Centrifuge Tests

Event	Motion	a_{max} base input (g)
A	Kobe	0.055
B	Kobe	0.055
C	Kobe	0.016
D	Kobe	0.20
E	Kobe	0.58

Spectra Comparison - Superstructure

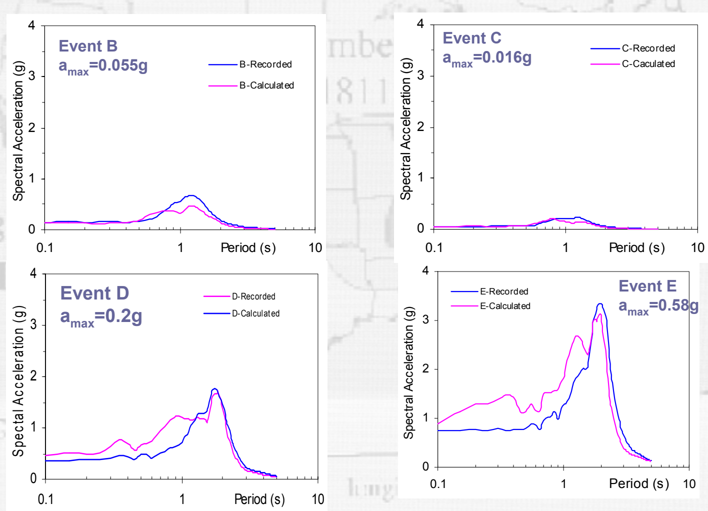

Comparison of Spectral Acceleration at Superstructure for Events B-E (5% damping)

Acceleration Time Histories Comparison

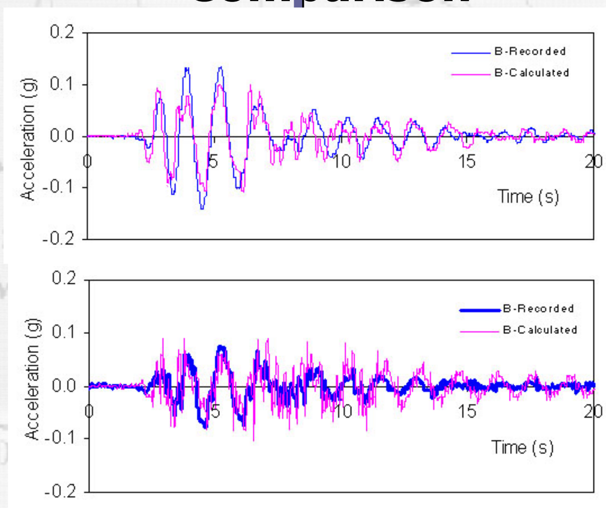

Comparison of Time Histories during Event B (a) Superstructure (b) Pile Head

Displacement and Moment Comparison

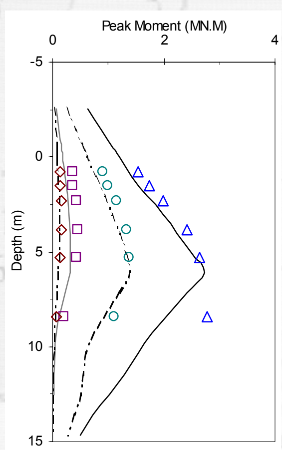

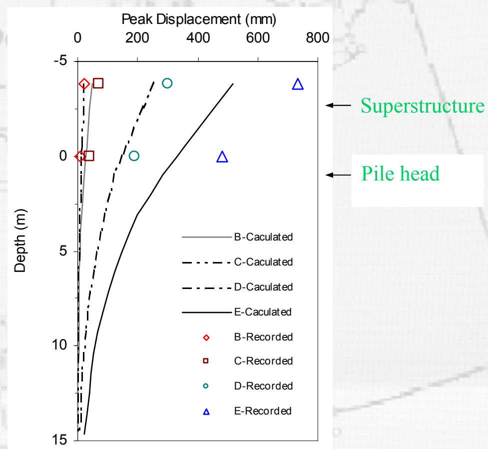

Comparison of Calculated and Recorded Peak Relative Displacements during Events B-E

Application in the NMSZ

- Presented SPSI analysis method is applied to a highway bridge (L472 site).
- Synthetic ground motions were used and propagated up to the bottom of the pile foundations using the site response analysis.

NATURAL HAZARDS MITIGATION INSTITUTE

UMR UNIVERSITY OF MISSOURI-ROLLA

Bridge Type

Elevation of Bridge L-472

This bridge was originally built as a multi-span simply supported steel girder bridge in the early 1950s, then enlarged and revised in 1971, and finally revised with deck repairs in 1984.

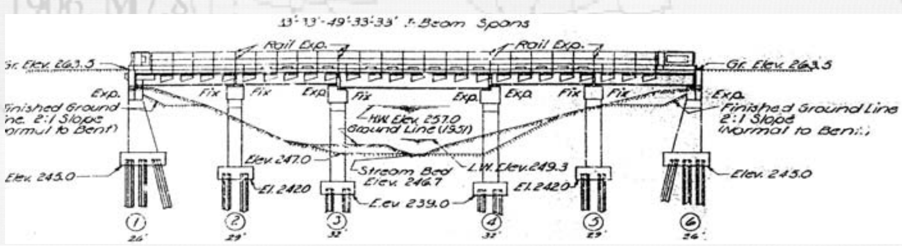

Elevation of Bridge L-472

NATURAL HAZARDS MITIGATION INSTITUTE

UMR UNIVERSITY OF MISSOURI-ROLLA

Application to L472

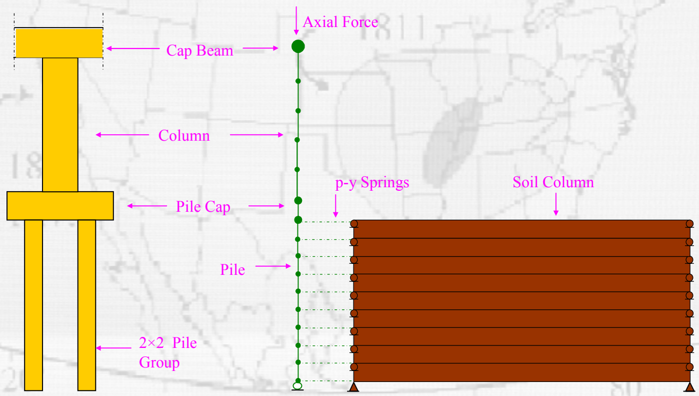

Finite Element Model for the Coupled SPSI Analysis

Results of Analysis

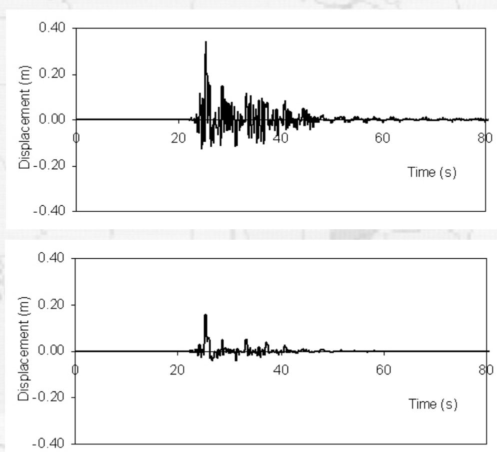

Displacement Histories for Analysis without Liquefaction Consideration in FN Direction (a) Beam Cap (b) Pile Cap

Results of Analysis

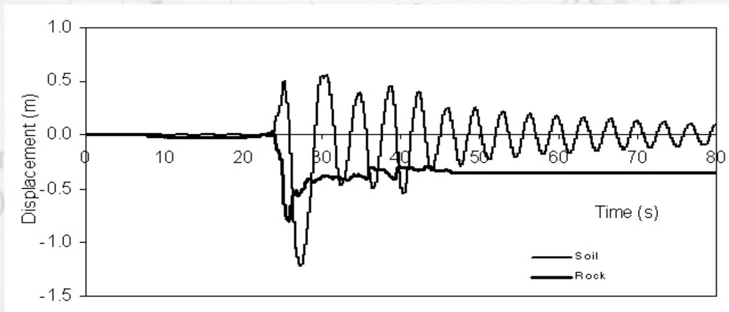

Displacement Histories at Rock Base and the Bottom of Pile Foundation for FN Direction

NATURAL HAZARDS MITIGATION INSTITUTE

UMR UNIVERSITY OF MISSOURI-ROLLA

Results of Analysis

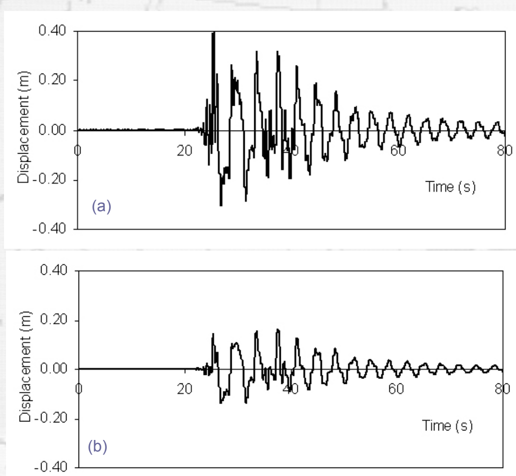

← Cap Beam

← Pile Cap

Displacement Histories for Analysis with Liquefaction Consideration in FN Direction (a) Beam Cap (b) Pile Cap

NATURAL HAZARDS MITIGATION INSTITUTE

UMR UNIVERSITY OF MISSOURI-ROLLA

Results of Analysis

Peak Moment Comparison in FN Direction

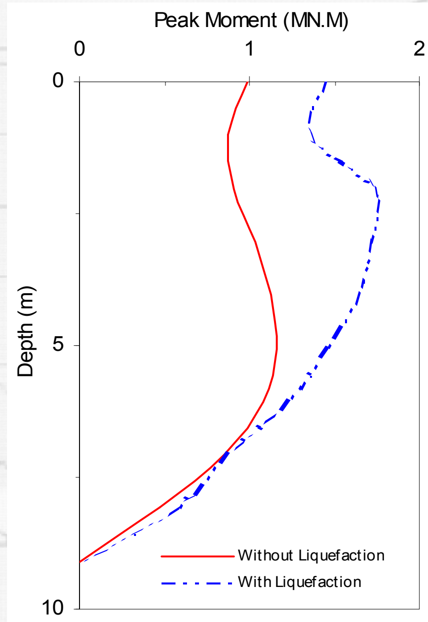

Other Considerations

- Dynamic Group Pile Effects
  - from scaled testing (Lok (1999)
- Effect of liquefaction was only considered in the saturated foundation soils. However, the impact on the embankment was considered.
- These different geotechnical components were assembled around the structure to simulate dynamic behavior.

Modeling Geotechnical Conditions to the Superstructure

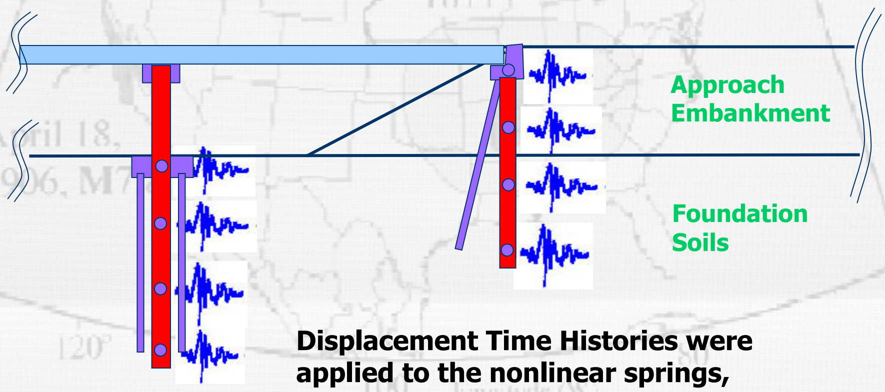

Displacement Time Histories were applied to the nonlinear springs, which include liquefaction effects

Summary & Conclusions

Summary of Findings

- A coupled SPSI analysis method was developed and verified with an instrumented centrifuge test results.
- This method has been applied to evaluate the seismic response of the highway bridges in the NMSZ.
- Dynamic nonlinear p-y method was adopted to simulate the interaction between pile and soil.

NATURAL HAZARDS MITIGATION INSTITUTE

UMR UNIVERSITY OF MISSOURI-ROLLA

Summary of Findings

- A degradation multiplier at the pile soil-interface is introduced to the p-y curve to consider softening due to pore water pressure generation which induces liquefaction.
- The results indicate that the degradation of soil spring due to the pore water pressure greatly influence the foundation and superstructure response. Larger displacements and moments were found due to the softening of the soil springs.

NATURAL HAZARDS MITIGATION INSTITUTE

UMR UNIVERSITY OF MISSOURI-ROLLA

Summary of Findings

- Near field energy pulse could be transmitted to the piles and other bridge components after propagating through the inelastic behavior of pile-soil interaction.
- However, near-field properties in the superstructure are not as significant as when the degradation of soil springs due to the pore water pressure is considered.

Final Comments

- The nonlinear effects near the surface tend to decrease the acceleration response spectra. However, there is a trade-off for these reduced spectra, that is, the larger deformations (straining) that the soil-structure undergoes to dissipate that energy. In saturated deposits these large nonlinear deformations may be a result of liquefaction which dramatically reduces the soil's ability to bear load.

PRESENSTATION 13

BRIDGE RESPONSE TO NEAR-FIELD GROUND MOTIONS

BRIDGE RESPONSE TO NEAR-FIELD GROUND MOTIONS

Genda Chen*, Ph.D., P.E., and Mostafa El-Engebawy, Ph.D.
*Associate Professor of Civil Engineering
Department of Civil, Architecture and Environmental Engineering
University of Missouri-Rolla
gchen@umr.edu

Geotechnical and Bridge Seismic Design Workshop
New Madrid Seismic Zone Experience
October 28-29, 2004

Participants

Genda Chen, Ph.D., P.E. (Team Leader)
Mostafa El-Engebawy, Ph.D.
Ronaldo Luna, Ph.D., P.E.
Richard Stephenson, Ph.D., P.E.
Wei Zheng, Ph.D. Graduate Student
Wenxig Liu, Ph.D. Graduate Student

NATURAL HAZARDS MITIGATION INSTITUTE

UMR UNIVERSITY OF MISSOURI-ROLLA

Outline of Presentation

- Objectives
- Description of Bridge Systems
- Foundation Model and Bridge Model
- Dynamic Characteristics of Selected Bridges
- Discussion of Results
  - Influence of Rupture Directivity
  - Influence of Vertical Acceleration
  - Influence of Liquefaction
  - Comparison with Far-Field Ground Motions
- Concluding Remarks
- Recommendations for including Near-Field Effects in Highway Bridge Design

NATURAL HAZARDS MITIGATION INSTITUTE

UMR UNIVERSITY OF MISSOURI-ROLLA

Objectives

- To evaluate the response of a multi-span simply supported bridge (L472) and a multi-span continuous bridge (A1466) to near-field ground motions from future earthquake scenarios in the NMSZ
- To compare the bridge response subjected to near-field ground motions simulated using the composite-source model with that of far-field motions of the point-source model
- To recommend a simple method for including near-field effects in highway bridge design

NATURAL HAZARDS MITIGATION INSTITUTE

UMR UNIVERSITY OF MISSOURI-ROLLA

Description of L472 Bridge

- Located on interstate highway I55, Pemiscot County
  - Multi-span simply supported (MSSS) bridge – 5 spans
  - Designed according to the 1949 AASHO specifications without seismic considerations
  - 57^{o} skew
  - Laterally-restrained steel plate girders
  - TYPE “C” fixed and expansion steel bearings
  - Supported by deep pile foundations

NATURAL HAZARDS MITIGATION INSTITUTE

UMR UNIVERSITY OF MISSOURI-ROLLA

Description of L472 Bridge

UMR UNIVERSITY OF MISSOURI-ROLLA

Description of L472 Bridge

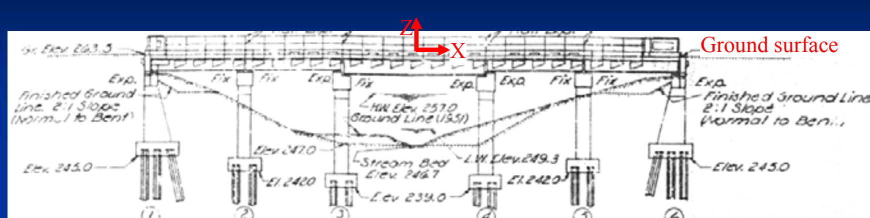

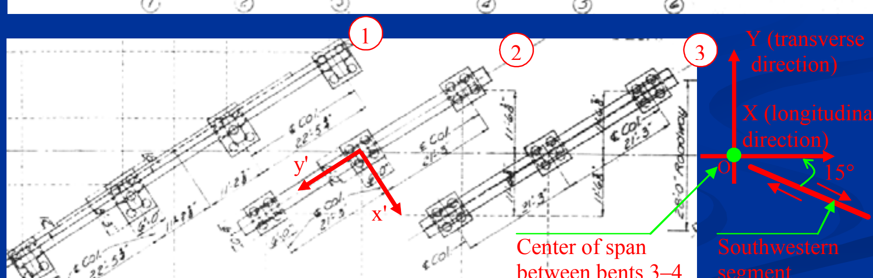

UMR UNIVERSITY OF MISSOURI-ROLLA

Description of A1466 Bridge

- Located on interstate highway I55, Pemiscot County
  - Multi-span continuous bridge – 4 spans
  - Designed according to the 1949 AASHO specifications without seismic considerations
  - 10^{o} skew
  - Laterally-restrained steel plate girders
  - TYPE "D" fixed and expansion steel bearings
  - Supported by deep pile foundations

NATURAL HAZARDS MITIGATION INSTITUTE

UMR UNIVERSITY OF MISSOURI-ROLLA

Description of A1466 Bridge

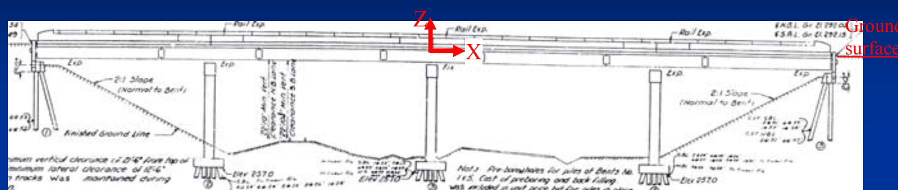

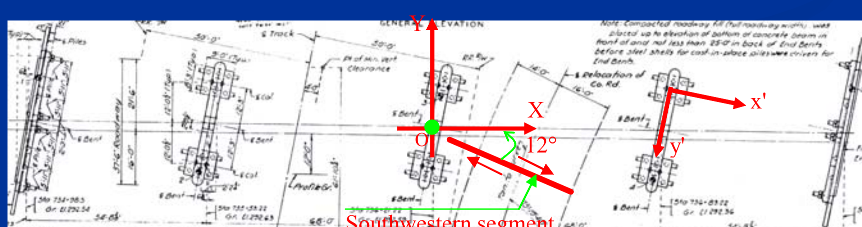

NATURAL HAZARDS MITIGATION INSTITUTE

UMR UNIVERSITY OF MISSOURI-ROLLA

Foundation Model

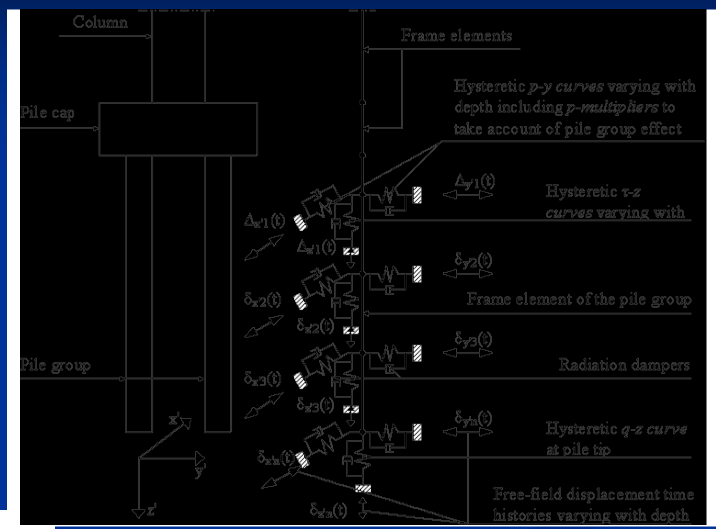

NATURAL HAZARDS MITIGATION INSTITUTE

UMR UNIVERSITY OF MISSOURI-ROLLA

Bridge Model

- Initial stiffness of all RC elements to account for concrete cracking, confinement, reinforcement yielding, and expected level of axial forces
- Nonlinear elements to account for:
  - *Plastic zones at the top and bottom of columns*
  - *TYPE "C" and "D" expansion bearings*
  - *Pounding*

NATURAL HAZARDS MITIGATION INSTITUTE

UMR UNIVERSITY OF MISSOURI-ROLLA

Bridge Model

Stress-Strain Relations

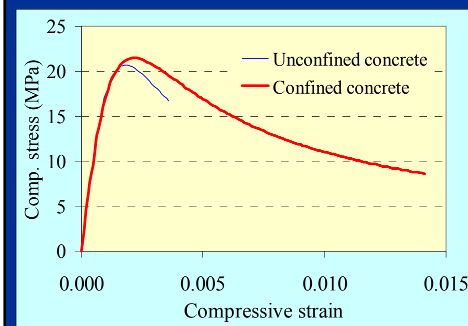

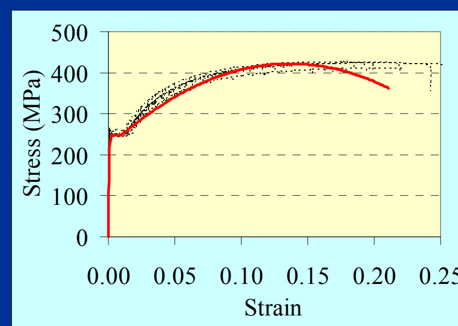

Bridge Model

Moment-Curvature Analysis

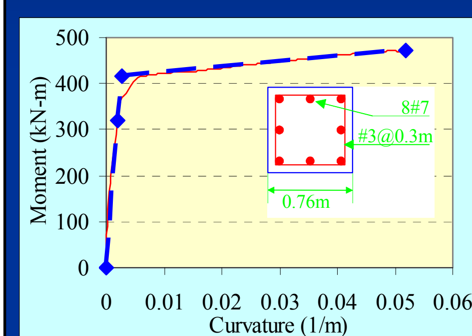

L472 Bridge Columns

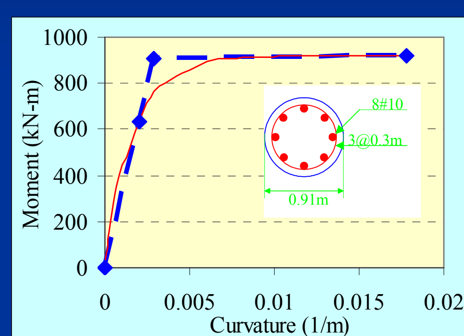

A1466 Bridge Columns

Dynamic Characteristics

L472 Bridge – Fundamental mode of vibration

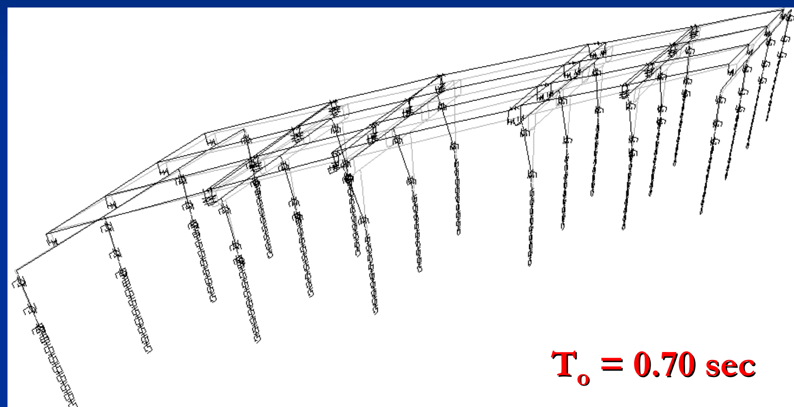

NATURAL HAZARDS MITIGATION INSTITUTE

UMR UNIVERSITY OF MISSOURI-ROLLA

Dynamic Characteristics

L472 Bridge – Second mode of vibration

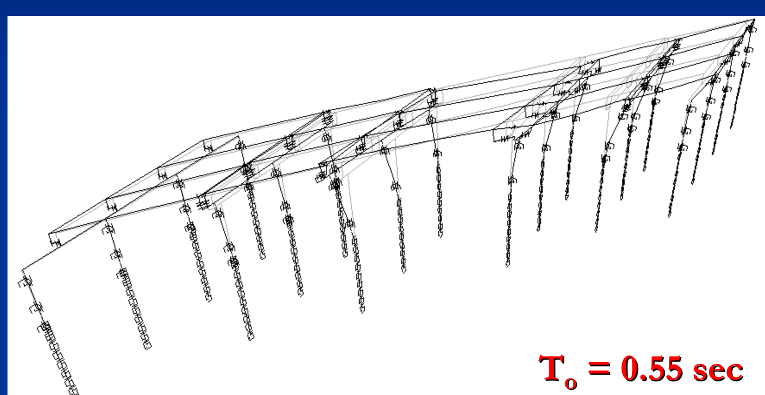

NATURAL HAZARDS MITIGATION INSTITUTE

UMR UNIVERSITY OF MISSOURI-ROLLA

Dynamic Characteristics

A1466 Bridge – Fundamental mode of vibration

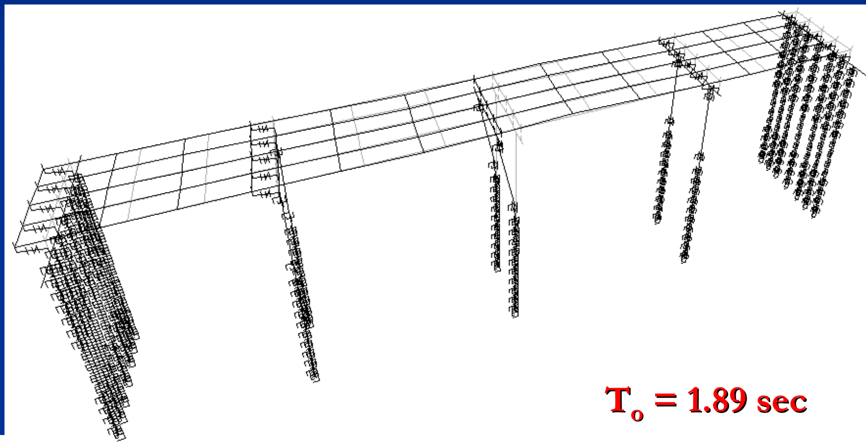

T_o = 1.89 sec

Dynamic Characteristics

A1466 Bridge – Second mode of vibration

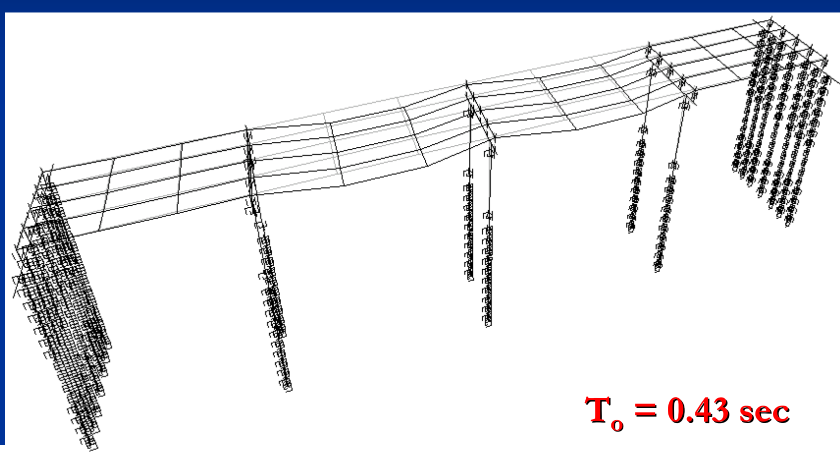

T_o = 0.43 sec

Discussion of Results

Influence of Rupture Directivity (L472)

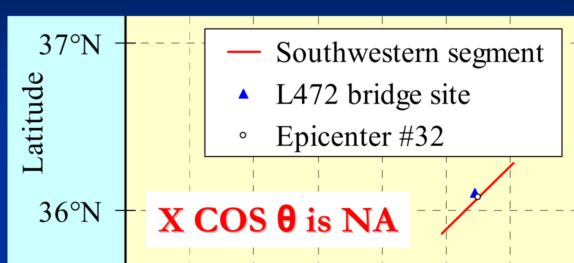

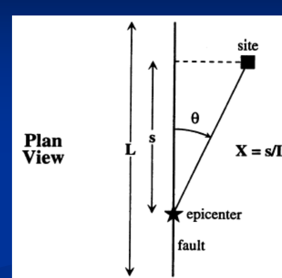

M_W 7.0

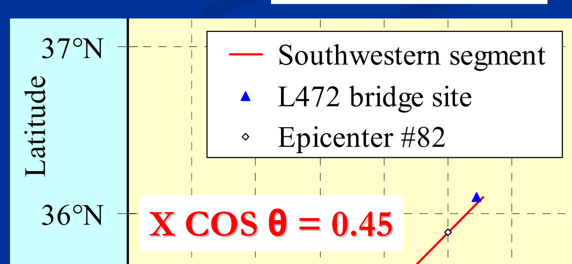

Influence of Rupture Directivity (L472)

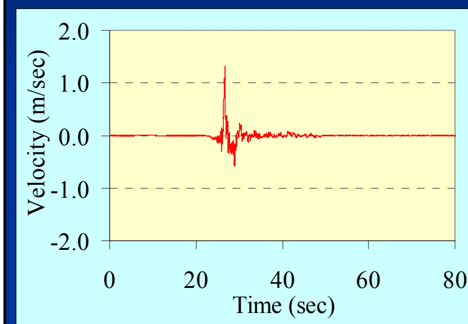

Sim #82 – FN rock motion with velocity pulses

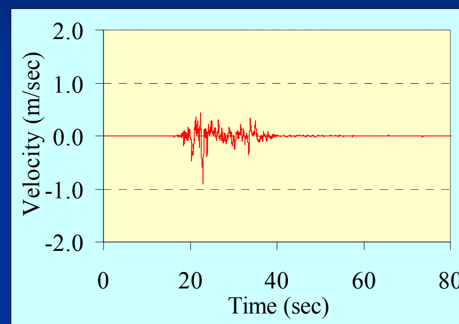

Sim #32 – FN rock motion without velocity pulses

Influence of Rupture Directivity (L472)

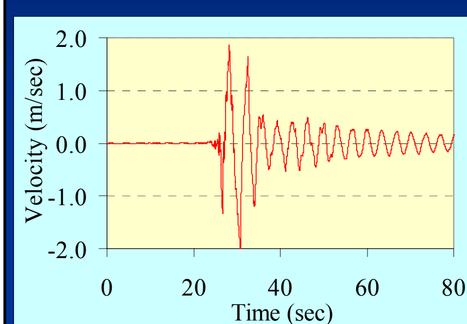

Sim #82 – FN ground motion with velocity pulses

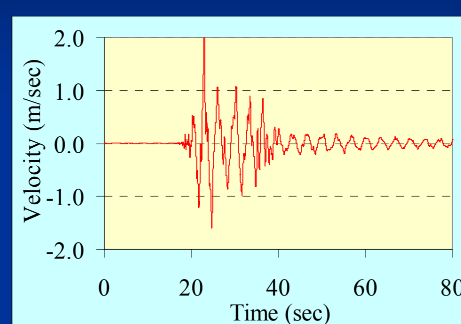

Sim #32 – FN ground motion without velocity pulses

Influence of Rupture Directivity (L472)

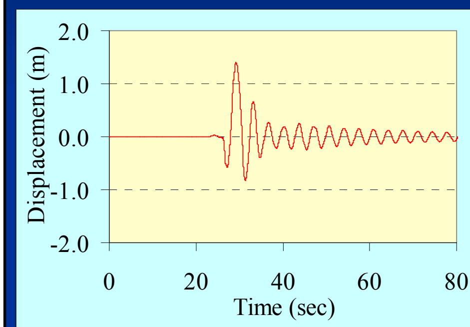

Sim #82 – FN ground motion with displacement pulses

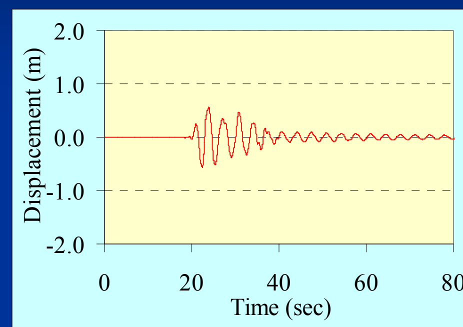

Sim #32 – FN ground motion without displacement pulses

Influence of Rupture Directivity (L472)

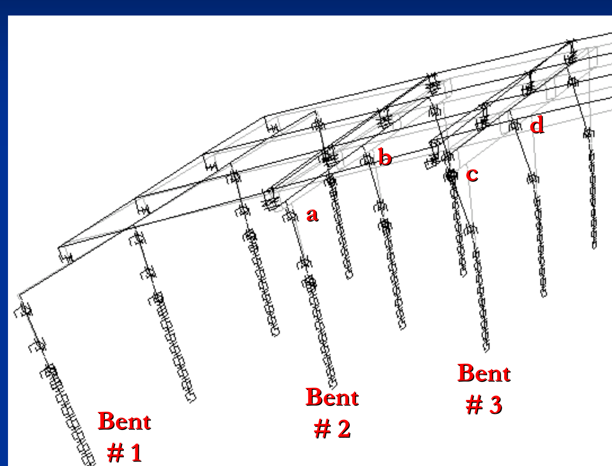

Location	Sim #32	Sim #82
a	1.7	2.3
b	2.3	2.8
c	2.5	2.7
d	3.1	3.2

In-plane curvature ductility

M_W 7.0

Influence of Vertical Acceleration (L472)

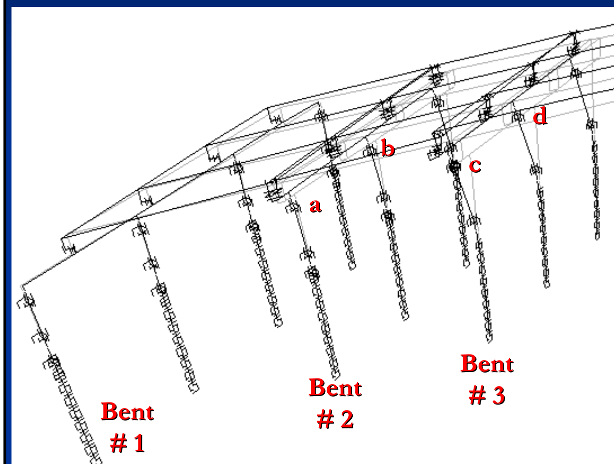

Location	with V	without V
a	-1386	-1006
b	-1679	-796
c	-1741	-1279
d	-1662	-897

Compressive force

M_W 7.5

NATURAL HAZARDS MITIGATION INSTITUTE

UMR UNIVERSITY OF MISSOURI-ROLLA

Influence of Vertical Acceleration (L472)

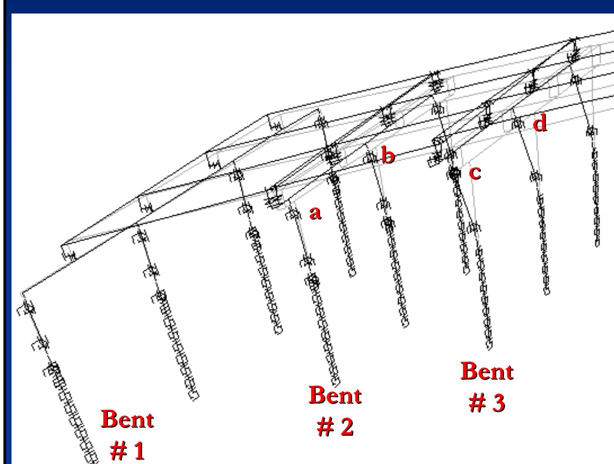

Location	with V	without V
a	4.2	5.3
b	5.6	6.5
c	6.7	8.1
d	8.1	9.4

In-plane curvature ductility

M_W 7.5

NATURAL HAZARDS MITIGATION INSTITUTE

UMR UNIVERSITY OF MISSOURI-ROLLA

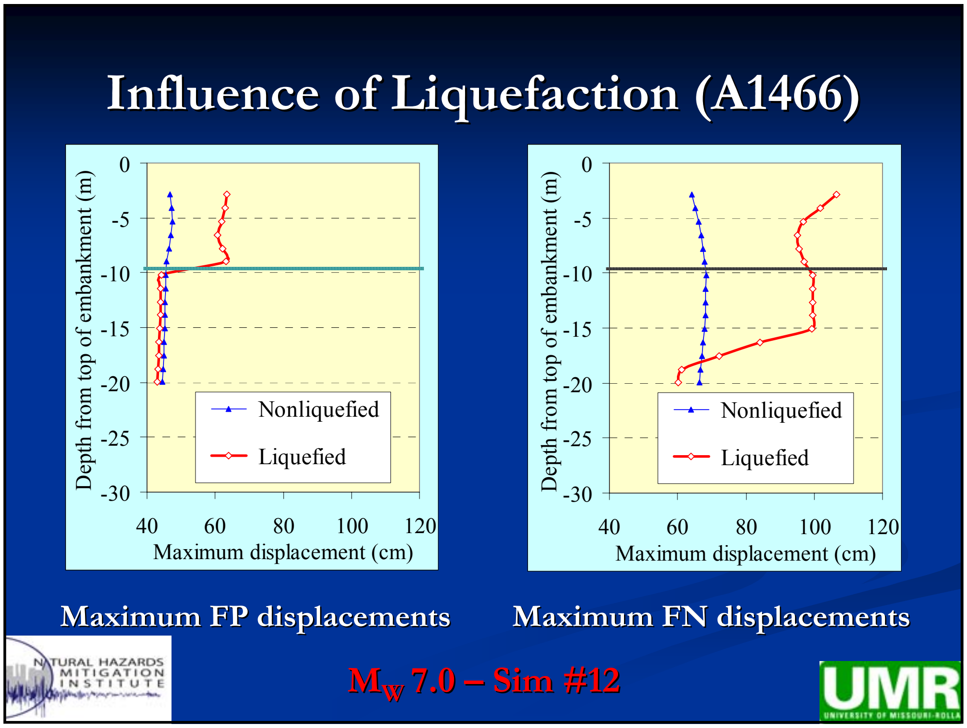
Influence of Liquefaction (A1466)
Depth from top of embankment (m)
0
-5
-10
-15
-20
-25
-30
Nonliquefied
Liquefied
40
60
80
100
120
Maximum displacement (cm)
Maximum FP displacements
Maximum FN displacements
NATURAL HAZARDS MITIGATION INSTITUTE
M_W 7.0 – Sim #12
UMR
UNIVERSITY OF MISSOURI-ROLLA

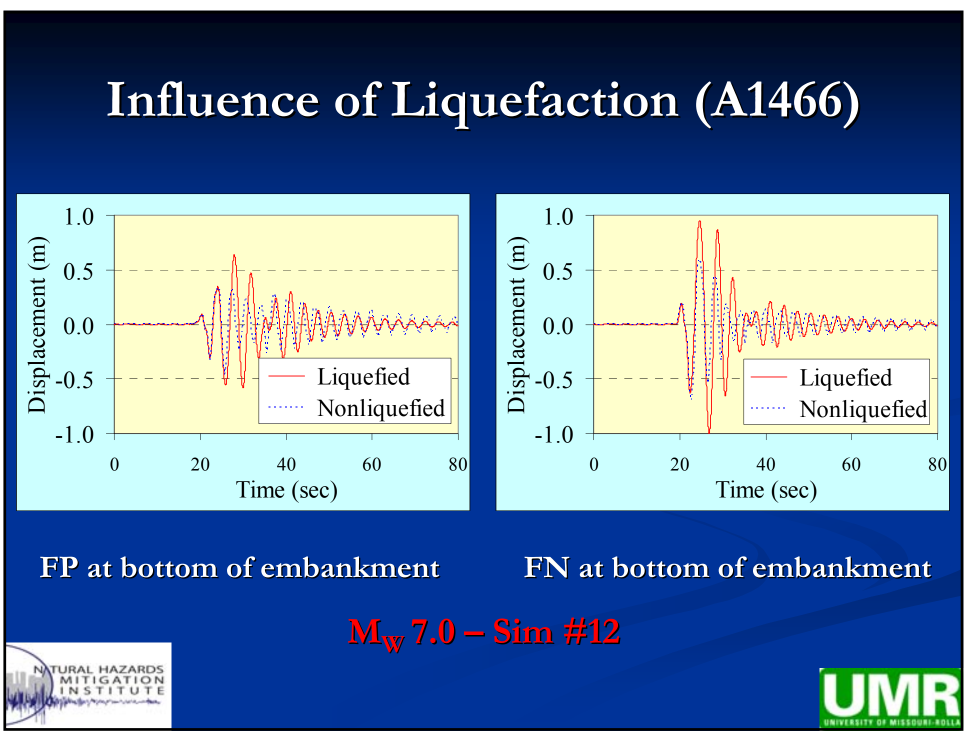
Influence of Liquefaction (A1466)
Displacement (m)
1.0
0.5
0.0
-0.5
-1.0
Liquefied
Nonliquefied
0
20
40
60
80
Time (sec)
FP at bottom of embankment
FN at bottom of embankment
M_W 7.0 – Sim #12
NATURAL HAZARDS MITIGATION INSTITUTE
UMR
UNIVERSITY OF MISSOURI-ROLLA

Influence of Liquefaction (A1466)

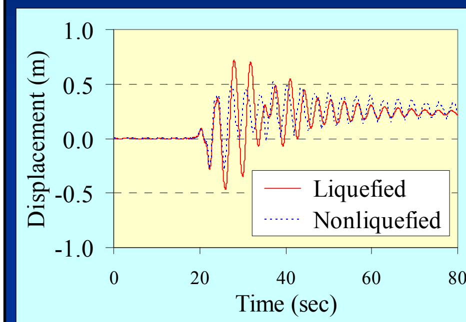

FP at top of embankment

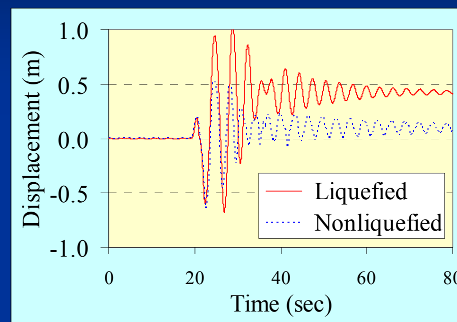

FN at top of embankment

M_W 7.0 – Sim #12

Influence of Liquefaction (A1466)

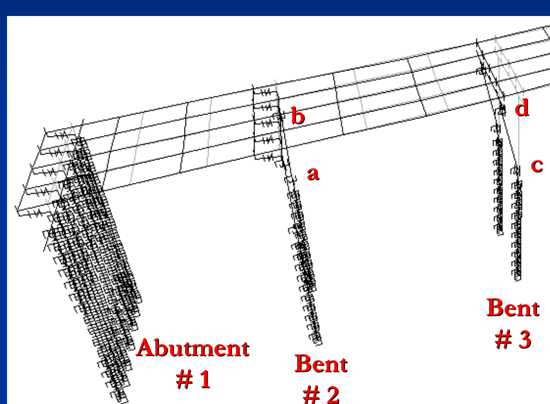

Location	with LIQ	without LIQ
a	31.6	6.3
b	20.2	6.1
c	31.0	6.4
d	18.9	6.3

In-plane
curvature ductility

M_W 7.0 – Sim #12

Comparison with Far-Field Motions

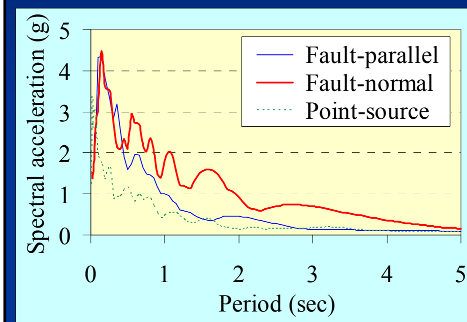

Rock motions

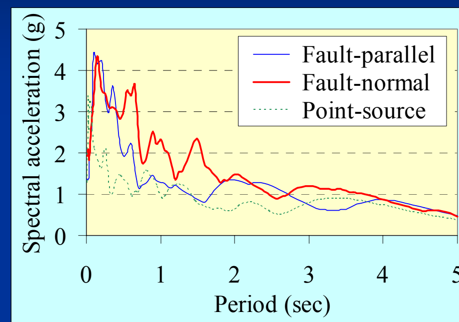

Ground motions

M_W 7.5 – L472

Comparison with Far-Field Motions

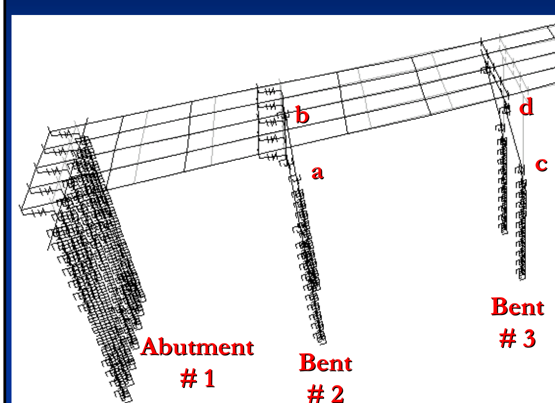

Location	Composite-source	Point-source
a	4.4	1.6
b	5.2	1.9
c	5.9	1.8
d	6.7	2.3

In-plane curvature ductility

Motions applied along the longitudinal axis of the bridge

M_W 7.5 – L472

Comparison with Far-Field Motions

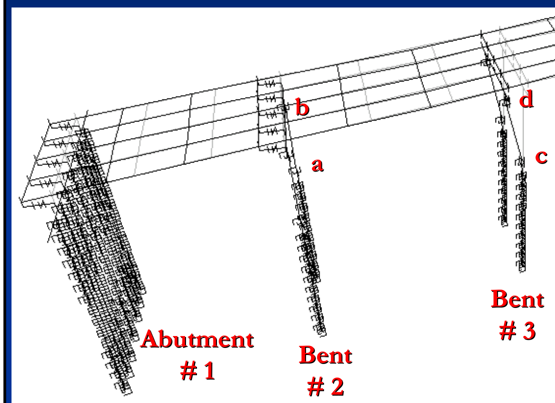

Location	Composite-source	Point-source
a	2.7	1.0
b	3.2	1.1
c	4.0	1.1
d	4.5	1.3

In-plane curvature ductility

Motions applied along the transverse axis of the bridge

NATURAL HAZARDS MITIGATION INSTITUTE

M_W 7.5 – L472

UMR UNIVERSITY OF MISSOURI-ROLLA

Recommendations for including Near-Field Effects in Highway Bridge Design

Based on Abrahamson's model (2000) and Somerville et al. (1997)

NATURAL HAZARDS MITIGATION INSTITUTE

UMR UNIVERSITY OF MISSOURI-ROLLA

Directivity model

STEP I

Scale factor for the average horizontal component AvH
(after Abrahamson, 2000)

$\ln[Dir(X, \theta, T)] = C1(T) + 1.88\, C2(T)\, XCos\theta \qquad XCos\theta \le 0.4$

$\ln[Dir(X, \theta, T)] = C1(T) + 0.75\, C2(T) \qquad XCos\theta > 0.4$

STEP II

Difference between FN and FP components of motion
(after Somerville et al., 1997)

$\ln(FN/AvH) = Cos(2\theta)\, [C3(T) + C4(T)\, \ln(r_{rup}+1) + C5(M_W-6)] \qquad \theta < 45°$

$\ln(FN/AvH) = 0 \qquad \theta \ge 45°$

$\ln(FP/AvH) = -\ln(FN/AvH)$

Upper bound of Directivity Conditions

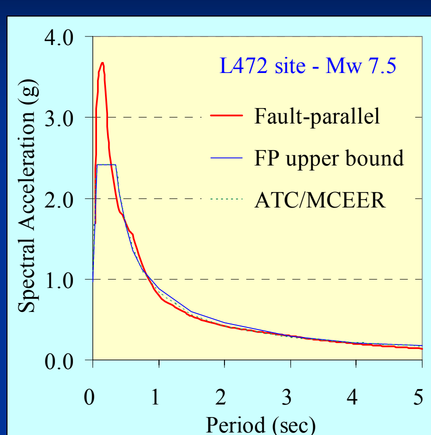

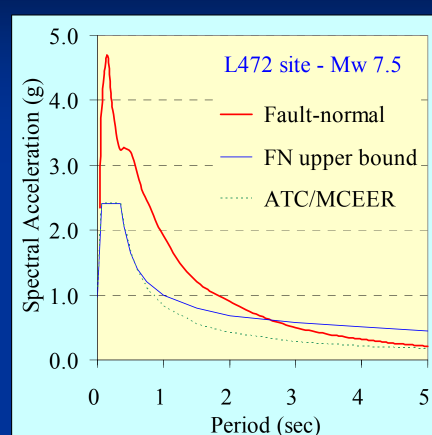

Assuming XCosθ=0.40 then θ=4.4° for L472 bridge (3.7 km from fault)

Upper bound of Directivity Conditions

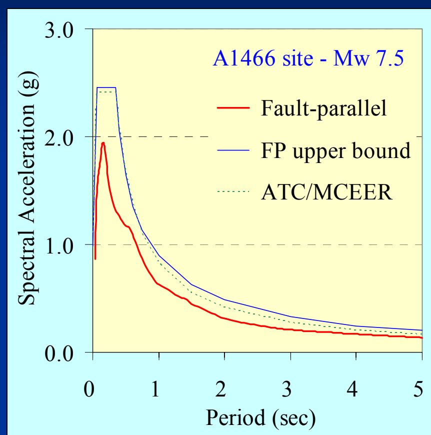

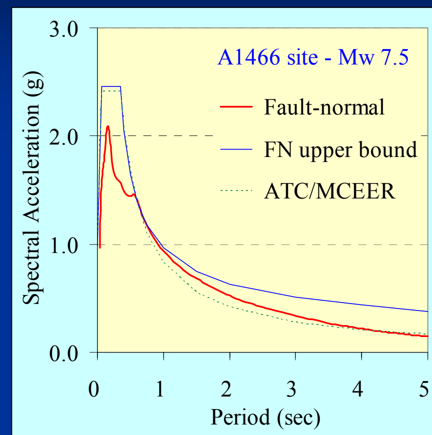

Assuming XCosθ=0.40 then θ=12.5° for A1466 bridge (10.9 km from fault)

NATURAL HAZARDS MITIGATION INSTITUTE

UMR UNIVERSITY OF MISSOURI-ROLLA

Average Directivity Conditions

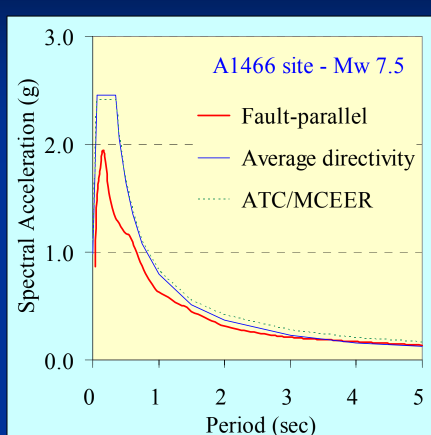

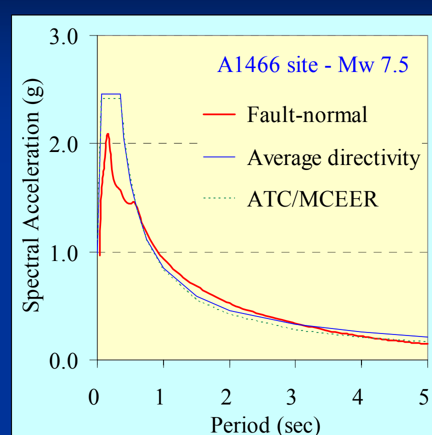

Assuming the epicenter at the middle of the fault then XCosθ=0.24 and θ=19.5° for A1466 bridge (10.9 km from fault)

NATURAL HAZARDS MITIGATION INSTITUTE

UMR UNIVERSITY OF MISSOURI-ROLLA

Concluding Remarks

- The curvature ductility ratio of columns increase significantly with the moment magnitude. Forward rupture directivity and liquefaction effects are the dominant reasons for the high ratios
- The vertical acceleration increases the compressive forces in the columns under the maximum considered earthquake. They are remarkably reduced with lower moment magnitudes
- Liquefaction yields large displacements in the fault-normal direction and permanent offset of the soil near the top of the embankment that develop extreme large deformations in the plane of the bridge bents leading to large in-plane curvature ductility ratios of the columns

NATURAL HAZARDS MITIGATION INSTITUTE

UMR UNIVERSITY OF MISSOURI-ROLLA

Recommendations

- A site-specific rock and ground motion simulations are recommended for highway bridges within 10 km from active faults in the NMSZ. The resulting rock motions should include forward rupture directivity while fling step is not likely to occur in future earthquake events
- For highway bridges located beyond 10 km, a simple methodology is recommended for considering near-field effects in their design response spectra based on the average directivity conditions at the site and the directivity models of Abrahamson (2000) and Somerville et al. (1997)

NATURAL HAZARDS MITIGATION INSTITUTE

UMR UNIVERSITY OF MISSOURI-ROLLA

PRESENTATION 14

SEISMIC EVALUATION AND RETROFIT OF BEAM-COLUMN JOINTS OF MID-AMERICA BRIDGES

Seismic Evaluation and Retrofit of Beam-Column Joints of Mid-American Bridges Part 1: Fiber Reinforced Polymer Retrofit

Pedro F. Silva, Ph.D., P.E.
Genda Chen, Ph.D., P.E.
University of Missouri-Rolla (UMR)
gchen@umr.edu

Geotechnical and Bridge Seismic Design Workshop
New Madrid Seismic Zone Experience

October 28-29, 2004, Cape Girardeau, Missouri

Participants

Pedro F. Silva, Ph.D., P.E.
Genda Chen, Ph.D., P.E.
Nick Ereckson, M.S. Graduate Student

Research Objectives

Develop a Comprehensive Research Program to Establish the Seismic Retrofit of a Beam/Column Joint According to Modern Seismic Design Principles Using CFRP Systems

- **Plastic hinges to form at the ends of the columns**
- **Beams protected against any significant flexural or shear inelastic actions**
- **Beam/column joints retrofitted in order to minimize inelastic rotations in the beam/column joint regions**

Current Design Deficiencies

Plastic Hinges Can Form Either in the Beams or Joints under Moderate Seismic Events

- ***Excessive*** - **Column flexural reinforcement**
- ***Inadequate*** - **Column shear reinforcement**
- ***Inadequate*** - **Beam shear reinforcement**
- ***Inadequate*** - **Beam flexural reinforcement**
- ***Inadequate*** - **Joint shear reinforcement**

Evaluation of Bridge Structures

- A) Column
  - A-1) Ductile Flexural Response
  - A-2) Brittle Shear Response
  - A-3) Confinement of Plastic Hinge
  - A-4) Buckling of Longitudinal Reinforcement
- B) Bent Cap
  - B-1) Ductile Flexural Response
  - B-2) Brittle Shear Response
- C) Bent/Cap Joint
  - C-1) Brittle Crushing of Diagonal Compression Strut
  - C-2) Brittle Joint Shear Failure with Reinforcement Pullout

Performance Levels for a Typical Bent Cap/Column-bent Connection

Evaluation of Bridge Structures

Bridge #	Year Built	Main Span Length	Girder Type	No. of Bents	No. of Columns/Bent
(#)	(Year)	(feet)	(type)	(#)	(#)
A-1466	1966	68	Steel Continuous	5	2
A-1931	1969	52	Steel Continuous	4	2
A-1938	1969	95	Steel Continuous	5	3
A-2024	1970	112	Steel Continuous	5	3
A-2332	1968	65	Steel Continuous	6	2
A-2333	1968	72	Steel Continuous	6	2
A-2334	1968	70	Steel Continuous	8	2
A-2336	1968	65	Steel Continuous	6	2
A-2427	1968	93	Steel Continuous	5	3
A-2429	1968	90	Steel Continuous	5	4
A-2430	1971	113.75	Steel Continuous	4	3
A-3478	1976	75	Steel Continuous	4	4
A-2428	1968	87	Steel Continuous	5	3

NATURAL HAZARDS MITIGATION INSTITUTE

UMR UNIVERSITY OF MISSOURI-ROLLA

Evaluation of Bridge Structures

Bridge #	Bent Cap		Column
	Flexural Failure	Joint Shear Failure	Column Shear
(#)	(PASS/ FAIL)	(PASS/ FAIL)	(PASS/ FAIL)
A-1466	FAIL	PASS	PASS
A-1931	PASS	MARGINAL	PASS
A-1938	PASS	MARGINAL	PASS
A-2024	PASS	MARGINAL	FAIL
A-2332	PASS	FAIL	MARGINAL
A-2333	PASS	MARGINAL	MARGINAL
A-2334	PASS	MARGINAL	MARGINAL
A-2336	PASS	FAIL	MARGINAL
A-2427	FAIL	PASS	PASS
A-2429	PASS	FAIL	PASS
A-2430	PASS	FAIL	PASS
A-3478	FAIL	FAIL	MARGINAL
A-2428	FAIL	FAIL	FAIL

UNIVERSITY OF MISSOURI-ROLLA

Test Matrix

Design of Two Test Units for Evaluation of Retrofit of Beam/Column Systems Using Carbon-FPP Composites

- **Unit 1 – Incremental retrofit at different performance levels**
- **Unit 2 – Complete retrofit before testing**

Prototype Structure

Longitudinal Section

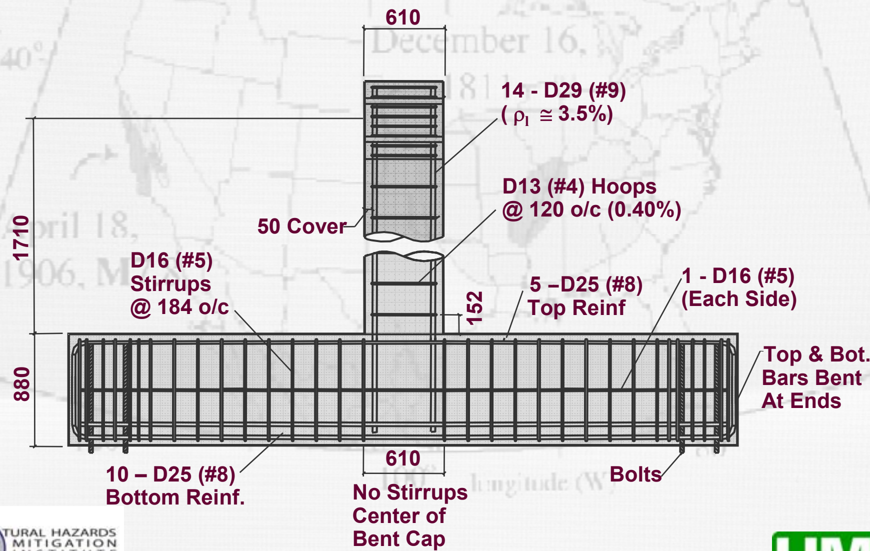

Beam & Column X-Sections

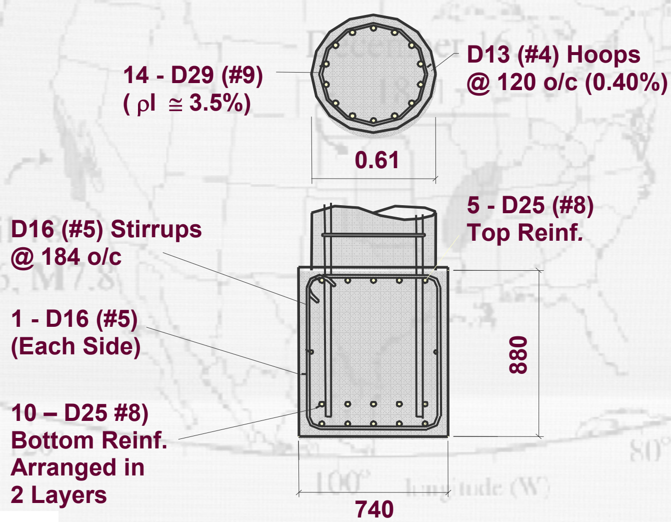


NATURAL HAZARDS
MITIGATION
INSTITUTE
UMR
UNIVERSITY OF MISSOURI-ROLLA

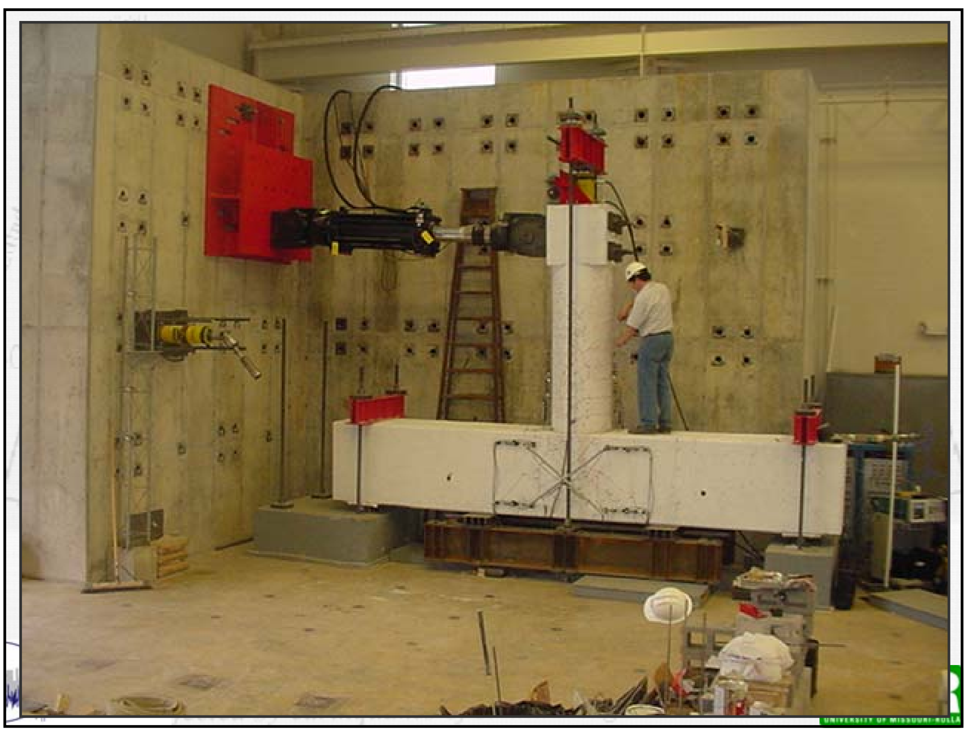

Demand Evaluation

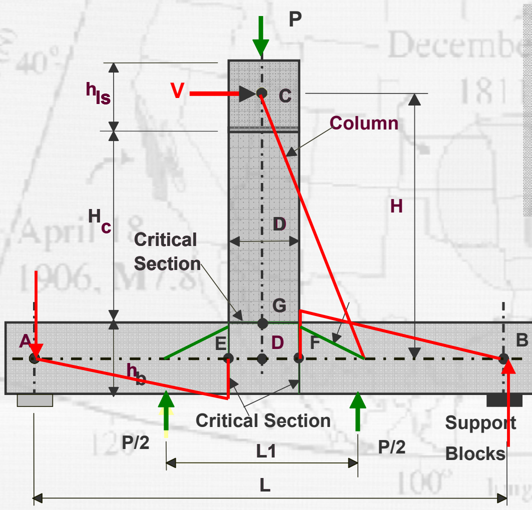

$$M_B^{cr} = \begin{cases} \dfrac{M_C^o}{2}\cdot\dfrac{H}{L}\dfrac{(L-D)}{\left(H-\frac{h_b}{2}\right)} + \\ \dfrac{P\cdot(L_1-D)}{4} \end{cases}$$

$$V_B^{cr} = \begin{cases} \dfrac{M_C^o}{L}\left(\dfrac{H}{H-\frac{h_b}{2}}\right) + \\ \dfrac{P}{2} \end{cases}$$

Material Properties

Concrete

		28 Day Strength	Strength at Time of Testing
		(psi)	(psi)
Specimen #1	Beam	5026	5342
	Column	3525	3697
Specimen #2	Beam	4216	4609
	Column	4993	5419

Steel Rebar

Bar #	Yield Strength (ksi)
4	87
5	60
8	80
9	78

Column Shear Capacity Evaluation

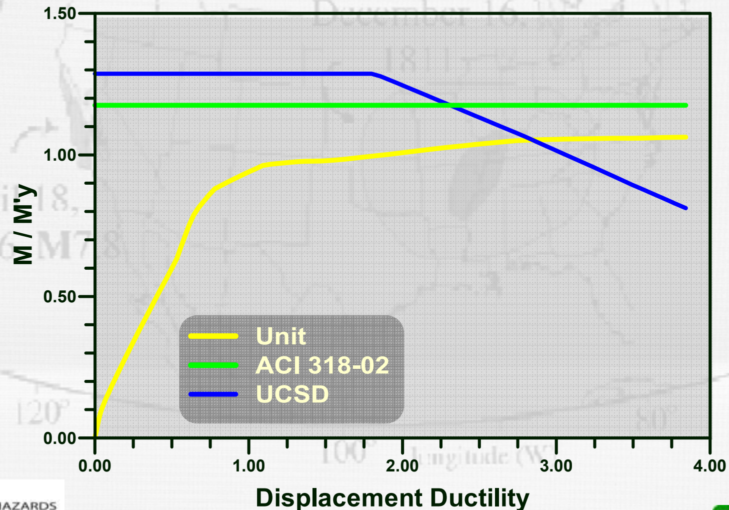

Beam Shear Capacity Evaluation

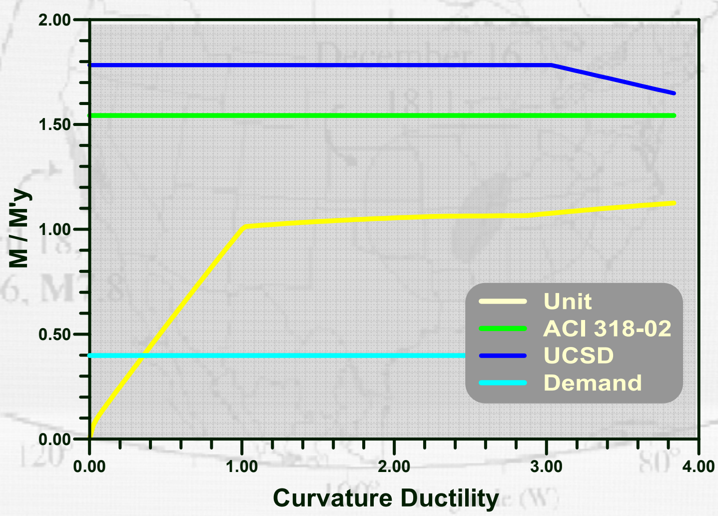

Negative Moment

Beam Shear Capacity Evaluation

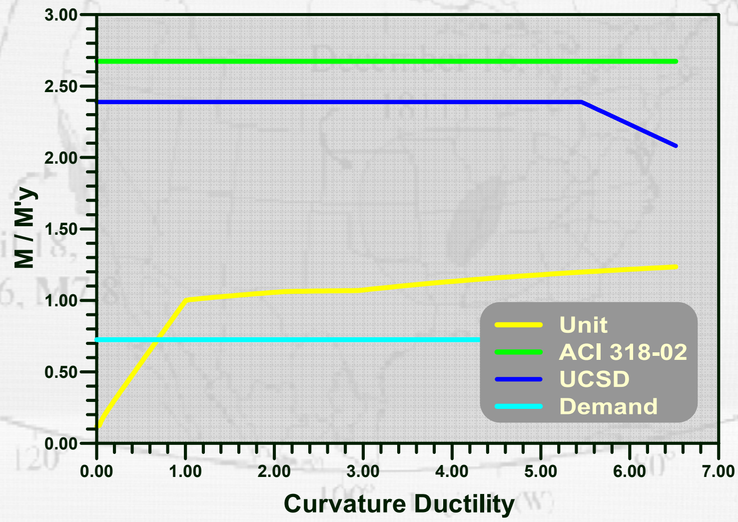

Positive Moment

Joint Principle Stresses Evaluation

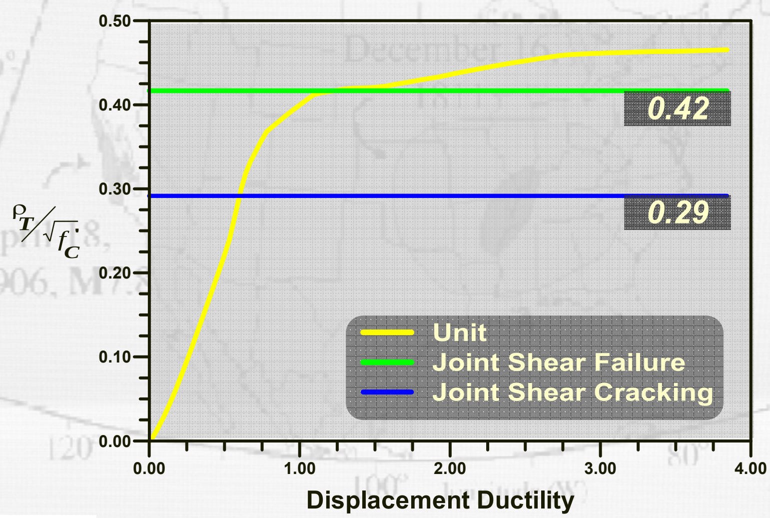

Principal Tensile Stresses

Predicted Seismic Response Un-strengthened System

1 Column shear failure at μ_Δ < 3 or onset of column cover concrete spalling
2 Onset joint shear failure at μ_Δ > 2

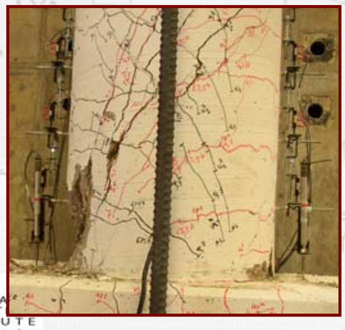

Column Retrofit

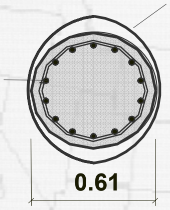

Shear (2 Plies)

$$t_j = \frac{V^\circ/\varphi_S - (V_C + V_S + V_P)}{0.5\,\pi\, f_{uj}\, D \cot\theta}$$

Confinement (9 Plies)

$$t_j = \frac{0.10\,(\varepsilon_{Cu} - 0.004)}{\varepsilon_{uj} f_{uj}} D\, f'_{CC}$$

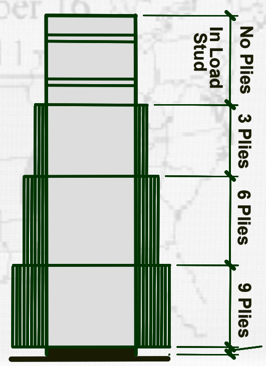

Retrofit Design Target μ_Δ=12.0

Column Retrofit Evaluation

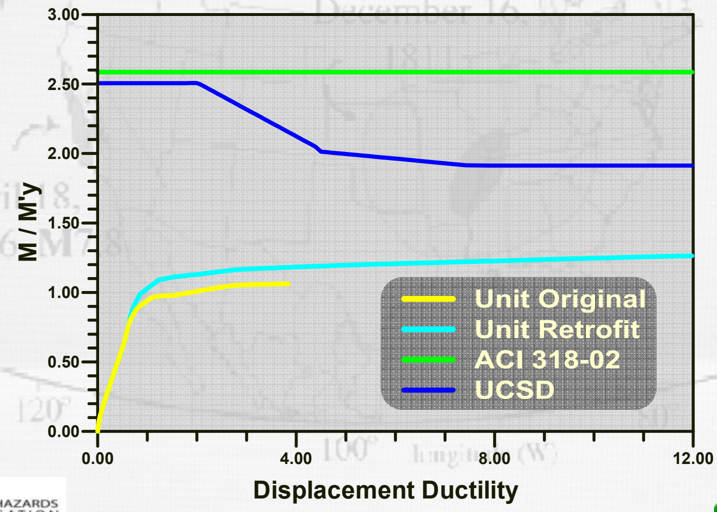

Material Properties

Carbon Fiber Reinforced Polymer (CFRP)

	Specimen # 1 and 2
Ultimate Tensile Strength	550 ksi
Ultimate Rupture Strain	1.67%
Tensile Modulus	33,000 ksi
Fabric Width	24 in.
Nominal Thickness	0.0065 in/ply

Column

Retrofit

Joint Retrofit

$$F_{CFRP} = \sqrt{(F_H)^2 + (F_V)^2}$$

$$F_H = T_C\left(\frac{0.7D - 0.5c_U}{0.5h_b}\right)$$

$$F_V = T_B\left(\frac{D - 0.5c_U}{0.5D}\right)$$

Joint Retrofit (3 Plies)

$$n_j t_j = \frac{F_{CFRP}}{2}\frac{1}{w_j f_{uj}}$$

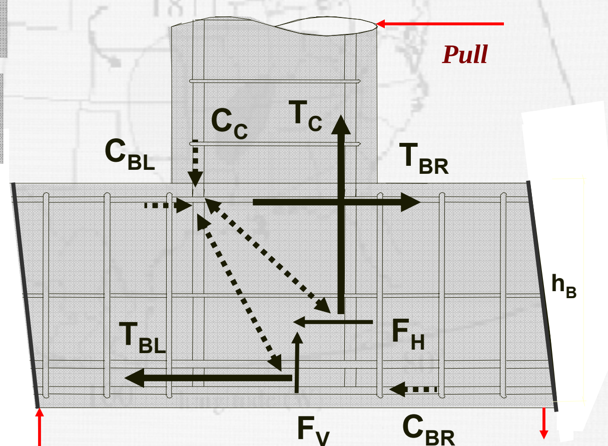

Joint Retrofit

Unit 2 – Retrofit Specimen

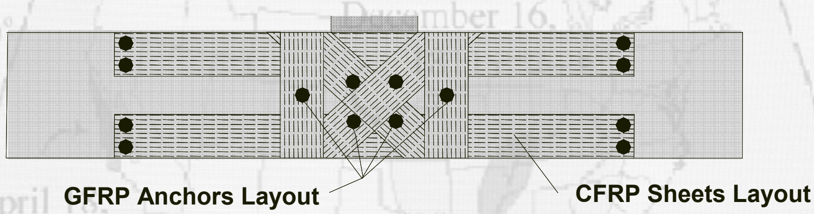

Experimental Results

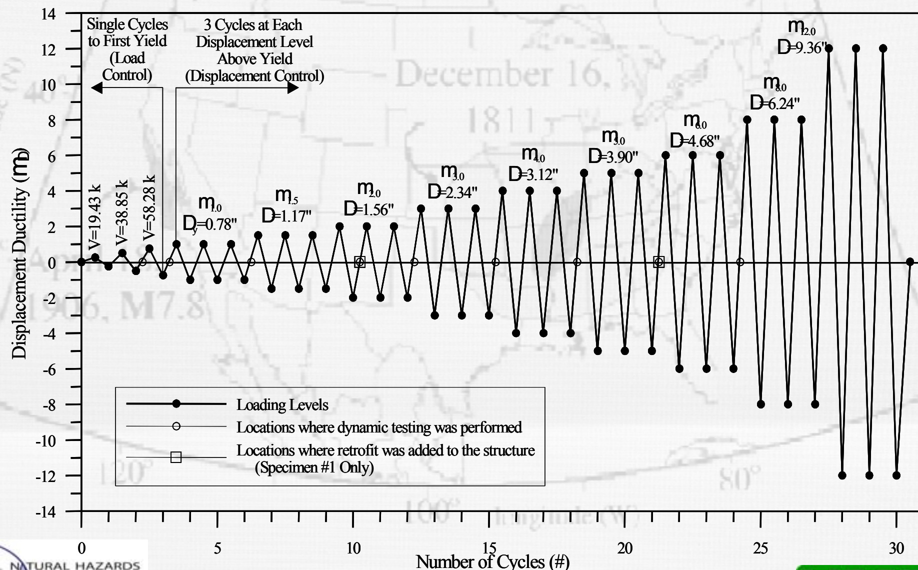

Unit 2: Experimental Results

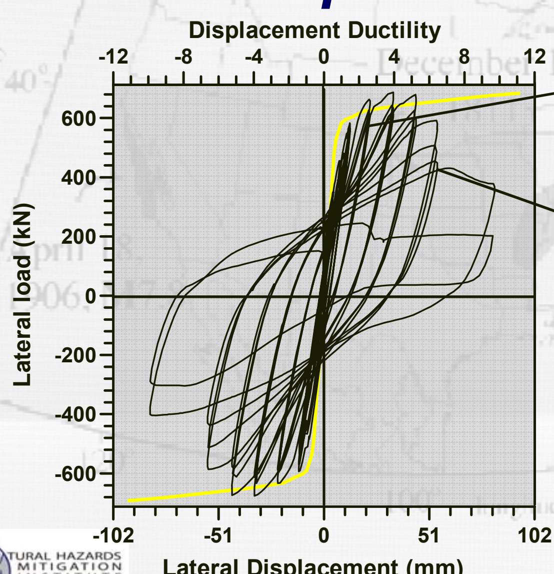

Occupational
MCE Reliable:
μ_{Δ}= 2
F_U=530kN

Life Safety
MCE Reliable:
μ_{Δ}= 6
F_U = 400kN

Unit 2: Experimental Results

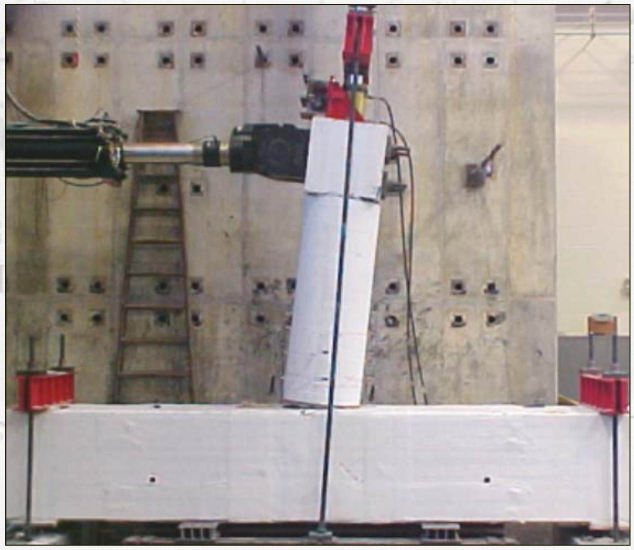

Unit 2 - Conclusions

- Column shear capacity was enhanced by applying CFRP sheets in the hoop direction
- Strengthening of the joint region was adequate in preventing joint shear failure
- Some level of strength degradation was observed in the joint region
- Main failure mode was characterized by fracture of the column long. reinforcement

Elastic Shear Forces

Distance From NMSZ (km)	SA %g	VE (kN)
1.60	2.99	2130
16.0	1.39	1000
160	0.91	650

Natural Period

$W = 710\text{kN}$

$F_Y = 320\text{kN}$

$\Delta_Y = 10.2\text{mm}$

$T_N = 0.31\text{sec.}$

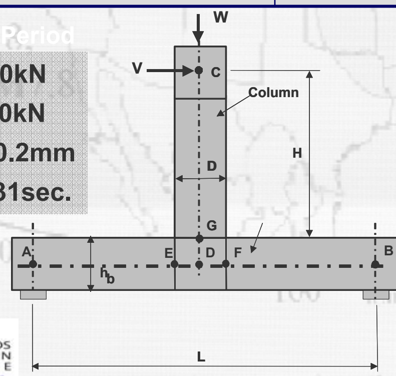

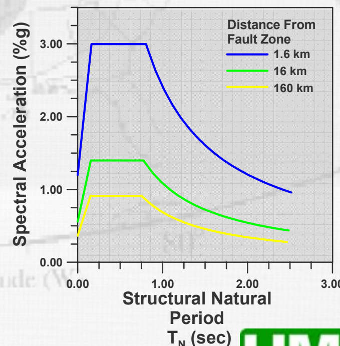

New Madrid Seismic Zone

Seismic Demand

Distance From NMSZ (km)	Performance Objective	R	Demand (kips)	System Capacity (kips)
1.6	Life Safety	2.55	832	400
	Operational	1.31	1623	535
16	Life Safety	2.61	378	400
	Operational	1.32	752	535
160	Life Safety	2.66	240	400
	Operational	1.33	485	535

Life Safety MCE Reliable:
$\mu_\Delta = 6$
$F_U = 400\text{kN}$

Occupational MCE Reliable:
$\mu_\Delta = 2$
$F_U = 530\text{kN}$

Response Modification Factor

$$R = 1 + (\mu_\Delta - 1)\frac{T}{1.25\,T_s}$$

Seismic Evaluation Conclusions

- ♦ **Column shear capacity was enhanced by applying CFRP sheets in the hoop direction**

  Adequate for any Seismic Level Hazard

- ♦ ***S*trengthening of the joint region was adequate in preventing joint shear failure**

  Life Safety: 16km from the NMSZ fault

  Operational: 160km from the NMSZ fault

Seismic Evaluation and Retrofit of Beam-Column Joints of Mid-America Bridges Part 2: Steel Sheet and Plate Retrofit

Genda Chen, Ph.D., P.E.
Associate Professor of Civil Engineering
Department of Civil, Architectural, and Environmental Engineering
University of Missouri-Rolla (UMR)
gchen@umr.edu

Geotechnical and Bridge Seismic Design Workshop
New Madrid Seismic Zone Experience

Cape Girardeau, MO, October 28-29, 2004

NATURAL HAZARDS MITIGATION INSTITUTE

UMR
UNIVERSITY OF MISSOURI-ROLLA

Participants

- Genda Chen, Ph.D., P.E. (team leader)
- Xiaofei Ying, Ph.D. graduate student
- Xi Huang, Ph.D. graduate student
- Pedro Silva, Ph.D., P.E.
- Roger LaBoube, Ph.D., P.E.

NATURAL HAZARDS MITIGATION INSTITUTE

UMR
UNIVERSITY OF MISSOURI-ROLLA

Background

- Both steel and FRP jacketing techniques are available for the seismic retrofitting of RC columns.
- Steel jacketing is ductile and durable. Engineers are confident with the reliable materials.
- FRP jacketing is light and easy to construct in field condition. It has no issue related to steel corrosion.
- It would be desirable to combine several advantages of the two techniques: ductile, durable, light in weight, and reliable materials. Using stiffened thin steel sheets (galvanized or stainless steel) seems to meet the above requirements.

NATURAL HAZARDS MITIGATION INSTITUTE

UMR UNIVERSITY OF MISSOURI-ROLLA

Objectives

- Develop a new seismic retrofit technique with stiffened thin steel sheets for columns and steel plates for beam-column joints
- Test concrete ring specimens wrapped with thin steel sheets to understand the strength and failure modes of nailed joints
- Design the retrofit scheme for an existing bridge in southeast Missouri
- Test two 4/5-scale beam-column specimens to validate the performance of the retrofit scheme

NATURAL HAZARDS MITIGATION INSTITUTE

UMR UNIVERSITY OF MISSOURI-ROLLA

New Retrofit Scheme

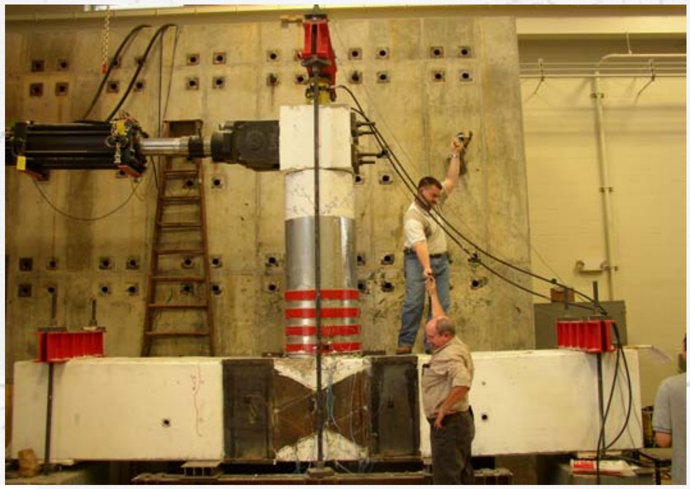

Nailed Joint Failure Modes

Specimens

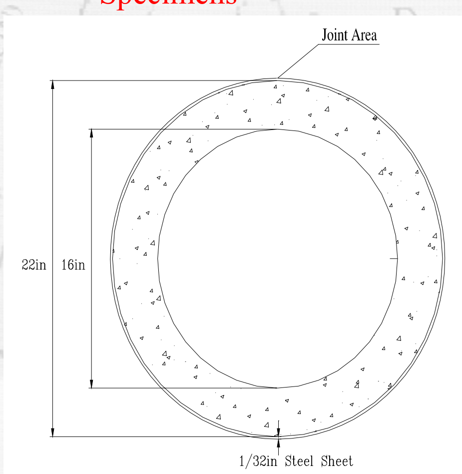

Top View

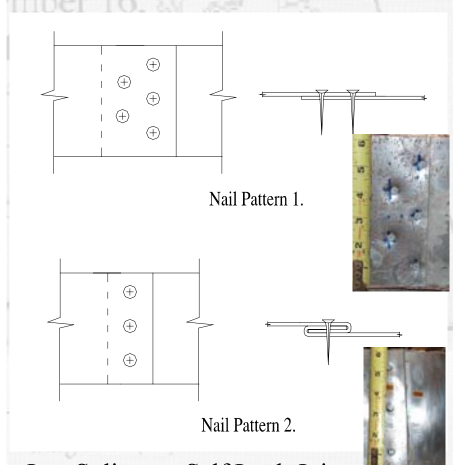

Lap Splice vs. Self Lock Joint

Nailed Joint Failure Modes

Test Setup

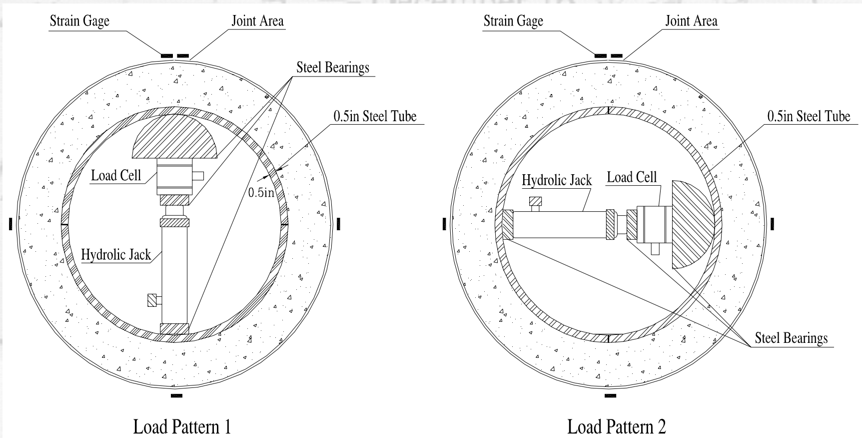

NATURAL HAZARDS MITIGATION INSTITUTE

UMR UNIVERSITY OF MISSOURI-ROLLA

Nailed Joint Failure Modes

Test Results (12 Specimens)

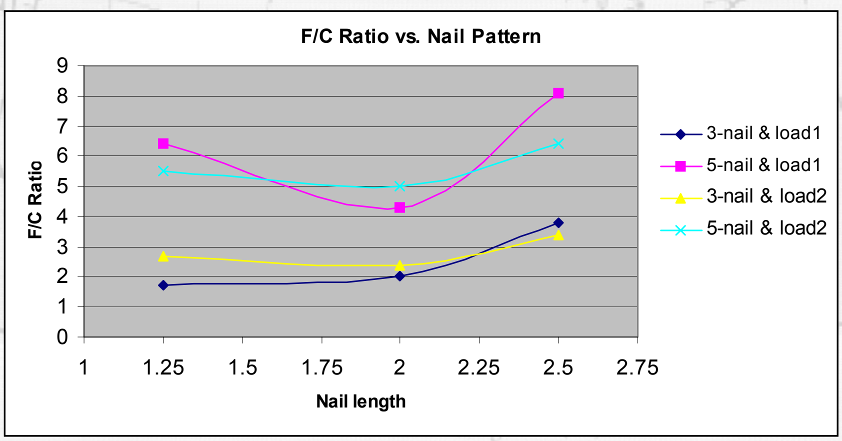

NATURAL HAZARDS MITIGATION INSTITUTE

UMR UNIVERSITY OF MISSOURI-ROLLA

Nailed Joint Failure Modes

Failure Modes and Summary

Lap splice joint   Self lock joint

- Self lock joints (3-nail pattern) always fail in pull-out of nails due to potential bending effects on the outer steel sheet while splice joints (5-nail pattern) always fail in bearing of the steel sheets.
- The ratio of failure to crack loads of the 5-nail pattern specimens are always greater than that of the 3-nail pattern specimens. Strength is proportional to the number of nails in joints.
- The strength of joints is independent of the length of nails.

Test Data of Lap Splice Joints

Rows of Nails	Number of specimens	Load at Peak (lbf)	Strain at Peak (%)	Strain at Break (%)
2	4	1990	0.39	0.59
3	4	2360	0.68	0.88
4	4	3370	1.94	2.66
5	3*	4100	3.23	3.36

* One specimen damaged before testing

Typical Load-Strain Relation

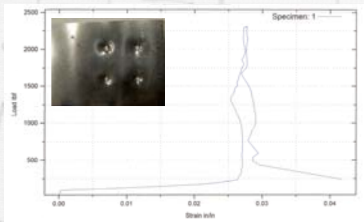
2-Nail Joint

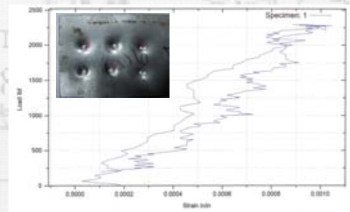
3-Nail Joint

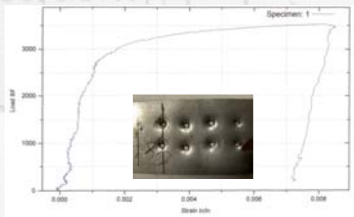
4-Nail Joint

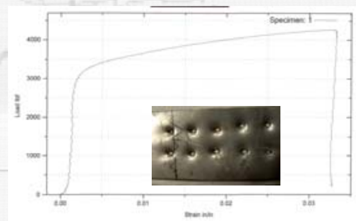
5-Nail Joint

Retrofit Goals

- Increase the ductility of the RC column
- Eliminate the potential shear failure of the column
- Increase the shear/flexural capacity of the cap beam
- Eliminate the potential shear failure and reduce the stiffness degradation at the beam-column joint

NATURAL HAZARDS MITIGATION INSTITUTE
UMR UNIVERSITY OF MISSOURI-ROLLA

Retrofit Design

Column Strengthening for Ductility

$$t_j = \frac{0.1(\varepsilon_{cu} - 0.004)Df_{cc}^{'}}{f_{uj}\varepsilon_{uj}}$$

$\varepsilon_{cu} = c\phi_u$

c -- neutral_axis_length -- 9.2in

$\phi_u = \mu_\phi \phi_y$

μ_ϕ -- objective_curvature_ductility -- 4.57

ϕ_y -- curvature_at_yield -- $0.00027in^{-1}$

D -- column_diameter -- 24in

$f_{cc}^{'}$ -- strength_of_the_confined_concrete -- 6.59ksi

f_{uj} -- ultimate_jacket_stress -- 50ksi

Retrofit Design

Column Strengthening for Shear

$$t_j \geq \frac{\frac{V_0}{\phi_s}(V_c + V_s + V_s)}{0.5\pi f_j D \cot\theta}$$

V_0 -- shear_demand_on_column = 128.56kips

ϕ_s -- factor_of_safety_for_shear = 0.75

V_c, V_s, V_p -- shear_strengths_due_to_the_concrete, stirrups_and_axial_force

$V_c = 29kips$

$V_s = 41.1kips$

$V_p = 35kips$

f_j -- design_jacket_strength = 50ksi

D -- column_diameter = 24in

θ -- the_greater_of_35° _or_the_column_corner_to_corner_angle = 35°

Retrofit Design

Statically Determinant (X-Shape Plate)

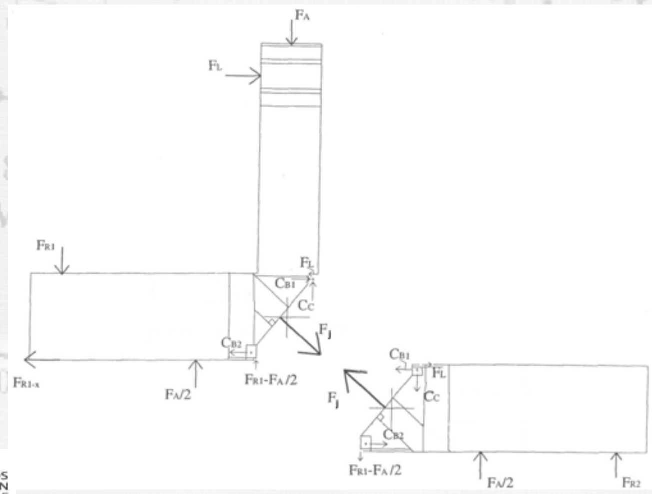

NATURAL HAZARDS MITIGATION INSTITUTE

UMR UNIVERSITY OF MISSOURI-ROLLA

Retrofit Design

Thickness of Horizontal Plates

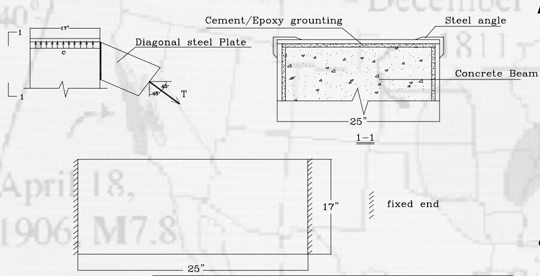

Analytical and computer models

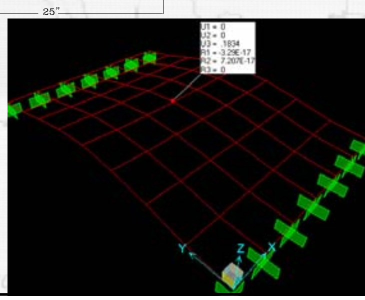

Assumptions:

1. Tension in vertical plates is significantly smaller (<20%) than that in diagonal plates. It is neglected in calculation.
2. Diagonal steel plates are fully yielded. The total tension force on two diagonal plates is T=2x50ksix12"x0.25"=300kips

- The load on the top plate is equal to $c = \frac{T\cos 45^\circ}{A}$ =0.5ksi
- A=25"x17"=425 in^2

U3=0.1834"<L/100=0.25"
The L/100 allowable deflection corresponds to that of the story drift of a steel frame (Table 1617.3.1, IBC2003)
Thickness=0.25"

NATURAL HAZARDS MITIGATION INSTITUTE

UMR UNIVERSITY OF MISSOURI-ROLLA

Retrofit Design

Summary

Retrofit component	**Design thickness (in)**	**Actual thickness (in)**
Steel ring for column ductility	0.25	0.5*
Steel sheet for column shear	0.025	0.036(20GA)*
Steel plate for beam-column joint shear	0.25	0.25
X-shape steel plate for joint shear	3/32	3/32

* Based on availability or ease of fabrication

Retrofit Design

3rd Specimen Details

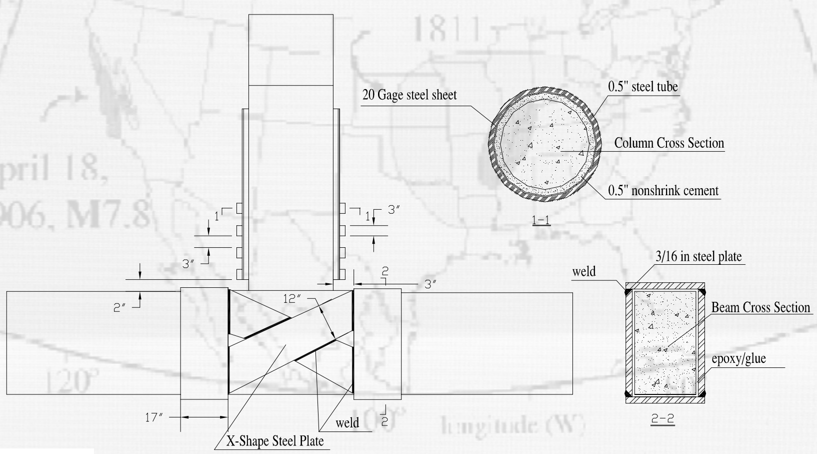

Retrofit Design

4th Specimen Details

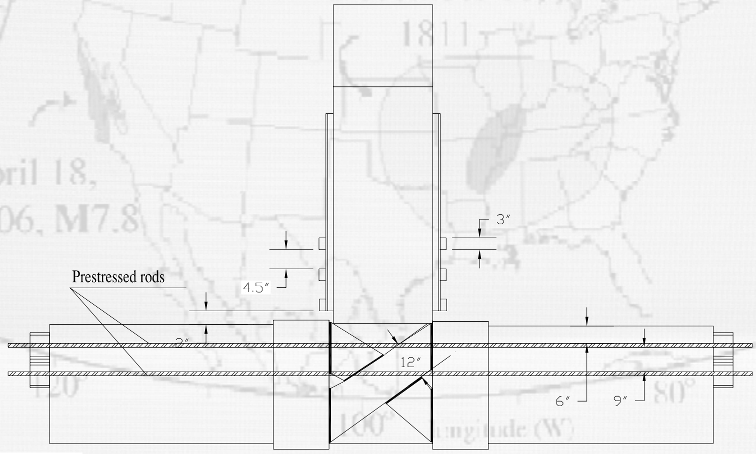

Test Setup

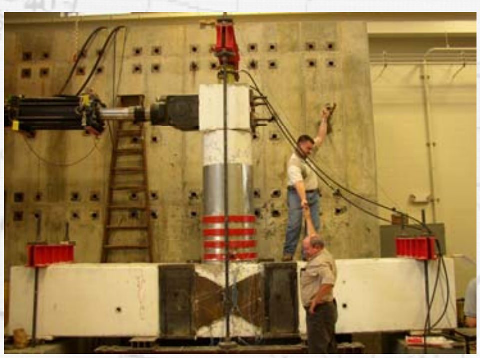

3rd Specimen

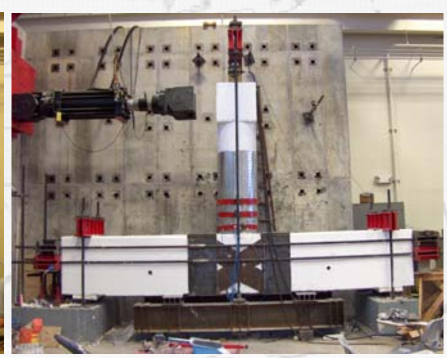

4th Specimen

Load vs. Displacement

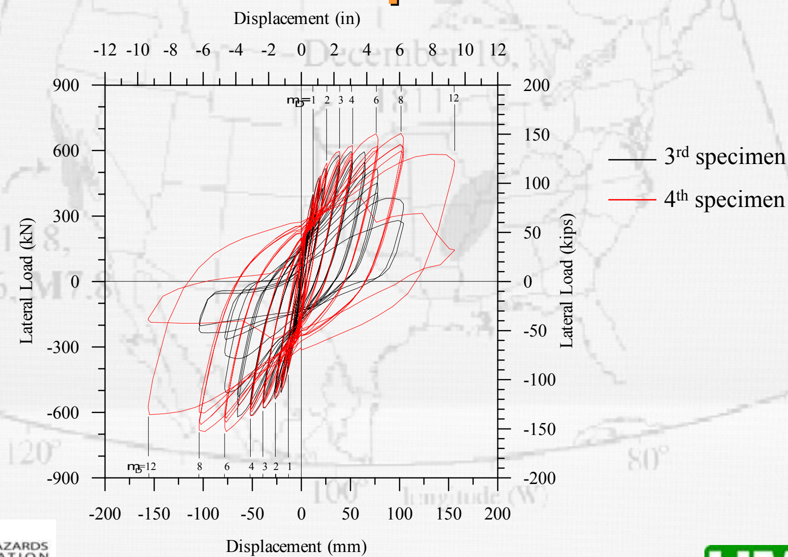

Axial Load vs. Displacement

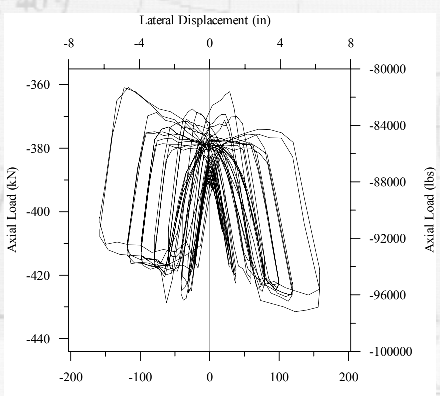

3rd Specimen

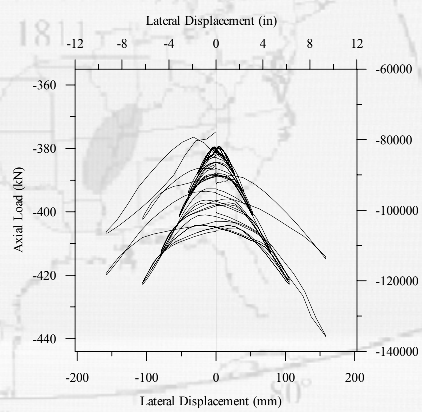

4th Specimen

Bent Cap Longitudinal Steel Strain (3rd Specimen)

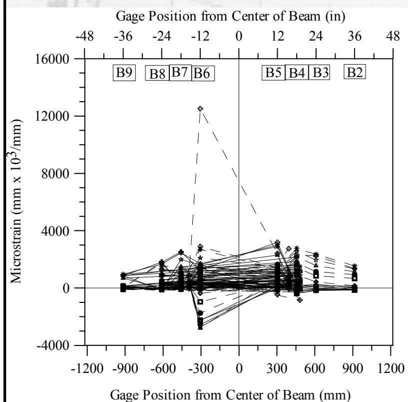

Top Longitudinal Bar

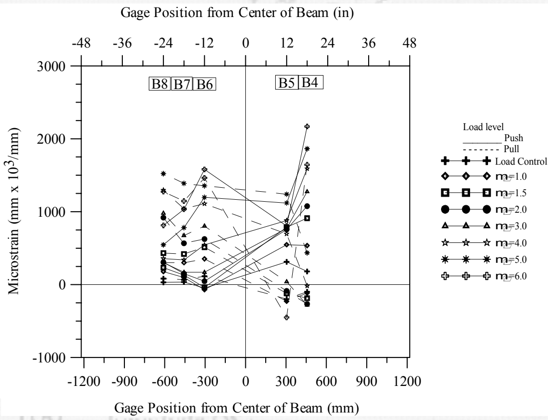

Bottom Longitudinal Bar

Bent Cap Longitudinal Steel Strain (4th Specimen)

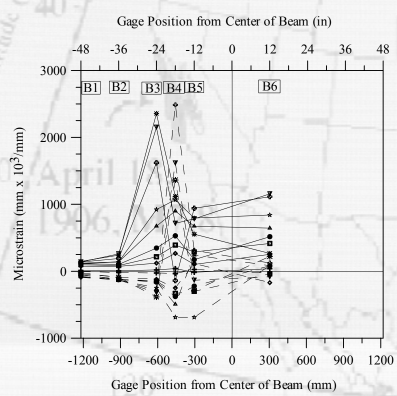

Top Longitudinal Bar

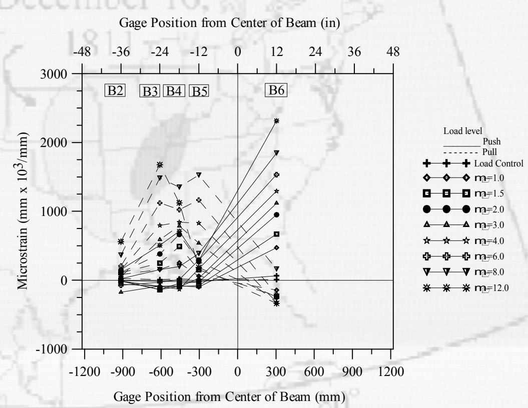

Bottom Longitudinal Bar

Bent Cap Stirrup Steel Strain

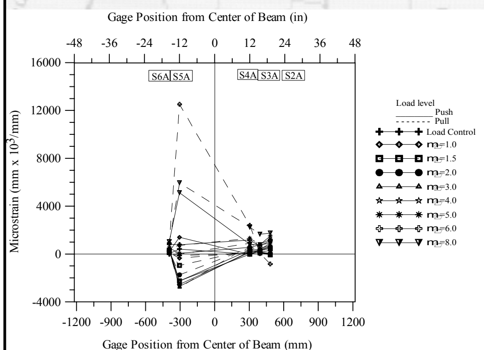

3rd Specimen

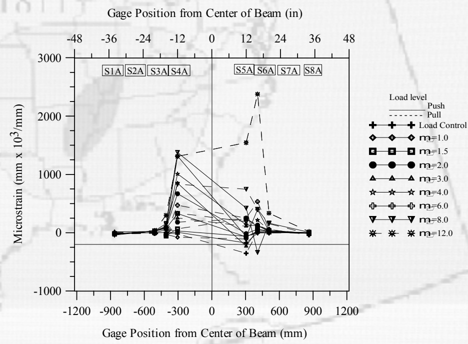

4th Specimen

Strain Gage Location on Retrofit Component

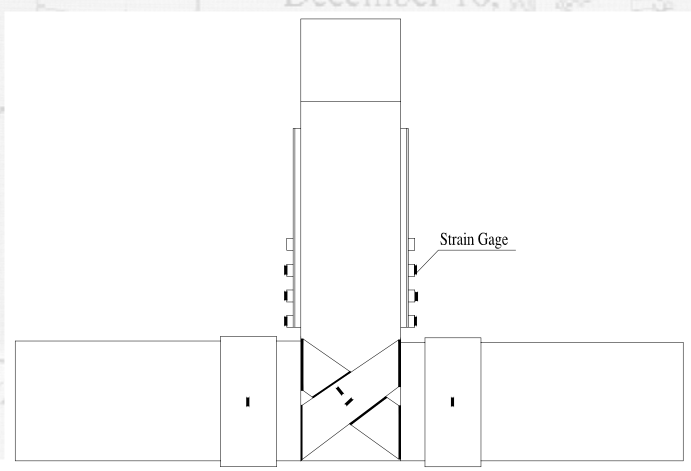

Strain on Steel Rings (3rd Specimen)

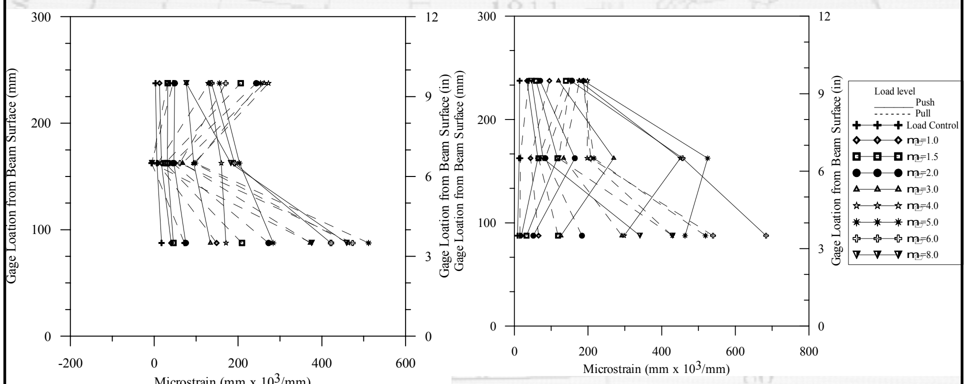

North side

South side

Strain on X-Shape Steel Plates (3rd Specimen)

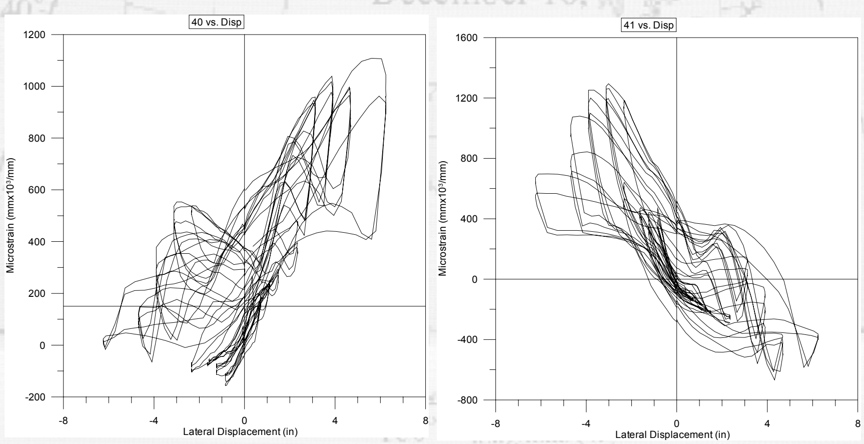

Strain on Vertical Steel Plates (3rd Specimen)

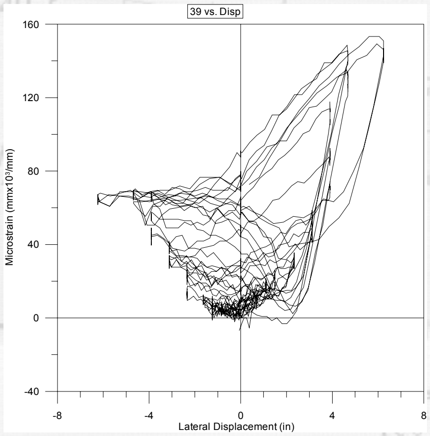

Left Side

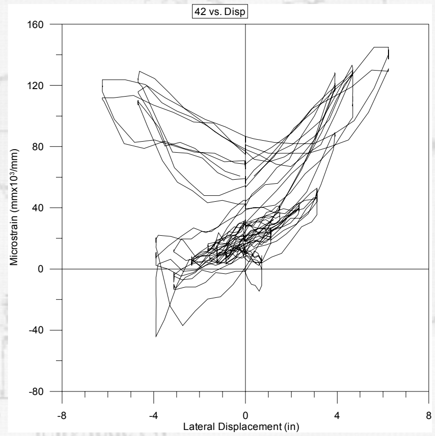

Right Side

Unretrofitted vs. Retrofitted Column (3rd Specimen)

Shear failure of unretrofitted specimen

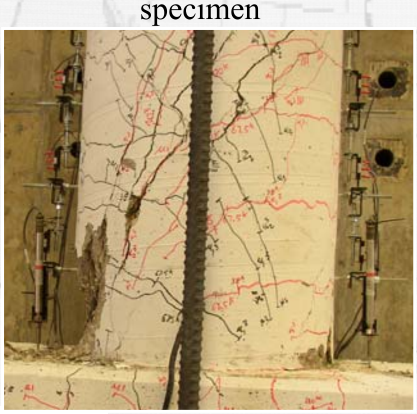

Plastic hinge formed at the beam-column joint of the retrofitted specimen

Unretrofitted vs. Retrofitted Joint (3rd Specimen)

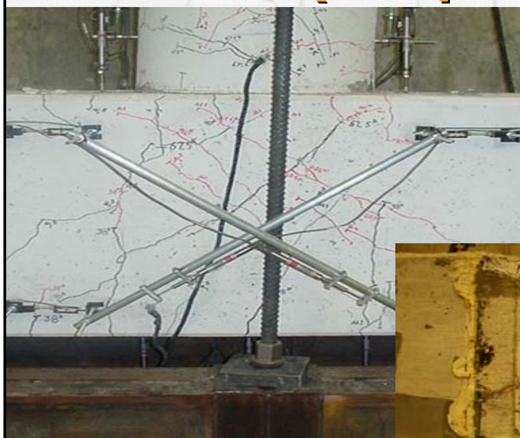

Excessive cracks of unretrofitted specimen

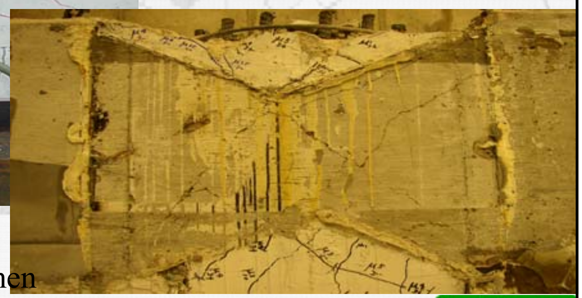

Few cracks of retrofitted specimen

Strain on Steel Rings (4th Specimen)

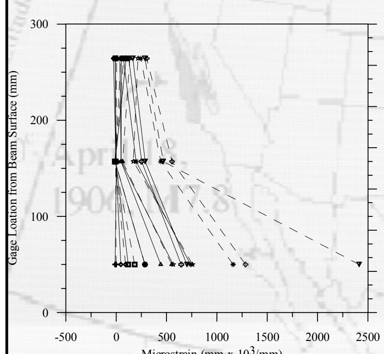

North side

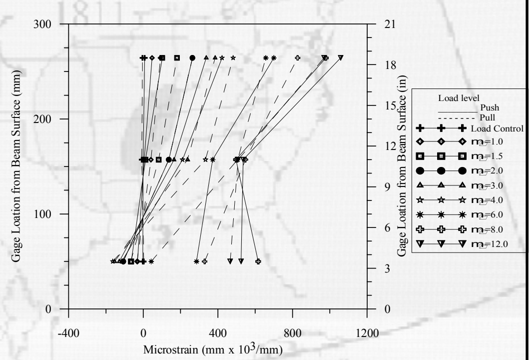

South side

Strain on X-Shape Steel Plates (4th Specimen)

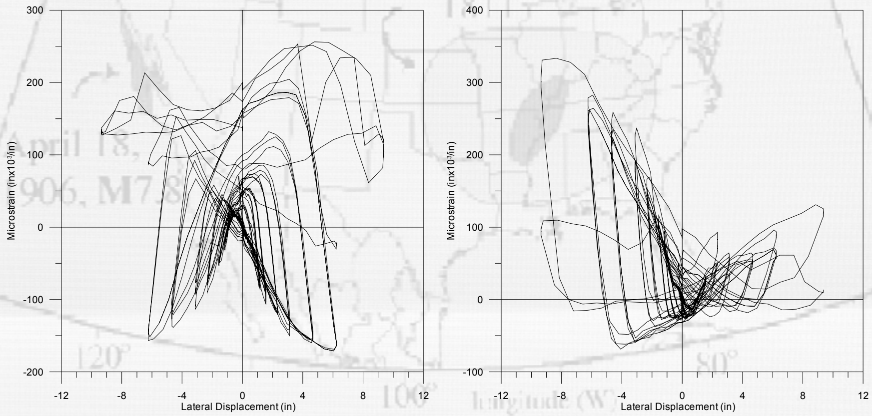

Strain on Vertical Steel Plates (4th Specimen)

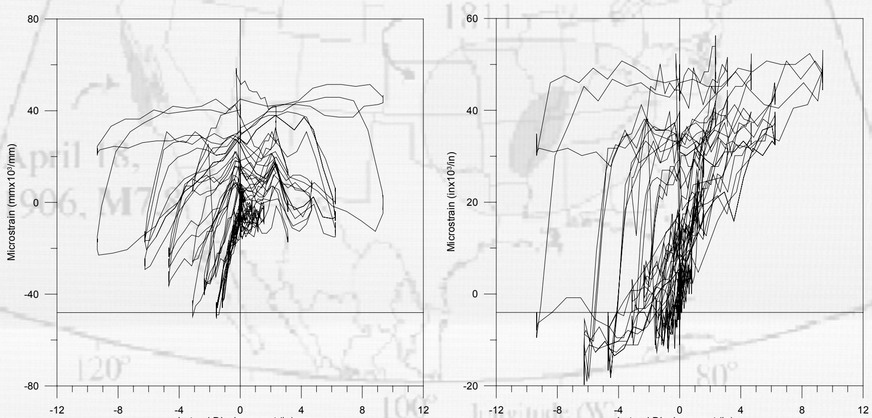

Left Side

Right Side

Conclusions

- Lap splice nailed joints of two thin steel sheets are very effective. Their strength is generally proportional to the number of rows of nails. Lap splice joints ultimately fail in bearing of the sheets.
- Self lock nailed joints of two thin steel sheets can be as effective as lap splice joints provided that sufficient space at the end of the sheets, nailed with two or more rows of nails, is available for shear deformation of the joints. Such a well-designed joint did not fail in pull-out of nails that happened to the concrete rings wrapped with a lock joint without space. The number of the rows of nails is significantly smaller than that of the lap splice joints.
- Both lap splice and self lock joints are sufficient in providing strength of nailed steel sheets for column shear retrofitting. Their strength is independent of the length of nails due to concrete cracks.

Conclusions

- Steel rings as stiffeners to thin steel sheets in the plastic hinge zone can enhance the column ductility substantially. A spacing of 7.5 cm seems reasonable to prevent buckling of the thin sheets.
- Retrofitting a beam-column joint with steel plates (one wrap around the cap beam on both sides of the column and x-bracing between two wraps) can effectively reduce the number and width of cracks at the joint. The shear force at the joint is mainly transferred by the x-bracing, not the vertical plates in the two wraps.
- Longitudinal prestress on the cap beam can further control the development of cracks at the beam-column joint so that the longitudinal rebar in column will not be pulled out of the joint and, as a result, the stiffness of the beam-column assemblage will not be degraded significantly.

PRESENTATION 15

Seismic Design of Long-Span Bridges

NATURAL HAZARDS MITIGATION INSTITUTE

UMR UNIVERSITY OF MISSOURI-ROLLA

Geotechnical and Bridge Seismic Design Workshop HNTB

Seismic Design of Long-Span Bridges

by

Steven T. Hague, P.E., S.E.

October 29, 2004
Cape Girardeau, Missouri

What makes a long-span bridge long?

- Type of Bridge
  - Prestressed Concrete Girders
  - Steel Plate Girders and Box Girders
  - Grade Separations
  - Interchanges

Generally DO NOT qualify

What makes a long-span bridge long?

- AASHTO

Primarily, the specifications set forth minimum requirements which are consistent with current practice, and certain modifications may be necessary to suit local conditions. They apply to ordinary highway bridges and supplemental specifications may be required for unusual types and for bridges with spans longer than 500 feet.

What makes a long-span bridge long?

- AASHTO Division IA

The provisions apply to bridges of conventional steel and concrete girder and box girder construction with spans not exceeding 500 feet (150 meters). Suspension bridges, cable-stayed bridges, arch type and movable bridges are not covered by these Specifications. Seismic design is usually not required for buried type (culvert) bridges.

AASHTO Division IA

- Four Methods of Analysis
  - Uniform Load Method
  - Single Mode Spectral Analysis
  - Multimode Spectral Analysis
  - Time History Method

AASHTO Division IA

TABLE 4.2A Minimum Analysis Requirements

Seismic Performance Category	Regular Bridges with 2 Through 6 Spans	Not Regular Bridges with 2 or More Spans
A	Not required	Not required
B, C, D	Use Procedure 1 or 2	Use Procedure 3

Geotechnical and Bridge Seismic Design Workshop

AASHTO Division IA

TABLE 4.2B Regular Bridge Requirements

Parameter	Value				
Number of Spans	2	3	4	5	6
Maximum subtended angle (curved bridge)	90°	90°	90°	90°	90°
Maximum span length ratio from span-to-span	3	2	2	1.5	1.5
Maximum bent/pier stiffness ratio from span-to-span (excluding abutments)	—	4	4	3	2

Note: All ratios expressed in terms of the smaller value.

Geotechnical and Bridge Seismic Design Workshop

What makes a long-span bridge long?

- AASHTO Division IA

The provisions apply to bridges of conventional steel and concrete girder and box girder construction with spans not exceeding 500 feet (150 meters). Suspension bridges, cable-stayed bridges, arch type and movable bridges are not covered by these Specifications. Seismic design is usually not required for buried type (culvert) bridges.

HNTB

Geotechnical and Bridge Seismic Design Workshop

What makes a long-span bridge long?

- AASHTO
  - Spans in excess of 500 feet
  - Arch Bridges
  - Suspension Bridges
  - Cable-stayed Bridges
  - Major Truss Bridges

HNTB

Geotechnical and Bridge Seismic Design Workshop

What makes a long-span bridge long?

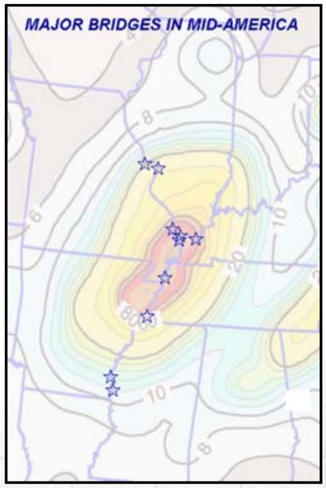

HNTB

Geotechnical and Bridge Seismic Design Workshop

What makes a long-span bridge long?

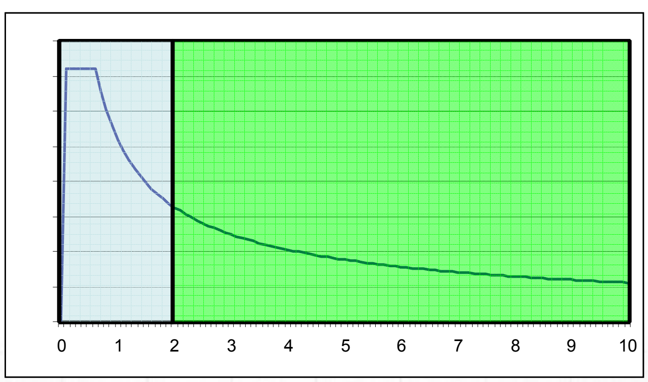

HNTB

Geotechnical and Bridge Seismic Design Workshop

What makes a long-span bridge long?

- AASHTO
  - Spans in excess of 500 feet
  - Arch Bridges
  - Suspension Bridges
  - Cable-stayed Bridges
  - Major Truss Bridges

Geotechnical and Bridge Seismic Design Workshop

AASHTO Division IA

- Time History Method
  - 5 spectrum-compatible time histories
  - Derived from a site-specific spectrum
  - Evaluate the sensitivity of the analysis to:
    - Time increment
    - Variations in materials
- We add to that
  - Effects of spatial incoherency
  - Effects of liquefaction

Geotechnical and Bridge Seismic Design Workshop

AASHTO Division IA

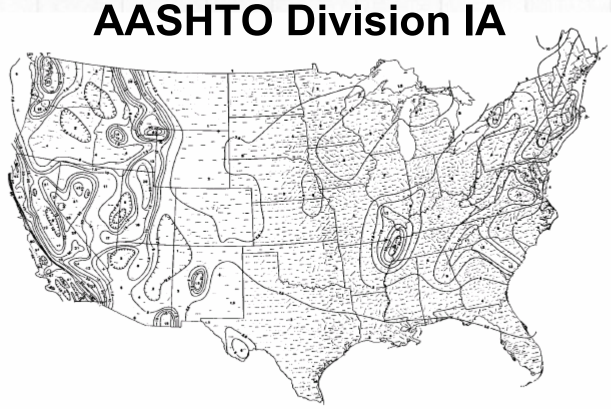

10% Probability of Exceedance in 50 Years
475-Year Return Period

HNTB

Geotechnical and Bridge Seismic Design Workshop

Bill Emerson Memorial Bridge

- 3,946-foot Mississippi River Bridge
- 1,150-foot Cable-Stayed Navigation Span
- $100 million
- HNTB Services
  - Preliminary & Final Design
  - Construction Consultation & Assistance
- Completion December 2003
- Design for Magnitude 8.5 Earthquake

HNTB

Bill Emerson Memorial Bridge

HNTB

Recurrence Interval for New Madrid Events

Magnitude	Recurrence Interval	Comments
1.0 - 1.9	2 Days	Not Felt
2.0 - 2.9	2 Weeks	Some Felt
3.0 - 3.9	4 Months	Almost Always Felt
4.0 - 4.9	4 Years	Minor Damage (1989)
5.0 - 5.9	40 Years	Damaging (1976)
6.0 - 6.9	80 Years	Destructive (1895)
7.0 - 7.9	200 Years	Devastating (1812)
8.0 - 8.9	500 Years	Disastrous (1812)

HNTB

Geotechnical and Bridge Seismic Design Workshop

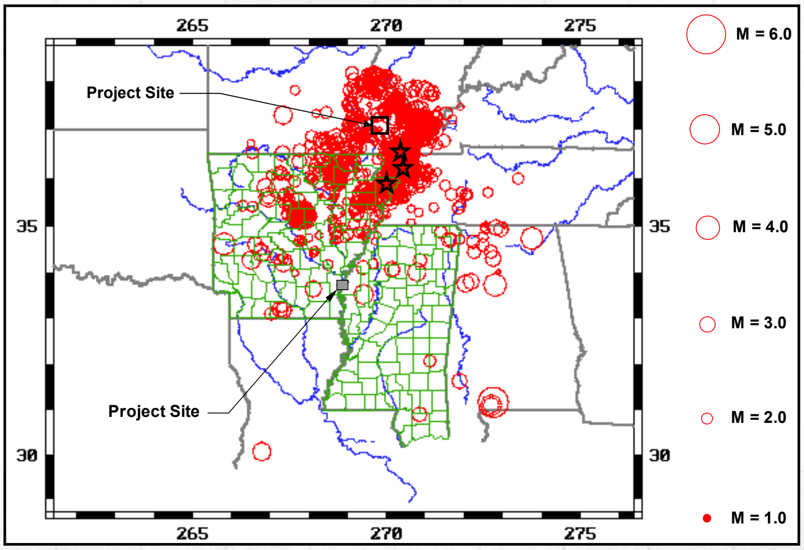

HNTB

Geotechnical and Bridge Seismic Design Workshop

So what do we do with this data?

- Determine earthquake hazard

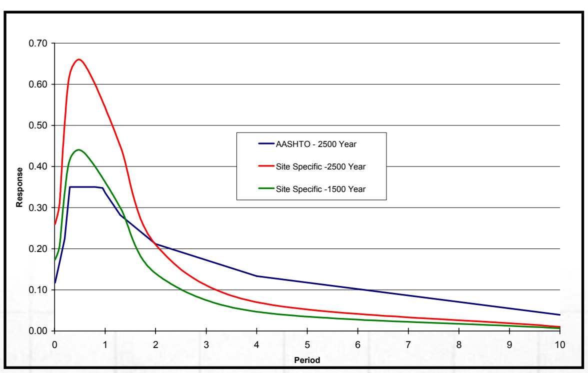

HNTB

Geotechnical and Bridge Seismic Design Workshop

So what do we do with this data?

- Determine design criteria
  - Cape Girardeau:
    - Design earthquake has 90% probability of not being exceeded in 250 years
    - Cable-stayed spans remain within the elastic range during the design event
    - Structure remains servicable after the design event

HNTB

Geotechnical and Bridge Seismic Design Workshop

So what do we do with this data?

- Determine design criteria
  - Great River Bridge:
    - 1500-year return period deterministic event
    - Cable-stayed spans remain within the elastic range during the design event
    - Structure remains serviceable after the design event

HNTB

So what do we do with this data?

- Site-specific geotechnical evaluation
  - Soil types
  - Shear wave velocity tests
  - Compression wave velocity tests
  - Hazard evaluation
- Develop site-specific spectrum
- Generate acceleration time history files

Geotechnical and Bridge Seismic Design Workshop

Generate acceleration time history files

- Caleta de Campos recordings from 1985 Michoacan (Mexico City), Mexico earthquake
- Valpariso recordings from 1985 earthquake in Chile
- Pichulema recordings from 1985 earthquake in Chile

HNTB

Geotechnical and Bridge Seismic Design Workshop

Generate acceleration time history files

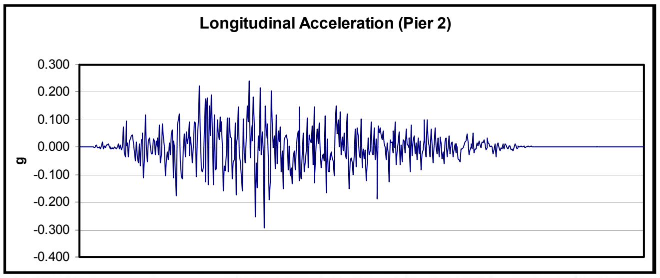

HNTB

Geotechnical and Bridge Seismic Design Workshop

Generate Structural Model

- Full 3-D model in T187
- Every member explicitly modeled
- Linear elastic member properties
- Geometric and boundary conditions non-linearity

HNTB

Geotechnical and Bridge Seismic Design Workshop

Generate Structural Model

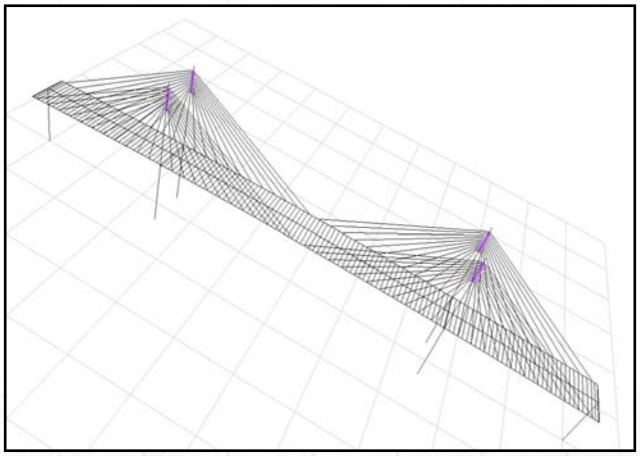

HNTB

Geotechnical and Bridge Seismic Design Workshop

Generate Structural Model

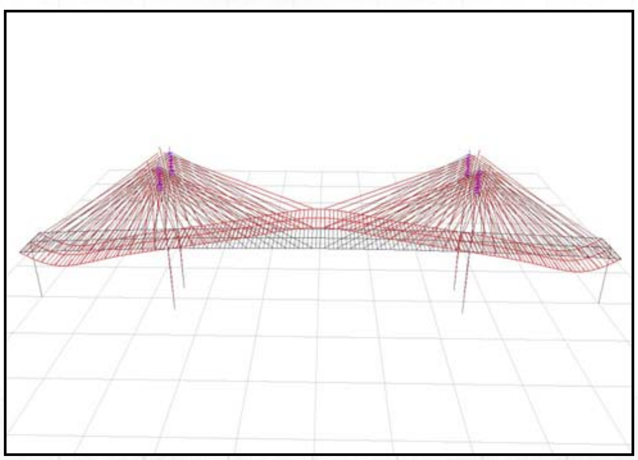

HNTB

Evaluate the performance of the Bridge

- Longitudinal translation and rotation free at anchor piers - All main pier options
- Translation free at both tower piers
- Translation fixed at one tower pier
- Translation fixed at both tower piers
- Isolation bearings at all piers
- Earthquake shock transmission devices at both tower piers

Consider Liquefaction Potential

- Soil Conditions
  - Missouri - Shallow Firm Clay on Limestone
  - Illinois - Deep Granular Alluvium on Limestone
- N = 25 Yields F.S. Against Liquefaction = 1.0
  - Missouri - No Liquefaction Hazard
  - Illinois - N = 10 to 30 to Depth of 70 feet (F.S. = 0.5)
- N > 15 Suggests No Lateral Spreading
  - Missouri - No Lateral Spreading
  - Illinois - N < 15 to Depth of 30 feet

Geotechnical and Bridge Seismic Design Workshop

Acknowledgements

- OWNERS
  - Missouri Department of Transportation
  - Illinois Department of Transportation
  - Federal Highway Administration
- SEISMIC DATA
  - Woodward-Clyde Consultants

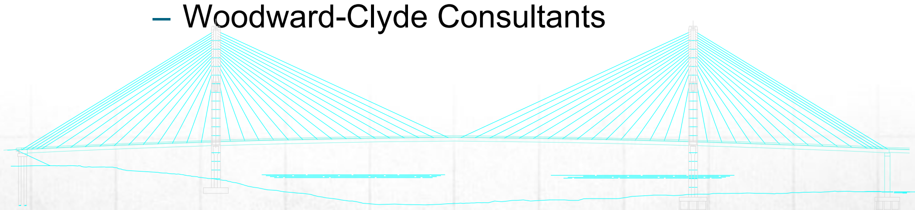

HNTB

Geotechnical and Bridge Seismic Design Workshop

Questions

HNTB

CLOSURE

This Geotechnical and Bridge Seismic Design Workshop represents the first of its kind, addressing the seismic hazard evaluation and mitigation of transportation structures in the vicinity of the New Madrid Seismic Zone (NMSZ). It draws the interest of over 60 engineers from the seven Midwest State Departments of Transportation and a number of leading consulting firms in the Central United States, and attracted faculty and students from several universities as well. Overall, the results are quite satisfactory and surpass my original expectations.

Although UMR leads the effort to organize this event, the turn out of this workshop is far beyond what UMR alone can achieve. The role of each Steering Committee member of the workshop is instrumental in bringing together the geotechnical and bridge engineers from various state agencies. As a Co-Chair of the workshop, I wish to express my sincere thanks to Mr. Peter Clogston from the FHWA regional office in Jefferson City, Mr. Thomas Fennessey and Mr. Timothy Chojnacki from MoDOT for their initiative and enthusiasm as well as their effort made in realizing this workshop.

The workshop is part of the technical transfer effort of the current UMR Earthquake Hazard Mitigation Research Program. The research team is currently summarizing the findings and recommendations in a final project report that will be due in Spring 2005. The participants of this workshop can request a copy of the final report through the FHWA report distribution center or UMR after permission has been granted by FHWA. Although every effort has been made to check the accuracy of the statements in all presentations, it is the responsibility of users to properly apply the presented results into their practice. Comments on the organization of this workshop or suggestions to future workshops should be addressed and emailed to Dr. Genda Chen, P.E. via gchen@umr.edu.

Genda Chen, Ph.D., P.E.
Associate Professor of Civil Engineering, UMR
Co-Chair of the Geotechnical and Bridge Seismic Design Workshop: NMSZ Experience